UNIVERSITY OF THE
FREE STATE
UNIVERSITEIT VAN DIE
VRYSTAAT
YUNIVESITHI YA
FREISTATA

UFS
UV

DEVELOPMENT OF ARTIFICIAL NEURAL NETWORK FOR MINE DEWATERING

By

Sage NGOIE

Thesis submitted in partial fulfilment for the degree of

***Philosophiae* Doctor**

In

Geohydrology

Institute for Groundwater Studies

University of Free State

Republic of South Africa

THESIS

Supervisor: Dr Francois Fourie

2017

- -

DECLARATION

I, Sage Ngoie, hereby declare that the present thesis, submitted to the Institute for Groundwater Studies in the Faculty of Natural and Agricultural Sciences at the University of the Free State, in fulfilment of the degree of Philosophiae Doctor, is my own work. It has not previously been submitted by me to any other institution of higher education. In addition, I declare that all sources cited have been acknowledged by means of a list of references.

I furthermore cede copyright of the dissertation and its contents in favour of the University of the Free State.

Signed _____

Student Number: 2015067057

Date _____

DEDICATION

To my mother and in memory of my father.

For their endless love and support

ACKNOWLEDGEMENTS

There are no proper words to convey my profoundest gratitude and respect to my thesis supervisor, Dr François Fourie. He offered me an unreserved guidance and inspired me to become an independent researcher. What I learned from him is not just what a brilliant and hardworking scientist can do, but how to view this world from a new perspective. Without his kind advice, this thesis would not have been completed.

My sincere thanks go to Derek McGregor and Heinrich Schreuder. Both of them generously gave me valuable comments toward improving my work.

There is no way to thank Dr Mark Schmelter enough for the time he offered me for refining my knowledge of statistics and my modelling skills. His inputs provided me with a constructive criticism, which helped me to develop my thesis.

I am grateful to Professors Jean-Marie Lunda Ilunga and Louis Kipata for being scientifically supportive during my research.

I deeply thank Franck Van de Wille, Leanice Hartz and Trevor Hille, managers at Freeport McMoran, for their financial support and encouragement.

I also have to thank Heritier Kabulo, Angele Ngoie, Deogratias Kahongo, Diane Ngoie, Pacifique Mwamba, Christelle Kasongo, Agnes Nde, Adeline Nde and all my friends for their patience with my moods during times of frustration.

Finally, I am grateful to my mother and my special sister, Estha Ngoie, for supporting my research without any complaint. They always told me to be very focused on my thesis and to follow my dream.

TABLE OF CONTENTS

LIST OF FIGURES

LIST OF TABLES

LIST OF ACRONYMS

ANN(s)	:	*Artificial Neural Network(s)*
BEM	:	*Boundary Element Method*
CM	:	*Collocation Method*
CPU	:	*Central Processor Unit*
GWL	:	*Ground Water Level*
K_{XX}	:	*Hydraulic conductivity along X axis*
K_{YY}	:	*Hydraulic conductivity along Y axis*
K_{ZZ}	:	*Hydraulic conductivity along Z axis*
mamsl	:	*Meters above mean sea level*
MLP	:	*Multi Layer Perceptron*
PI	:	*Performance Index*
r	:	*Pearson Correlation Coefficient*
ZBLSF	:	*Zero based Log Sigmoid Function*
BSF	:	*Bipolar Sigmoid Function*
FDM	:	*Finite Difference Method*
FEM	:	*Finite Element Method*
HTF	:	*Hyperbolic Tangent Function*
IFDM	:	*Integrated Finite Difference Method*
LSF	:	*Log-Sigmoid Function*
NRMSE	:	*Normalized Root Mean Square Error*
NSE	:	*Nash Sutcliffe Efficiency*
PBIAS	:	*Percent BIAS*
q	:	*Groundwater abstraction rate [m^3/day]*
RMSE	:	*Root Mean Square Error*
RSR	:	*RMSE - observations Standard déviation RATIO*
SQP	:	*Sequential Quadratic Programming*
T	:	*Transmissivity [m^2/day]*

CHAPTER 1: INTRODUCTION

1.1 BACKGROUND

Groundwater models are often used to represent and simulate the impacts of various activities on the aquifer systems. Such activities could include: potable groundwater provision to communities, irrigation from aquifer systems, groundwater abstraction for industrial and manufacturing use, evaluating the efficiency of remedial actions on contaminated aquifers, and studying the impacts of abstraction from aquifers for dewatering purposes at open pit mines. Groundwater models can also be used to simulate natural processes such as the interaction between groundwater and surface water. Apart from these applications, there are other geohydrological problems which also need to be solved by predicting the hydrodynamic potentiometric field and its behaviour with respect to time. In recent decades, groundwater models based on the Finite Element Method (FEM) and Finite Difference Method (FDM) have been used to simulate groundwater behaviour in many studies. However, due to the fact that these models require large quantities of data, it is often a costly and laborious process to develop such models for mine dewatering studies.

1.2 MOTIVATION FOR THE RESEARCH

Dewatering is critically important to open pit mining operations to provide access to ore for removal and transport to processing facilities, as well as for the safety of mining personnel. One of the methods used to plan dewatering programmes, and to support ongoing dewatering programmes, is based on the results from numerical groundwater modelling.

Groundwater models simulate the lowering of the water level elevation as the mines develop deeper below the original ground surface and into the groundwater table. The behaviour of aquifers is typically complex. Aquifers are often highly

heterogeneous and anisotropic and their behaviour depends on the physical and chemical properties of the geological unit forming the aquifer. They are controlled by numerous hydraulic and physical parameters.

Numerical models based on FDM and FEM are often used to solve geohydrological problems (Konikow, 1996). These methods discretize continuous media and assign to them some principles of behaviour and conservation characterized by constitutive parameters found from field and laboratories investigations (Levasseur, 2007). Their main disadvantages are that they typically require many inputs, including the geomorphology and geology of the area, hydraulic parameters, geohydrological characteristics, structural data, piezometer records and pumping data, which are often expensive to gather. The models are also limited by uncertainties associated with the availability and quality of the data.

By contrast, Artificial Intelligence, in particular Artificial Neural Networks (ANNs), is known to be able to model complex systems in various disciplines (Sarkar, 2012). These networks can be defined as systems that reproduce the cognitive function by simulating the architecture of the brain. ANNs are powerful tools that can provide simple and accurate solutions to very complex systems. The accuracy of these solutions are, however, also typically dependent on the number and quality of the available data used as inputs to train the networks to perform specific tasks (Hsu *et al.*, 1995). These observations lead to the following research question:

Is it possible to develop ANNs, using limited input data, that can accurately predict aquifer behaviour during the dewatering of open pit mines?

1.3 AIM AND OBJECTIVES OF THE RESEARCH

When a scientist develops a numerical model to predict the behaviour of an aquifer, some past records of that aquifer are typically used to compare the model predictions to the observed behaviour. Based on the degree of agreement between the observed and modelled data, some inputs of the model may be adjusted to better simulate the observed behaviour. This process is called *calibration*. Calibration becomes difficult

when limited data are available for the calibration process. This observation leads to the aim of this thesis, which is to investigate the possibility of simulating dewatering at open pit mines where limited data are available, using ANNs. This research will be undertaken with the following objectives:

- To develop an ANN capable of simulating and predicting the groundwater behaviour during mine dewatering;
- To assess the success of the predictions made by the ANN under conditions of varying, but limited, input data availability;
- To apply the developed ANN to real open pit mines to predict the behaviour of the aquifer systems at these mines; and,
- To find simple mathematical equations to describe the hydraulic heads in observation wells at the mine. These equations could be used to make future predictions related to the impacts of dewatering strategies on the aquifer system.

1.4 RESEARCH METHODOLOGY

To achieve the aim and objectives of the study, the following actions will be taken:

- A hydrogeological model will be developed using FEM to produce synthetic "observations" of the hydraulic heads at piezometers of a fictional mine to represent "true conditions" that a subsequent ANN will try to reproduce under varying data availability conditions;
- Different ANNs will be developed to predict the hydraulic head response at the fictional mine. The modelled hydraulic head data (the synthetic observations) from the FEM will be used to train the ANNs and to do performance analysis;
- The ANN most capable of simulating and predicting the groundwater behaviour for mine dewatering at the fictional mine will be identified by changing the architecture and algorithms used by the ANN through trial-and-error adjustments;

- The strengths and weakness of the final ANN will be evaluated by doing performance analyses during which the predicted (by the ANN) and modelled (by the FEM) hydraulic heads will be statistically evaluated;
- The ANN will be used to predict the hydraulic head response at two real open pit mines (the Kabwe and Shimbidi mines) in order to evaluate the model's performance under real-world conditions; and,
- Mathematical equations will be found to predict the hydraulic heads in piezometers at the Kabwe and Shimbidi open pit mines. These equations will be based on the predictions made by the ANN.

1.5 THESIS STRUCTURE

The thesis will comprise seven chapters:

- In Chapter 1, the research will be presented through the background of the study, aim and objectives, motivation of the research and the methodology followed to achieve the aim and objectives;
- Chapter 2, will give a review of the literature on groundwater modelling approaches, the physiological and mathematical models of Artificial Neural Networks, and mine dewatering processes. The theoretical background to the current investigations will be described;
- In Chapter 3, a numerical groundwater model of an ideal mine will be developed using FEM. The numerical model will be used to simulate the behaviour of the groundwater system under different conditions of groundwater abstraction. These modelled groundwater responses (outputs) will be used to present "real" or "observed" measurements used as inputs to train the ANN developed in Chapter 4;
- In Chapter 4, an Artificial Neural Network will be developed. This ANN will use the outputs from the numerical groundwater model developed in Chapter 3 as inputs during training. The strengths and weaknesses of the ANN in predicting

the aquifer response will be evaluated through statistical and graphical techniques. The architecture of the ANN will be adjusted to find the network yielding the best results;

- In Chapter 5, the selected ANN will be applied to the Kabwe and Shimbidi open pit mines to explore its strengths and weaknesses in predicting aquifer behaviour under real-world conditions. Mathematical equations will be found to predict the groundwater behaviour at the mines during dewatering;
- Chapter 6 will summarise the findings of the study, draw conclusions from the results of the study and make recommendations for future research.

CHAPTER 2: LITERATURE REVIEW

2.1 INTRODUCTION

This chapter will discuss the literature on groundwater modelling with its application for mine dewatering, the background of Artificial Neural Networks, and the evolution of Artificial Neural Networks in geohydrology. The understanding of advective groundwater behaviour is very important in water management. Although there are some variables (for example, physical and chemical soil properties) which affect groundwater flow in the subsurface, aquifers are conceptually easy to understand.

Although water in the subsurface may also occur in the form of soil water and capillary water, the term *groundwater* often refers to the water below the water table (the upper surface of the zone of saturation). The groundwater media below the water table are saturated because the pore space in these media is completely filled with water. Above the water table, the soil is unsaturated and the pore space contains both air and water. After precipitation, water can flow across the ground surface (runoff), evaporate or infiltrate. Infiltration induces a local rise of the water table which could lead to groundwater flow if hydraulic gradients are formed (Kumar, 1992).

2.2 GROUNDWATER MODELLING

Modelling is a simplification of a more complex reality. Groundwater modelling is an approximate representation of an underground water system. The main aim of groundwater models is the prediction of groundwater behaviour under different conditions and different impacts (Anderson and Woessner, 1992).

Groundwater models are very useful tools for solving a wide range of groundwater problems and for supporting decision-making processes, such as with water supply projects and pit dewatering strategies. Models can be physical, analog or mathematical (Mercer and Faust, 1980).

2.2.1 PHYSICAL MODELS

Physical models mimic, on a small scale, physical processes found in nature. In groundwater studies, they are commonly used to teach, demonstrate and perform experiments to simulate aquifer conditions. Physical models were the first models used in groundwater flow studies (Sarkar, 2012).

2.2.2 ANALOG MODELS

Some geohydrological problems cannot be solved by ordinary mathematical formulations. If boundary conditions and related factors are well defined, analog models can be used to solve such problems. Analog models are models that use two physical systems and the system that is easier to compute is used to model the other. The strength of analog modelling is the ease with which it can analyse very complex boundary-value problems with simple physical interpretations.

In theory, there are two types of analog models which are prominent for groundwater flow:

- **Electric analog models** are used to simulate geohydrological conditions based on the similitude between electrical laws and laminar liquid flow. An electrical analog model for groundwater studies in porous media is carried out by connecting generators that produce potential energy on the system, which leads to an energy-dissipative field. The electrical network assembled for that purpose is called an “analog computer”. The analog computer simulates the geometry and internal state of the region to reproduce analogically the geology of the aquifer (Jorgensen, 1974);
- **Viscous fluid analog models** are based on the similitude between laminar liquid flow and the movement of viscous fluid flowing through two parallel plates separated by an infinitesimal distance (Todd, 1954). This model is based on the analogy between the groundwater flow and the movement of liquid flow between two parallel plates. This model can be built by using two parallel

plastic sheets separated at a small distance and connected to a reservoir of oil or glycerine. In the horizontal position, the viscous fluid analogue model can simulate confined or phreatic aquifers (Santing, 1957). According to Varrin and Fang (1967), geohydrological parameters can be simulated by varying the interspace between the plates, varying the viscosity of the fluid by using either glycerine or oil, and by changing the angle of the plates to model different hydraulic gradient conditions.

2.2.3 MATHEMATICAL MODELS

Mathematical models can be deterministic or statistical (stochastic), or a combination of these. The latter provides a window of solutions relative to probabilities while deterministic models are based on cause-and-effect relationships for well-known systems. Deterministic models can be analytical and numerical (Thangarajan, 1999).

2.2.3.1 ANALYTICAL MODELS

Analytical models are any solutions of numerical equations that can be expressed as polynomial, logarithmic, exponential or trigonometric functions (Craig and Read, 2010).

Several methods can be used to predict the impact of groundwater flow in open pit mining. For a single excavation face, one-dimensional methods are more frequently used (McWhorter, 1981). If inflow predictions are needed for the entire mine, the combination of radial flow and one-dimensional methods can give better first order estimates (Saunders, 1983). If enough data are available, numerical models have the potential to provide accurate prediction for complex conditions.

In the last several years, analytical models have provided accurate predictions in various domains of geohydrological research. Below are some case examples:

- Koch (1985) developed an analytical model to predict inflows to open pit mines and to assess the geohydrological impacts of mining;
- Holland *et al.* (2004) produced an analytical model of a lowland river floodplain. This model required inputs which could be easily found from published papers and it had lower requirements compared to numerical models done based on the FDM;
- Craig and Read (2010) made a hybridisation of analytical and numerical models to increase the accuracy of prediction for non-linear problems;
- Kelson *et al.* (2002) developed a model based on an analytical element code and non-linear parameter estimation. They concluded that analytical element models are able to predict hydraulic parameters well;
- Brown and Trott (2014) developed an analytical model to solve water resource problems in a mining operation with limited available data.

According to Csoma (2001), analytical models are preferable if:

- There is a lack of information on the physical conditions at the boundaries of the model, since the method does not require specified boundary conditions around the area;
- Several structures and surface water behaviour impact the aquifer throughout the model, as the description of their joint effects with the corresponding elements is simple and sufficient.

2.2.3.2 NUMERICAL MODELS

Numerical methods used for groundwater modelling may be classified as follows:

- The **Finite Difference Method (FDM)** solves differential equations where finite differences approximate the derivatives on rectangular elements (Gilberto and Urroz, 2004);

- The **Integrated Finite Difference Method (IFDM)** is conceptually similar to FDM but uses an integrated form to have another differential form where the area to model can be easily discretised into subdomains (Ferrarresi, 1989);
- The **Finite Element Method (FEM)** is based on finding approximate solutions for partial differential equations using triangular elements (Dhatt *et al.*, 2012);
- The **Boundary Element Method (BEM)** denotes any method that approximates the solution of differential equation on the boundary of the domain using integral equations (Costabel and Stephen, 1985);
- The **Collocation Method (CM)** takes account of the finite-dimensional space of solutions and determines a number of points in the domain (called collocation points). The solution which satisfies the equation at the collocation point has to be selected to solve ordinary or partial differential equation or integral equations (Gomez and Lorenzis, 2016).

2.3 MODELLING PROCESS

The groundwater modelling process starts with planning the type of model needed and defining the modelling objectives. Then comes the conceptualisation of the model for defining known physical components of the area. In the design stage of the model, it is decided how to make a good representation of the conceptual model through a mathematical model. After calculating the model response, if the output is found to give a poor representation of the measured data, adjustments have to be made to either the model type, the conceptual model or the mathematical model (Barnett *et al.*, 2012). On the other hand, if the model response is found to give a fair representation of the measured data, the model may be further improved by calibration during which the input parameters are adjusted to reduce the difference between the measured and modelled responses. Furthermore, sensitivity analyses may be carried out to determine which input parameters have the strongest influence on the modelled response. The model may then be used to predict the behaviour of the groundwater system. At any time during this process, adjustments

to the model should be made if the modelled response is found to give a poor representation of the measured response (refer to Figure 2-1).

2.3.1 CONCEPTUAL MODELS

When constructing a model, the first step is to understand the physical system and to define how it operates through the development of a conceptual model. For a mathematical model as generalized in Figure 2-2, a conceptual model can be defined as a graphical representation of the groundwater system, based on geomorphological, hydrological, geological and hydrogeological data, in a simple block diagram or 2D section (Anderson and Woessner, 1992).

After analysing the topography of the area of interest, the next step to produce the conceptual model is to define geological parameters, taking into account thicknesses of layers, layer continuity, tectonic features and lithology. These data can be found from geophysical surveys, geological maps, bore logs or some additional field mapping (Wilson *et al.*, 2005). To construct a more objective model, additional data can be obtained from the government or private sources and investigations.

A conceptual model takes into account all exterior constraints to the area by assigning boundary conditions to the model.

2.3.2 MATHEMATICAL MODELS

According to Fowler (1998), mathematical models of real-world situations are generally complex and it is difficult to describe the real physical phenomena in mathematical terms. When applied mathematicians attempt to construct a model, they start with a phenomenon of interest, which has to be described mathematically by considering the physical laws that govern the particular phenomenon.

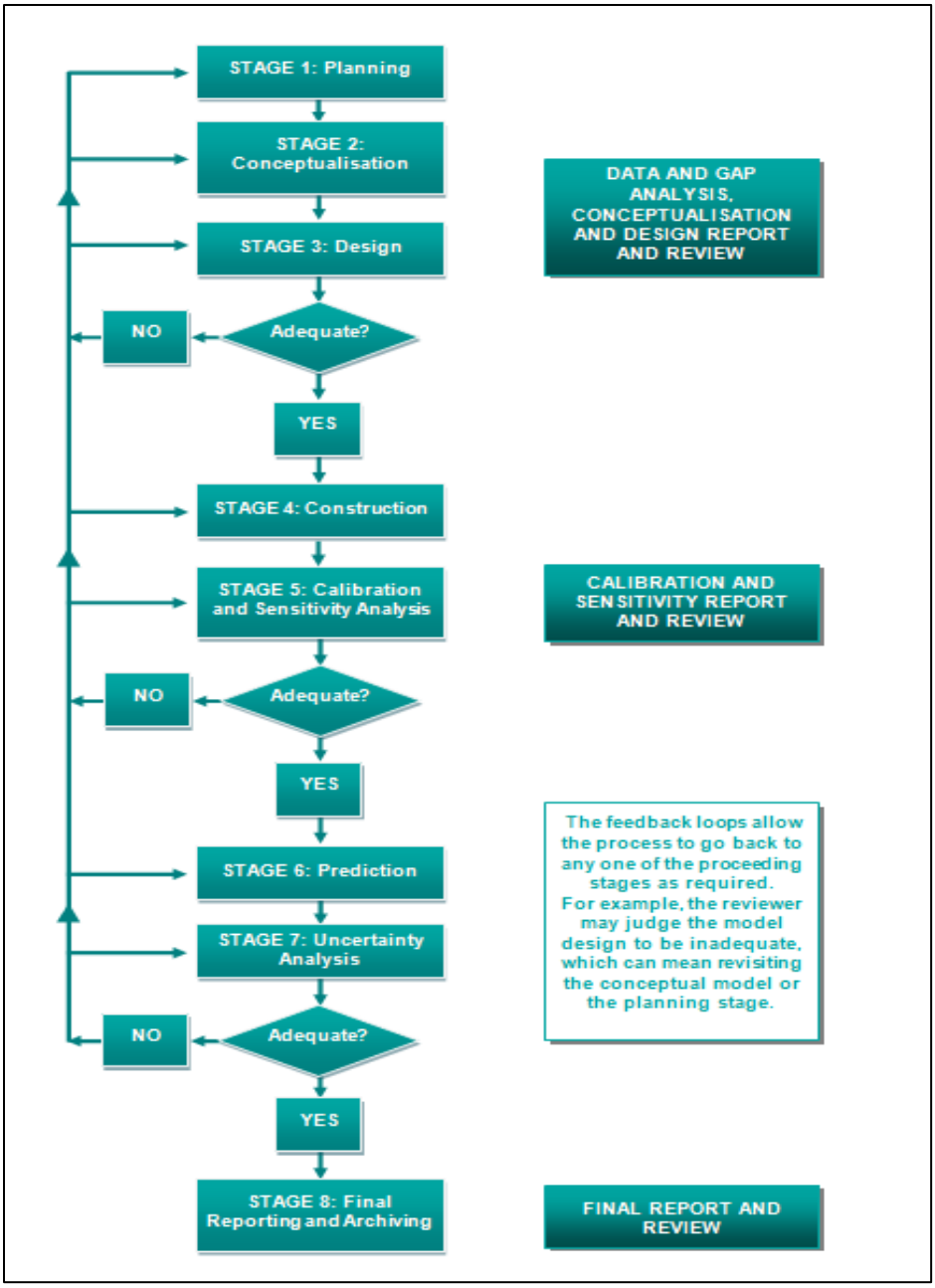

Figure 2-1: Groundwater modelling process (modified from Yan et al., 2010)

Observation of the phenomenon often leads to an understanding of the mechanisms that control the phenomenon. The main purpose of the mathematical model is to provide quantitative descriptions of the mechanisms and therefore, illustrate the phenomenon.

Quantitative description is usually done based on some physical variables. A mathematical model is constructed based on equations that depend on these variables. There are three ways to formulate the dependence of the equations on the variables. The equations can be expressed as (Fowler, 1998):

- Exact conservative laws;
- Constitutive relation between variables; and,
- Hypothetical laws.

Mathematical models are analysed by comparing their outputs with observations made in situ. Some adjustments to the model can be done to ensure that the mathematical formulation gives an accurate description of the mechanisms governing the phenomena. The model can also lead to predictions that help to assess the accuracy of the model.

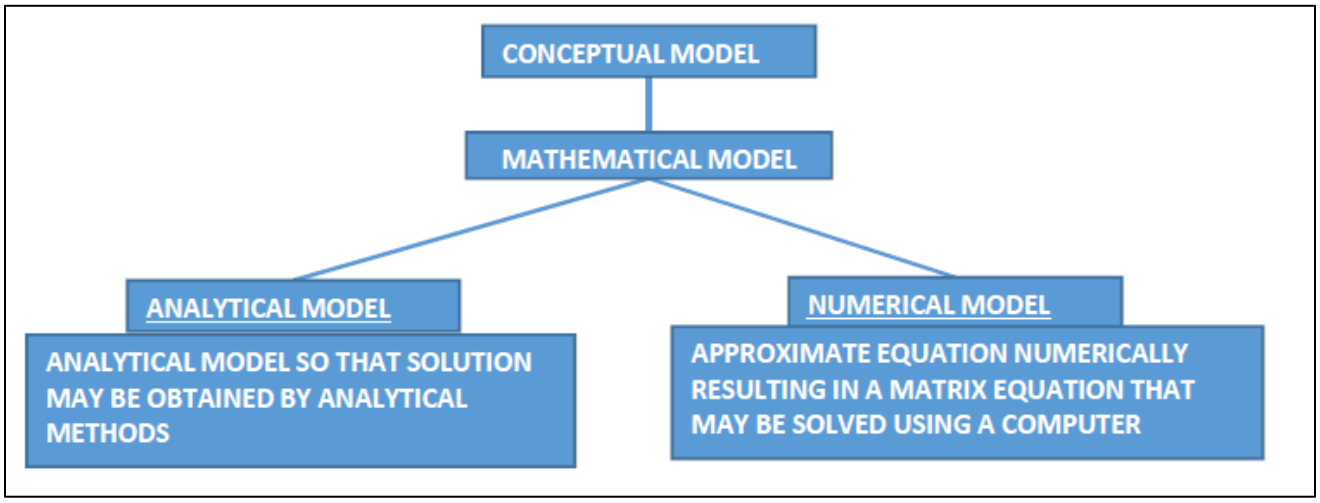

Figure 2-2: Logical diagram for developing a mathematical model (Mercer and Faust, 1980)

All models are idealisations and are limited in their applicability. Mathematical models are usually first done with simple formulations. If the modelled responses give acceptable estimations of the observed data, then the formulation can be made more complex to allow for the modelling of complex structures (Balint and Balint, 2007).

Mathematical models are frequently used in studying groundwater systems. They can be used to simulate or predict groundwater flow and contaminant transport (Kumar, 1992). From the available literature it can be seen that groundwater models have been used in many studies relating to groundwater (Ardejani and Tonkaboni, 2009; Aryafar *et al.*, 2007; Shamim *et al.*, 2004; Lohani and Krishnan, 2015; Haitjema and Brucker, 2005). As discussed in the preceding sections, groundwater models generally require many data, which are often difficult and expensive to acquire. It is thus important to find alternative methods of predicting aquifer behaviour in cases where little information on the aquifer systems is available. In the current study, an Artificial Neural Network is developed to address this problem.

2.4 ARTIFICIAL NEURAL NETWORKS

2.4.1 INTRODUCTION

Artificial Neural Networks (ANNs) are part of Artificial Intelligence. They are a mechanism that reproduces the cognitive function of the brain by simulating its architecture. By imitating the human brain's structure and function, ANNs are well-known to be powerful in solving complex, noisy and non-linear problems (Hsieh, 1993). They are successfully used for approximating functions, task classifications and clustering (Allende *et al.*, 2002; Hsieh, 1993; Khashei and Bijari, 2009; Wilamowski, 2007). ANNs learn from the available data describing the behaviour of a system and attempt to establish a relationship between these data, even if the physical mechanisms controlling the behaviour of the system are poorly understood. They are thus suitable to model the complex behaviour of aquifers which by nature are anisotropic and heterogeneous.

The learning and generalisation processes of ANNs are based on neurophysiological processes, and are described through mathematical relations that mimic the neurophysiological functioning.

2.4.2 NEUROPHYSIOLOGICAL PROCESSES

The human brain contains almost 100 billion neurons with 1 000 to 10 000 synapses by neuron. The way the brain processes information is not yet well known, although there are many available applications (Ellis *et al.,* 1995; Park et *al.*, 2009, Goh *et al.*, 2005; Cho, 2009; Shi, 2000). Neurons can be defined as biological cells which have body cells and nuclei. Information is collected by fine structures called dendrites. A neuron produces an electrical signal and sends it through an axon, which is divided into several branches. That electrical signal is converted in an effect at each end of the branch by a synapse which then generates activity in connected neurons.

When a neuron is excited enough, compared to its input, it generates electricity and sends its signal to its axon. Learning occurs when the effectiveness of the synapses changes, causing neurons to influence each other.

2.4.3 MATHEMATICAL MODELS

Biological neurons can perform various tasks such as body recognition, signal processing and generalisation. The performance of the neurons can be described by mathematical relations, which can be transformed into algorithms, leading to the development of Artificial Intelligence. ANNs are models of the neurophysiology of the brain that may be described by their components, descriptive variables and interactions between components (Rojas, 1996). Together, the components of the ANNs and the interactions between these components form the architecture of the ANNs.

2.4.3.1 NEURAL NETWORK ARCHITECTURE

An ANN is based on an interconnection of nodes, called neurons, that works as a collective system. This system comprises neurons and links. Each link has a weight, which is a numerical value representing the connection strength between the

neurons (see Figure 2-3). The sum of the input weights is converted to outputs through a transfer function (TF) (refer to Section 2.4.3.2) (Wilamowski, 2003).

ANNs contain three kinds of layers:

- An **input layer** which has the predicator variable;
- One or more **hidden layers** which function as a collection of feature detectors;
- An **output layer** used to produce a response relative to the inputs.

ANNs can function using either feed-forward or feedback methods, using single or multiple hidden layers.

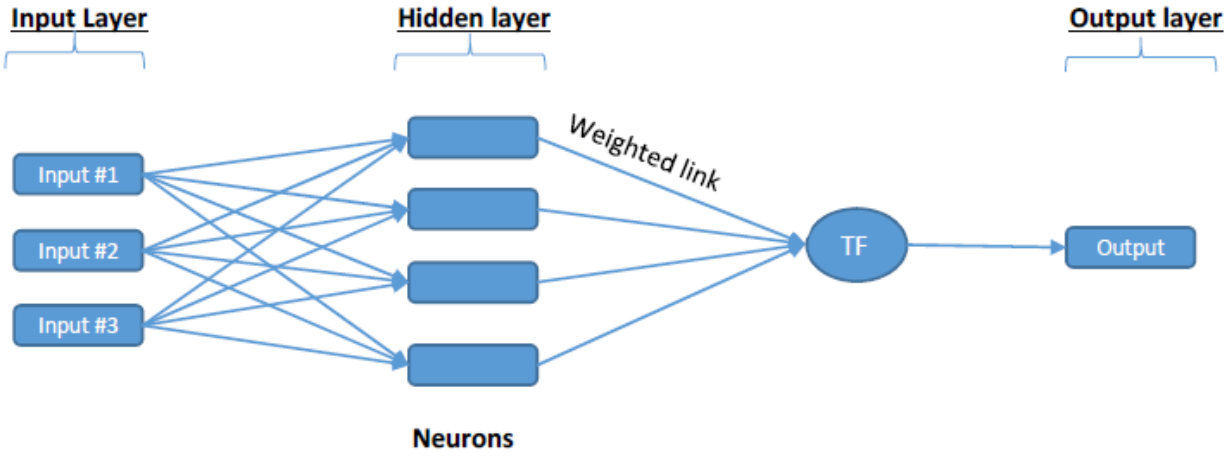

Figure 2-3: Example of an ANN with one hidden layer (Li E., 1994)

2.4.3.1.1 FEED-FORWARD NETWORKS

Feed-Forward Neural Networks (FFNNs) are widely used. One such FFNN is the Multi-Layer Perceptron (MLP). In these neural networks, information progressions are unidimensional going from input layer to output layer through hidden layers (Millar and Calderbank, 1995).

2.4.3.1.2 FEEDBACK NETWORKS

Feedback Networks (FBNs) are neural networks that process information in both directions by introducing loops in the network. They have an interactive or recurrent architecture. Their output is often used to create feedback connections in single layer organization. They can become very complex, but are often useful for solving complex problems (Rojas, 1996).

2.4.3.2 TRANSFER FUNCTION

An ANN should be able to reproduce the correct output for the related inputs. Its behaviour depends on the weights and the input-output function operating at each neuron, called the transfer function. While using an ANN, the choice of the transfer function can deeply impact the behaviour of the whole network. The most commonly used transfer functions are (Hajek, 2005):

- **Linear**, where the output from the neuron is directly proportional to the total weighted input that it receives from the other neurons connected to it;
- **Threshold**, where the output is set to a higher or lower level depending on whether the total input is greater or less than some threshold value;
- **Sigmoidal (logistic)**, where the output changes progressively but not linearly according to changes in the weighted input;
- **Hyperbolic tangent**, where the fluctuation between consecutive inputs is relative to the hyperbolic tangent derivative.

It is important to note that the threshold, sigmoidal and hyperbolic transfer functions are non-linear (Pushpa and Manimala, 2014).

2.4.4 OPTIMISATION OF THE MODEL

The process of optimisation of ANNs is also called the “training” or “learning” process. According to Rumelhart *et al.* (1986), the most commonly used method is the back-propagation algorithm. This algorithm is non-linear and is more often applied when

using multi-layer perceptrons (Brown and Harris, 1994). Perceptrons are algorithms which can be computed by a binary variable coding. They can be linear or spherical according to the way outputs are computed. It is expensive to compute the back-propagation algorithm, especially during the learning process. It is then important to find an alternative simplified method which can speed the learning process and produce reasonable outputs for new inputs.

2.4.5 STOPPING CRITERIA

When optimising ANNs, it is important to decide when the training process has to be stopped. The stopping criteria determine when the ANN has been optimally trained. The training process can be stopped when a) a fixed number of training inputs have been reached, or b) when the training error becomes acceptably small. The first stopping criterion could lead a prematurely cessation of training, while the second could lead to over-training.

Cross-validation is a valuable technique to avoid such problems (Smith, 1993). When available inputs are limited, Amari *et al.* (1997) suggested using the cross-validation technique because it presents many advantages. In this technique, the data are divided in three parts: training, testing and validation. The training part is used to train and build the model. The testing part measures the ability of generalisation of the model. The training is stopped when the error of the testing set starts to increase, even if the number of iterations has not been reached. The validation part is used for performance analysis. It is also possible to divide the dataset into two parts where one part is used for training and the other for validation.

2.4.6 PERFORMANCE ANALYSIS OF THE MODEL

The main purpose of the performance analysis is to ensure that the ANN is able to generalise what was used for its training, rather than just memorising the relationship between the inputs and outputs of the training dataset. The ANN can

be assumed to be robust only if the performance on an independent dataset (not used during training) is adequate.

Most model evaluations are done through statistical and graphical techniques (Moriasi *et al.*, 2007). The main statistical evaluation techniques are:

- The **Slope and Y-intercept method** shows how well the predicted data match the observed data. In this techniques it assumed that compared data have a linear relationship, measured data are free of error and all errors come from predicted data. In reality, the measured data often have errors. For this reason, the Slope and Y-intercept method has to be used carefully;

- The **Pearson correlation coefficient (*r*)** describes the degree of collinearity between the observed data and the model output (predicted data). The Pearson correlation coefficient ranges from -1 (the observed and predicted data are negatively correlated) to +1 (the observed and predicted data are negatively correlated). An *r*-value of zero indicates that there is no correlation between the data. The coefficient can be defined as follows:

$$r = \frac{\sum_{i=1}^{n}[(X_i - X_{mean}) * (Y_i - Y_{mean})]}{\sqrt{\sum_{i=1}^{n}(X_i - X_{mean})^2 * \sum_{i=1}^{n}(Y_i - Y_{mean})^2}}$$

  Where n is the number of data points, X_i is the observed value of data point i, Y_i is the predicted value for data point i, and X_{mean} and Y_{mean} are the mean values of the observed and predicted data, respectively.

- The **Nash-Sutcliffe Efficiency coefficient** (NSE or E) is a statistical method that calculates the magnitude of the measured data variance compared to the residual variance (Nash and Sutcliffe, 1970). The NSE can range from -∞ to 1 (inclusive). If the value is equal to 1, it means that the model outputs match the observations perfectly. Values between 0 and 1 indicate acceptable

performance, whereas negative values indicate unacceptable performance. The NSE is defined as:

$$NSE = 1 - \frac{\sum_{i=1}^{n}(X_i - Y_i)^2}{\sum_{i=1}^{n}(X_i - X_{mean})^2}$$

- The **Percent Bias (PBIAS)** measures the general trend of predicted data values compared to the observed data values. Data values are compared to determine whether the predicted values are generally smaller or larger than the observed values (Gupta *et al.*, 1999). Positive values for the PBIAS indicate that the model is biased towards underestimation, while negative values indicate that that the model is biased towards overestimation. The optimal value for the PBIAS is zero, indicating no bias in the predicted data. The PBIAS is calculated as:

$$PBIAS = \frac{\sum_{i=1}^{n}(X_i - Y_i)^{*}100}{\sum_{i=1}^{n} X_i}$$

- The **Root Mean Square Error (RMSE)** is based on the difference between the observed and predicted values. That difference is called the "residual". According to Singh *et al.* (2005), a lower RMSE indicates better performance of the model. It can be defined as:

$$RMSE = \sqrt{\frac{\sum_{i=1}^{n}(X_i - Y_i)^2}{n}}$$

- The **RMSE-Observations Standard Deviation Ratio (RSR)** is a ratio of the RMSE and standard deviation of the observed data. It is a way of standardising the RMSE. The lower the RSR, the better the performance of the model (Moriasi *et al.*, 2007). The optimal value of the RSR is zero, indicating a perfect fit between the observed and predicted data. The RSR is defined as:

$$RSR = \frac{\sum_{i=1}^{n}(X_i - Y_i)^2}{\sum_{i=1}^{n}(X_i - X_{mean})^2}$$

- The **Normalised RMSE (NRSME)** allows the comparison of the performance of models where differences in the mean data values of the models may lead to different performances if evaluated using the standard RMSE. The optimal value of the NRMSE is zero. It is calculated as follows:

$$NRMSE = \frac{RMSE}{X_{max} - X_{min}}$$

Where X_{max} and X_{min} are the maximum and minimum values of the data in the observed dataset.

- Lin and Cunningham III (1995) developed a new approach to fuzzy-neural knowledge extraction, which can be used to check the accuracy of complex models. They defined a parameter called the **Performance Index (PI)**. They concluded that the lower the PI, the better the model. The PI is defined as followed:

$$PI = \frac{\sqrt{\sum_{k=1}^{m}(X_i - Y_i)^2}}{\sum_{k=1}^{m}|X_i|}$$

- **Graphical residual analysis** is a technique which allows a modeller to evaluate at first glance the performance of the model. It is based on the residual (difference between predicted and observed data) and is used to evaluate whether the four following assumptions are satisfied (Osborne and Waters, 2002):

    - Data from the different datasets display a **linear** relationship. There are several methods to investigate the linearity of models (Cohen and Cohen, 1983; Pedhazur, 1997). The commonly used method is the plotting of residuals as function of predicted values, called *residual plots*. The spread of residuals has to be approximately constant from left to right

of the plot (random pattern) to assume that the model is linear. In the case of non-random pattern (U-shaped or inverted U), the model is said to be non-linear.

- Data are **independent**. As for the linearity, the independence of variables is detected based on the residual plots. From the residual plots, a datasets can be judged independent (randomly distributed), positively correlated or negatively correlated.
- Data are **normally** distributed. A histogram and a point-point plot (PP plot) can be used to test if the output data from the model are normally distributed. In a histogram, the observation that the data lie on a bell curve can be sufficient to indicate a normal distribution. The PP plot is a scatter diagram which compares two datasets (predicted and observed) of the same size and on the same scale. Data are assumed to be normally distributed if the scatter points lie close to a line with slope 1. A normal probability plot, formed by plotting the percentile versus the residual, can also be used to check the normality of the model. If the plot is almost linear it can be assumed that data are normally distributed.
- Data have an **equal variance**. The residual plot is also used to check the error variance. If a residual plot shows an increasing or decreasing trend, it can be concluded that the data do not have an equal variance.

If any of the above assumptions are violated, the results of the analysis may be misleading or completely wrong. In such a case, data have to be refined or transformed to meet the assumptions of the linear regression model. If the problem still remains unsolved, then it will have to be assumed that the model is non-linear.

2.4.7 APPLICATION OF ANNs IN GROUNDWATER STUDIES

An ANN can be seen as a universal approximator. Its ability to learn and generalise makes the ANN a powerful tool able to solve various complex problems, such as:

pattern recognition, stock forecasting, non-linear modelling, and classification of data according to type. In geohydrology, ANNs have had a significant growth since Rumelhart *et al.* (1986) developed their computational mechanism. This approach is now used in all branches of engineering and the sciences.

Many water-related problems need to be solved by prediction and estimation. Most hydrogeological processes show high fluctuation, both spatially and temporally. They are often non-linear physical processes. Often there is large uncertainty in the parameters affecting the processes (McCuen, 1997).

Geohydrologists have to provide answers to complex problems related to water management. To provide answers to these problems, ANNs offer the possibility of finding relationships between the inputs and outputs of processes even if these processes are not well understood. The applicability of ANNs in geohydrology is extensive. These networks can identify the relation between noisy data and help to generate simple rules (Sarkar, 2012).

ANNs can be applied to mimic temporally and spatially distributed human influences, such as water extraction patterns, on a regional scale with high predictive accuracy for complex groundwater system, as shown by Feng *et al.* (2008). Sensitivity studies done with ANNs are an effective and efficient tool which can help decision-makers to understand the impact of human activity on the aquifer.

Using ANNs, Joorabchi *et al.* (2009) found that tide variation is the main parameter impacting the water table in coastal anisotropic aquifers. Abrahart and See (2007) concluded that these networks can be used to produce understandable non-linear transformations in the study of aquifers.

The power of ANNs to model complex non-linear problems is one of its strengths which can provide output datasets ready to be used in other areas of groundwater research, such as hydrochemistry (Seyam, 2010) and hydrodynamics (Aziz and Wong, 1992).

ANNs are known to be able to generate accurate predictions. The accuracy of these networks may be further improved by using them in combination with numerical models (Szidarovszky *et al.*, 2007). This hybridisation method can be used to evaluate the performance of Finite Difference-based models and ANNS, as shown by Mohanty *et al.* (2013).

ANNs are able to forecast time series (Sudheer *et al.*, 2002; Yoon *et al.*, 2007; Kumar *et al.*, 2013) and compared to the performance of a hybrid model, the results suggest that both the ANN and hybrid model can successfully be used for the prediction of the temporal behaviour of groundwater levels.

ANNs combined with numerical based-models have been used for predicting liquefaction potential in soil deposits (Farrokhzad *et al.*, 2010). This combination provides results that are more accurate.

In studies to protect coastal aquifers against seawater intrusions, ANNs have been developed, optimized and then combined with numerical models to provide better predictions, even for complex pumping system (Kourakos and Mantoglou, 2009). Additional to the study of groundwater quality in coastal areas, Yoon *et al.* (2011) developed two hydrogeological models based on Support Vector Machines (another form of machine learning) and ANNs to forecast the short-term fluctuations of the groundwater table of a coastal aquifer in Korea. It was observed that the Support Vector Machines gave more accurate results for long prediction times than ANNs. Seawater intrusion can increase the salinity of islands. It was observed by Banerjee *et al.* (2011) that when the pumping rate increases, the salinity of the aquifer also increases. Thus, they used both ANNs and SUTRA (Saturated-Unsaturated Transport; an FEM code) to predict the minimum acceptable pumping rate which would leave the salinity below an acceptable threshold. Comparing the results founds with SUTRA and ANNs to the observations, they concluded that ANNs provided more accurate predictions even though these networks required fewer inputs than SUTRA.

Juan *et al.* (2015) used ANNs to forecast suprapermafrost groundwater levels. Since permafrost areas are typically harsh environments, data collection in these areas is demanding, with the result that only a limited number of studies have focussed on understanding the behaviour of the aquifers in such areas. Juan *et al.* (2015) stated that the groundwater hydrodynamics of permafrost areas is not controlled by Darcy flow, but by thermodynamics. The authors employed ANNs in their investigations and used temperature, rainfall data and previous suprapermafrost groundwater levels as inputs to the ANNs to predict the suprapermafrost groundwater level. They observed that the results were satisfactory when compared to the field observations, although the accuracy of the predictions decreased with increasing prediction time.

Mohanty *et al.* (2013) developed a groundwater model based on FDM, as well as ANNs, to predict the depletion of water in a region of India. After comparing the results of these studies to the field observations, they found ANNs to be more accurate for short-term predictions while FDM are more suitable for long-term predictions. They therefore recommended the combined use of these two methods to complement one another and ensure good decision-making in groundwater management.

The coupling of numerical models and ANNs have been used to evaluate the interaction between rivers and aquifers, providing rapid results. These hybrid models can easily be extended to other complex scenarios (Parkin *et al.*, 2001). Tapoglu *et al.* (2014) combined the use of ANNs and Kriging methods to predict the groundwater level changes in Bavaria (Germany). They used the hydraulic head data recorded at 64 piezometers to train 64 ANNs, one for each piezometer. At positions removed from the piezometers interpolation with Kriging was used to estimate the hydraulic heads. It was found that this approach was powerful and required few inputs, making it a useful tool for the prediction of groundwater level changes in areas with limited geological and hydrogeological data.

Hybridisation of approaches were shown in the last decade to be a more powerful technique for estimation and prediction of groundwater behaviour (Yeh, 1992; Das

and Datta, 2001). Thus, Bahrami *et al.* (2016) developed a hybrid model to predict the groundwater inflow during the advance of an open pit during mining. First they developed an ANN to perform the predictions. Since the performance of ANNs depends on the architecture of the network and a proper selection of weights for the connections between neurons, the authors used the Genetics Algorithm (GA) and Simulated Annealing (SA) to determine initial weights so as to obtain more accurate solutions. Thus, they developed a hybrid model based on ANN-GA and ANN-SA to predict the groundwater inflow during the pit advance. The comparison between the measured groundwater inflows and the predicted inflows gave better results for hybrid models than when using a simple ANN.

Ardejani *et al.* (2013) used ANNs to predict the water table rebound in an excavation were the water table was below the floor of the pit. The authors stated that the methods commonly used to predict groundwater rebound require a lot of inputs, such as hydraulic conductivities, transmissivities, initial hydraulic heads, rainfall data and specific storages. Accurate information on these parameters is often difficult to obtain. Furthermore, since the system is nonlinearly dependent on these parameters, inaccuracies in the parameter estimates could lead to large errors in the predicted responses. To avoid such errors, the authors used ANNs to predict the behaviour of the groundwater level during rebound in the open pit mine. The predicted hydraulic heads were compared to the observed field data, and a correlation coefficient (R value) of 0.986 was obtained, showing good agreement between the observed and predicted water levels.

However, if the available input data are sparse, it is important to use alternative methods, which start by using real or synthetic observations where the number of inputs can be reduced. Using this approach, Mohammadi (2008) employed synthetic observations generated from a groundwater model based on the finite difference method to implement an ANN model. The objective of his study was to investigate the applicability of ANNs in groundwater level simulation without any well boundary conditions and with limited data. In this research, different ANNs were used to predict the groundwater elevation. Although a few networks gave poor results, the

majority of the ANNs predicted the groundwater elevations with a high degree of accuracy. It was therefore concluded that ANNs can be effectively used for groundwater modelling.

2.5 DEWATERING STRATEGIES AT MINES

Modelling has been used for many years to simulate groundwater behaviour during pit dewatering operations. Open pit mine operations often extend below the groundwater table. This becomes a serious challenge and can have negative impacts on safety, operations and benefits. It is preferable, and at times mandatory, to perform mining in dry conditions by applying pit dewatering strategies at the mine. This usually requires a geohydrological assessment of the mine site.

Individual mines often use a combination of dewatering methods, depending on the specific geohydrology and the experience of the geohydrologist. Based on the geology and the type of mine, different dewatering strategies may be applied, as described below:

2.5.1 GROUTING

Grouting is one of several methods of ground treatment for excluding water in mining operations. The advantage of this method is the permanence of the ground treatment, which may enhance dewatering and increase stability. Although ground freezing may also be used for water exclusion during mining, this method is only temporary in nature (Kipko *et al.*, 1993; Heinz, 1997; Nel, 1997).

Grouting of water-bearing strata is a highly efficient water exclusion method in underground mines and many practical applications indicate that a significant reduction of flow through the grouted strata is achievable. With the introduction of ultrafine and chemical grouts even low permeable strata can be efficiently grouted. The disadvantage of grouting is the relatively high cost over large areas and therefore, grouting is typically used in the sealing of smaller areas such as faults or fracture systems (Straskraba and Effner, 1998).

Note that in mining and tunnelling infrastructures, the application of cement-based grouts is more common than other types of grout (Daw and Pollard, 2006).

2.5.2 STORM WATER CONTROL

In open pits, storm water can be defined as water coming from precipitation events such as rainfall, snow or ice melts. The water can infiltrate into the soil, evaporate, or flow overland in the form of runoff. The goal of storm water control is to prevent water from entering the open pits at the mine, and to minimise contact of the water with materials or products which could lead to the pollution of the aquifer.

2.5.3 WELLPOINTS AND BOREHOLES

Wellpoints and boreholes accomplish pit dewatering through pumping from the surrounding aquifers. Pumping creates a cone of depression in the aquifer by reducing the water level elevation or hydraulic head around the borehole. For improved dewatering, more than one pumping borehole may be used to enhance the reduction in the hydraulic head through interference between the cones of depression. Boreholes may be located next to each other to cause an overlap in the cones of depression for more effective reduction of the water table. Using several pumping boreholes in conjunction often improves the dewatering of large areas.

In the same way, wellpoints may be used to for dewatering operations in unconsolidated rocks. The casings of wellpoints typically have much smaller diameters than the casings of boreholes, and may be driven directly into the unconsolidated rocks. The effectiveness of wellpoints during dewatering is controlled by the permeability of rocks and the atmospheric pressure (Dowling *et al.*, 2013).

Due to their limited depths, wellpoints are used to dewater aquifers that occur close to the surface. For more efficient dewatering of a multi-layered aquifer, they are used in combination with deep dewatering boreholes. This process was used in South Africa to dewater some coal mines (Morton and Niekerk, 1993). Wellpoints are mostly

used to dewater aquifers during construction when foundations are cast below the water table.

Water management is one of the expensive tasks in mining operations. Good groundwater control can limit mining expenses by reducing waste stripping and improving safety. Inclined and vertical boreholes are common methods for open pit dewatering. Boreholes and wellpoints often interfere with mining operations when they are installed on the pit floor. To avoid this interference, it is important to place them outside the pits (Morton, 2009).

2.5.4 SUB-HORIZONTAL DRAINS

Sub-horizontals drains are holes of five to eight centimetres diameter, drilled in the rock near the toes of slopes. These drains are usually sub-horizontal and are used for aquifer depressurisation. They are very useful dewatering strategies, particularly if used supplementary to the main system for lowering the groundwater table (Libicki, 1985).

To decrease the build-up of pore pressure, another alternative is to blast entire benches without excavating them during the winter month. The increase in permeability acts as a drain which allows water to seep from the slope. This water has to be collected in sumps and pumped out of the pit (Brawner, 1982).

2.5.5 CUT-OFF WALLS

Cut-off walls are a useful method against groundwater inflow during mining operations. There are several types of cut-off walls. Usually, a special excavator is used to dig a ditch sealed to provide support for the walls and, in this way, to decrease the infiltration of water. The applicability of this method is limited by the operating range of the excavator (Libicki, 1993).

Another type of cut-off wall may be constructed by grouting. It consists of drilling a borehole which is sealed with a special substance under pressure based on the regional pressure conditions. This method can be applied at significant distance from

the topographic surface. However, one disadvantage of the method is the fact that the grout wall has to be changed regularly as conditions change at the mine. This is especially true for grouting over large areas (Libicki, 1993).

Cut-off walls can be used as impermeable layers to prevent inflow in overburden aquifers. If it is not extended to an impermeable layer, it can lose its efficiency by inducing damming of groundwater, which can increase the velocity through the non-sealed area (Libicki, 1993).

It is highly recommended to use cut-off walls in high permeable aquifers which are in direct contact with lakes or rivers. Another advantage of cut-off wall is that they can reduce or avoid the development of cones of depression far from the drained area and thus, keep the hydrodynamic behaviour of surrounding surface water system intact. This method is known to be expensive during construction, but may be cost-effective in the long term by reducing the costs associated with continuous dewatering of pits during mining operations (Libicki, 1993).

2.5.6 ARTIFICIAL GROUND FREEZING

Ground freezing is a technique which converts pore water into ice by continuous circulation of cryogenic fluid in small diameter pipes installed into the ground. The frozen pore water acts as a part of the soil or rock and decrease its permeability. Freeze pipes are vertically installed into the soil and they are connected in parallel arrangements. The liquid nitrogen is pumped down into the freeze pipe, thus withdrawing the heat from the rock. When the rock temperature reached zero degree Celsius, there ice is formed around the pipe in a cylindrical shape. The radius of each cylinder increases until adjacent cylinders come in contact, thereby creating a continuous wall. This method is minimally invasive and requires limited penetration of pipes into the ground, since the “ice wall” is created by the propagation of heat out of the rock (Chang and Lacy, 2008).

Ground freezing has been used with success in different applications, from industrial construction to geotechnical engineering, as well as in mine dewatering and groundwater management (Straskraba and Effner, 2012).

In the climate conditions of the Northern Hemisphere, slope freezing is commonly used to avoid seepages from the slopes.

2.5.7 PIT SUMPS

A sump is a hole dug at the bottom of the mine with the main purpose of collecting water coming from adjacent areas through channels or ditches. The water that collects in the sump is then removed through pumping. Slurry or sump pumps are used to remove water from shallow sumps. In the case of deep sumps, submersible pumps can be required (Quinion and Quinion, 1987).

If the sump is dug in unconsolidated rock, the sides of the slopes have to be flattened to increase its stability. It is important to evaluate the stability of the surrounding foundation before pumping to avoid any settlement or erosion which could lead to high instability of existing structures (Quinion and Quinion, 1987).

CHAPTER 3: NUMERICAL MODELLING OF AQUIFER RESPONSE TO PIT DEWATERING

3.1 INTRODUCTION

Synthetic data have long been employed in geohydrology for model development and testing. The objective of this chapter is to generate a synthetic dataset of geohydrological responses during dewatering operations at a fictional open pit mine. The synthetic dataset is generated by using a numerical model. In the model, different pumping scenarios are considered. The model uses nine observation points (piezometers) and three, six, nine and 12 pumping wells in the four different pumping scenarios. The purpose of the pumping wells is to dewater the open pit under different pumping conditions. The response of the aquifer to these different pumping scenarios is examined. The datasets of hydraulic heads versus time thus generated allows for very different hydraulic head responses against which the performance of the ANNs in predicting the hydraulic heads under different pumping conditions can be tested (Chapter 4).

3.2 MODEL DESCRIPTION

Aquifers are complex and not often directly visible. For better understanding these aquifers for modelling purposes, they have to be represented by simplified versions in the form of conceptual models (refer to Section 2.3.1). The conceptual model may influence the choice of numerical method used for simulating the behaviour of the aquifers. For example, a conceptual model with complex aquifer boundaries may have to be modelled using FEM instead of FDM, since the rectangular cells used in FDM do not allow for adequate refinement of the modelling grid.

If the conceptual model give an accurate representation of the real aquifer, the numerical model will also be more accurate (Anderson and Woessner, 1992).

The conceptual model of the current investigation includes information on the pit geometry, geomorphology, rainfall, surface water bodies, and aquifer units as derived from the geological layers.

3.2.1 GEOMETRY OF THE MODELLED OPEN PIT MINE

For the purposes of the current study, a model of a fictional open pit mine is developed. The fictional open pit mine is treated as a real mine and a degree of complexity in the geology, topography and boundary conditions is allowed so as to create a dataset of modelled hydraulic heads under conditions similar to those experienced at real-world open pit mines. This complexity allows for non-linear behaviour in the system, as would be expected at a real mine.

The open pit mine is assumed to be excavated in a sedimentary deposit with the top and bottom elevations at 1 250 mamsl and 1 166 mamsl, respectively. The plan view of the pit can be compared to a smooth closed curve, which is symmetric about its centre with the transverse, and conjugate diameters of 880 m and 370 m, respectively (refer to Figure 3.1).

The mine is exclusively excavated in the first geological layer (dolomite), which is 160 m thick. The pit is assumed to be excavated in an unconfined aquifer, since it is assumed that water in the voids and fractures of the dolomite is in contact with the atmosphere and is therefore under atmospheric pressure.

The vertical distance between the highest point on the perimeter of the pit and the pit floor is 84 m. The pit has nine benches with an average bench height of 9.3 m (see Figure 3.2).

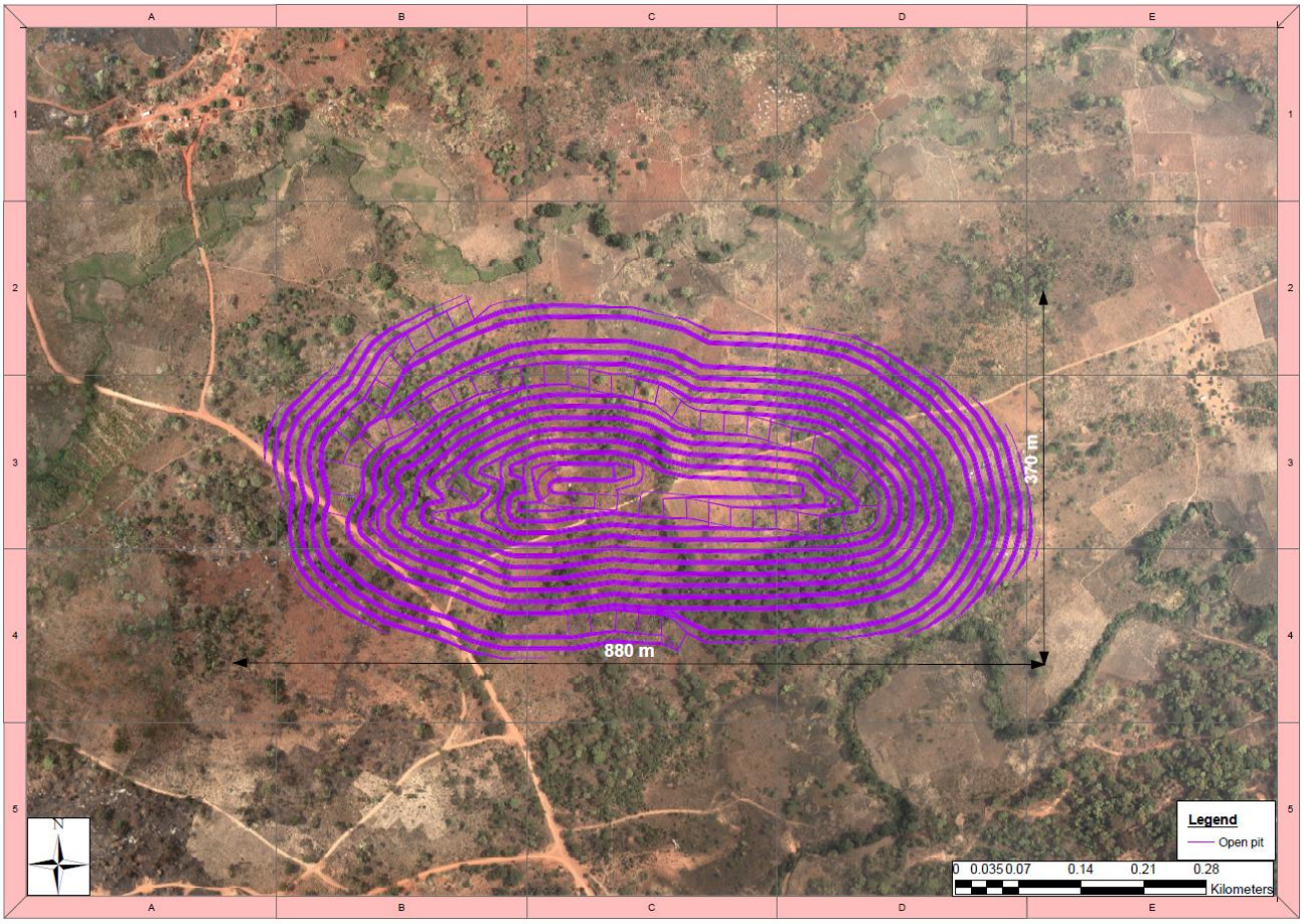

Figure 3.1: Plan view of the open pit of the model

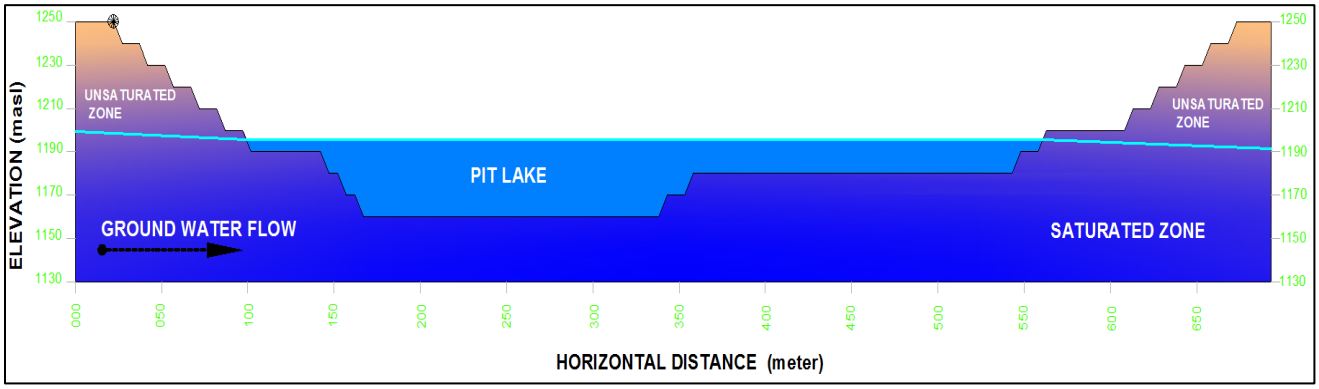

Figure 3.2: Cross-section through the open pit of the model

3.2.2 TOPOGRAPHY AND HYDROGRAPHY OF THE MODELLED AREA

The general topography of the region is gentle. The pre-mining topography shown in Figure 3.3 is an existing topography of a tropical area in the Democratic Republic of Congo (DRC). This particular area was chosen because of the variation in the surface topography (higher elevations in the south–western parts and lower elevations in the north-eastern parts). Since groundwater elevations generally emulate the surface topography, topographic gradients are often also associated with hydraulic gradients and thus with groundwater movement (Haitjema and Mitchell-Bruker, 2005). In this research, it is therefore assumed that the groundwater flows in the direction of the topographic gradient.

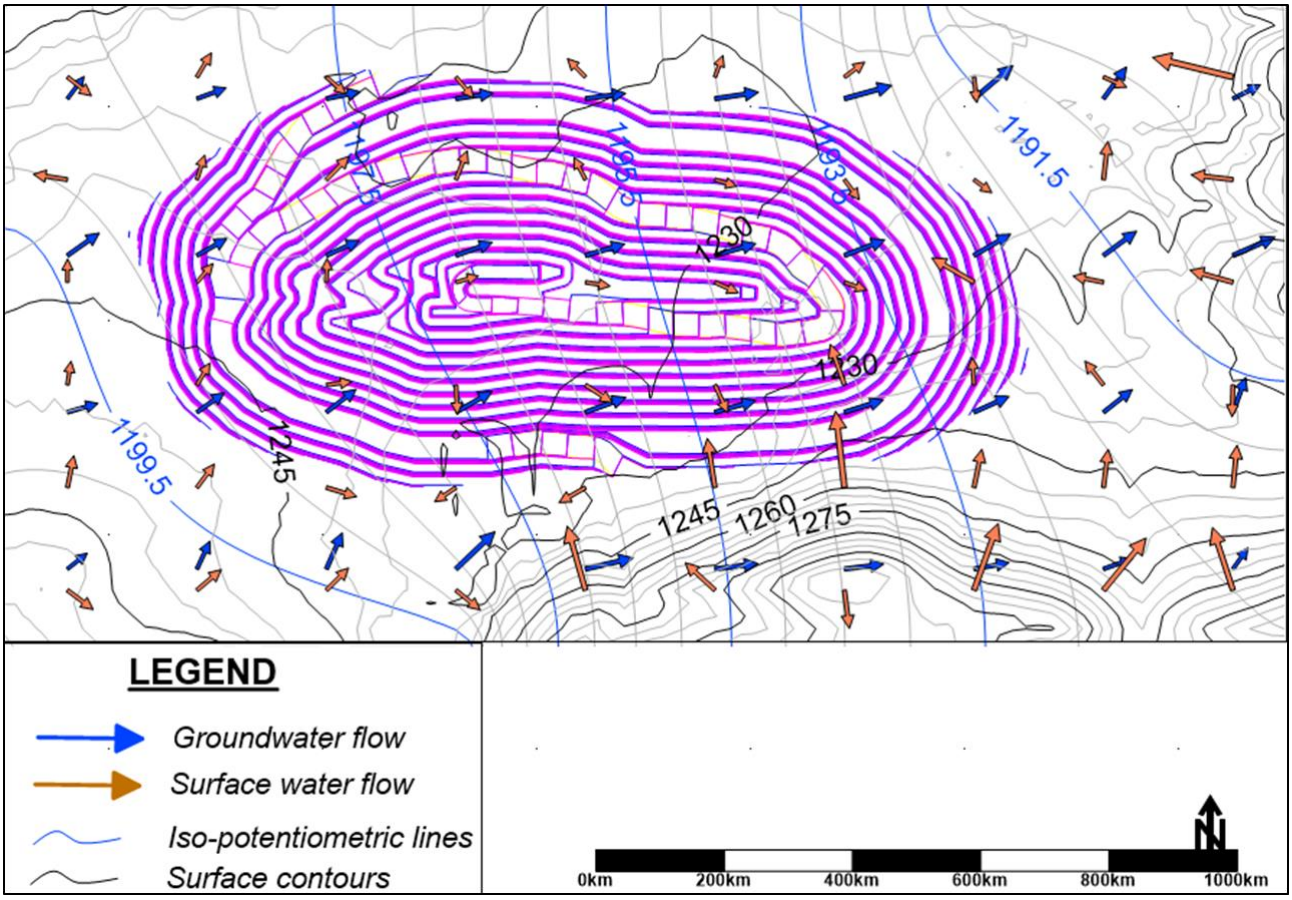

Figure 3.3: Pre-mining topography of the model

The open pit is located on the watershed between two catchments as shown in Figure 3.4. Each catchment drained by a river flowing from south-west to north-east. These two rivers are simulated as constrained head boundaries. The constrained heads were assigned values that ensure a gradient in the direction of the river flow (down-gradient, according to the ground topography). It was further assumed that the water from the river infiltrates the aquifer at a constant rate of 30 m^3/h. This latter infiltration rate was chosen because it was observed by Norris (1983) in the Scioto River in south-central Ohio (from 0.06 to 0.19 million gallons per day for one acre) and also in the Dipeta River in the Democratic Republic of Congo (30 m^3/h for a river with a length of 1.3 km and a width of 3 m).

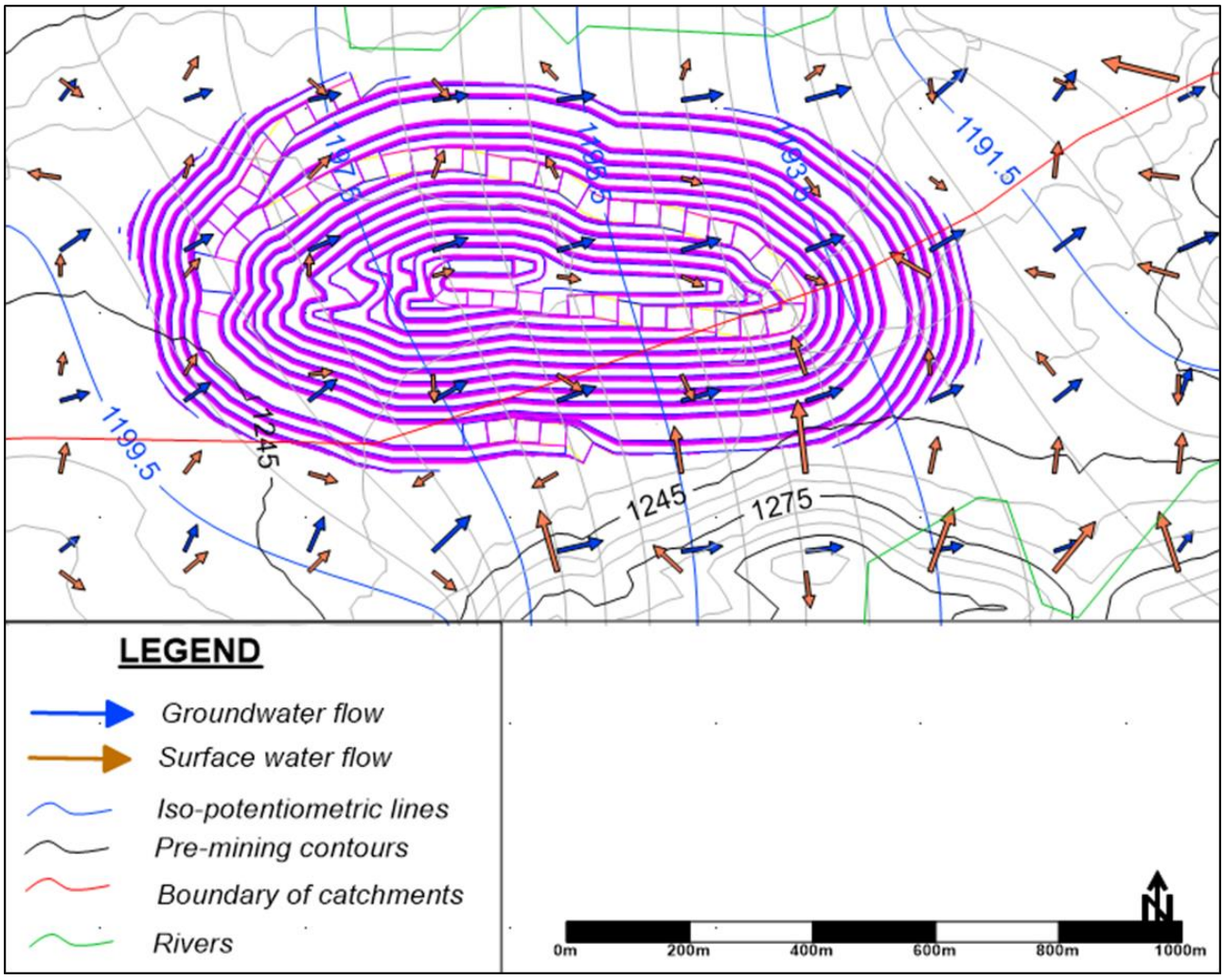

Figure 3.4: Catchments and rivers of the model

Based on the topography of the model, some of the surface runoff drains directly into the open pit. Such runoff water could pose problems to the management of surface water at real mines. However, in this research, surface runoff water entering the pit will not be considered in the synthetic model, since the aim is to model pit dewatering by using abstraction wells.

3.2.3 GEOMETRY OF THE GROUNDWATER MODEL

The model domain is 1 126 m long, 574 m wide and 240 m high. As shown in Figure 3.5, the geology of the region is assumed to be sub-horizontal, consisting of only two layers, namely: a dolomite layer (160 m thick), overlying a shale layer (80 m thick). No prominent tectonic features, such as faults, occur within the model domain. The open pit mine is excavated exclusively in the dolomite layer to depth of 84 m.

3.2.4 HYDRAULIC PARAMETERS

In Figure 3.5, the spatial distribution of the hydraulic parameters is shown. It is seen that these parameters are directly related to the geological units, and that these parameters do not vary within the geological units. As indicated in Table 3-1, the hydraulic conductivity is the only hydraulic parameter that differs for the two layers in the model. It is also seen that that the vertical hydraulic conductivities (K_{ZZ}) of the layers are significantly smaller than the horizontal hydraulic conductivities (K_{XX} and K_{YY}). These hydraulic conductivity values are based on the work of Morris and Johnson (1967) who conducted studies on the hydraulic parameters of several rock types. The specific storages, and the specific yields of the two layers are taken as the default values for dolomites and shales, as defined in the software.

Table 3-1: Hydraulic parameters of the synthetic model

Lithology	K_{XX} (m/s)	K_{YY} (m/s)	K_{ZZ} (m/s)	Specific yield	Specific storage	Thickness (m)
Dolomite	10^{-7}	10^{-7}	5.10^{-8}	0.2	10^{-4}	160
Shale	10^{-12}	10^{-12}	10^{-13}	0.2	10^{-4}	80

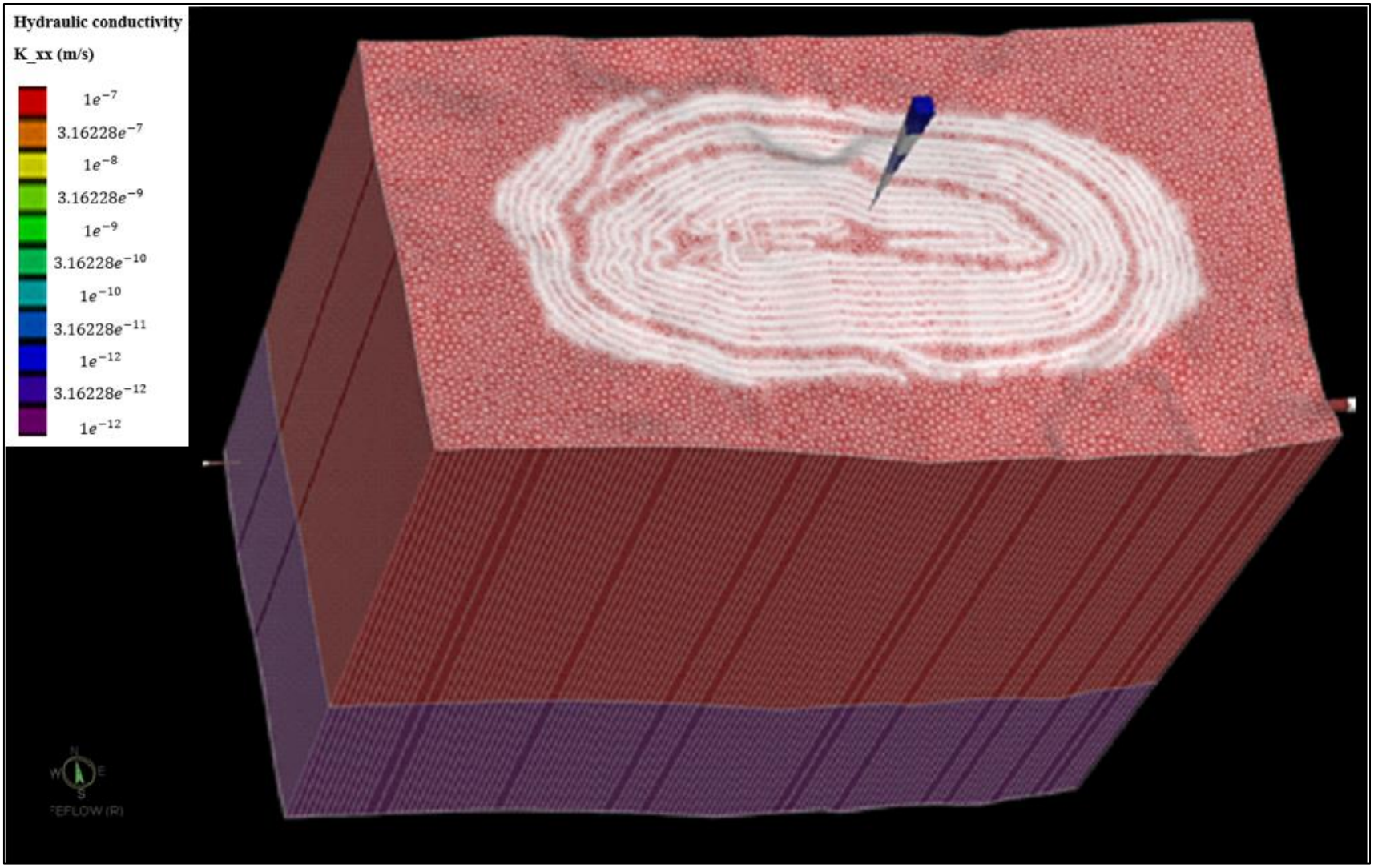

Figure 3.5: The synthetic model setup with hydraulic conductivity distribution

3.2.5 RECHARGE

The main recharge of the aquifer is through rainfall. The mean annual rainfall (MAR) in the modelled area is assumed to be 1 200 mm, corresponding to the rainfall figures in a tropical climate. A large percentage of the rainfall flows to rivers as runoff. In Feflow, rainfall is modelled as aerial groundwater recharge by using sink/source formulations. Recharge values for carbonate rocks such as limestone and dolomite range from 3 to 10% (MWR, 2009). This boundary condition was applied to the top of the first geological layer of the numerical model. Recharge calculation is then performed automatically according to the hydrogeological parameters (permeability, storativity, etc.) of the layers in the model.

3.2.6 DEWATERING AND OBSERVATION WELLS

While performing the dewatering simulations, the behaviour of the aquifer will be observed at nine observation points (OBS_1 to OBS_9) spatially distributed as shown in Figure 3.7. Observation point OBS_9 is used to evaluate the water elevation according the bottom of the pit because it is located right in the middle of the pit. Four dewatering scenarios will be run with three, six, nine and twelve dewatering wells. The dewatering wells are numbered BH_1 to BH_12.

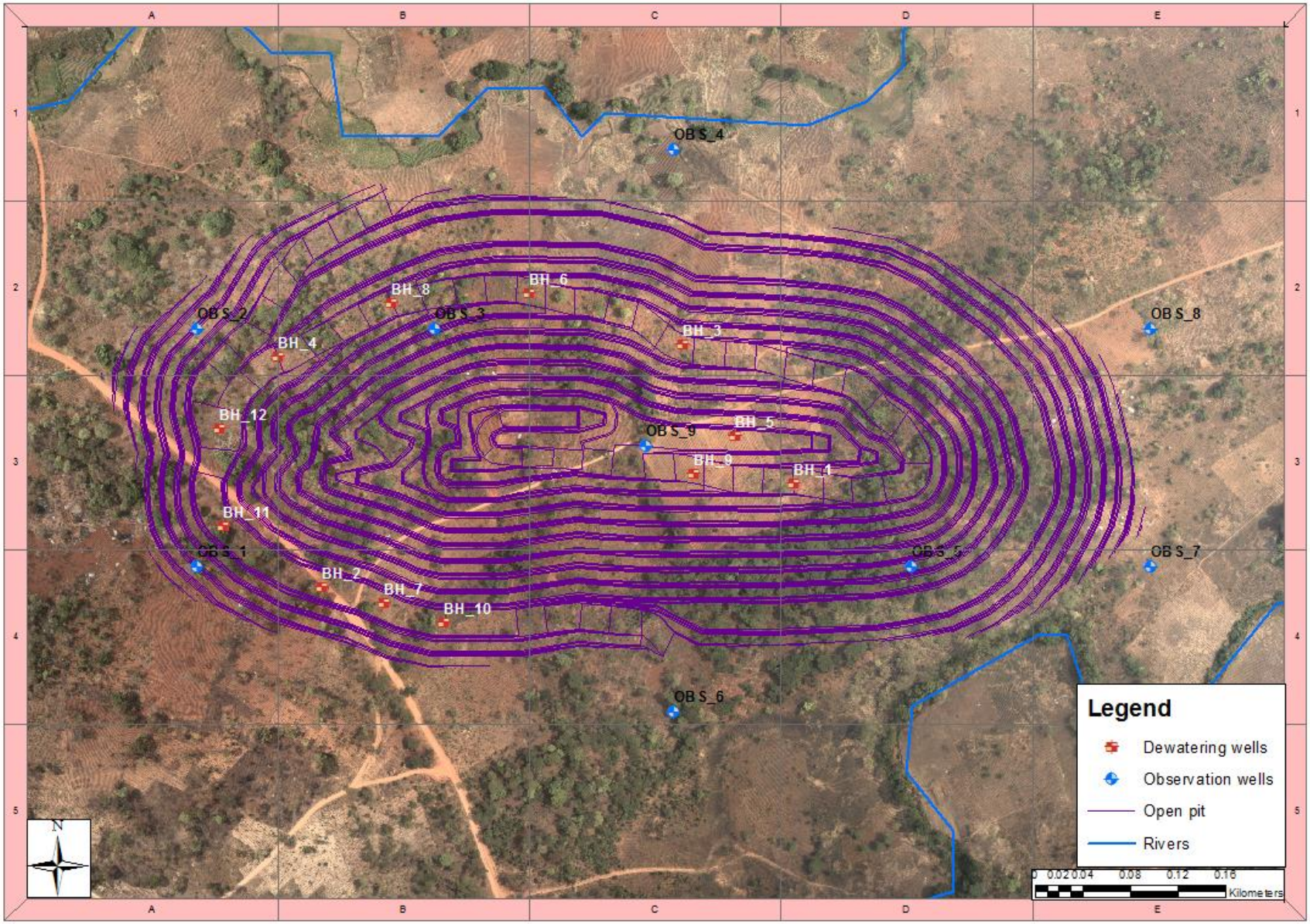

Figure 3.6: Spatial distribution of observation points and dewatering well

3.2.7 BOUNDARY CONDITIONS

The base of the model (the bottom of the shale layer) is assumed to be impermeable. The numerical model used in this study incorporates the following boundary conditions:

- Recharge (3 to 10% of the MAR) is represented by areal fluxes applied at the top slice of the synthetic model (the top of the dolomite layer);
- The well boundary conditions applied to the dewatering wells describes the impact of water abstraction at a single node in m^3/d;
- The model assumes that the rivers and groundwater are in dynamic connection. Hydraulic head boundary condition with flow-rate constraints were used for definition of rivers.
- Constant head boundary conditions are assigned to the boundaries of the model domain. These constant heads were determined by considering the surface topography at the boundaries.

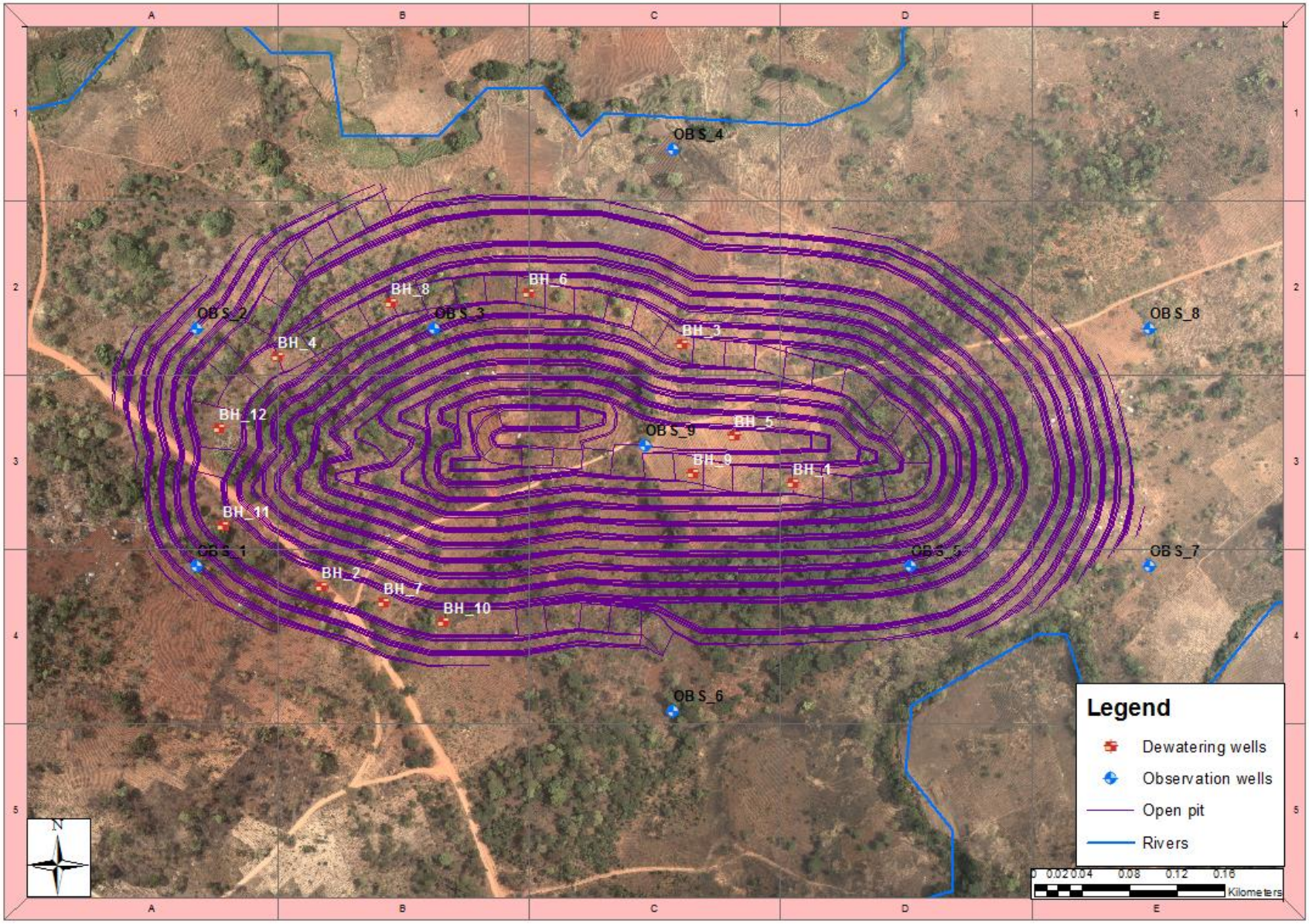

Figure 3.7: Spatial distribution of observation points and dewatering well

3.3 MODEL DEVELOPMENT

3.3.1 MODEL PACKAGE

The finite element software Feflow® v6.2 from DHI-WASY was used to simulate the behaviour of groundwater. Feflow is a three dimensional finite element package able to simulate unsaturated and saturated flow. It also has a mesh generation method which allows for flexible and quick editing of the model. This code allows rapid execution, development and analysis of the model (Diersch, 2004).

The capabilities of Feflow to interact with ArcGIS (ESRI) and spreadsheets is one of the important features of this software. Its flexibility is the reasons why it is one of the modelling packages preferred by scientists (Knapton, 2009).

3.3.2 SPATIAL DISCRETIZATION

The discretization of the model is done with the Feflow® package. Meshes are generated by applying the automatic triangle algorithm (Shewchuk, 2002). This algorithm is very versatile and extremely fast, and can deal with complex geometrical setups of polygons, lines, and points.

The mesh of the current model has 169 386 elements with 84 873 nodes. The regional mesh was refined in the synthetic model using the Mesh Geometry Editor. The resulting mesh used in the modelling is presented in Figure 3.8.

3.3.3 MODEL SETTINGS

The synthetic model assumed saturated and unconfined conditions, and also assumed only groundwater flow (not mass transport). The total duration of the modelling was for a period of 5 months.

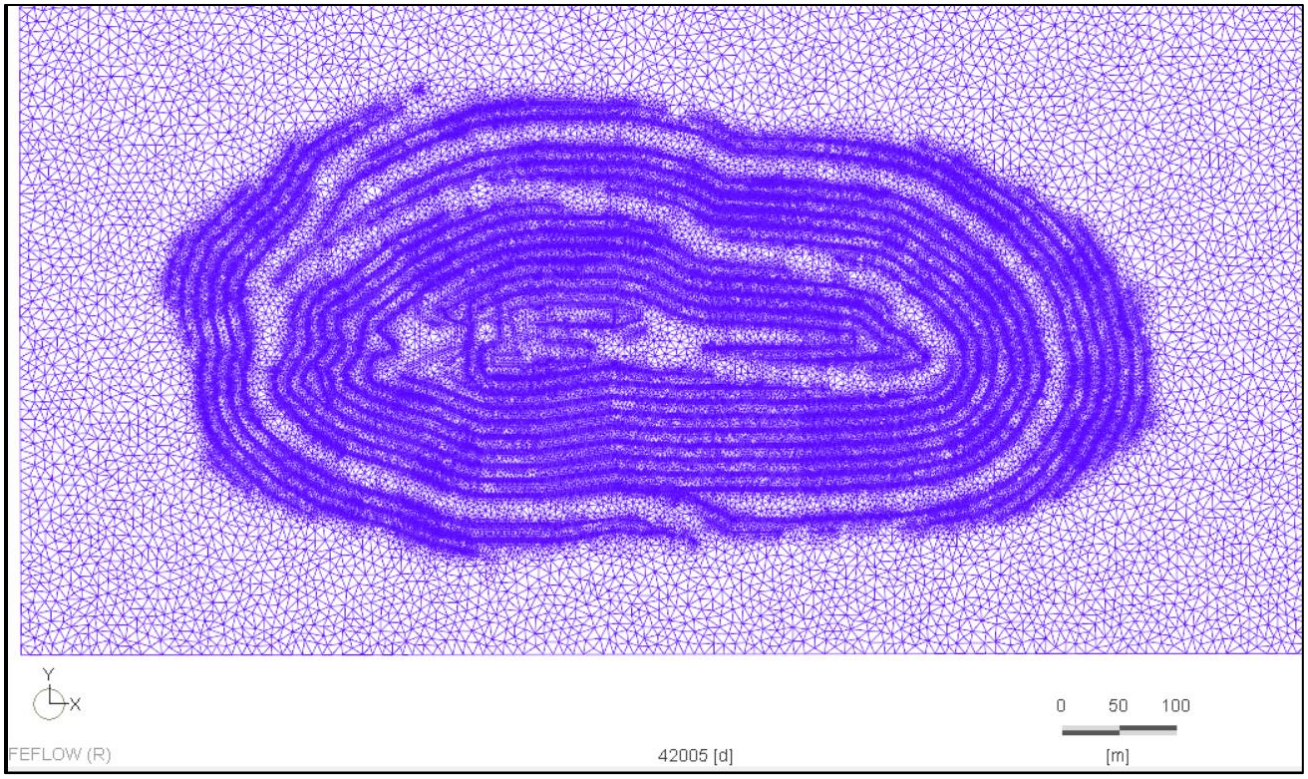

Figure 3.8: Finite element mesh used in the synthetic model

3.3.4 DEWATERING STRATEGY AND MODEL RESULTS

3.3.4.1 PRE-MINING GROUNDWATER LEVELS

The natural pre-mining hydraulic gradient in the vicinity of the pit is shown in Figure 3.9. It can be seen that under natural conditions, the groundwater generally flows from south-west to north-east within the model domain.

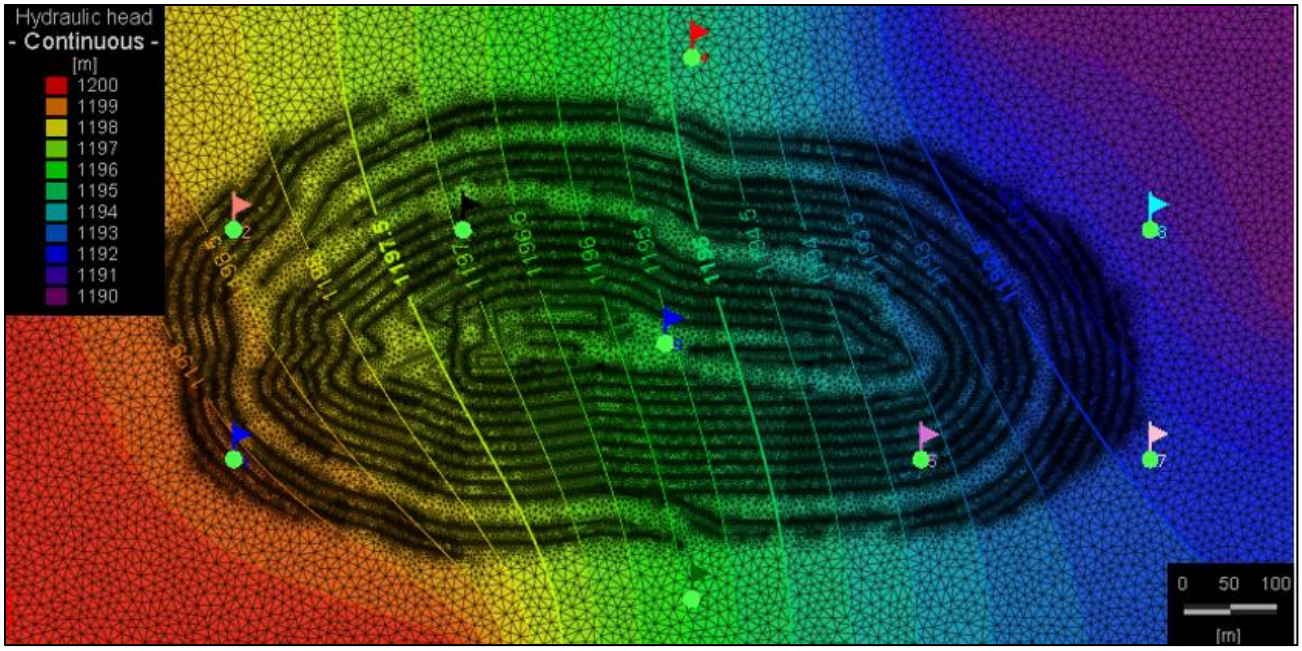

Figure 3.9: Pre-mining hydraulic heads within the model domain

3.3.4.2 STATIC GROUNDWATER LEVELS AFTER MINING

After excavating the pit, and allowing equilibrium (static) conditions to be reached, the bottom level of the mine is located at an elevation of 1 166 mamsl, while the highest hydraulic head within the model domain is at 1 200 mamsl.

Figure 3.10 shows the water elevations in all the observation wells under static (no groundwater abstraction) conditions. As expected, all the wells display constant heads (horizontal lines), because, under static conditions, the water table is not impacted by dewatering. The difference between the highest (OBS_1) and lowest (OBS_8) hydraulic heads at the observation wells is 8 m within the boundary of the model, as shown in Figure 3.10.

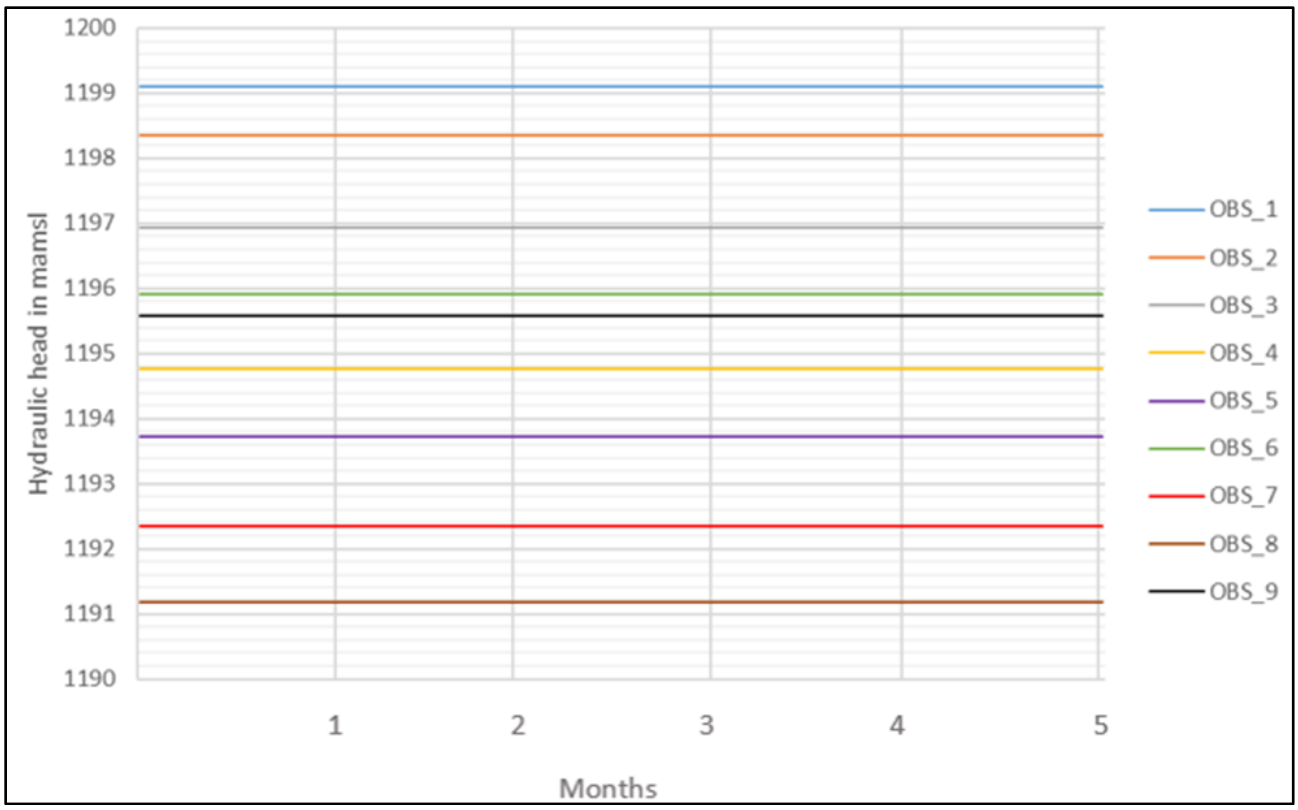

Figure 3.10: Modelled hydraulic heads of the observation wells when no abstraction takes place

Under conditions of no abstraction, a pit lake occurs with a water elevation of 1 195.58 mamsl (a depth of approximately 30 m as measured from the bottom of the pit), as shown in Figure 3.11.

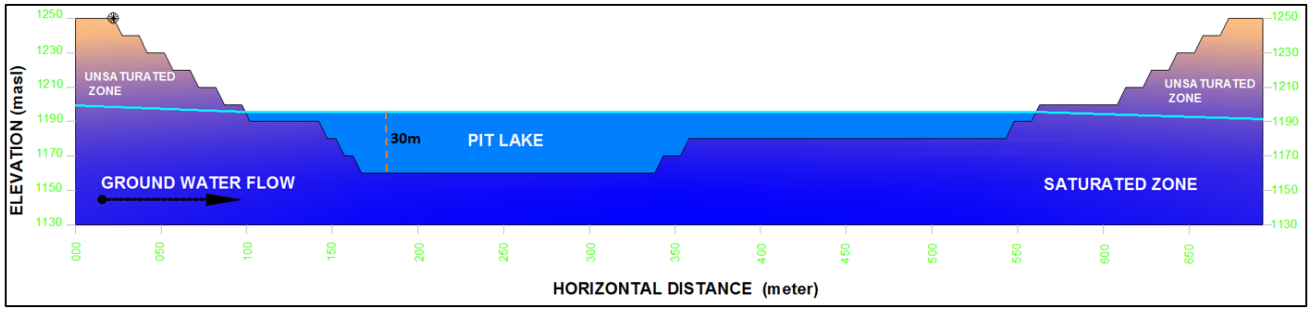

Figure 3.11: East-west profile of the pit for the model at initial conditions.

3.3.4.3 DEWATERING USING THREE ABSTRACTION WELLS

One or more dewatering strategies described in the second chapter could be applied to lower the water level. In this research, vertical pit boreholes are used in the dewatering strategy. Each borehole pumps at a constant rate of 300 m^3/h. Four scenarios, taking into account three, six, nine and 12 dewatering wells, running for a 5-month abstraction period, were considered during the modelling of pit dewatering. These scenarios correspond to different dewatering strategies that have lesser or greater impacts on the hydraulic heads in the aquifers surrounding the mine.

To lower the water level, the first scenario consists of installing three wells (BH_1 to BH_3) along the iso-potentiometric line on the eastern ramp of the open pit in order to decrease the water inflow to the mine. After pumping commences, the water elevations at all the monitoring points decrease due to the formation of cones of depression around the abstraction wells (refer to Figure 3.12). However, from approximately two and a half months after pumping commenced all observation points indicate stable water levels, as equilibrium conditions are attained.

After simulating three dewatering wells pumping for 5 months, the water level in the pit lake decreased to an elevation of 1 191.6 mamsl, as shown by the Figure 3.13. During the initial conditions, the water level at monitoring point OBS_9 was 1 195.6 mamsl. After simulating three wells pumping for 5 months, the water level in the lake dropped by approximately 4 m. The water in the pit lake then had a depth of 26 m.

3.3.4.4 DEWATERING USING SIX ABSTRACTION WELLS

With six dewatering wells (BH_1 to BH_6) in the model pumping for 5 months, the depth of the water in the pit lake was reduced to 8.2 meters (observation point OBS_9 in the pit had a water elevation of 1173.8 mamsl). The water levels in the observation wells during the 5-month period are shown in Figure 3.14, while a cross-section through the pit showing the groundwater elevation is presented in Figure 3.15. It

can be seen that the pit is still flooded after 5 months of pumping from the six dewatering boreholes. Under these circumstances, it would therefore be difficult to re-start mining operations unless some additional dewatering wells are installed.

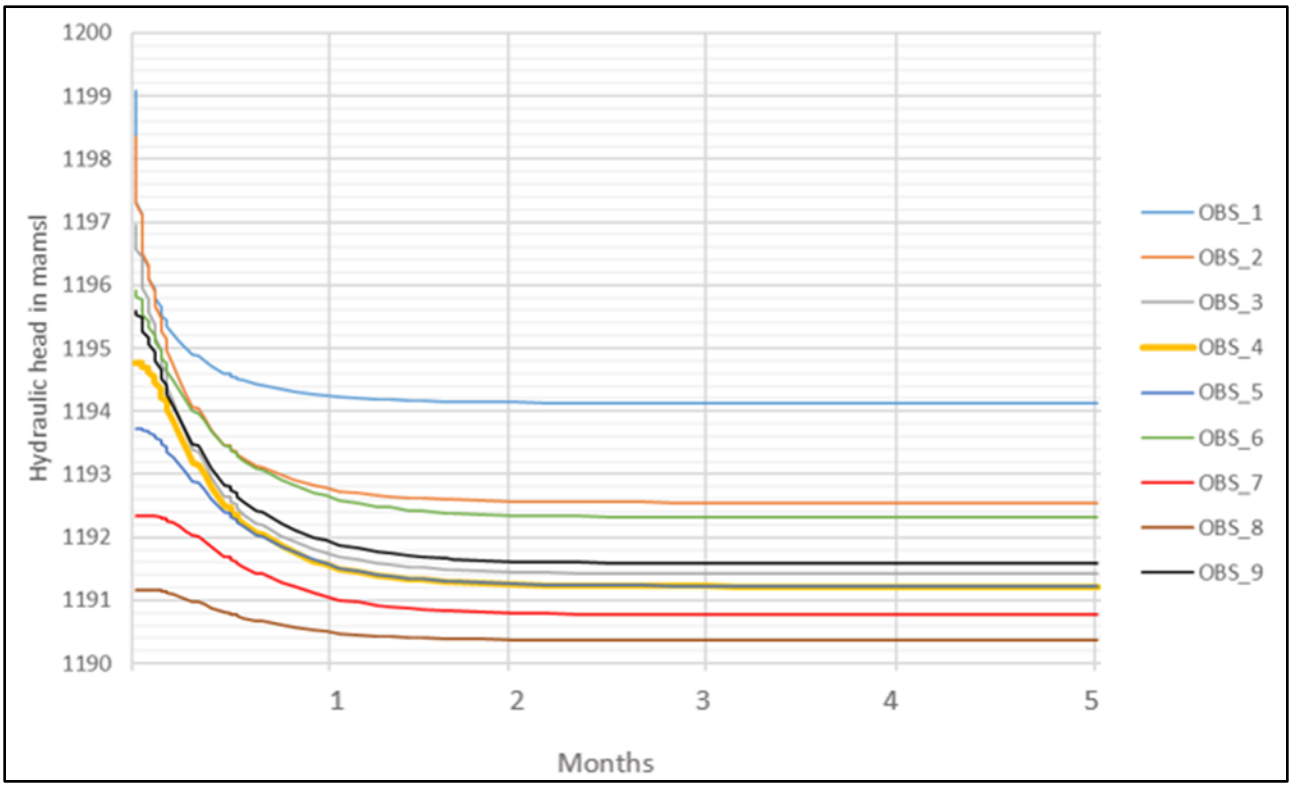

Figure 3.12: Modelled hydraulic heads of the observation wells for the model using three dewatering wells

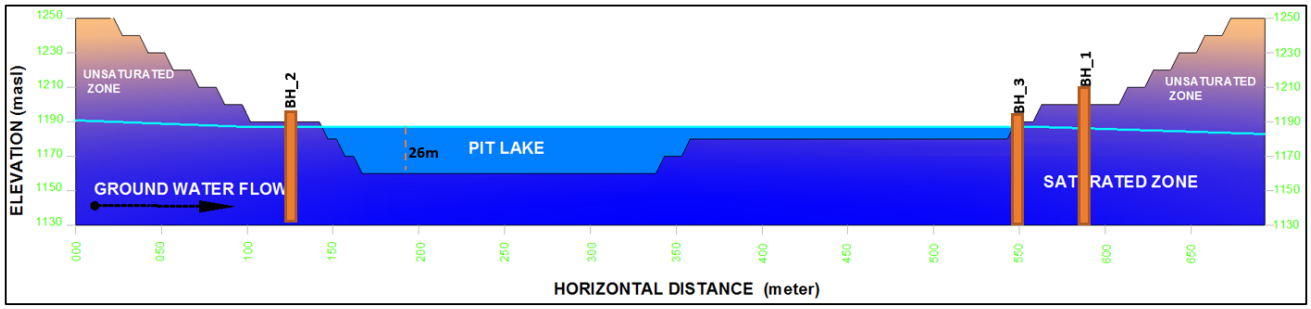

Figure 3.13: East-west profile of the pit for the model using three dewatering wells

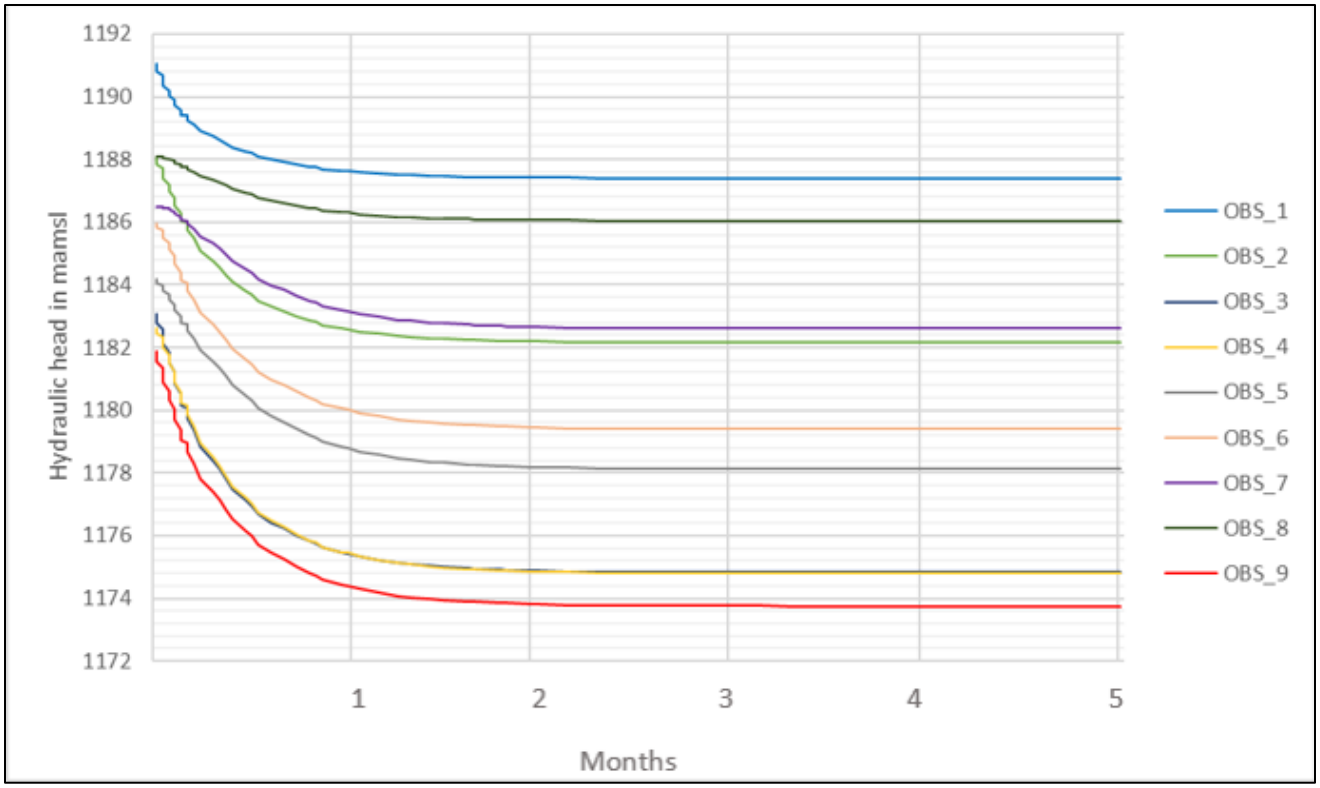

Figure 3.14: Modelled hydraulic heads of the observation wells for the model using six dewatering wells

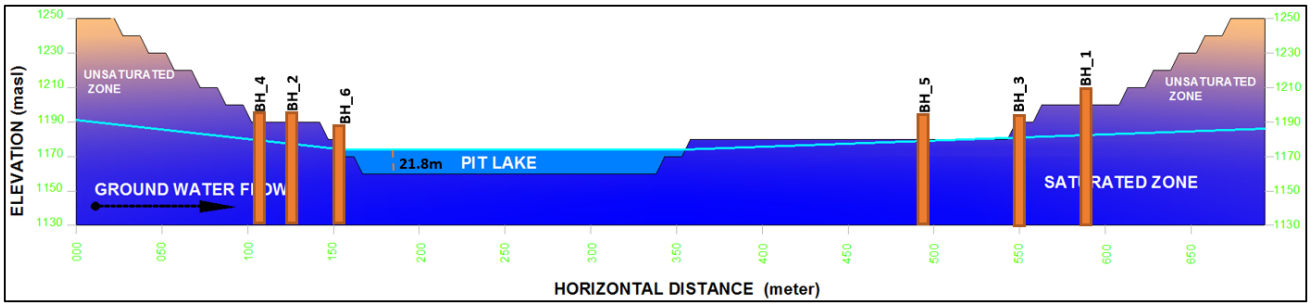

Figure 3.15: East-west profile of the pit for the model using six dewatering wells.

3.3.4.5 DEWATERING USING NINE ABSTRACTION WELLS

The third scenario takes into account nine dewatering wells (BH_1 to BH_9). Abstracting water from these wells over a 5-month period reduced the water level of the pit lake (as observed at monitoring point OBS_9) to 1166.6 mamsl. The graphs of the water levels in the observation wells (Figure 3.16) show that the impact of the dewatering for 5 months is significant, with a steep cone of depression around the

boreholes, but that the water level in the pit is not reduced enough to allow the extraction of minerals under dry conditions.

The water depth in the pit lake has now been reduced to only 1.0 meters (see Figure 3.17). Although this water level is low, it is still not possible to extract minerals without further dewatering procedures.

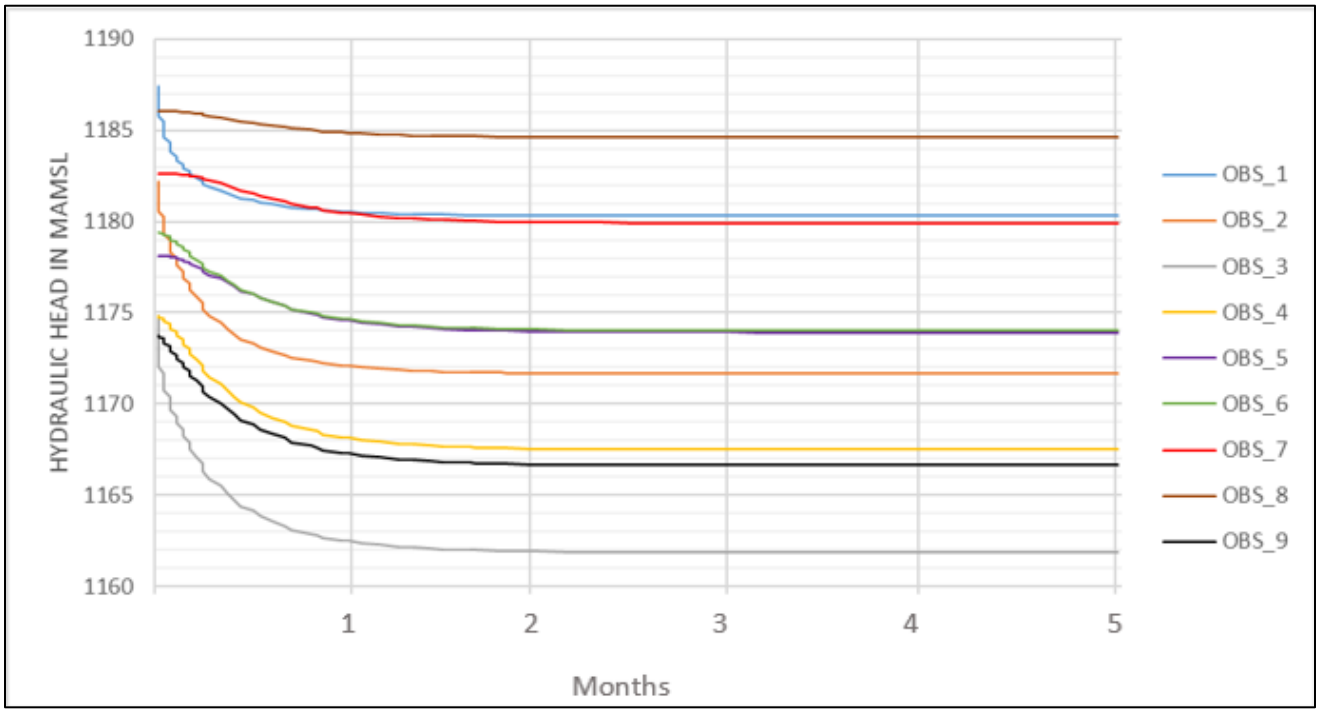

Figure 3.16: Modelled hydraulic heads of the observation wells for the model using nine dewatering wells

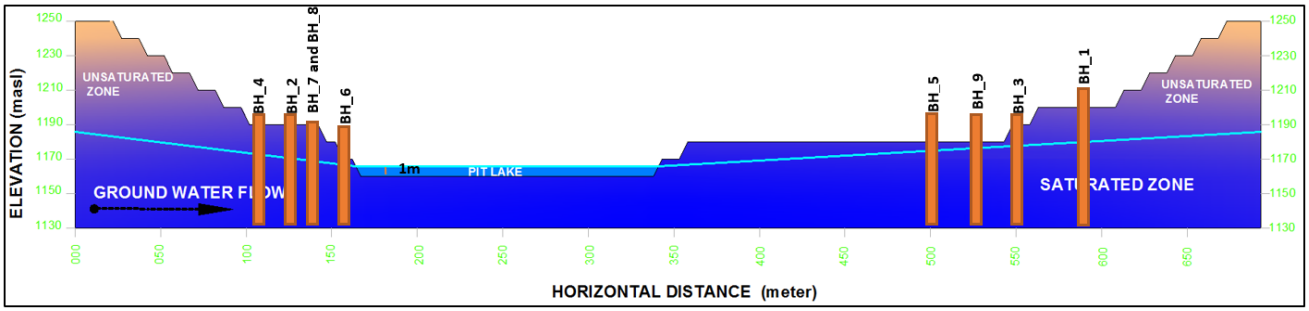

Figure 3.17: East-west profile of the pit for the model using nine dewatering wells

3.3.4.6 DEWATERING USING 12 ABSTRACTION WELLS

Since nine abstraction wells were not able to dewater the pit completely, another modelling scenario with more abstraction wells is required. This scenario takes into account 12 dewatering wells to lower the water level up to one bench lower than the bottom of the pit. After 5 months of dewatering, the water level at OBS_9 in the pit stabilises at 1151.2 mamsl (refer to Figure 3.18). This elevation is 14.8 m below the bottom elevation of the pit floor.

A cross-section through the pit after 5 months of pumping with 12 abstraction wells is shown in Figure 3.19. The groundwater level is now below the bottom of the pit and the extraction of minerals can commence.

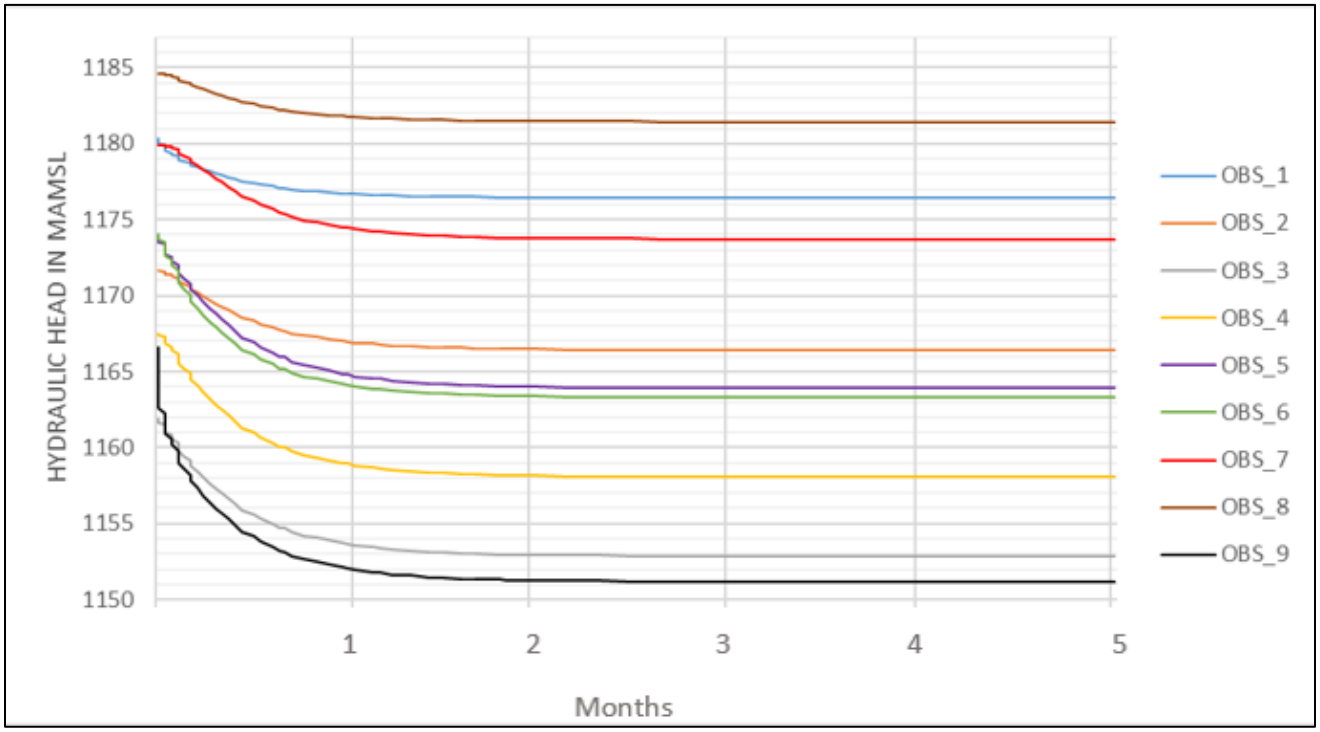

Figure 3.18: Modelled hydraulic heads of the observation wells for the model using 12 dewatering wells

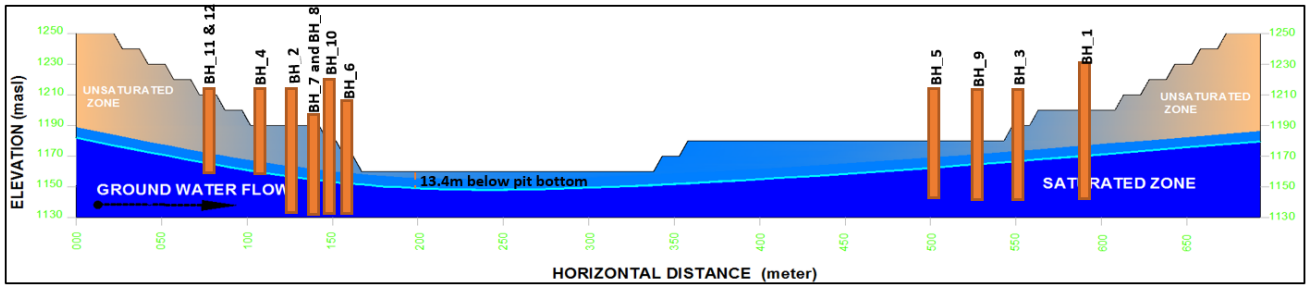

Figure 3.19: East-west profile of the pit for the model using 12 dewatering wells

3.3.4.7 DISCUSSION

In Figure 3.20, the results of the different modelling scenarios are summarised by plotting the pit water level (OBS_9) against the number of abstraction wells used in the dewatering strategy. From this figure it is clear that the different modelling scenarios had significantly different impacts on the groundwater and pit water levels. The model results also showed under which conditions complete dewatering of the pit will be attained.

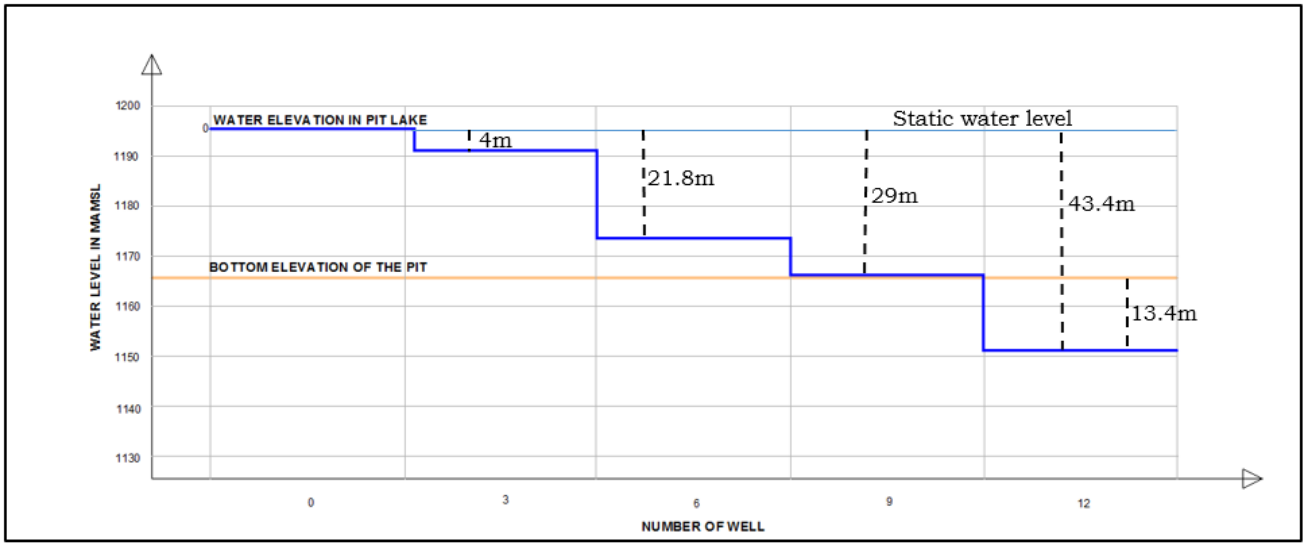

Figure 3.20: Summary of the dewatering impact relative to the bottom of the pit

The model results provide valuable datasets of hydraulics heads measured against time for the different pumping scenarios. These synthetics datasets will be used in the next chapter to train, test and validate ANNs.

CHAPTER 4: DEVELOPMENT AND EVALUATION OF ANNS FOR MINE DEWATERING PREDICTIONS

4.1 INTRODUCTION

This chapter is dedicated to the development of ANNs able to simulate the behaviour of aquifers, intersected by open pits, during pit dewatering. The ANNs will be trained using the dataset generated by the groundwater model based on FEM in Chapter 3.

As described in Section 2.4, ANNs are able to mimic the functioning of human brain to recognise patterns in data. Each neuron of the ANNs has a transfer function which determines the output for the inputs that it receives from the previous layer. Since groundwater is known to have non-linear behaviour under abstraction conditions, non-linear transfer functions are required at the neurons to relate the inputs received to the outputs generated. Thus zero-based log-sigmoid functions, hyperbolic tangent functions, log-sigmoidal functions, and bipolar sigmoidal functions will be used as transfer functions in this study to find the best ANN capable of simulating and predicting the behaviour of groundwater when impacted by dewatering wells.

4.2 METHODOLOGY

In Chapter 3, a synthetic numerical model was created to model the aquifer response at an open pit during various dewatering strategies. The calculated responses formed a dataset that can now be used to train ANNs and evaluate their performances in predicting the aquifer behaviour under different conditions. The developed ANNs will be used to reproduce the FEM datasets using various non-linear transfer functions. Of these ANNs, those yielding the smallest error will be selected for the validation of real data from open pit mining environments (Chapter 5).

4.3 IMPLEMENTATION OF THE NEURAL NETWORK MODEL

NeuroXL Predictor, an add-in to Microsoft Excel and part of NeuroSolutions software, was used to develop the ANNs. The most commonly used ANNs in the sciences are multi-layer perceptron networks (MLPs). MLPs have an input layers, one or more hidden layers and an output layer. They make use of a feed-forward architecture, and have a process where parameters (momentum, weight and number of neurons in the hidden layer) are manually adjusted until the targeted output is reached.

According to Cybenko (1989), an MLP with just one hidden layer can be used to approximate any non-linear function. The choice of the transfer function is also very important in the model construction.

The available dataset used for training and testing the ANNs has only two inputs, namely: time (date) and water levels. Seventy-five per cent of the *time-water level* data are used as inputs (time) and outputs (water level) during training. The remaining 25% is used to validate the performance of the ANNs. Based on a supervised learning process, the trial-and-error method is used by adjusting the weights, iteration numbers, learning rate momentums, transfer functions and number of neurons in the single hidden layer until the smallest error is attained.

When designing any ANN, it is important to find a transfer function which can accurately predict the system of the study. Among the transfer functions discussed in the literature review (Chapter 2), only hyperbolic tangent and sigmoidal functions are used in this thesis, because they are known to be able to make non-linear approximations, and are therefore well suited to predict the non-linear behaviour of groundwater impacted by dewatering processes (Pushpa and Manimala, 2014). Also, NeuroXL Predictor is used in this study because it has the capability to handle non-linear transfer functions.

4.4 ARCHITECTURE OF ARTIFICIAL NEURAL NETWORKS

There are several possible architectures for ANNs that are suitable for groundwater studies. The feed-forward ANNs used in this research, have a unidirectional signal

flow. After several trial-and-error adjustments of the network architectures, four ANNs, using sigmoidal and hyperbolic tangent transfer functions, were found to give acceptable results in reproducing the hydraulic heads of the synthetic observations made during the numerical modelling of mine dewatering simulation (Chapter 3). These ANNs are described in Table 4-1.

Table 4-1: The ANNs best suited for groundwater level predictions

ANNs PARAMETERS	ANN 1	ANN 2	ANN 3	ANN 4
Learning rate	0.3	0.3	0.3	0.3
Momentum rate	0.2	0.2	0.1	0.2
Initial weight	0.2	0.2	0.1	0.2
Neurons in hidden layers	6	6	15	6
Transfer function	ZBLSF	HTF	LSF	BSF

Three of the ANNs (ANNs 1, 2 and 4) have the same architecture in terms of learning rates, momentum rates, initial weights and the number of neurons in the hidden layer. The remaining model (ANN 3) has quite a different structure, as can be seen when comparing the network architectures (refer to Figure 4-1 and Figure 4-2). As mentioned above, these architectures correspond to those ANNs yielding the smallest errors after several trial-and-error adjustments. The architectures that provided the most accurate water level predictions for dewatering purposes have the following characteristics:

- ANNs 1, 2 and 4 have two inputs layers, six hidden layers and one output layer for the zero-based log-sigmoidal function (ZBLSF), bipolar sigmoidal function (BSF) and hyperbolic transfer function (HTF);
- ANN 3 has two inputs layers, 15 hidden layers and one output layer for log-sigmoid transfer function (LSF).

The minimum weights assigned in the ANNs was 0.001, and the training involved a maximum number of 20 000 complete cycles (epochs).

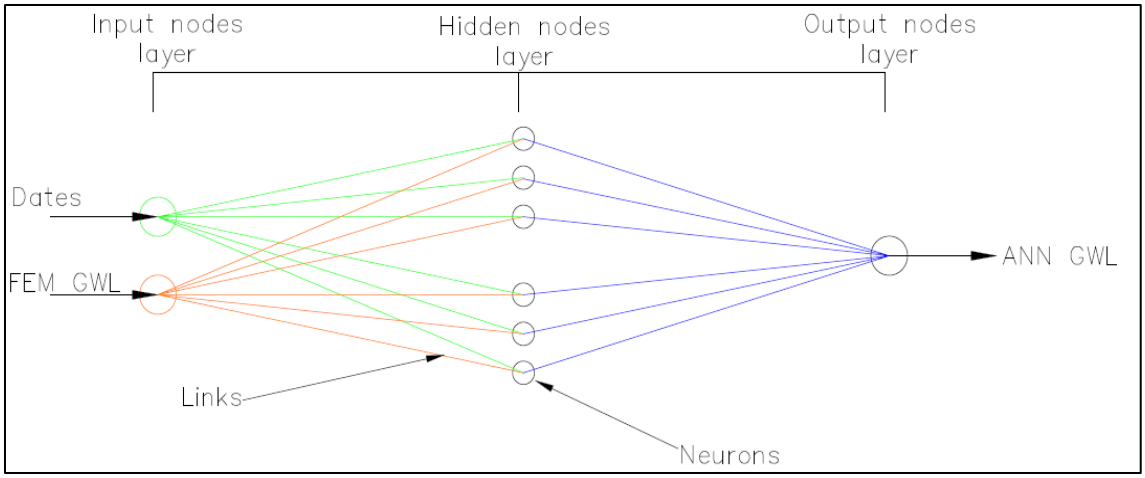

Figure 4-1: Architecture of the ANNs 1, 2 and 4, using the zero-based log sigmoid, hyperbolic tangent, and bipolar sigmoidal transfer functions

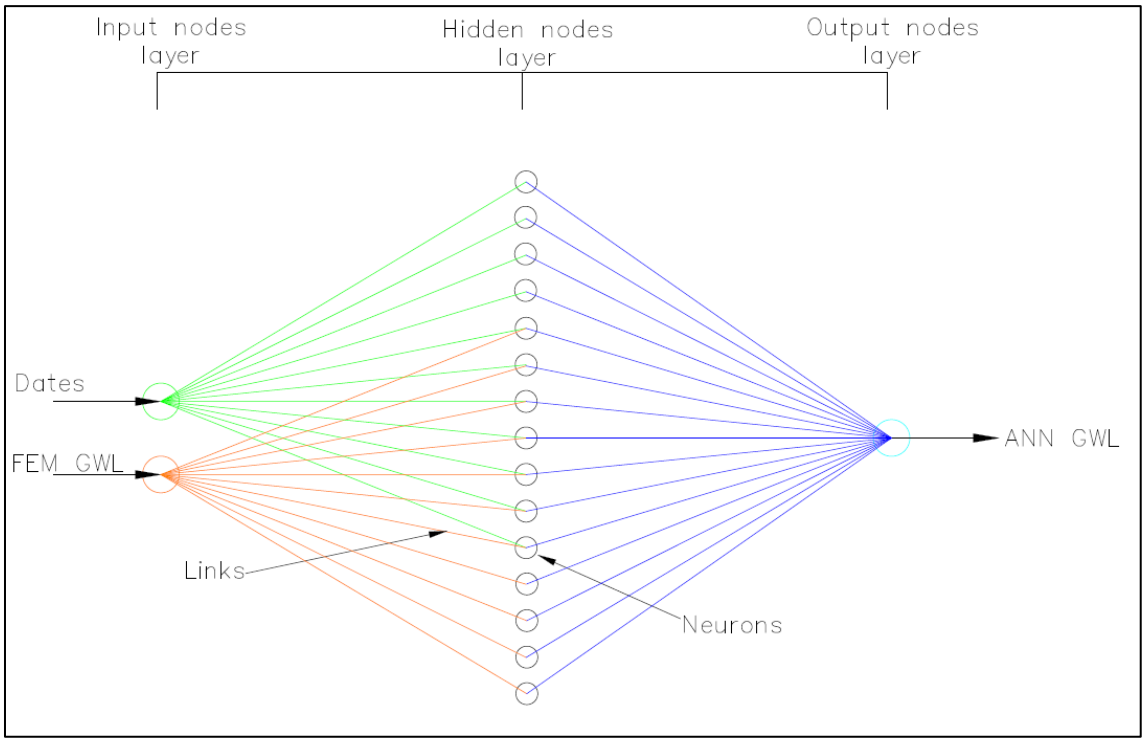

Figure 4-2: Architecture of the ANN 3, using on log-sigmoidal transfer function

4.5 EVALUATION OF THE DEVELOPED ANN

4.5.1 INTRODUCTION

In Section 4.4, ANNs were developed to predict the impacts of mine dewatering on the groundwater elevations. Different architectures were considered for the ANNs, and the abilities of the ANNs to accurately predict the groundwater levels were investigated by using synthetic datasets, generated with a numerical groundwater model (refer to Chapter 3), for training and validation. From trial-and-error adjustments to the architecture, the four architectures yielding the best results were identified. These four ANNs make use of four different transfer functions at the neurons of their hidden layers.

The aim of this section is to use the four identified ANNs, and to investigate which transfer function allows the most accurate prediction of the groundwater levels. To do this, performance analyses will be carried out by using statistical and graphical evaluation techniques. The groundwater levels predicted by the ANNs will again be compared to the groundwater levels obtained from the numerical model.

Seven statistical performance evaluation techniques will be used. These are the RMSE, NRMSE, NSE, PI, PBIAS, RSR and Pearson's *r* techniques (Anderson and Woessener, 1992). Graphical evaluation techniques that will be used to investigate the performance of the ANNs include normal plots and residual plots.

4.5.2 STATISTICAL EVALUATION

Since the finite-difference numerical model included nine observation wells, and since four abstraction scenarios (3, 6, 9 and 12 abstraction wells) were modelled, a total of 36 different datasets of modelled groundwater elevations are available against which the performance of the ANNs can be evaluated. Each dataset consists of 36 modelled values of the groundwater elevations at different times.

Since the performances of four different ANNs using four different transfer functions are to be evaluated in this section, it will not be possible to include the evaluations

for each observation well, under each abstraction scenario, for each choice of transfer function. For this reason, only a selected number of evaluations will be shown and discussed.

In Figure 4-3 to Figure 4-6, the modelled and predicted groundwater elevation at observation well OBS_9 are shown for the four dewatering strategies as examples of the responses obtained. Similar graphs for the other eight observation wells are presented in Appendix A. In these figures, the modelled (FEM) groundwater elevations, as well as the groundwater elevations predicted by four ANNs using different transfer functions, are plotted against the dates of measurement.

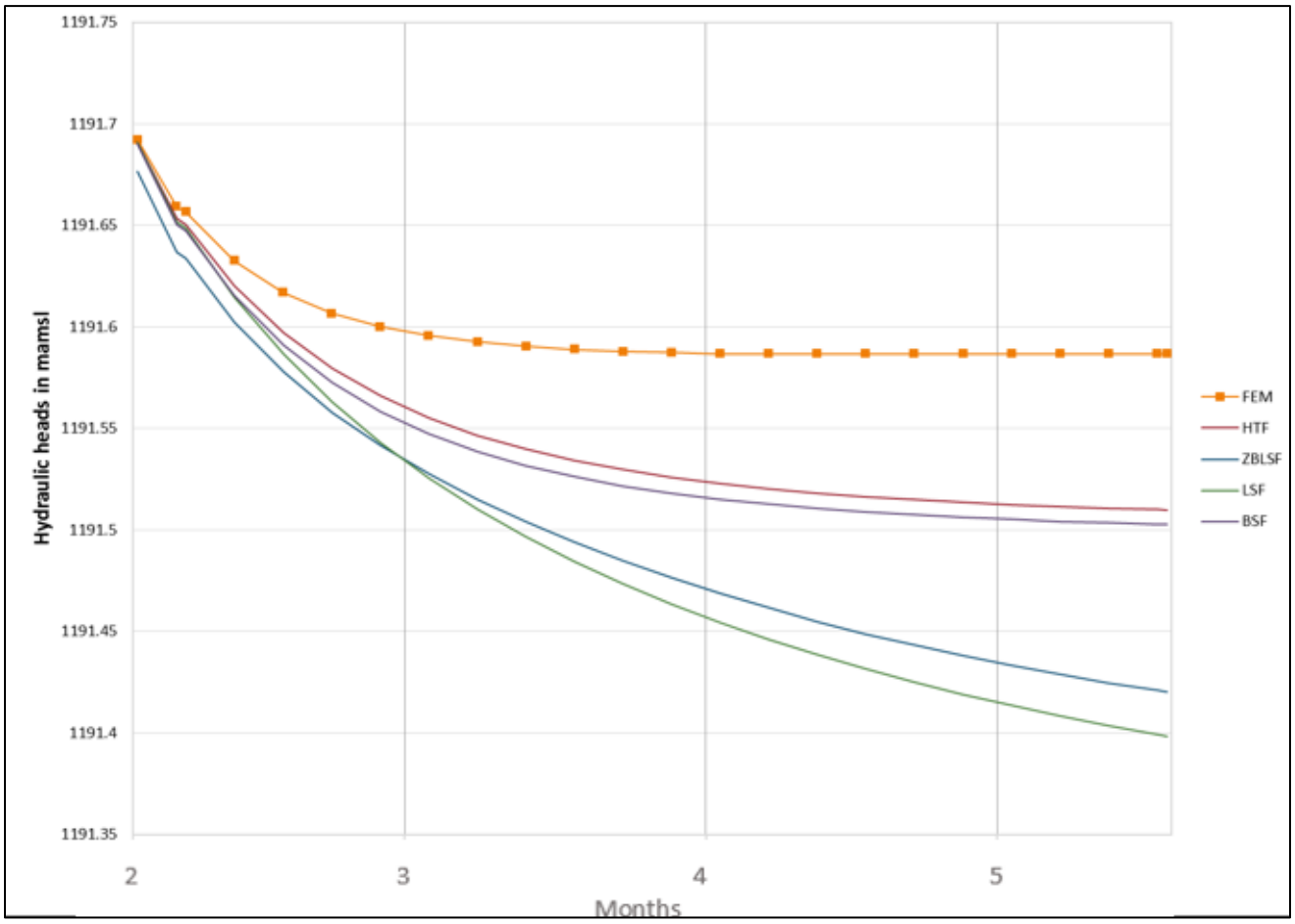

Figure 4-3: Modelled and predicted hydraulic heads at observation well OBS_9 for a dewatering strategy using three dewatering wells

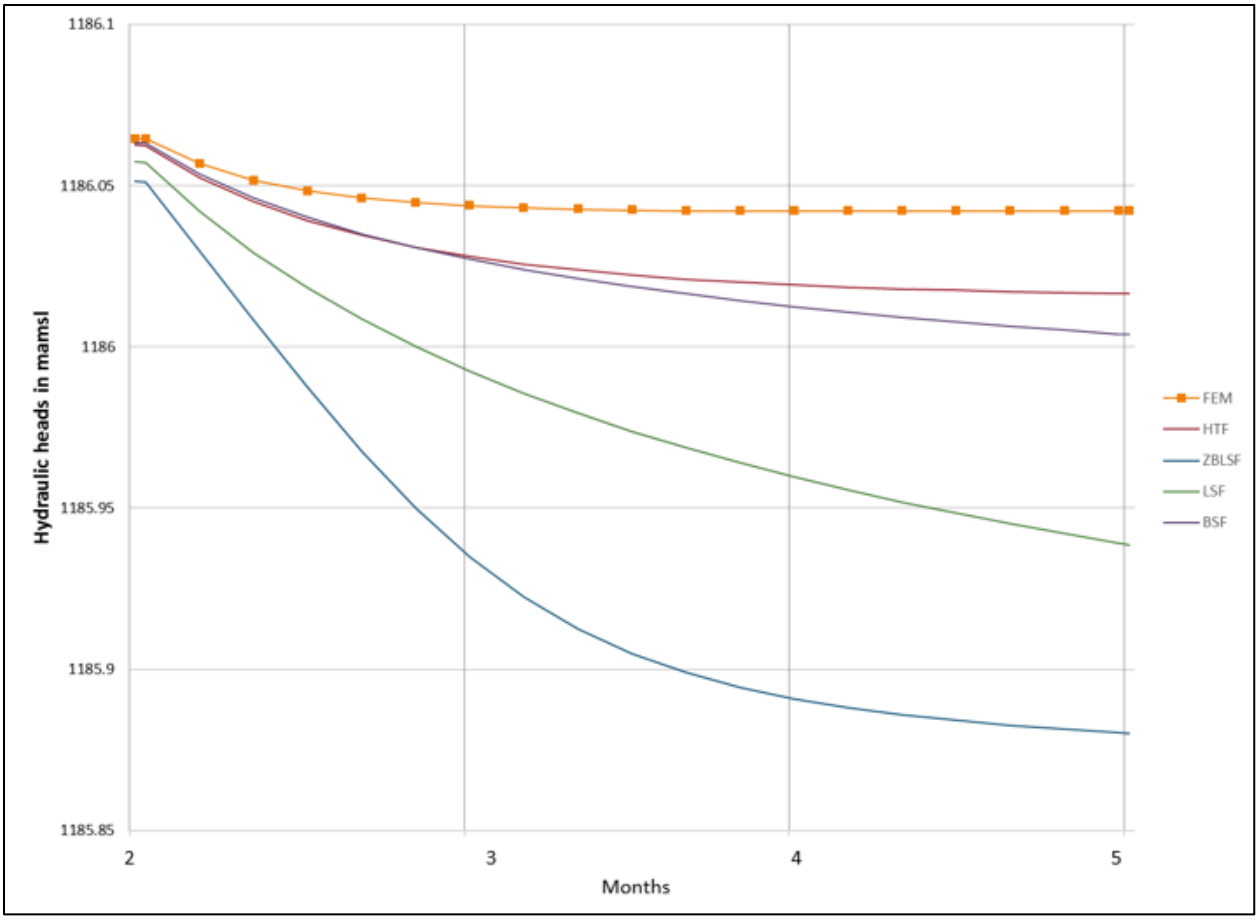

Figure 4-4: Modelled and predicted hydraulic heads at observation well OBS_9 for a dewatering strategy using six dewatering wells

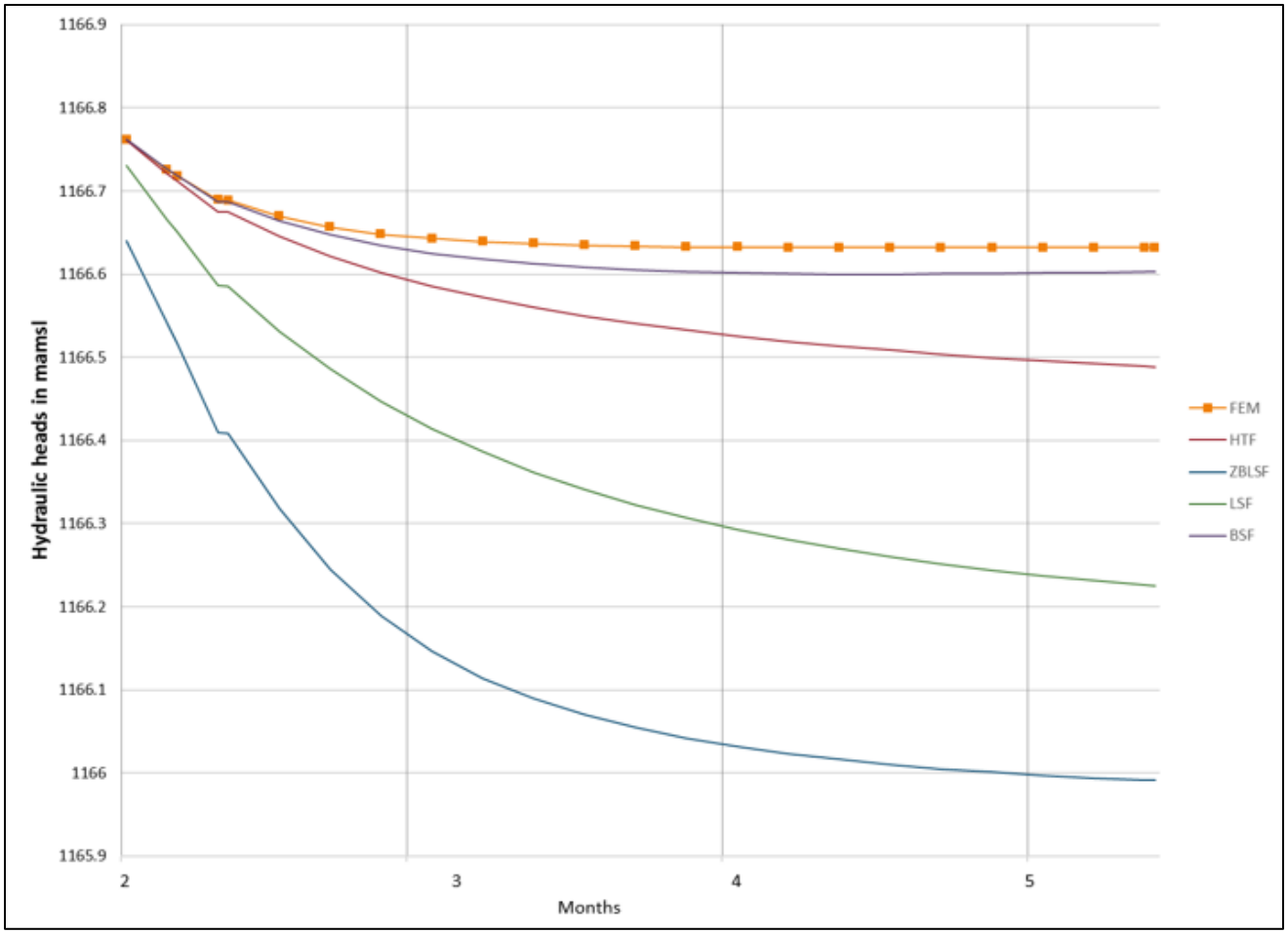

Figure 4-5: Modelled and predicted hydraulic heads at observation well OBS_9 for a dewatering strategy using nine dewatering wells

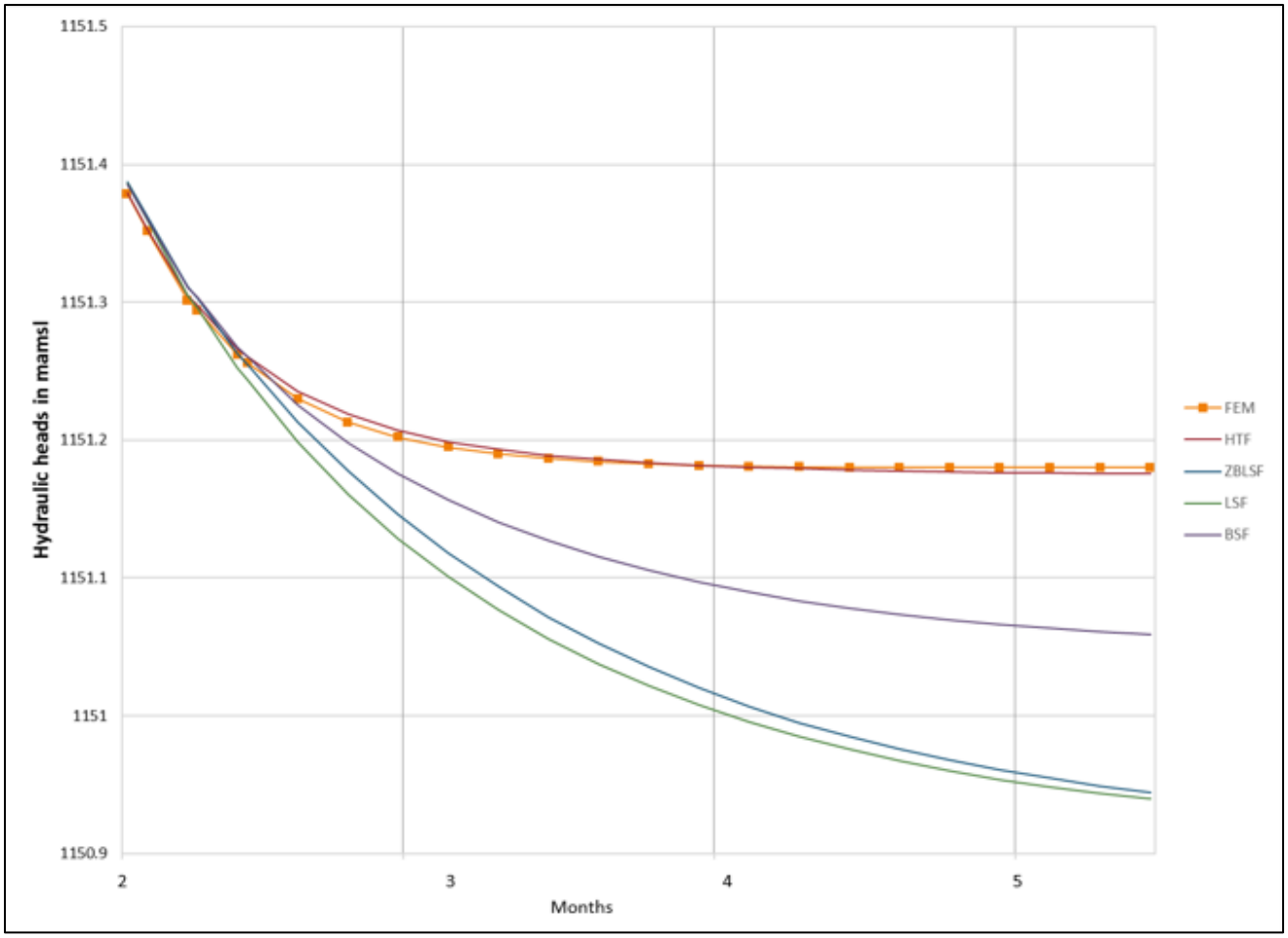

Figure 4-6: Modelled and predicted hydraulic heads at observation well OBS_9 for a dewatering strategy using 12 dewatering wells

From Figure 4-3 to Figure 4-6 it can be seen that the predictions of hydraulic heads made by the ANNs models generally underestimate the hydraulics heads from the numerical model. It can be also seen that ANN using the hyperbolic transfer function (HTF) yielded the best predictions of the modelled (FEM) hydraulic heads for three of the four dewatering scenarios (3, 6, 9 and 12 abstractions wells). It can furthermore be seen that the accuracy of the head predictions made by the ANNs generally decreased over time. However, the difference between the modelled and predicted hydraulic heads seldom exceeded 0.5 m.

To verify the accuracy of the hydraulic head predictions, statistical techniques were used to assess the performance of the different ANNs. The performance analyses were carried by considering the modelled and predicted hydraulic heads at all nine

observation points (OBS_1 to OBS_9) for all four dewatering simulations (using 3, 6, 9 and 12 abstraction wells).

In Figure 4-7, the Root Mean Square Errors (RMSEs) for the hydraulic head predictions made by the ANNs using the four different transfer functions are shown at all nine observation points. The RMSEs for the ANNs using the BSF, LSF, ZLBSF and HTF are shown in green, blue, brown and orange, respectively. From this figure it can be seen that the HTF yielded the smallest errors at most observation wells, followed by the BSF. The ANN using the ZLBSF and LSF gave the largest errors (poorest predictions). Similar observations can be made when considering the Normalised Root Mean Square Errors (NRMSEs) (refer to Figure 4-8).

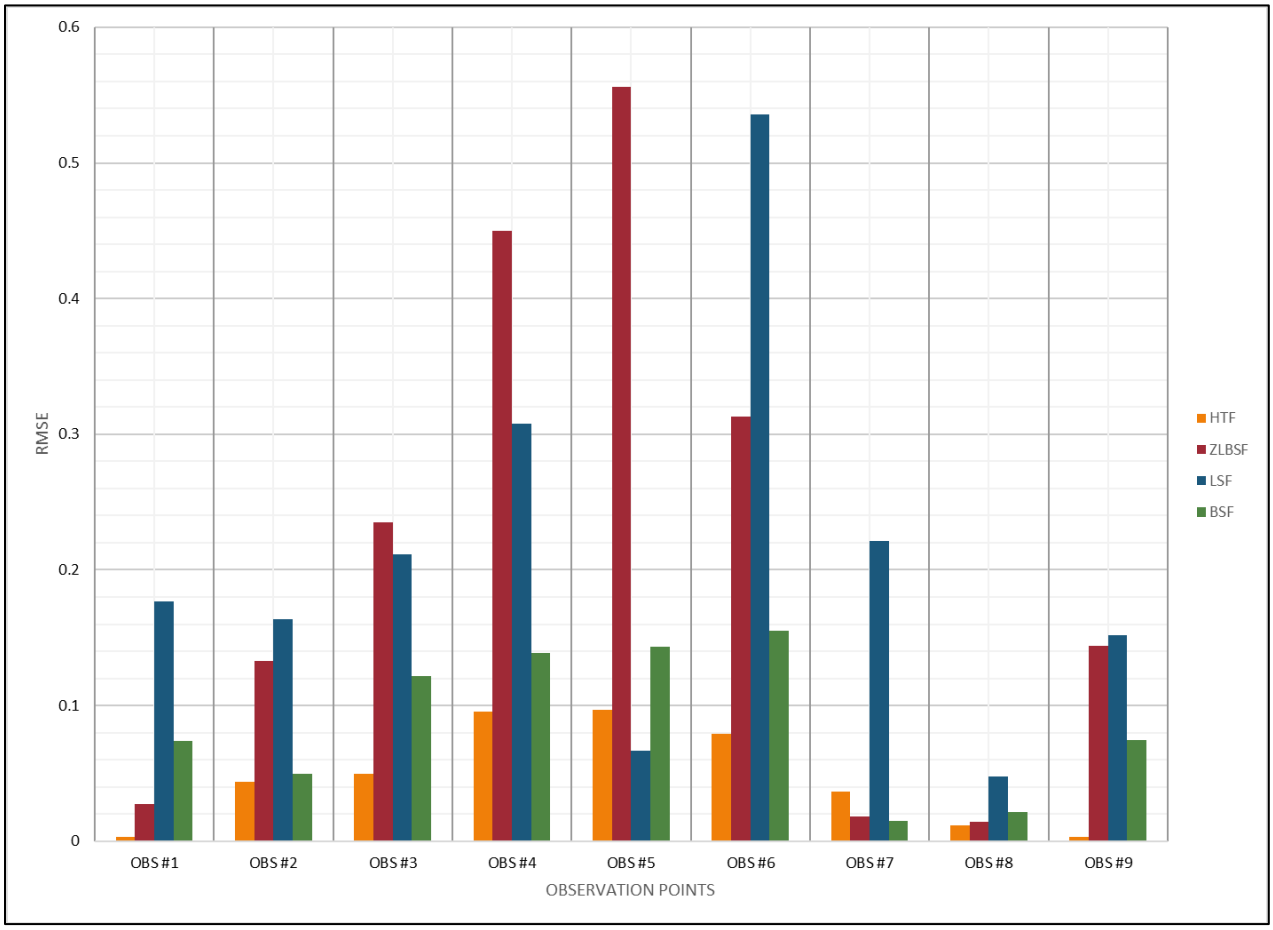

Figure 4-7: Root Mean Square Errors (RMSEs) for the hydraulic head predictions at the different observation wells

In Figure 4-9 the Person's *r* value is shown for all the observation wells. These values all range between approximately 0.88 and 1. According to Section 2.4.6, this means that there is a strong positive correlation between the datasets. The positive correlation implies that increases or decreases in the observed data correspond to similar increases and decreases in the predicted data. The Pearson's *r* correlation coefficients therefore indicate that the ANN was able to successfully predict changes in the hydraulic heads. At six of the nine observation wells, the ANN using the HTF had *r*-values closer to 1 than the ANNs using the other transfer functions. It can therefore be concluded that the ANN using the HTF performed better than the other ANNs in predicting the hydraulic heads at the observations wells.

Figure 4-10 shows the NSE at all the observation wells. As explained in Section 2.4.6, NSE-values between 0 and 1 indicate acceptable performance, whereas negative values indicate unacceptable performance. From Figure 4-10 it is seen that large negative NSE-values were calculated at some of the observation wells for the predictions made by the ANNs using the ZLBSF, LSF and BSF. Positive or small negative NSF-values were calculated for the ANN using the HTF. This ANN therefore outperformed the others in its predictions of the hydraulic heads.

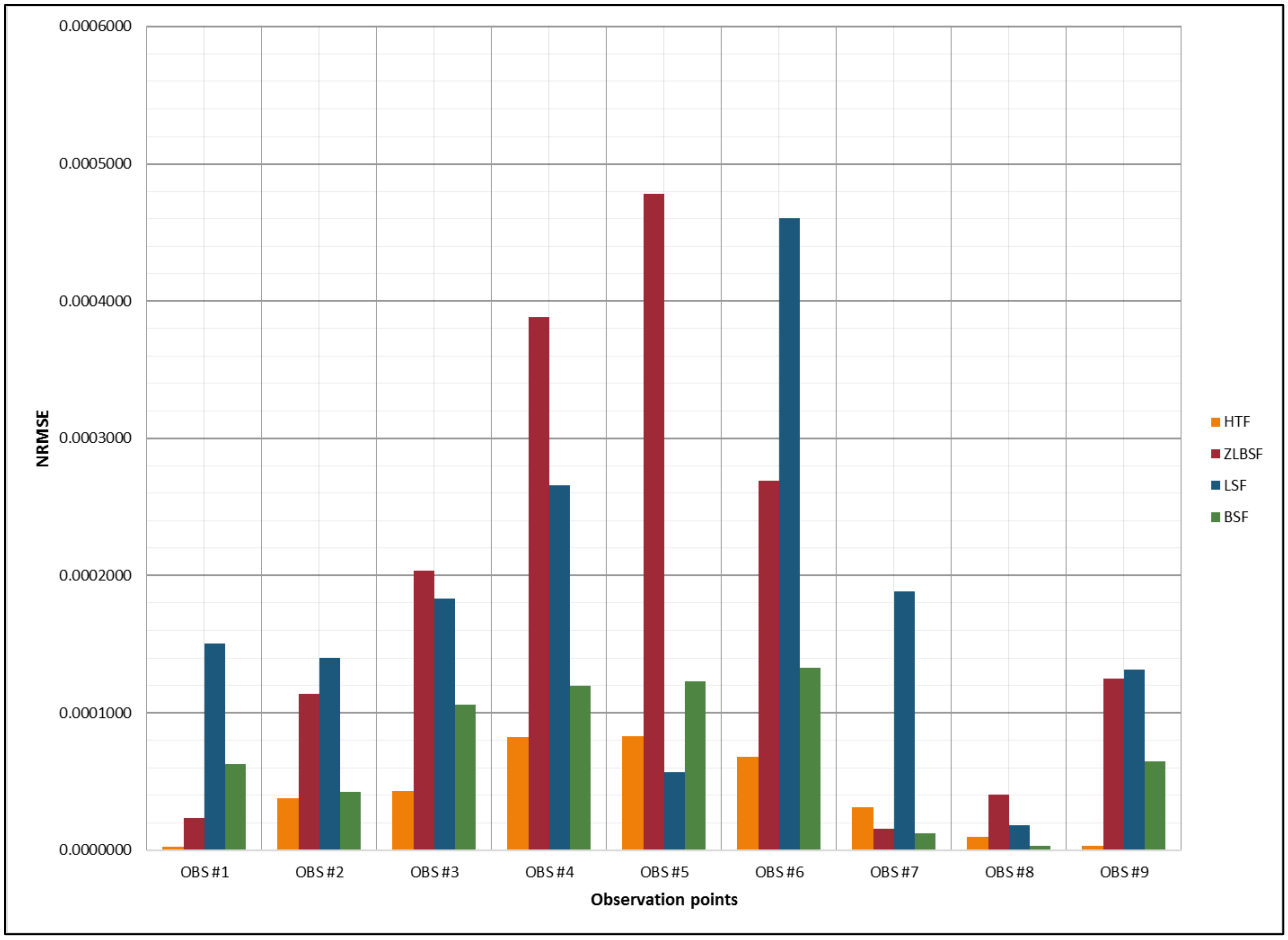

Figure 4-8: Normalised Root Mean Square Error (NRMSE) for the hydraulic head predictions at the different observation wells

In Figure 4-11 the PIs calculated at all the observation wells are shown. The correspondence between two datasets is deemed satisfactory when low PI values are calculated for these datasets (Lin and Cunningham III, 1995). From Figure 4-11 it can be seen that, at most wells, the lowest PI values were calculated for the ANN using the HTF. This transfer function therefore yielded the best results.

Figure 4-12 shows the RSR calculated for the hydraulic head data at all the observation wells. From this figure it is seen that the ANN using the HTF yielded the lowest RSR values at most observation wells, and therefore gave the best performance in predicting the hydraulic heads at the different piezometers.

In Figure 4-13 the PBIAS for the groundwater elevation data at all the observations wells is shown. Again the ANN with the HTF gives the lowest (closest to zero) values for the PBIAS at most observation wells. This ANN therefore performed the best in predicting the hydraulic heads.

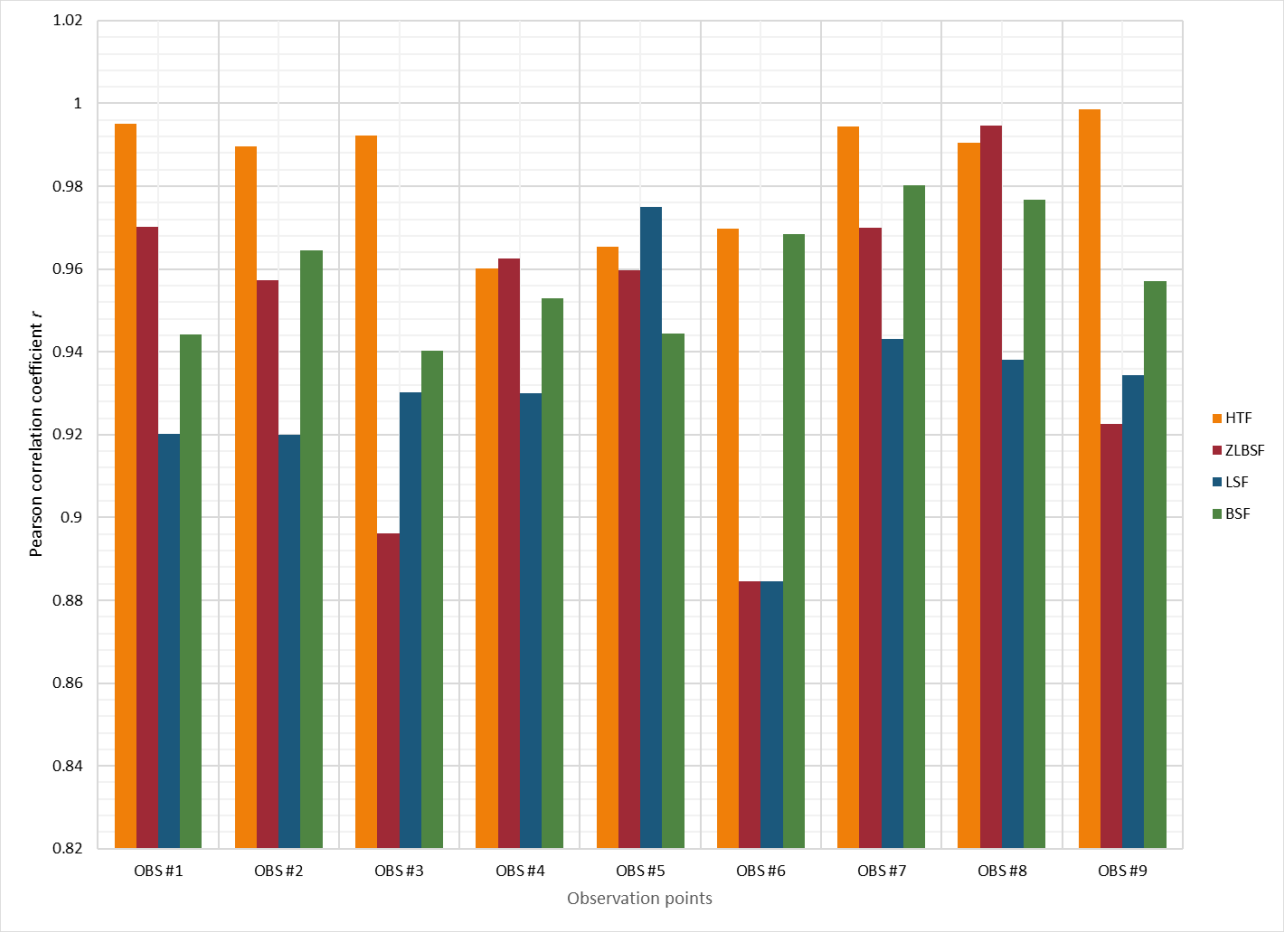

Figure 4-9: Pearson correlation coefficient (r) for the hydraulic head predictions at the different observation wells

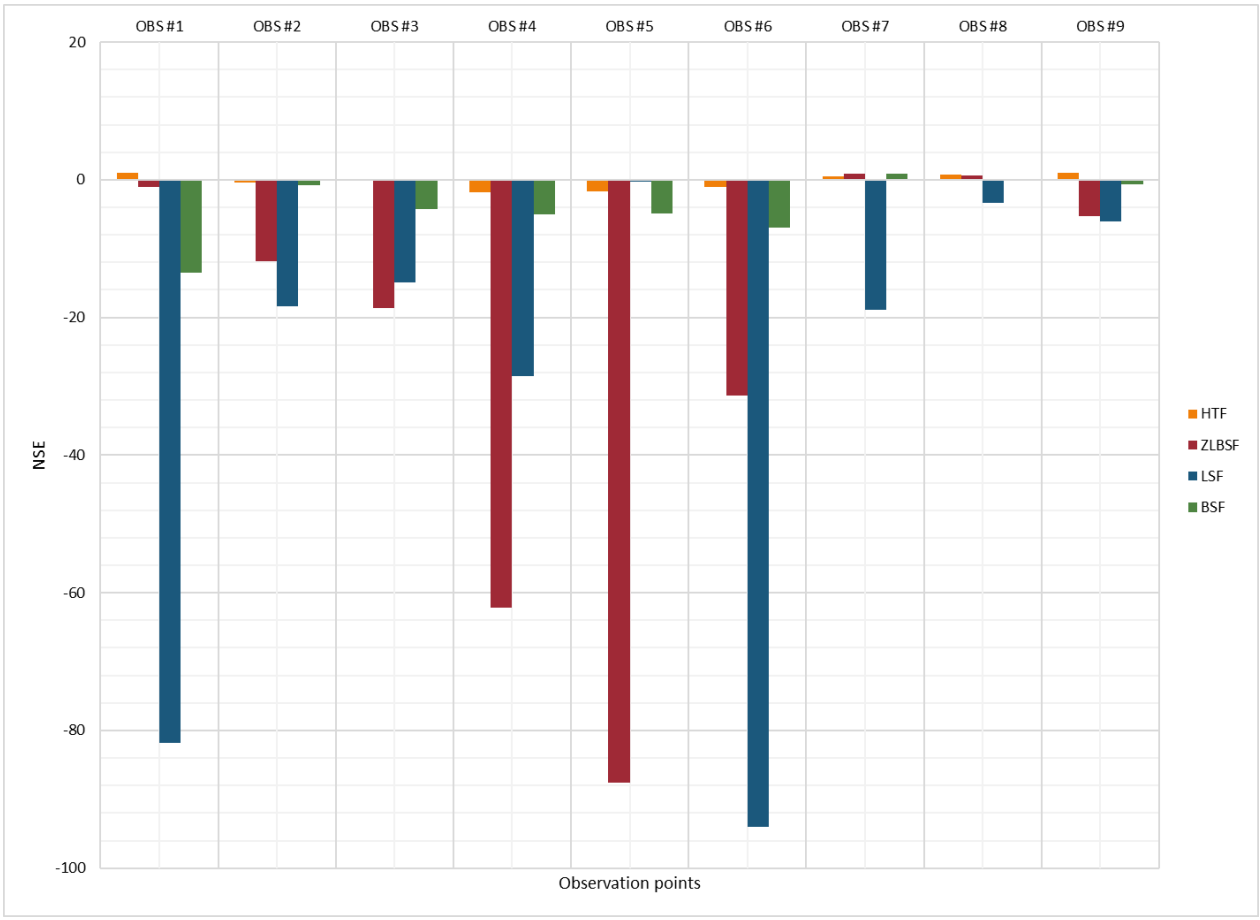

Figure 4-10: Nash-Sutcliffe Efficiency (NSE) for the hydraulic head predictions at the different observation wells

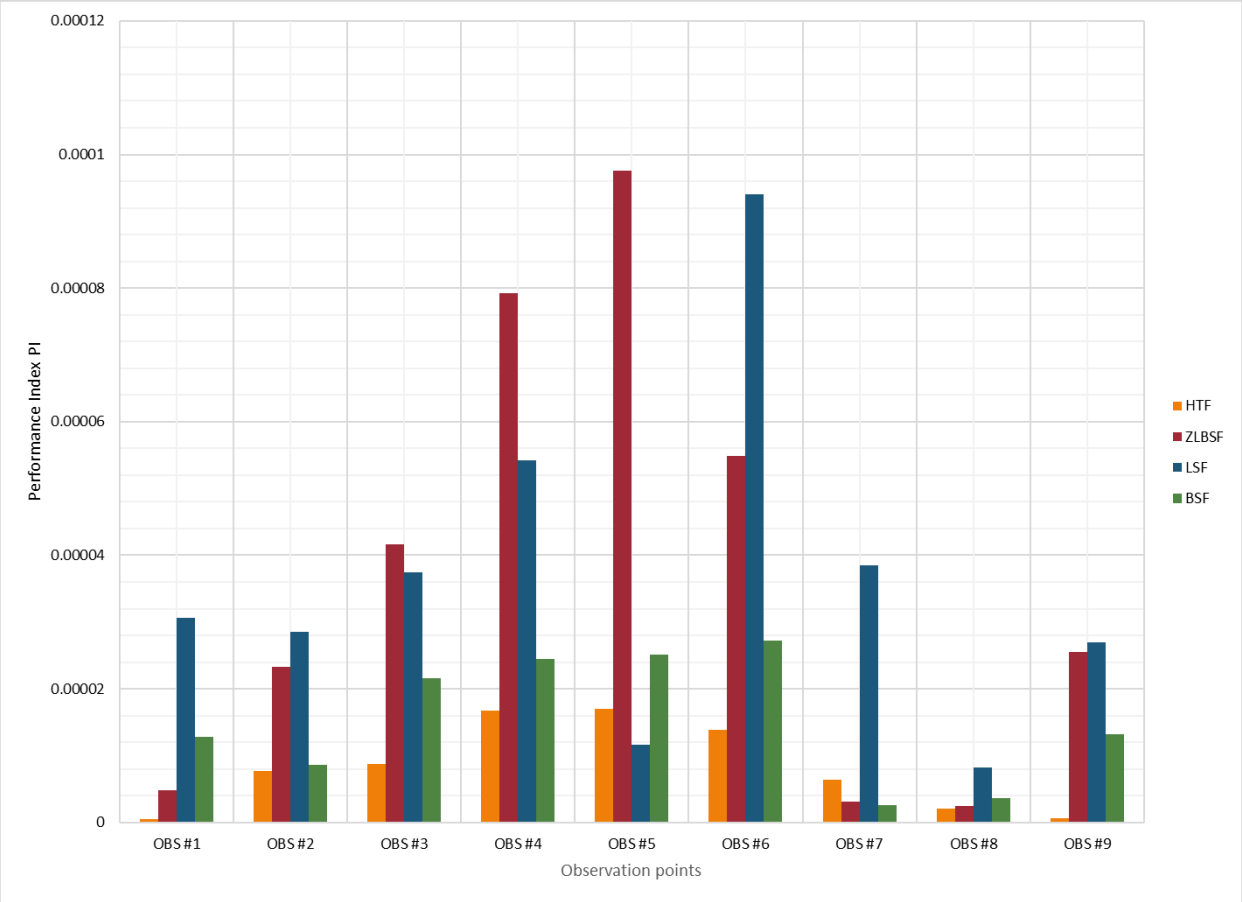

Figure 4-11: Performance Index (PI) for all observation points

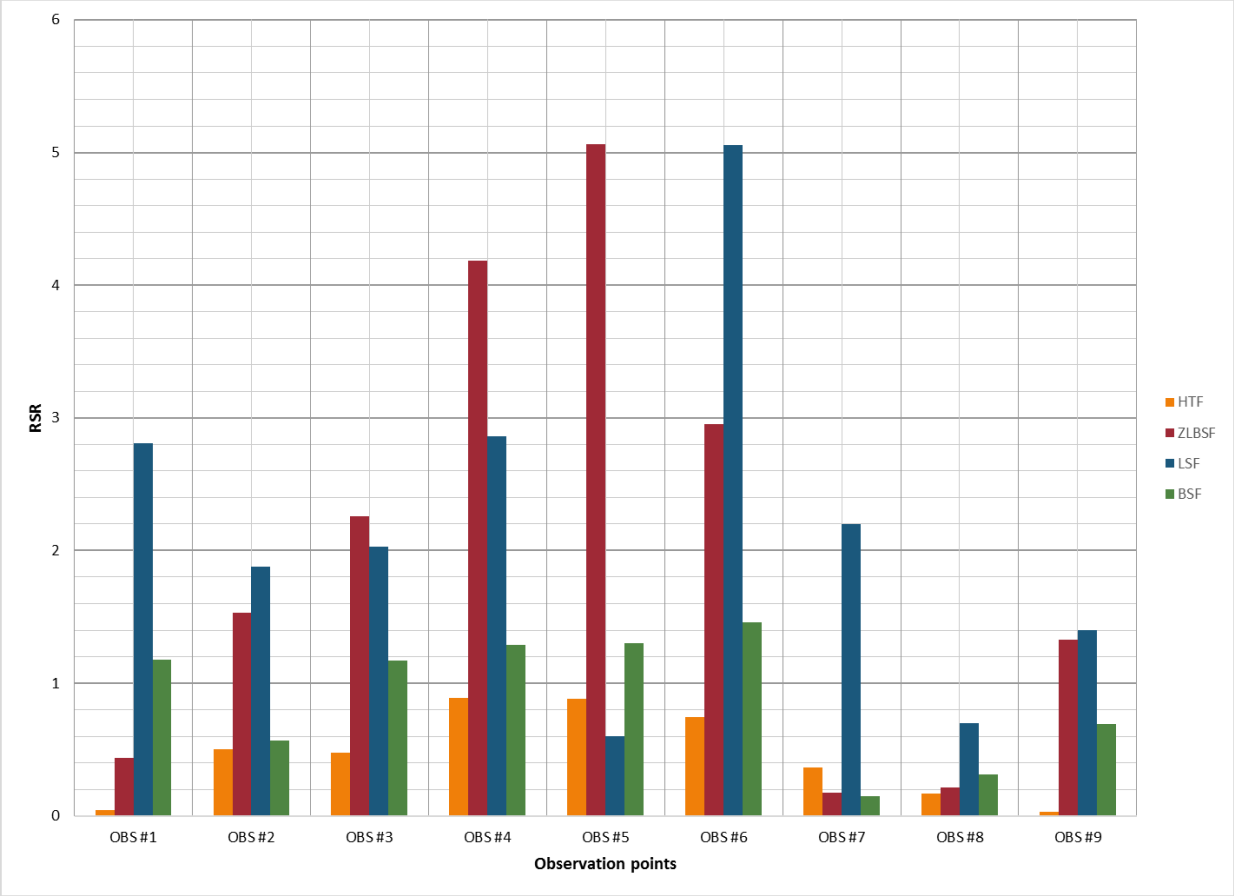

Figure 4-12: RMSE-observations Standard deviation RATIO (RSR) for all observation points

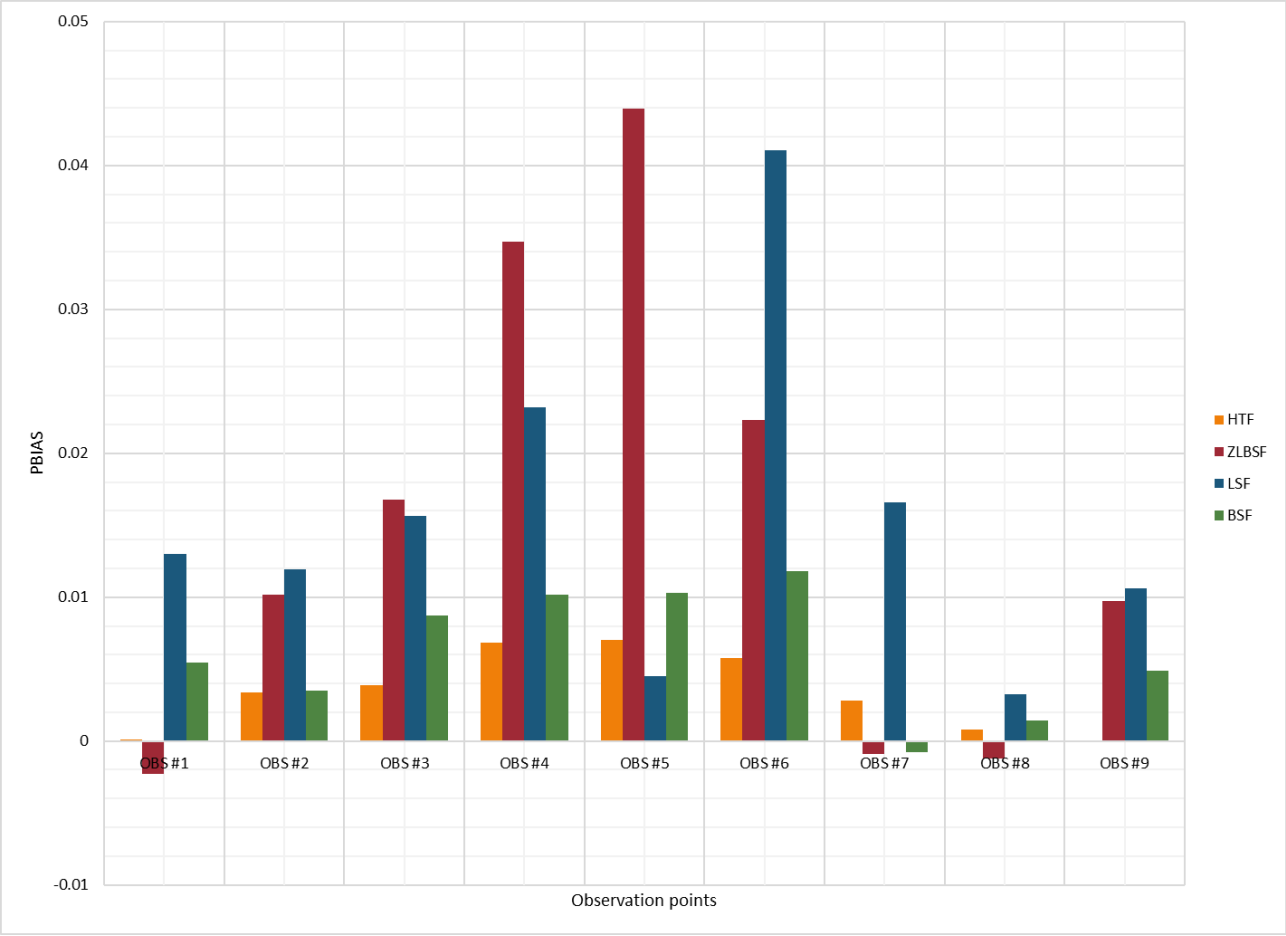

Figure 4-13: Percent BIAS (PBIAS) for all observation points

4.5.2.1 DISCUSSION

The main objective of this section was to use statistical methods to evaluate which transfer function used by the different ANNs results in the best prediction of the hydraulic heads obtained from the numerical model. ANNs using four different transfer functions were used and their performances were evaluated based on seven statistical evaluation techniques. The statistical evaluation results show that the ANN using the HTF best predicts the effects of the dewatering process at the open pit.

4.5.3 GRAPHICAL EVALUATION

From the statistical evaluation techniques, the model based on the HTF was found to be most suitable to predict the groundwater elevations. In this section, graphical residual analysis will be used to further assess the performance of the ANN using this transfer function.

In Figure 4-14 to Figure 4-17 the hydraulic heads predicted at OBS_9 by the ANN using the HTF are plotted against the modelled (FEM) hydraulic heads for the four dewatering scenarios (3, 6, 9 and 12 dewatering wells). Similar graphs for the other observation wells are presented in Appendix B. From these figures it can be seen that predicted values give good approximations of the modelled values. The R-squared values of the linear fits range between 0.91 and 0.99, indicating that hydraulics heads predicted by ANN fit the regression line well.

However, it is known that the R-squared value cannot determine if the hydraulics heads predicted by the ANN are biased. For this reason, normal probability plots and residual plots were constructed for the data at the different observation wells. There are several methods to test the normality of data distribution. For graphical analysis, the common techniques are the quantile-quantile (Q-Q) probability plot and the normal probability plot. The Q-Q plot is a technique used to determine if the data used for the analysis are from populations with the same distribution. The normal probability plot helps to evaluate if the dataset follows a normal or Weibull distribution (Chambers *et al.*, 1983). In the current study, normal probability plots were used. These plots are graphs showing the percentile of the normal distribution against the residual values.

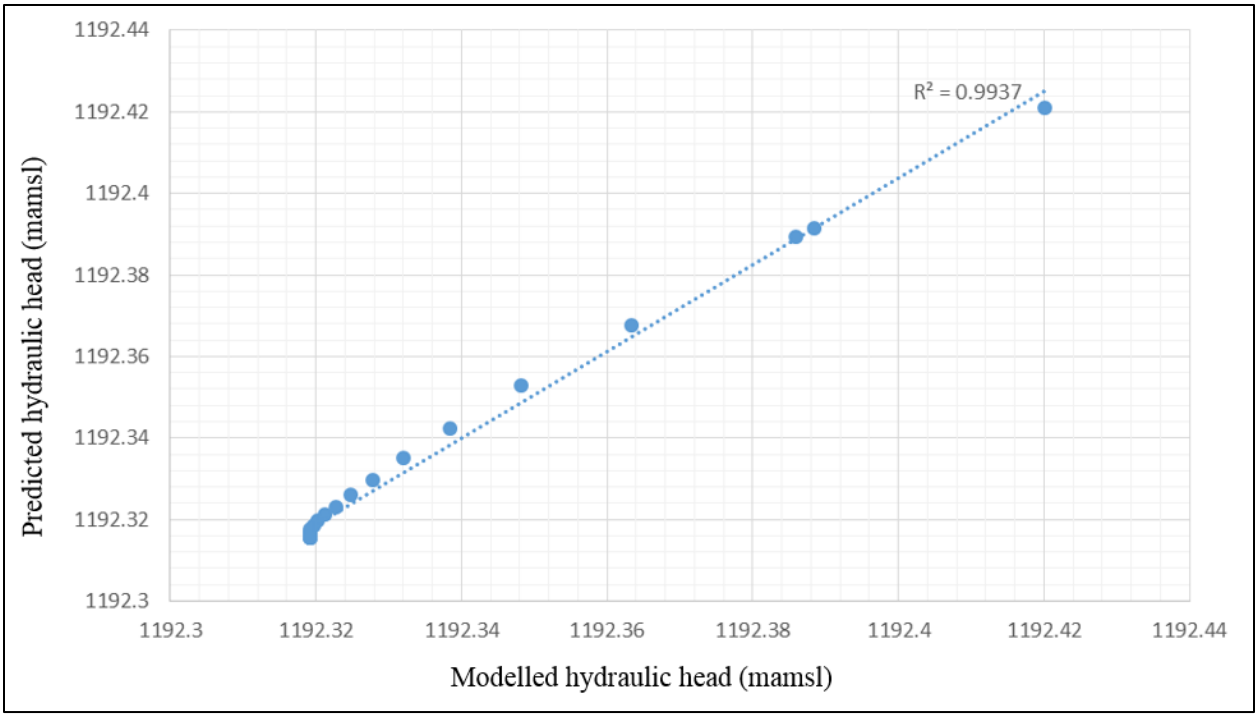

Figure 4-14: ANN versus FEM hydraulic heads for observation point OBS_9 using three dewatering wells

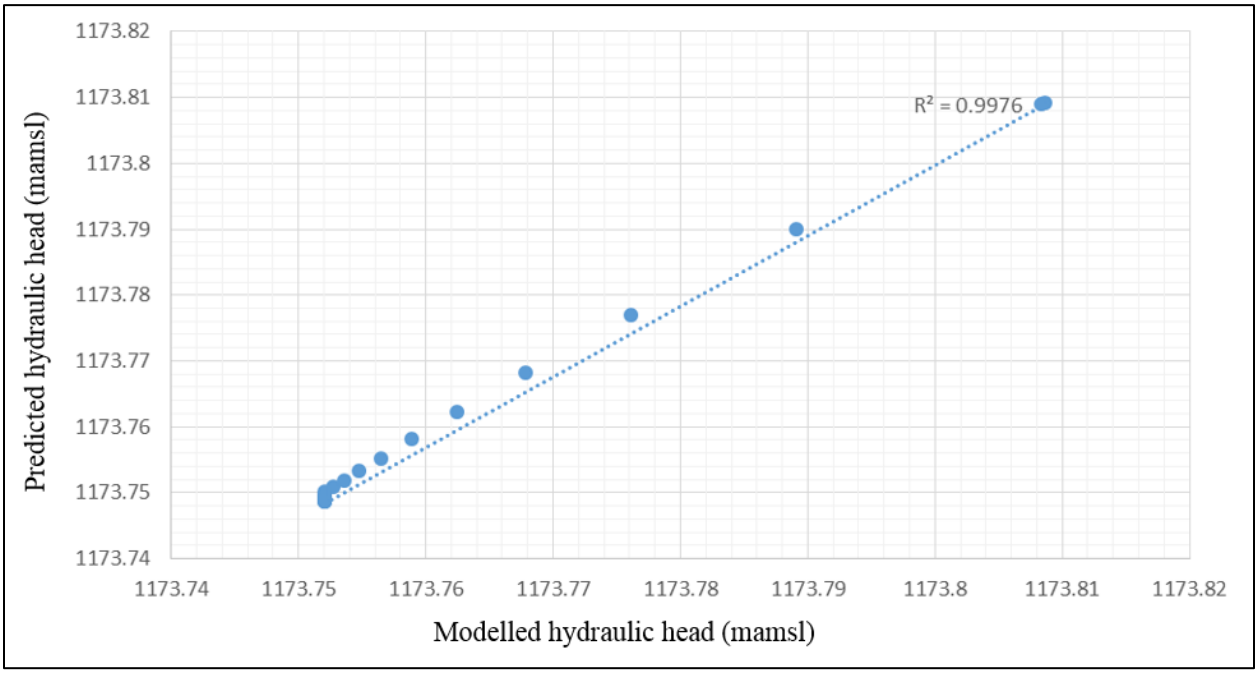

Figure 4-15: ANN versus FEM hydraulic heads for observation point OBS_9 using six dewatering wells

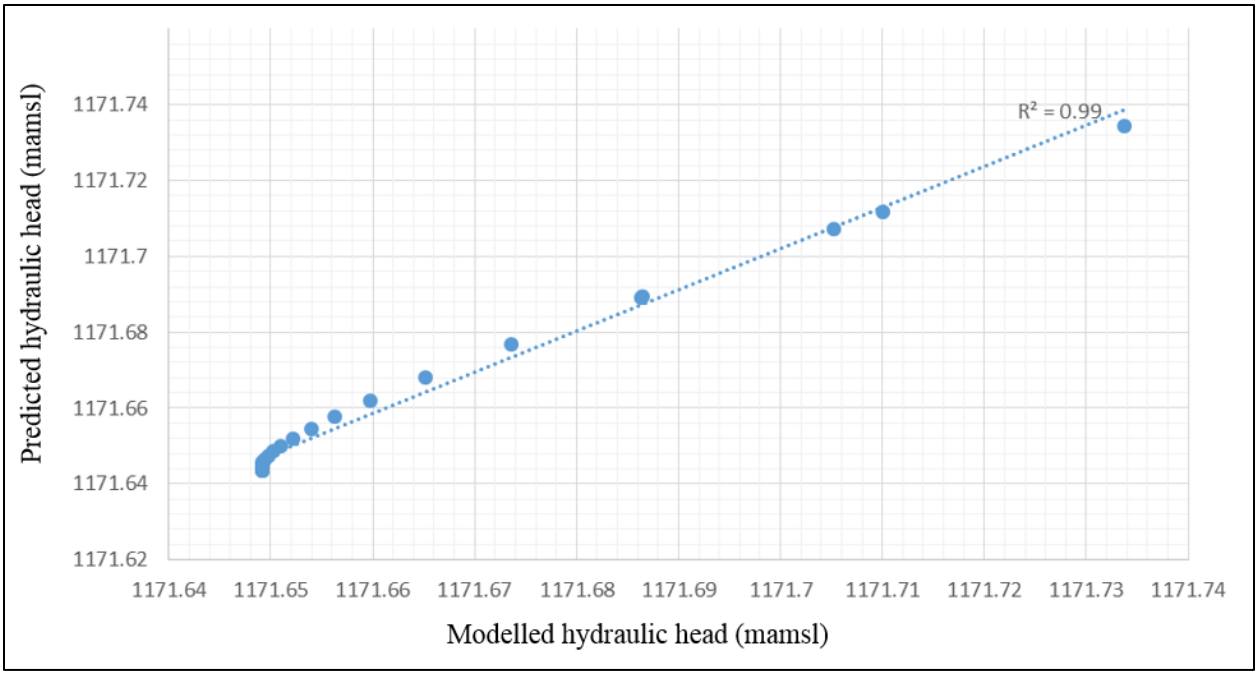

Figure 4-16: ANN versus FEM hydraulic heads for observation point OBS_9 using nine dewatering wells

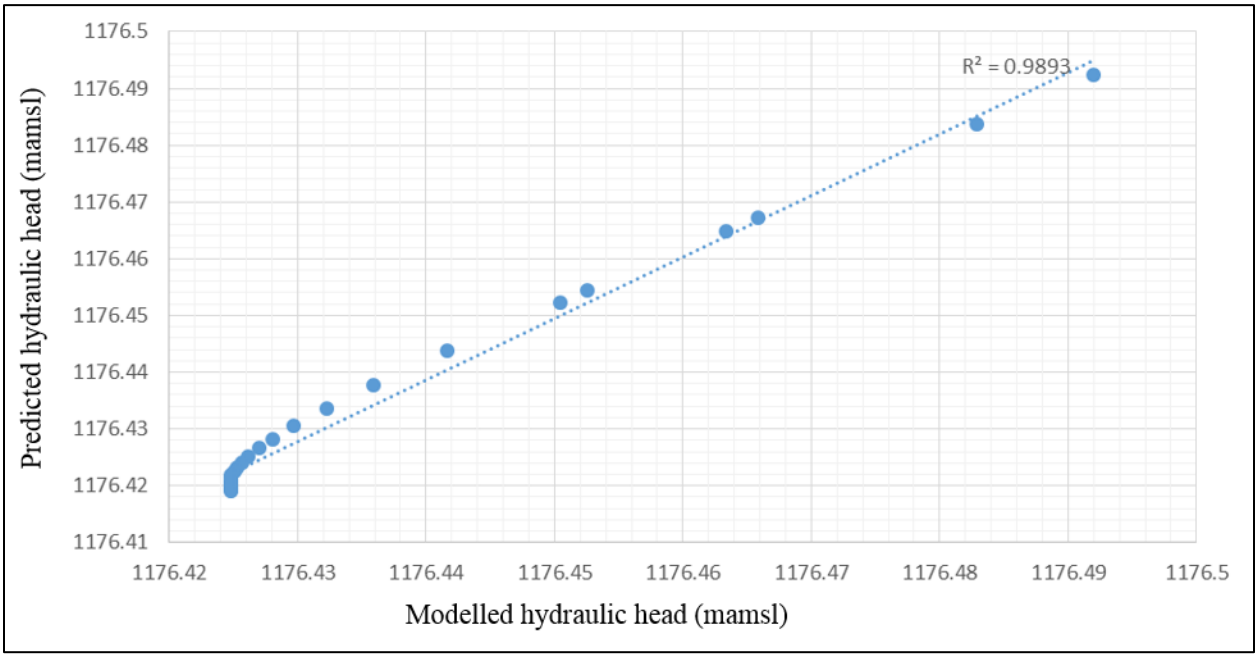

Figure 4-17: ANN versus FEM hydraulic heads for observation point OBS_9 using 12 dewatering wells

The normality plots for observation well OBS_9 during the four dewatering strategies are presented in Figure 4-18 to Figure 4-21. Similar plots for the other observation

points may be perused in Appendix C. From these figures it can be observed that there are minor deviations from the straight line fit. It can therefore be concluded that the data are normally distributed, since these plot show strong linear patterns with R-squared values close to 1. No significant outliers are observed in the data.

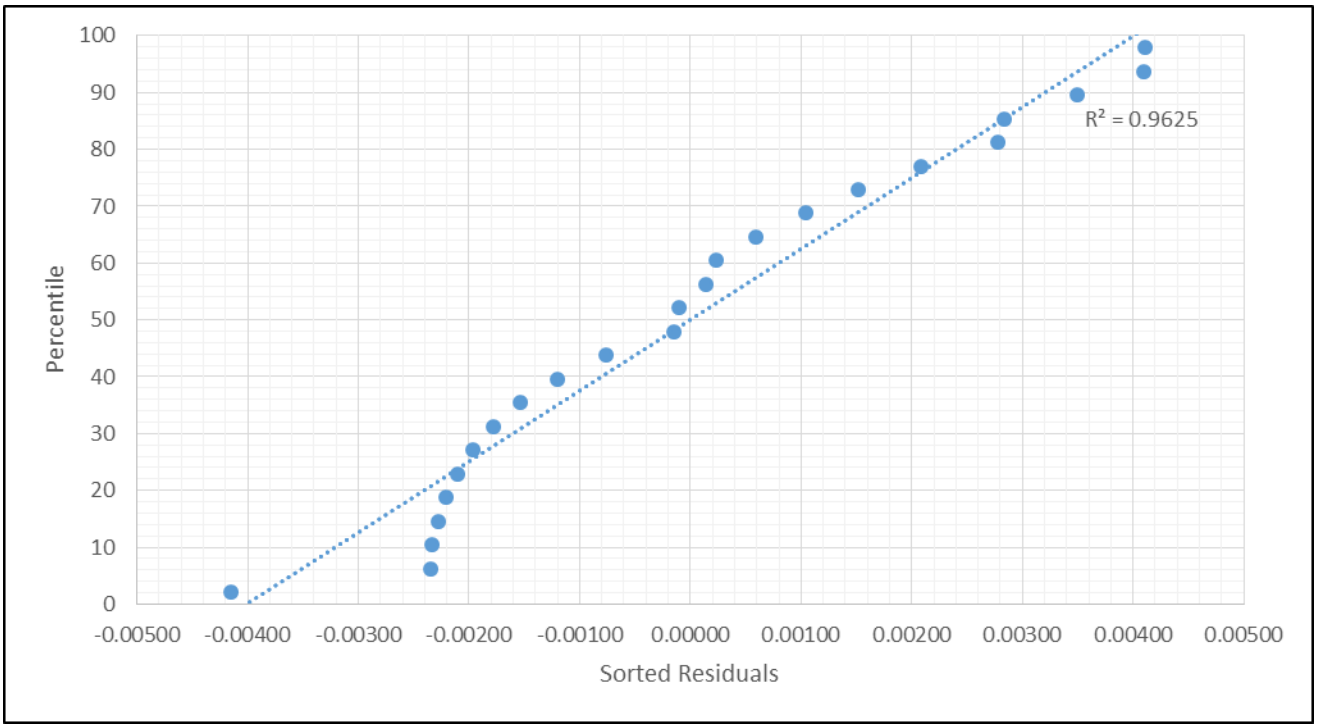

Figure 4-18: Normal probability plot for observation point OBS_9 using three dewatering wells

The comparison between the outputs from the ANN and the FEM revealed good agreement between these two datasets. However, further examination of the data by means of residual plots could reveal systematic differences between the two datasets. Graphical residual analysis is used in this research to verify the quality of the agreement between the modelled and predicted data to determine whether the ANN needs further refinement for linearization.

Residual plots are firstly used to determine if the data fits the linearity and homogeneity of the variance assumptions. The plots have to be randomly distributed if the variance is homogeneous. To meet the linearity requirement, the residuals have to be equally scattered above and below the *x*-axis of the plot.

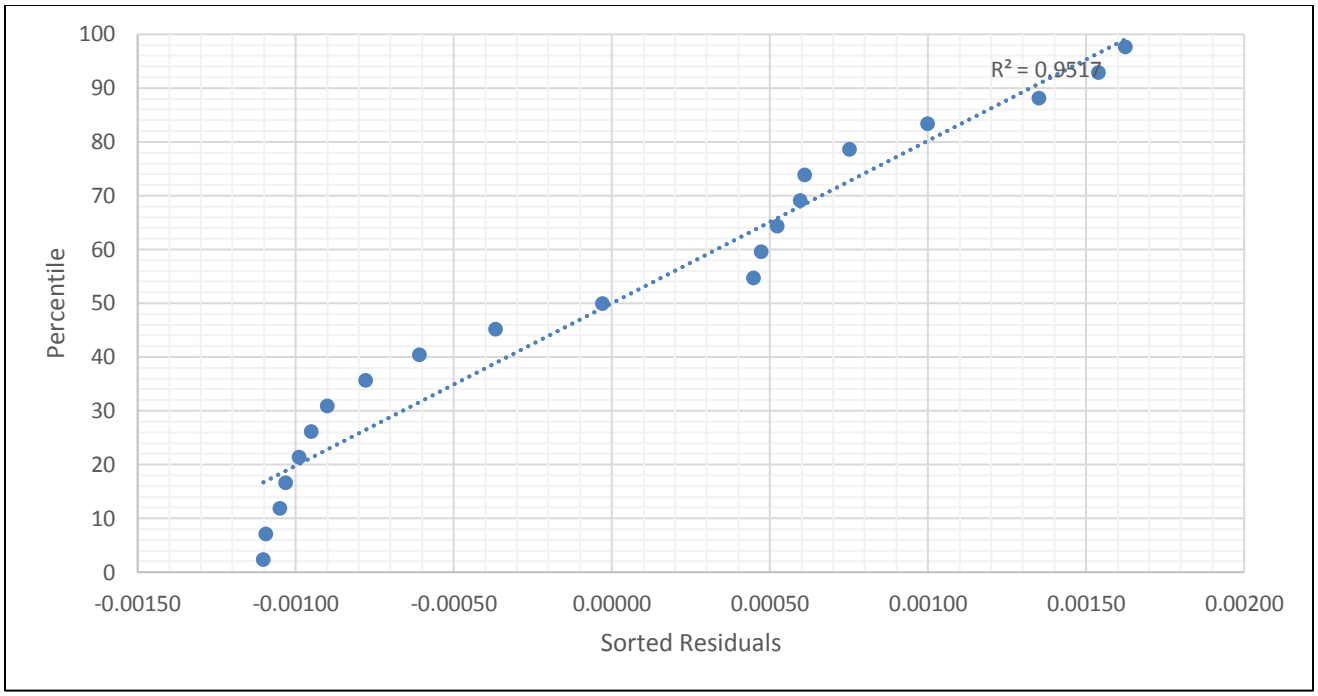

Figure 4-19: Normal probability plot for observation point OBS_9 using six dewatering wells

The residual plots of observation well OBS_9 are shown in Figure 4-22 to Figure 4-25 for the four dewatering strategies. Similar plots for the other observation wells are presented in Appendix D. From these figures it is seen that the residual plots have non-random, inverted U-shaped patterns, suggesting that a better fit to the data could have been obtained using a non-linear model. The shapes of the residual plots suggest that the function used to describe data should be quadratic.

In an attempt to improve the predictions of the ANN, the ANN was refined by transformation of the data to achieve linearity. Transforming a dataset is to re-express it with another measurement scale using an appropriate mathematical operation. A non-linear transformation increases or decreases a linear relationship between variables, changing their correlation by so-doing.

The challenge of variable refinement is to find the method of transformation appropriate to linearize the dataset at hand. Several transformation methods were used in the current investigation to randomize the residual plots in order to meet

the linearity assumptions. However, it was found that none of these transformations were able to achieve linearity.

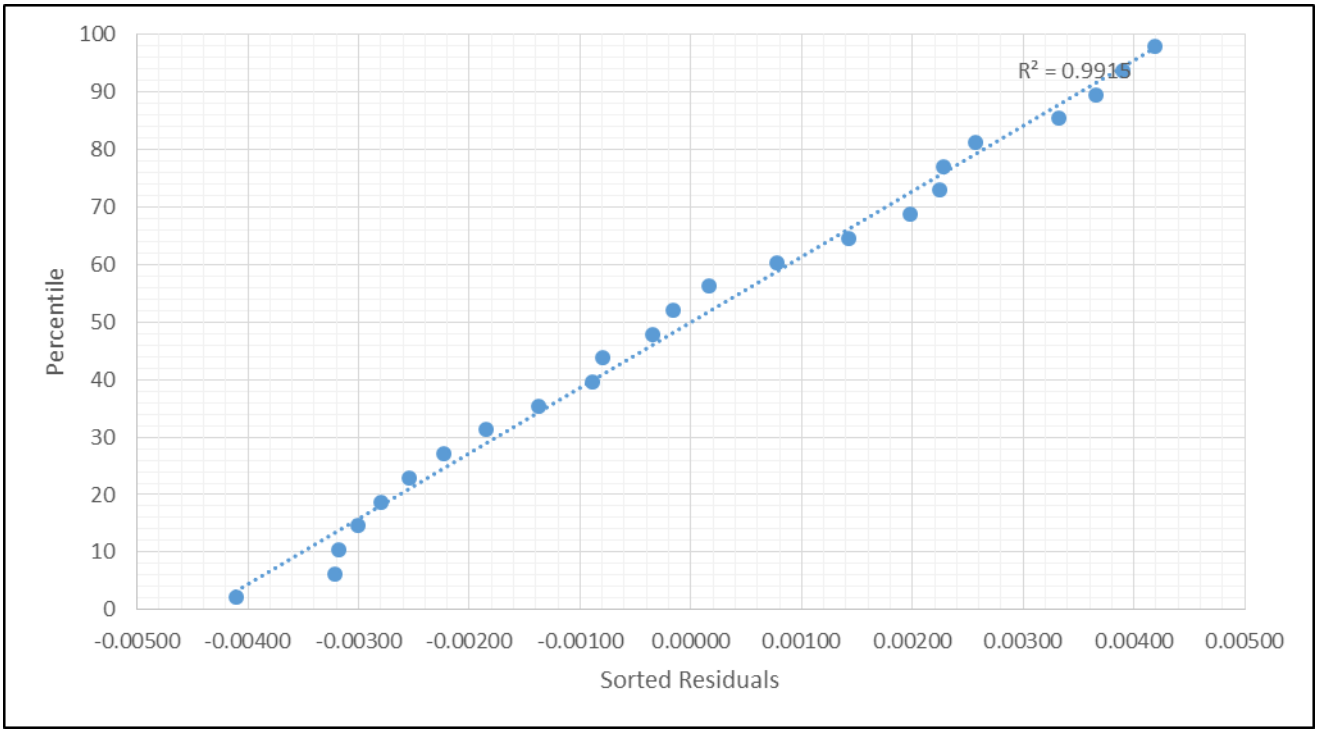

Figure 4-20: Normal probability plot for observation point OBS_9 using nine dewatering wells

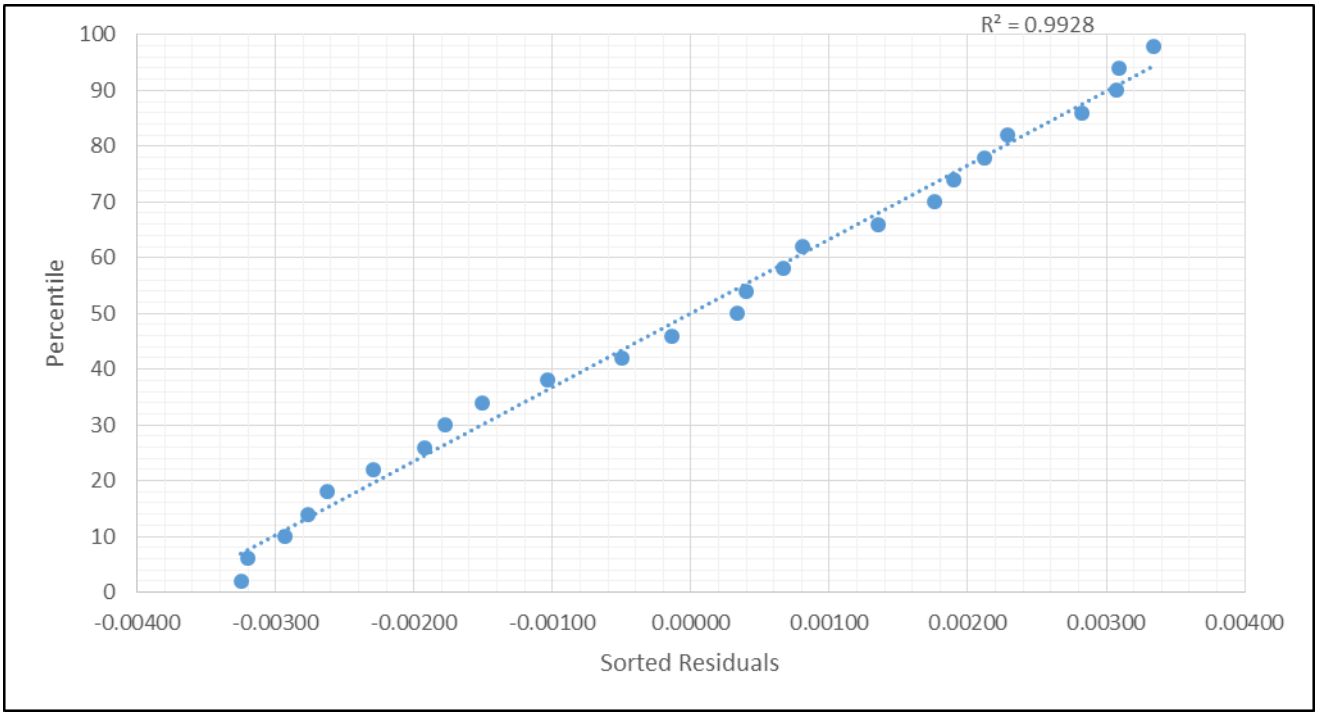

Figure 4-21: Normal probability plot for observation point OBS_9 using twelve dewatering wells

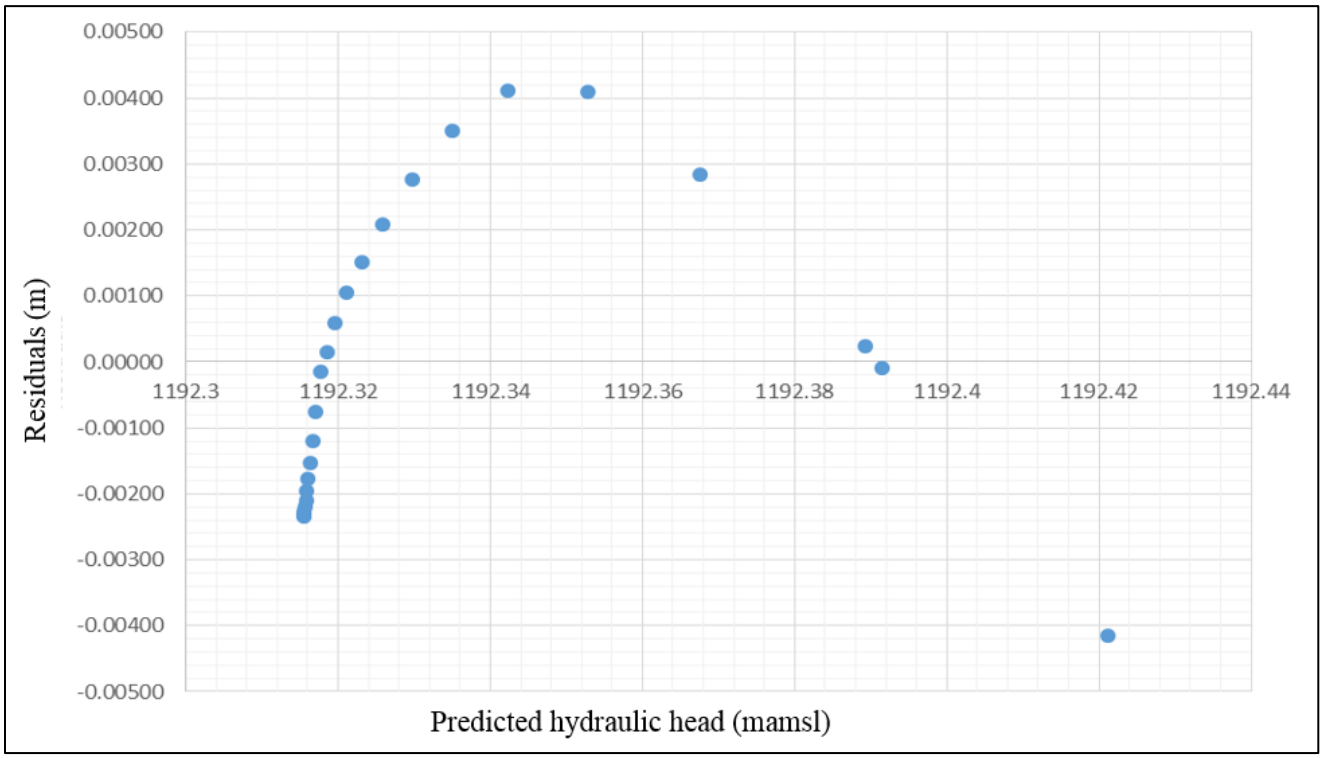

Figure 4-22: Residuals plots for observation point OBS_9 using three dewatering wells

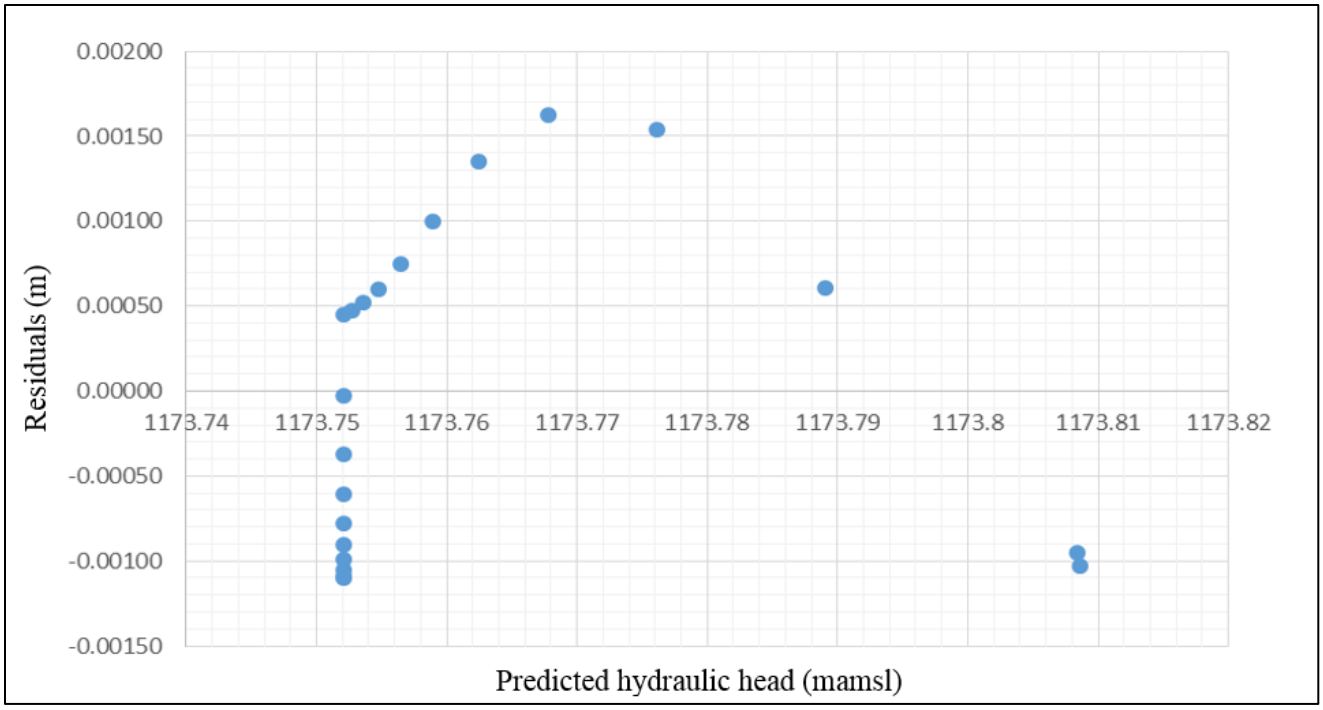

Figure 4-23: Residuals plots for observation point OBS_9 using six dewatering wells

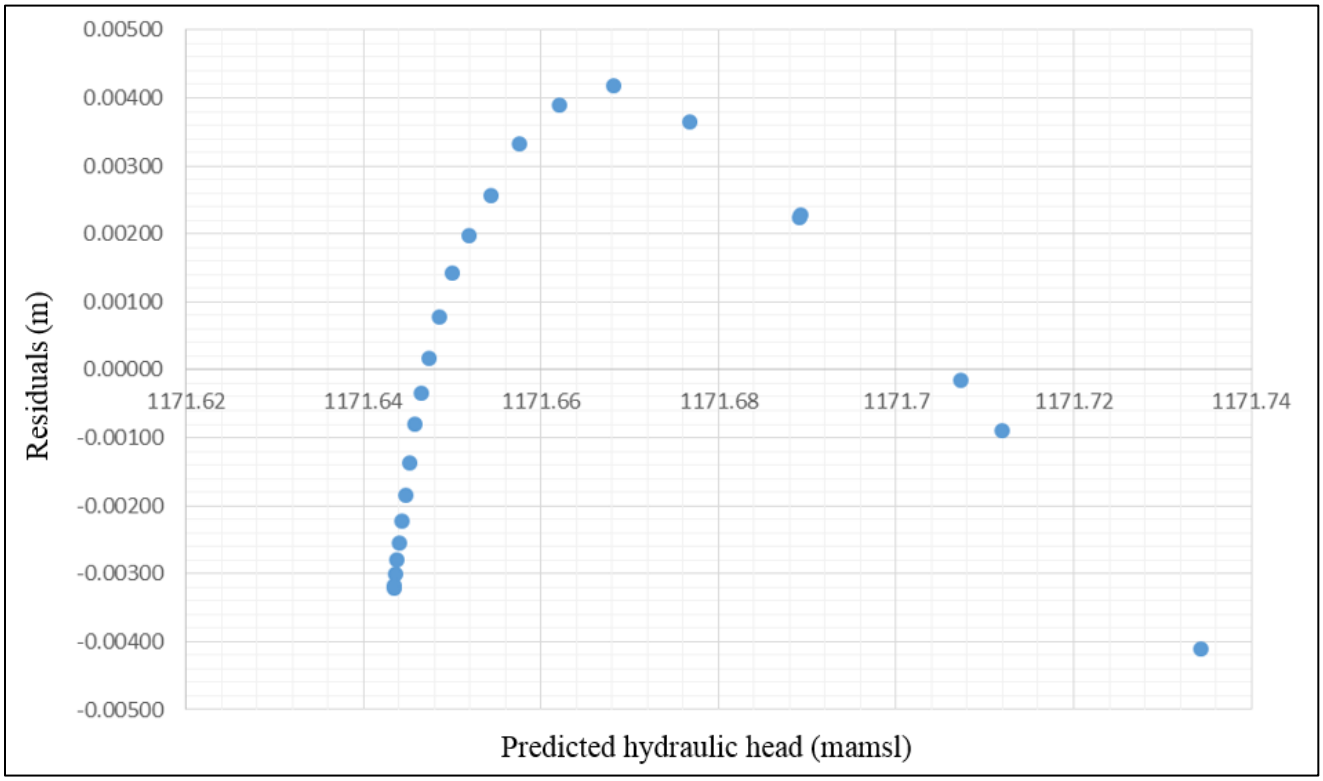

Figure 4-24: Residuals plots for observation point OBS_9 using nine dewatering wells

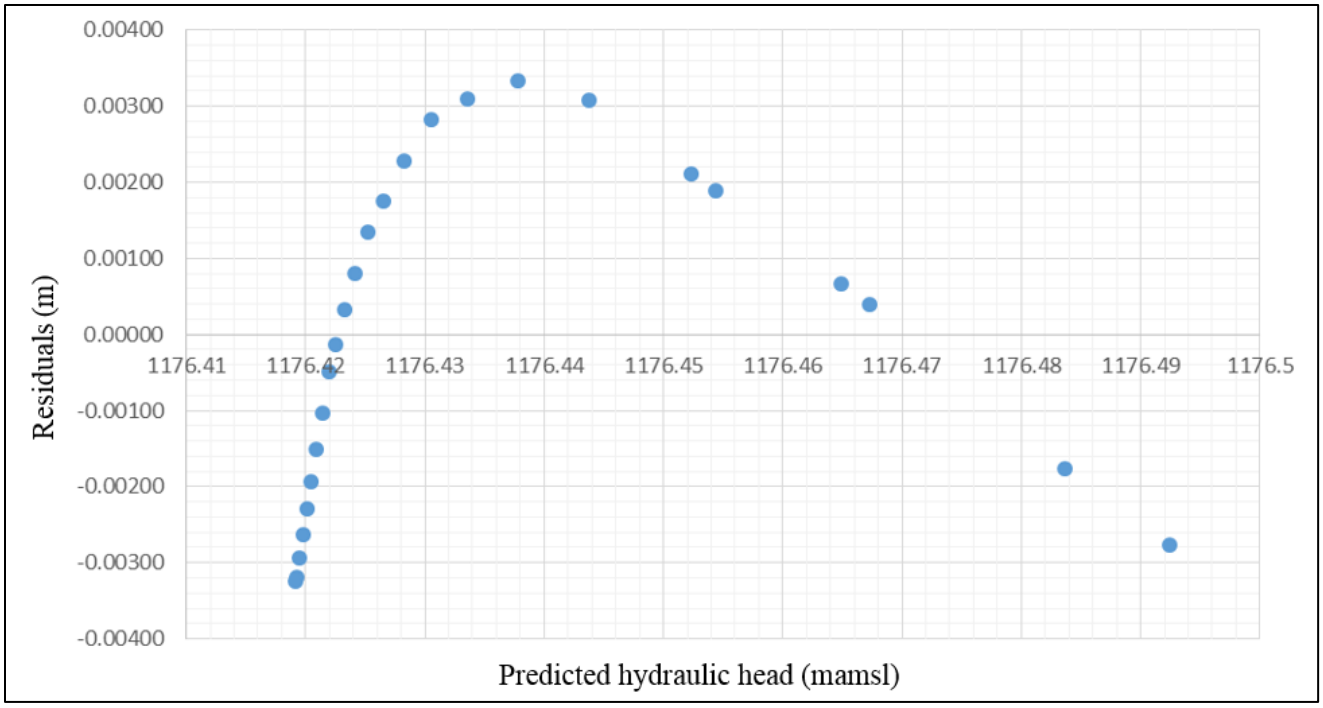

Figure 4-25: Residuals plots for observation point OBS_9 using twelve dewatering wells

4.5.3.1 DISCUSSION

From the graphical residual analysis it is seen that there is a systematic non-linearity between the modelled and predicted datasets. Despite this non-linearity, all the other graphical evaluation techniques showed that the ANN was successful in predicting the hydraulic heads with high accuracy. In Chapter 5, the developed ANN will be applied to a real open pit mine to predict the impact of dewatering strategies.

CHAPTER 5: HYDRAULIC HEAD SIMULATION FOR DEWATERING OF OPEN PIT MINES IN THE TENKE COMPLEX

5.1 INTRODUCTION

In open pit mining, dewatering of the pits is important to support the mining operations to prevent flooding and slope stability problems. One of the tools used to plan future dewatering programmes is groundwater modelling. The aim of groundwater modelling is to simulate the behaviour of aquifers during dewatering operations aimed at lowering the water table below the pit floor. Modelling usually requires large datasets for several input parameters, such as hydraulics conductivity, storativity, geology, tectonic features, rainfall and pumping rates. Many mining companies have only limited data available for the input parameters, since the acquisition of these data is usually a difficult, time-consuming and costly process. Alternative methods are therefore required to simulate or predict the groundwater behaviour at mines where limited input data are available.

In this study, the ANN developed in Chapter 4 will be used to simulate and predict the impacts of mine dewatering strategies at a real mine with limited input data.

5.2 STATEMENT OF THE PROBLEM

The Democratic Republic of Congo (DRC) is a country with many mineral deposits. Several mining companies are extracting these minerals. Tenke Fungurume Mining (TFM) is currently extracting copper and cobalt in the Tenke Complex deposit. Two of their open pit mines are the Kabwe and Shimbidi Mines. These two mines have been active for some years. The Kabwe open pit is 1 100 m long, 347 m wide and 90 m deep, while the Shimbidi open pit is 410 m long, 405 m wide and 45 m deep. The main dewatering strategy at the Kabwe and Shimbi Mines is the use of dewatering boreholes.

Recently, mining operations were shut down to allow expansion of the two pits to the north to form one single pit. When mining operations were stopped, almost all the dewatering boreholes were shut down and the water table rebounded to its equilibrium level. The only bench currently accessible for mining will be depleted of ore within six months. Dewatering of the pits is therefore required if mining is to continue. This will require the rebounded water table to again be dropped to a level of 10 meters below the pit floor elevation.

For numerical and analytical calculations, geohydrologists and hydrogeological engineers need to have information on the geohydrological characteristics and physical properties of soil, and the hydraulics characteristics of the geological units intersected by mining. Much of this information is absent or incomplete at the two mines considered in this investigation, making the development of numerical models to accurately simulate the behaviour of the system a near impossibility.

However, temporal data on the hydraulic heads at a number of piezometers are available at the two mines. Hydraulic head data are gathered at these mines using automatic loggers. This study aims to investigate whether these measured hydraulic heads can be used to predict the water elevations during mine dewatering at the two mines where the existing lack of other input data would yield poor numerical models.

5.3 AIM AND OBJECTIVES OF THE STUDY

In Chapter 4 an ANN was developed for the prediction of the impact of mine dewatering on the aquifer system intersected by mining. The ANN using a HTF was found to provide the accurate predictions and simulations. This ANN will be used in this section to predict the water table elevations at two open pit mines in the DRC. These pits are currently flooded and the water levels in these pits will have to be lowered by 7.5 meters within six months to allow mining operations to restart. The ANN will use temporal hydraulic head data recorded at a number of piezometers at the mines as training data. The performance of the ANN will be evaluated by comparing the hydraulic head observations and predictions.

5.4 TOPOGRAPHICAL SETTINGS OF THE STUDY AREA

The pre-mining topography of the study area was rugged, consisting of hills which alternate with valleys, as shown in Figure 5-1. Mining activities have significantly altered the topography, transforming hills into flat areas and pits, as shown in Figure 5-2. The current study was carried out in an area with two such open pit mines, namely the Shimbidi and Kabwe Mines. Before mining commenced, the Dipeta River flowed at a position between the current locations of these two open pits. Since dewatering operations started, the flow of the river decreased drastically. The river is currently located at a distance of 130 m from the Kabwe open pit and 75 m from the Shimbidi open pit, and has a negligible impact on the water volumes in the pits.

5.5 CLIMATE

Kabwe and Shimbidi mines are located in the Democratic Republic of Congo in the Katanga province close to the city of Kolwezi. The area of TFM experiences a dry season (May to October) which is totally distinct to its rainy season (November to April). According to Golder Associates (2007), the climate of the area is cool and dry between May and August, hot and dry between September and October and rainy between November and April. Based on the meteorological station of Kolwezi, the MAR varies from 870 mm to 1 420 mm with an average of 1 150 mm. Being close to the equator (10° latitude), daylight (from 6:00 to 18:00) and night time (from 18:00 to 6:00) are of almost equal duration.

5.6 GEOLOGICAL SETTINGS

The Tenke Complex occurs in the Tenke-Fungurume district in the African Copper Belt. The latter is a Neoproterozoic sedimentary and metasedimentary complex located between the south-eastern part of the DRC and the northern part of Zambia. The African Copper Belt, in its Katanga Supergroup, is one of the most important source of copper and cobalt in the world. The Shimbidi and Kabwe Mines extract ore from the Tenke Complex through open pit mining activities (Fay and Barton, 2011).

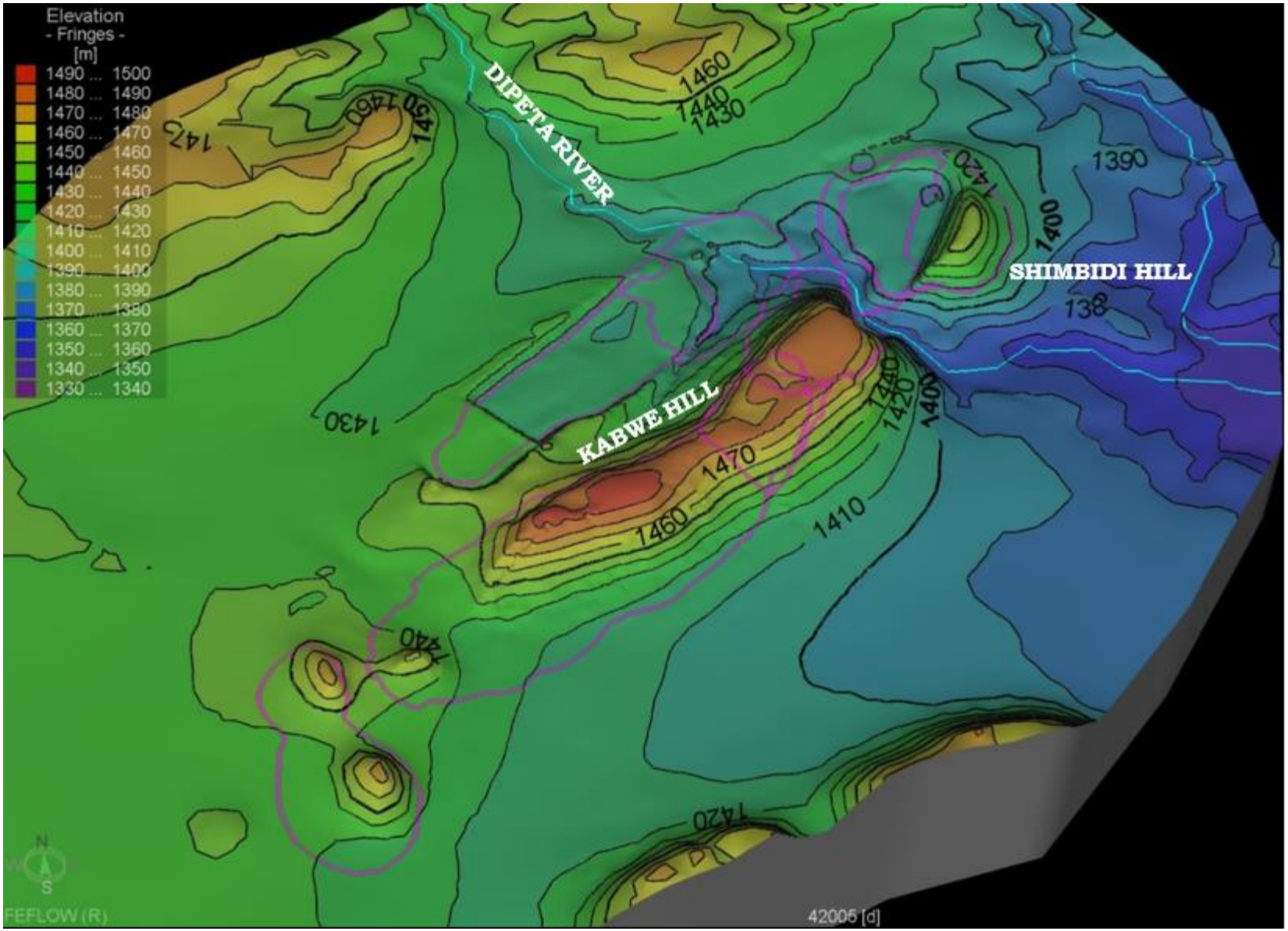

Figure 5-1: Pre-mining topography at the Kabwe and Shimbidi Mines

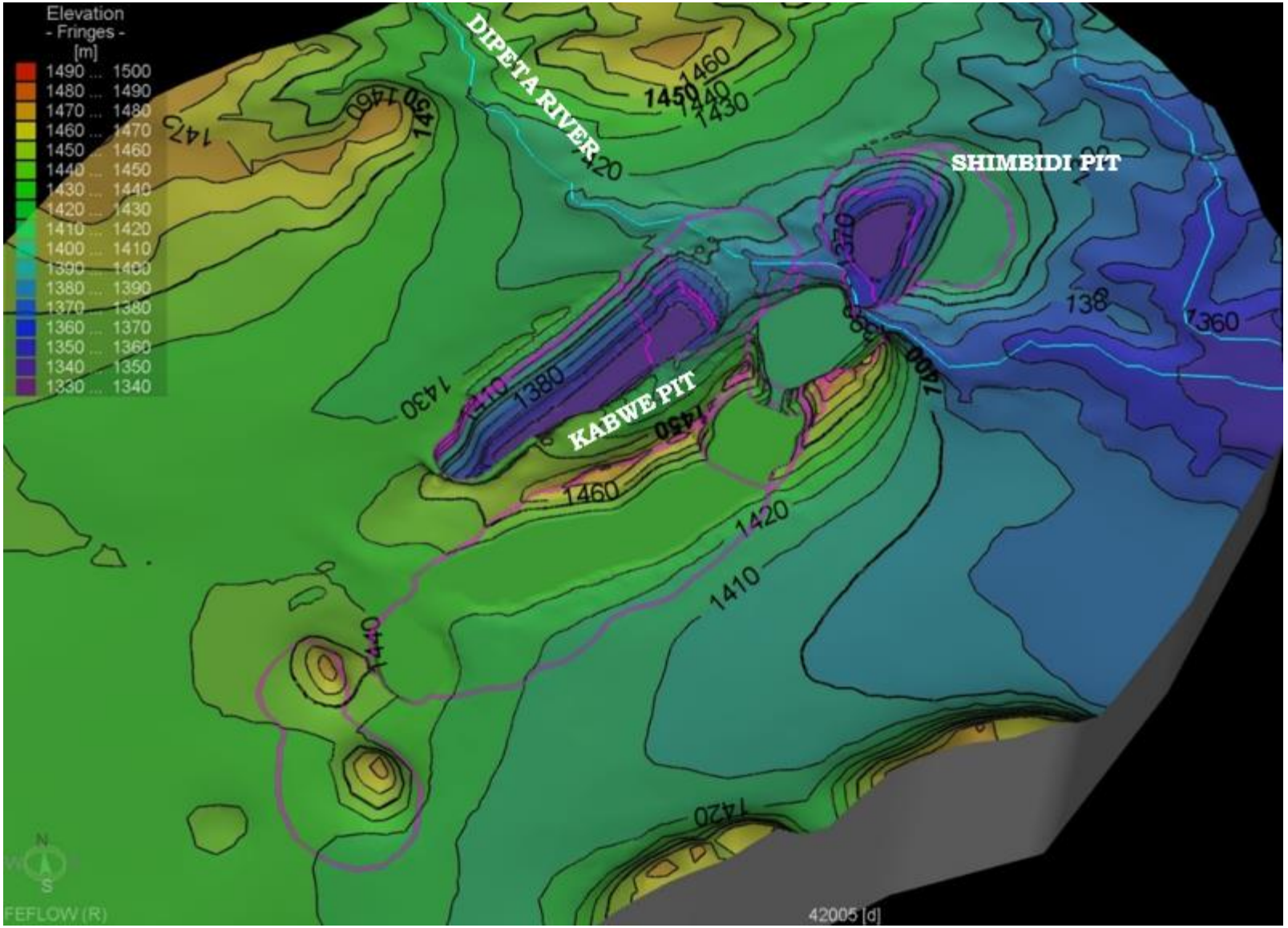

Figure 5-2: Current topography at the Kabwe and Shimbidi Mines

The Katanga Supergroup is divided into the Nguba, Roan and Kundelungu Groups (Batumike *et al.*, 2007). As shown in Table 5-1, the study area of this investigation is located in the Roan Group. This latter has four subgroups, which are from top to bottom: Mwashya (R4), Dipeta (R3), Mines (R2) and Roche Argilo-Talqueuse (RAT) (R1). The Mwashya Subgroup is composed of carbonaceous shales, siltstones and sandstone deposits (Cailteux *et al.*, 2007). According to François (1987), the Dipeta Subgroup consists of sandy-argillaceous rocks. As shown in Table 5-1 the Mines Subgroup consists of dolomite and dolomitic shales (Cailteux *et al.*, 2005). The RAT Subgroup mainly consists of sandy-argillaceous and dolomitic rock (François, 1995).

Occurring mainly in the Roan Group, the geological stratigraphy of the Tenke Complex has at its base the RAT Group (or clay talceous rocks). It is important to note that the abbreviation RAT refers to both the RAT Subgroup and to argillaceous talceous rocks in general. RAT (the rock type) occurs in both the RAT Subgroup (lilac to red in colour) and the Mines Subgroup (grey in colour) (refer to Table 5-1). In the Tenke Complex the lilac and grey RAT are respectively approximately 15 and 6 meters thick. Above the grey RAT in the Mines Subgroup, stratified dolomite (DStrat), followed by Roche Siliceuse Feuilletée (RSF) or fissile siliceous rocks, occur. The distribution of these different rock types within the study area are shown in Figure 5-3 (also refer to Table 5-1).

The Tenke Complex had a long and complex brittle evolution influenced by local and regional events (Kipata, 2013). The geological formations of the Tenke-Fungurume district are highly tectonised. The main trend of fault axes is north-west/south-east. All of these faults intersect the aquifer. Evidence for brittle tectonism is abundant in the study area. This tectonism caused extensive fracturing of the aquifers.

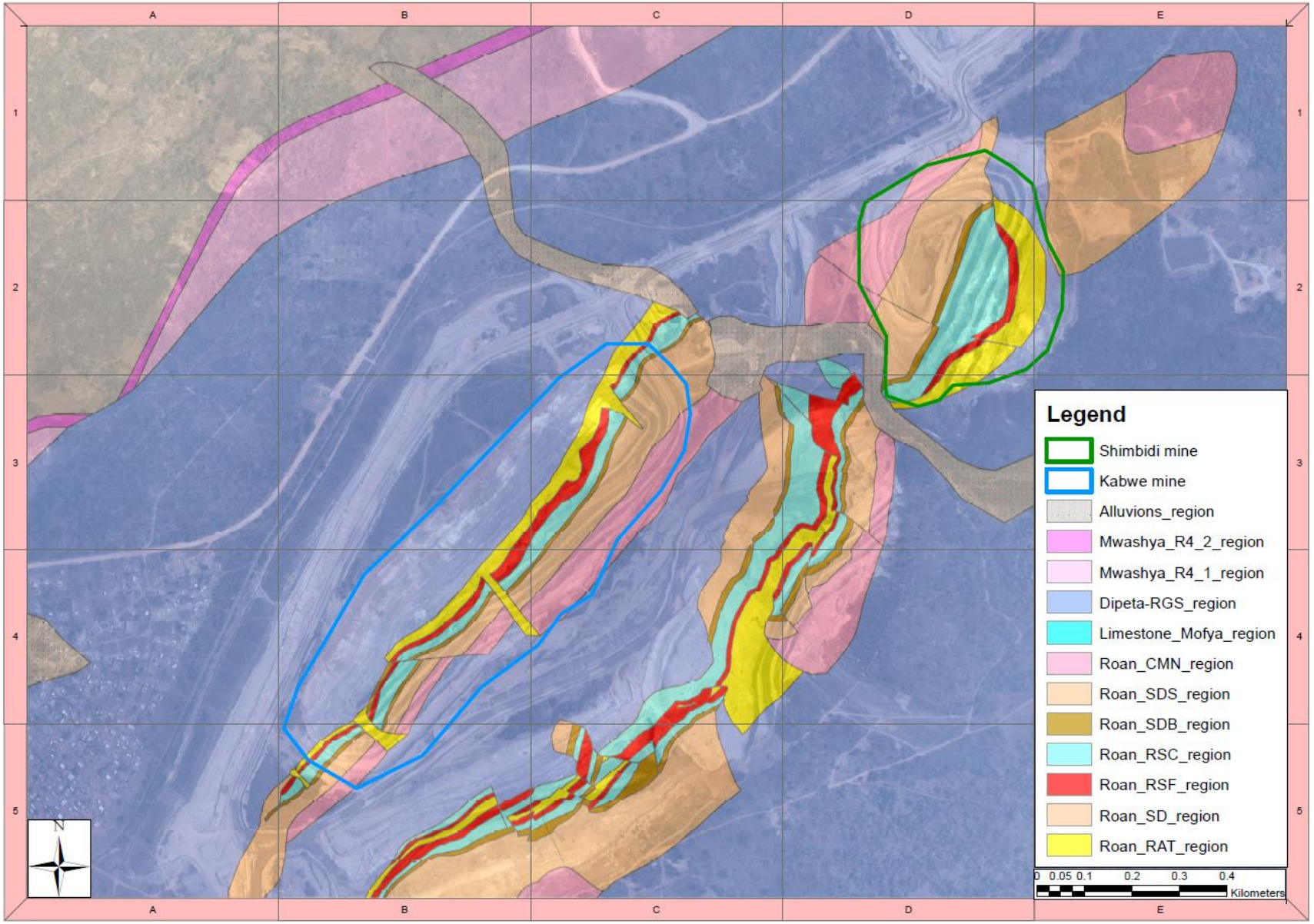

Figure 5-3: Geology of the Tenke Complex

Table 5-1: Stratigraphic columns of the Katangan Super-group in Congo compiled from Kipata et al. (2013) and Batumike et al. (2007).

Age (Ma)		Group	Subgroup	Formation	Lithology
±320	**Karoo**				
<573	**Katangan Supergroup**	**Kundelungu - Ku**	Biano - Ku 3		Arkoses, conglomerates and argillaceous sandstones
			Tectonic unconformity (orogenic paroxysm)		
			Ngule - Ku 2	Sampwe, Kiubo, Mongwe	Dolomitic pelites, dolomitic sandstones, siltstones and sandstones
±635			Gombela - Ku 1	Lubudi, Kanianga, Lusele, Kyadamu	pink oolithic sandstones, sandy carbonate beds, carbonates siltstones, micritic dolomite and glacial diamictites called " Petit conglomerat"
		Nguba - Ng	Bunkeya - Ng 2	Monwezi, Katete	dolomitic sandstones, siltstones, pelites, dolomites beds and shales
±730			Muombe - Ng 1	Kipushi, Kakontwe, Kaponda, Mwale	carbonates, carbonate shales, siltstones, dolomites, dolomitic shales and glacial diamictites called "Grand conglomerat"
		Roan - R	Mwashya - R 4	Kanzadi, Kafubu, Kamoya	Dolomitic shales, grey to black carbonaceous shales, quartzites
			Dipeta - R 3	R 3.4 (Kansuki), R 3.3 (Mofya), R3.2, R 3.1 (R.G.S)	Dolomitic shales, dolomites and shale with grit
			Mines - R2	CMN	Limestone, dolomite and carbonaceous clays
				SDS	Shale and sandstone with algal dolomite
				SDB	dolomitic shale
				RSC	Silicified algal dolomite
				RSF	Laminated dolomite
				Dstrat	Bedded dolomite
				Grey RAT	Grey argillaceous dolomitic siltstone
			RAT - R1	Lilac RAT	Argillaceous dolomitic silts-sandstones
±880		**Basal pebble and cobble conglomerate**			
±2050	**Kibaran and pre-Kibaran**				

5.7 HYDROGEOLOGICAL CHARACTERISTICS

The Mines Group of the Tenke Complex consists mainly of dolomite and dolomitic shale. Some of these rock units are more permeable than others. The dolomitic formations, especially the “Roche Siliceuse Cellulaire” (RSC), are karstic and their hydraulic parameters (permeabilities, hydraulic conductivities, storativities) are much higher than those of the sandstones layers or the dolomitic sandstone, such as RAT. The permeability of the rocks is controlled by the presence of fractures and cavities. The main aquifer comprises the SD, RSC, RSF, DSTRAT and RSF (refer to Figure 5-3 and Table 5-1). The RGS and RAT are generally not very permeable but these rock units can obtain secondary permeability if brecciated.

In some other areas of the Roan Group, geohydrological tests were performed by a government company (Gecamines) along with consultants, such as Geomines Inc. They found hydraulic conductivity values (vertical and horizontal) of rocks ranging from 0.00011 to 6.2 m/day.

Unfortunately, no known pumping tests have yet been performed on the aquifers of the Tenke Complex. The available hydraulic head data were recorded at existing wells and monitoring points at the open pit mines extracting ore from the complex. The positions of the wells and monitoring points relative to the mining activities in the study area are shown in Figure 5-4. The monitoring points are used to record hydraulics heads at a pre-defined time step. These head-vs-time measurements form the dataset that will be used in this chapter to investigate the applicability of the ANN developed in Chapter 4 in the prediction of the behaviour of the aquifers of the Tenke Complex during dewatering of the Kabwe and Shimbidi open pits.

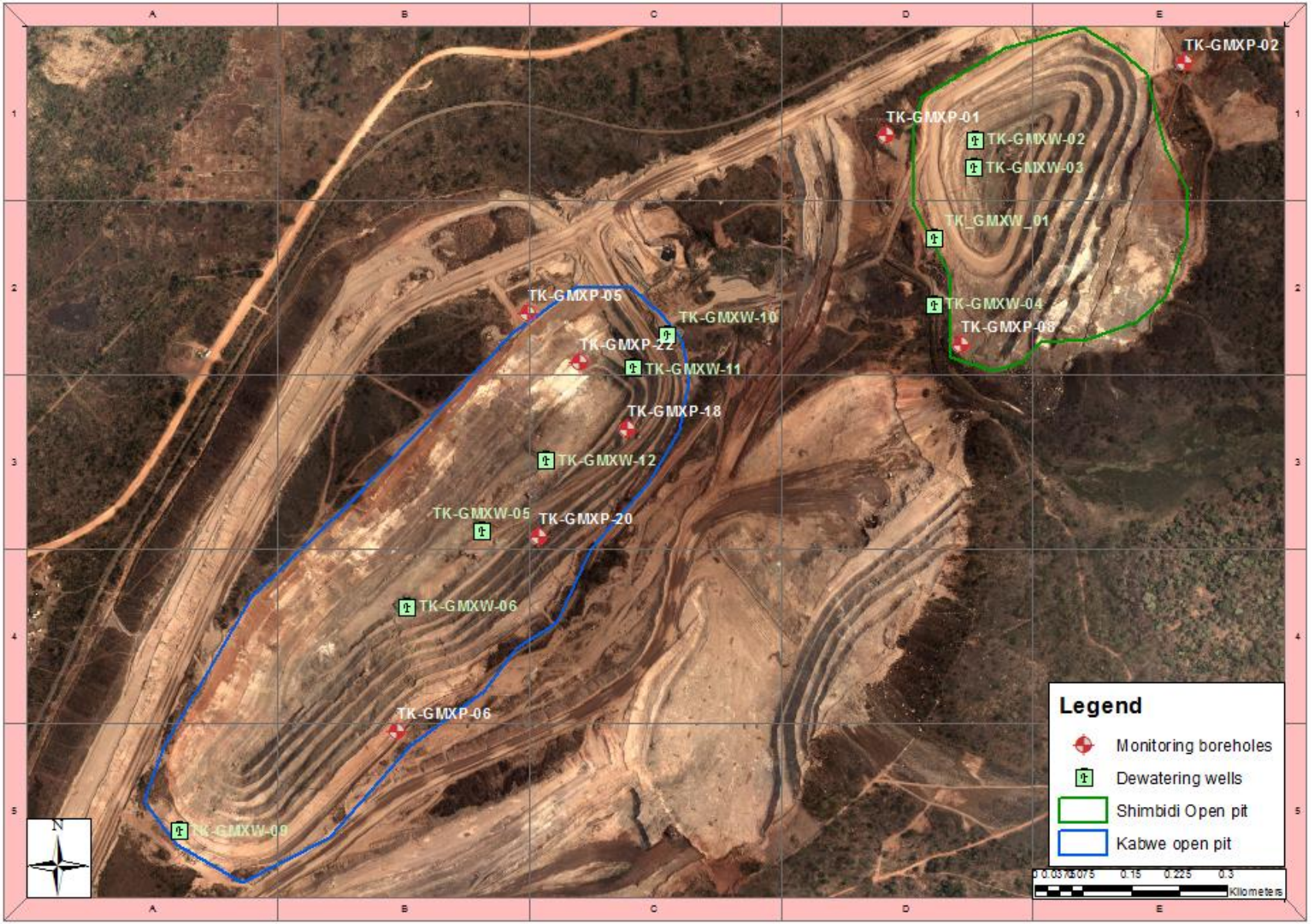

Figure 5-4: The positions of monitoring and pumping wells at the Kabwe and Shimbidi Mines

During dewatering of the open pits at the Kabwe and Shimbidi Mines, continuous monitoring of water levels, pumping rates and inflows was done. Nine dewatering wells were in operations at these two open pits. Some of these dewatering wells were pumping continuously while others encountered mechanical problem which put them out of commission for a couple days. The pumping rates of the dewatering wells were not constant during the dewatering activities. After air-lifting, some wells yielded up to 250 m^3/h, but the average flow of all wells was approximately 108 m^3/h.

5.8 HYDRAULIC HEAD PREDICTION USING THE ANN

For accurate predictions with an ANN, it is important to have a dataset of good quality, containing as much data as possible (Smith and Eli, 1995). In this study, hydraulics heads automatically recorded with Geokon data loggers at eight piezometers (TK-GMXP-01, 02, 05, 06, 08, 18, 20 and 22), as well as manual measurements, were used to train and validate the ANN.

The ANN used to predict hydraulic heads at the Kabwe and Shimbidi Mines was trained using observed hydraulic heads for the period from 03 January 2015 to 30 September 2015. The validation of the ANN was done using data recorded during the period from 05 October 2015 to 30 December 2015.

The ANN used for prediction is the network that performed best during the evaluation (refer to Chapter 4). This ANN is based on a feed-forward algorithm, has a single hidden layer, uses two inputs (hydraulics heads and date), and makes use of the hyperbolic tangent transfer function (HTF) to relate the inputs at each cell to an output from the cell. The maximum weight assigned to the connections of the ANN was 0.001, while the network was trained for up to 20 000 epochs.

5.8.1 RESULTS

The hydraulic head predictions made by the ANN are shown in Figure 5-5 along with the observed hydraulic heads. To allow visual comparison, the predictions at only three piezometers (TK-GMXP-01, 02 and 18) are shown in this figure.

From Figure 5-5, it can be seen that the ANN was successful in predicting the general behaviour of the hydraulic heads in terms of their absolute values and trends. However, the ANN was less successful at those piezometers where large fluctuations in the hydraulic heads were recorded. This is to be expected, since the ANN makes predictions based on patterns recognised in the training data. The ANN is therefore more adept at making predictions about the general temporal and spatial behaviour of the system, while short-period fluctuations are inherently unpredictable.

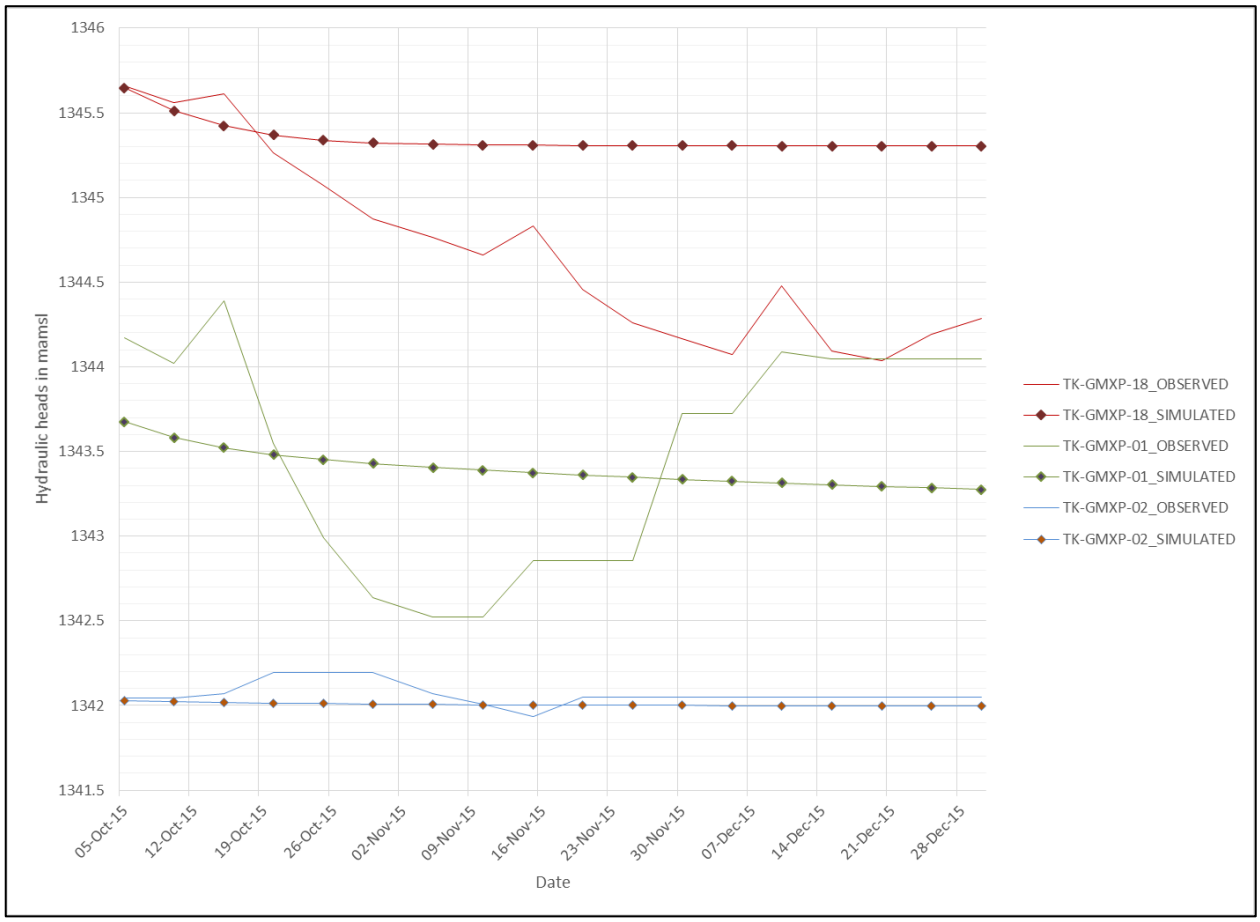

Figure 5-5: Observed and predicted hydraulic heads at three piezometers

It is also apparent from Figure 5-5 that the accuracy of the predictions at some piezometers become worse over time. This is especially noticed at piezometer TK-GMXP-18 where the initial prediction (05 October 2015) of the hydraulic head was good, but where the observed and predicted hydraulic heads diverged over time. Nonetheless, over the prediction period of approximately 3 months, the difference between the observed and predicted hydraulic heads never exceeded 1.5 m.

Profiles of the observed and predicted hydraulic heads across the open pits on 30 December 2015 are presented in Figure 5-6. From this figure it is seen that ANN successfully predicted the general behaviour of the hydraulic heads around and within the open pits. However, the predicted hydraulic heads were too high at certain positions, and too low in other positions. Particularly in the vicinity of the Shimbidi pit, where low hydraulic heads occur, the ANN overestimated the hydraulic head by more than 1.5 m.

It should be kept in mind that the ANN was trained using hydraulic head data recorded at eight piezometers during active pit dewatering. As stated in Section 5.7, the pumping rates of the dewatering wells were not constant during the dewatering activities and not all the dewatering wells were in operation during the period from 03 January 2015 to 30 December 2015. The variable pumping rates necessarily caused fluctuations in the hydraulic heads. The ANN's performance in predicting the general behaviour of the hydraulic heads is therefore quite remarkable. One cannot expect the ANN to predict the unpredictable.

From the profiles of the hydraulic heads in Figure 5-6, it seems that the ANN was more successful in predicting the hydraulic heads at positions were smaller drawdown occurred (in the vicinity of the Kabwe open pit), and less successful at positions where larger drawdowns occurred (in the vicinity of the Shimbidi open pit). This may prove to be a weakness of ANNs in predicting aquifer behaviour near dewatering wells.

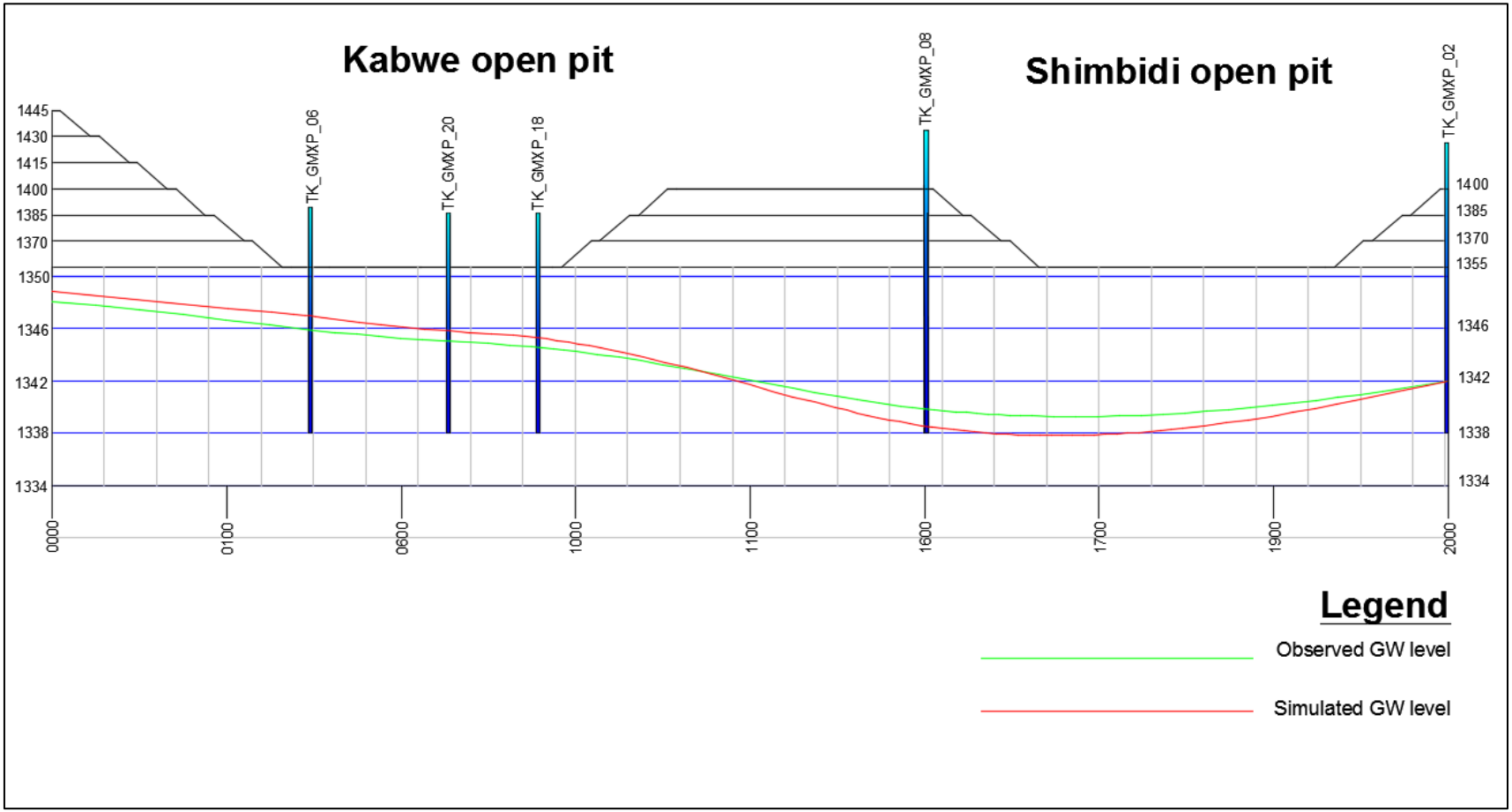

Figure 5-6: Observed and predicted (simulated) hydraulic heads on 30 December 2015

5.9 PERFORMANCE ANALYSIS

By comparing the predictions of the ANN with the observed hydraulic heads, it is seen that the ANN was more successful in predicting the hydraulic heads at some monitoring points than at others. For example, predictions for monitoring point TK-GMXP-02 were more accurate than for monitoring point TK-GMXP-18 (refer to Figure 5-5).

Furthermore, when comparing the results of the hydraulic head predictions at the Kabwe and Shimbidi Mines with the results of the predictions made for the synthetic (numerical) example (refer to Chapter 4), it is seen that the ANN performed much better with the synthetic data than with the real data. This is to be expected since the real hydraulic head data exhibited much more fluctuation due to factors such as the varying abstraction rates from the dewatering wells at the mines. Since ANNs function by recognising patterns in the training data and using these patterns to make general future predictions, such localised short-period fluctuations cannot be predicted.

Despite the above limitations, the ANN was able to predict the general behaviour of the aquifer system at the Kabwe and Shimbidi Mines. The values of the predicted hydraulic heads were generally within 1.5 m from the values of the observed hydraulic heads.

To further analyse the performance of the ANN in predicting the hydraulic heads at the Kabwe and Shimbidi Mines, the statistical and graphical evaluation techniques described in Section 2.4.6 will now be applied. Figure 5-7 shows the RMSE between the predicted and observed hydraulic heads. The RMSE is seen to vary from 0.08 for piezometer TK-GMXW-02 to 1.0 for the piezometer TK-GMXW-08. The RMSE is less than 1.0 at all the other piezometers, indicating a high agreement between the observed and predicted hydraulic heads.

Also shown in Figure 5-7 are the Pearson correlation coefficients, *r*, calculated at the different piezometers. This coefficient is less than 0.2 at piezometers TK-GMXW-08 and TK-GMXW-01, indicating very weak correlations between the observed and modelled data at these piezometers. However, the *r*-value at the other piezometers ranged from 0.2 to 0.94, which according to Smith (1995), shows that there is a good correlation between observed and simulated hydraulics heads. As

the ANN produced low values of RMSE and relatively high *r*-values, it can be concluded that the model was able to accurately predict the behaviour of aquifers of the Tenke Complex under dewatering conditions.

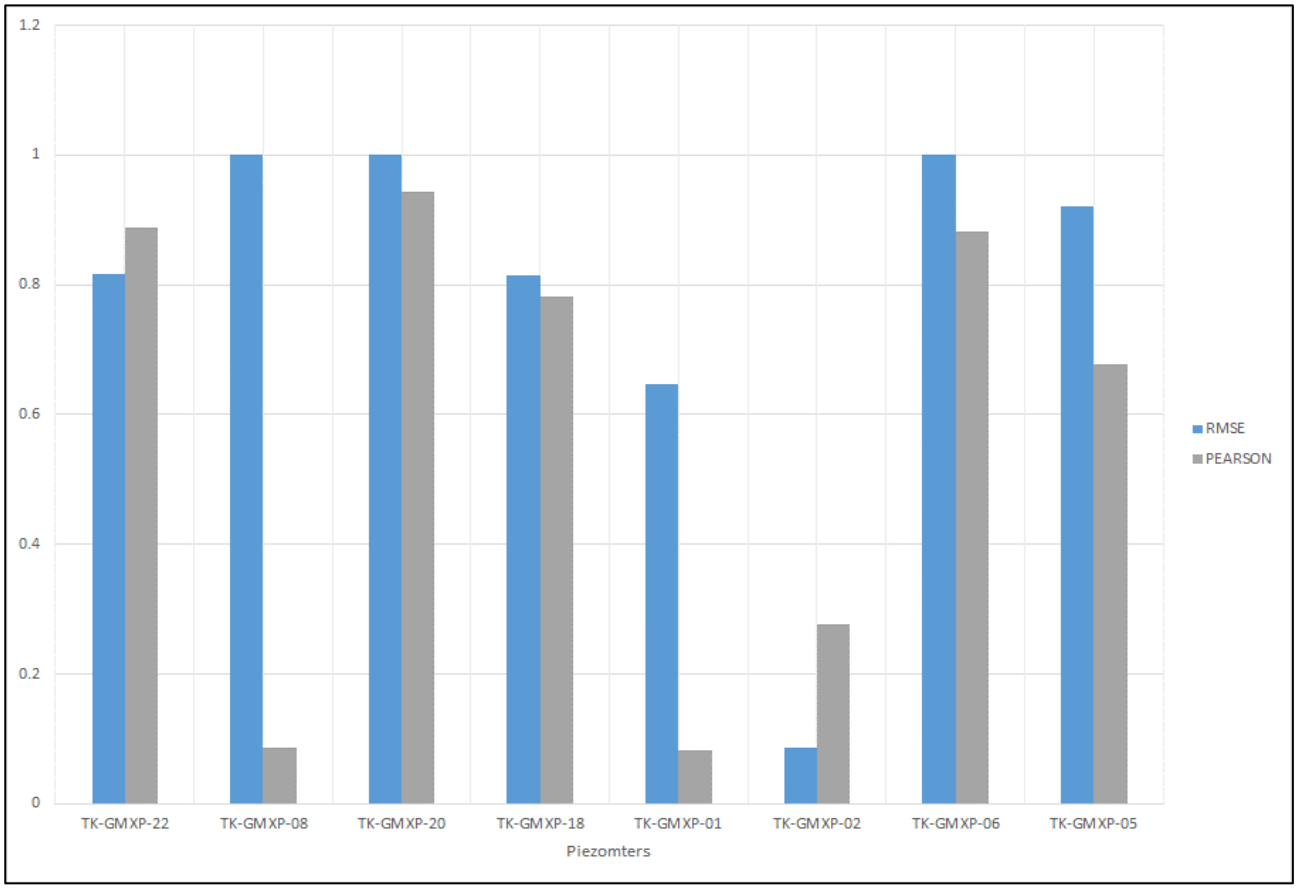

Figure 5-7: RMSE and Pearson correlation coefficient of the ANN model for each piezometer

Each evaluation technique has its strength and weakness (Chai and Draxler, 2014; Willmott and Matsuura, 2005). For greater certainty in the results of the performance analysis, other statistical techniques, such as the NSE, PBIAS, RSR, NRMSE and PI, were also used to evaluate the performance of the ANN.

The values of NRMSE and PI ranged respectively from 0.0001 to 0.0019 and from 0 to 0.0004 as shown in Figure 5-8. As these values are low, it can be concluded that the performance of the ANN model is good indicating that the model can well simulate the behaviour of groundwater for mine dewatering.

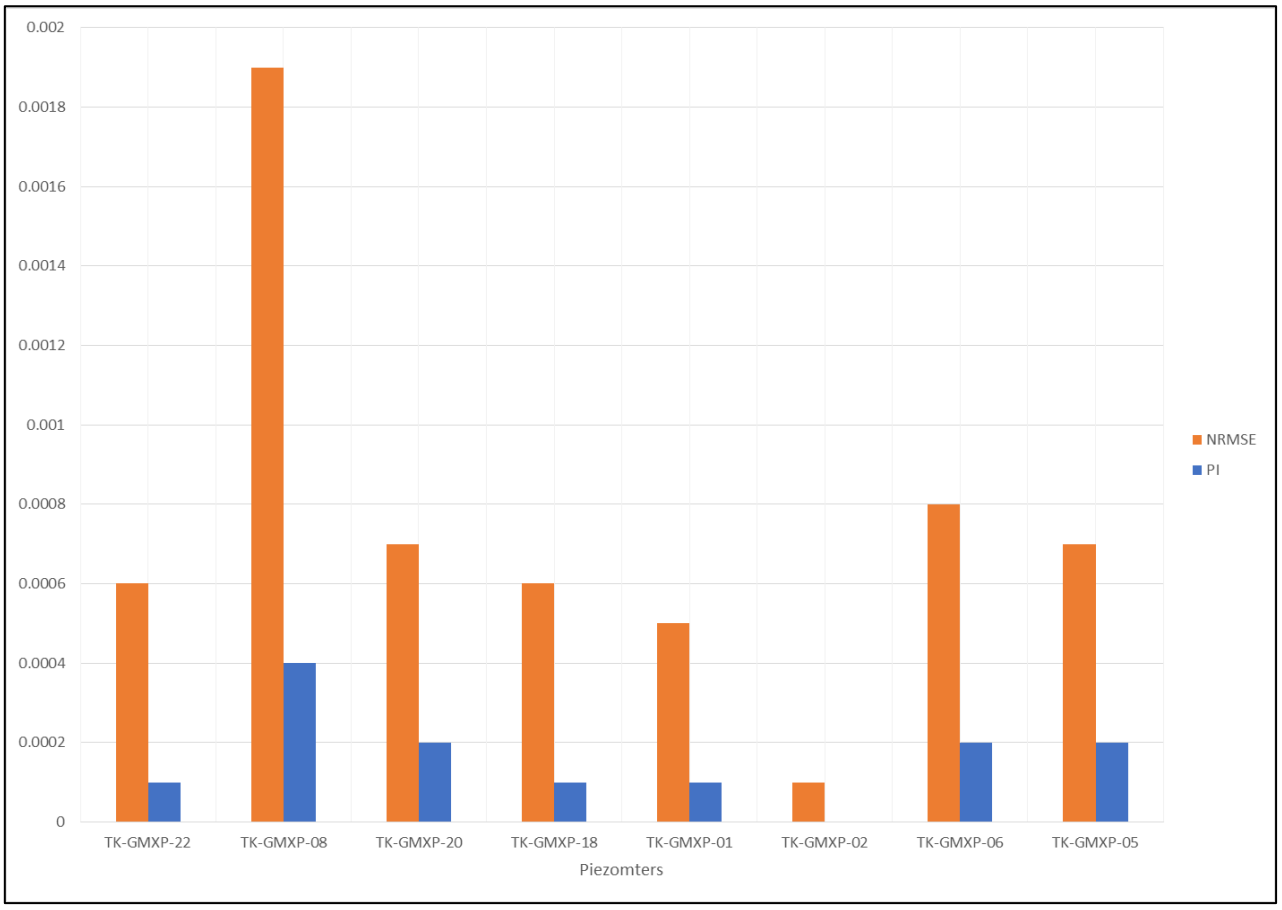

Figure 5-8: NRMSE and PI of the ANN model for each piezometer

Neglecting the outlier value (11.3) at piezometer TK-GMXP-08, the RSR-values calculated for the data at the other piezometers ranged from 0.7 to 2.7 (see Figure 5-9). Although these values of the RSR index suggest that the performance of the model was unsatisfactory, the NSE-values ranged from 0.9 to 1.0, which according to Moriasi *et al.* (2007) shows that the ANN was successful in predicting the groundwater behaviour at the Kabwe and Shimbidi Mines during dewatering.

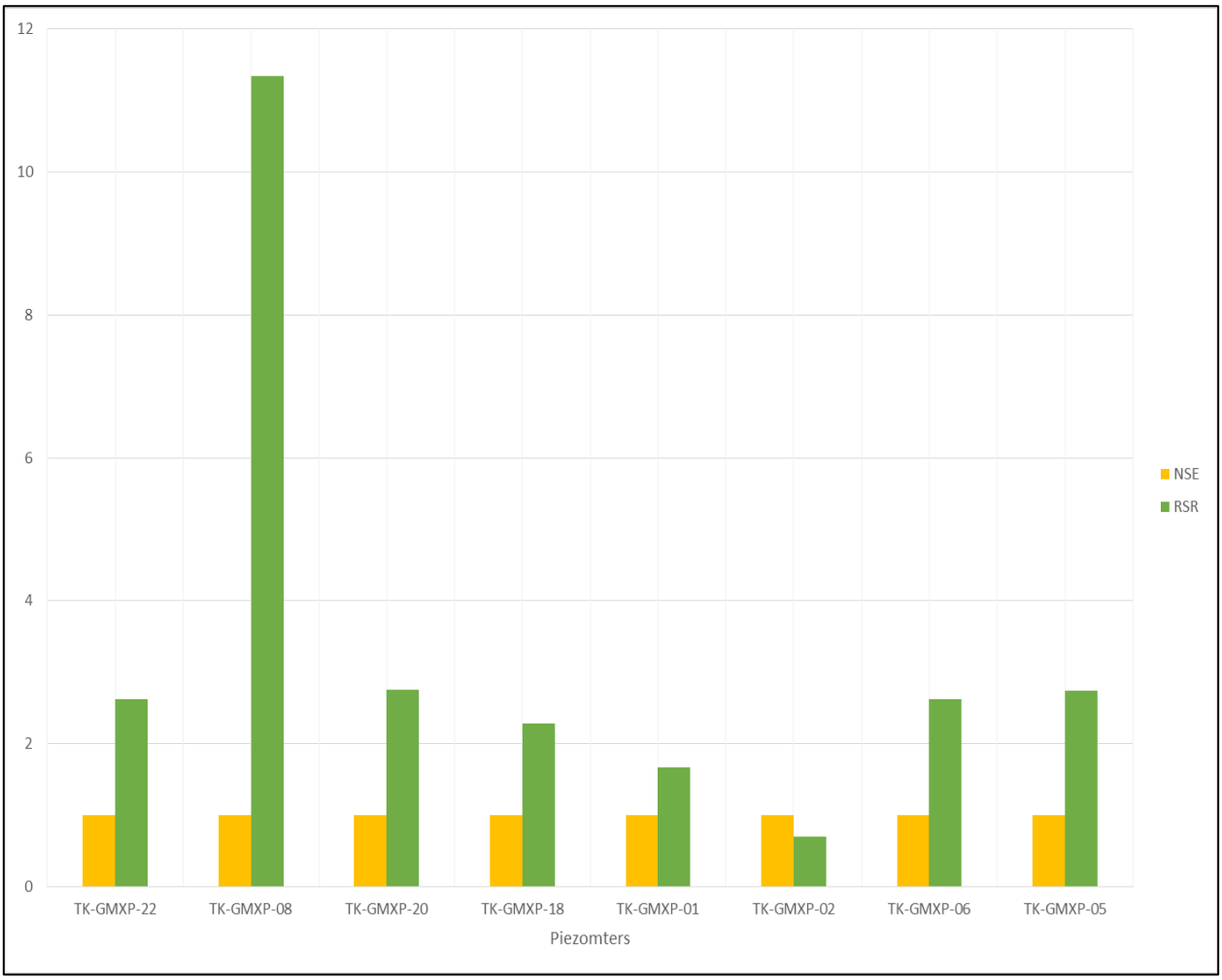

Figure 5-9: NSE and RSR of the ANN model for each piezometer

Figure 5-10 shows that the PBIAS calculated for the hydraulic head datasets at the different piezometers varied between -7% and 19%. These values show that the performance of the ANN ranged from good to very good according to the classification system suggested by Moriasi *et al.* (2002).

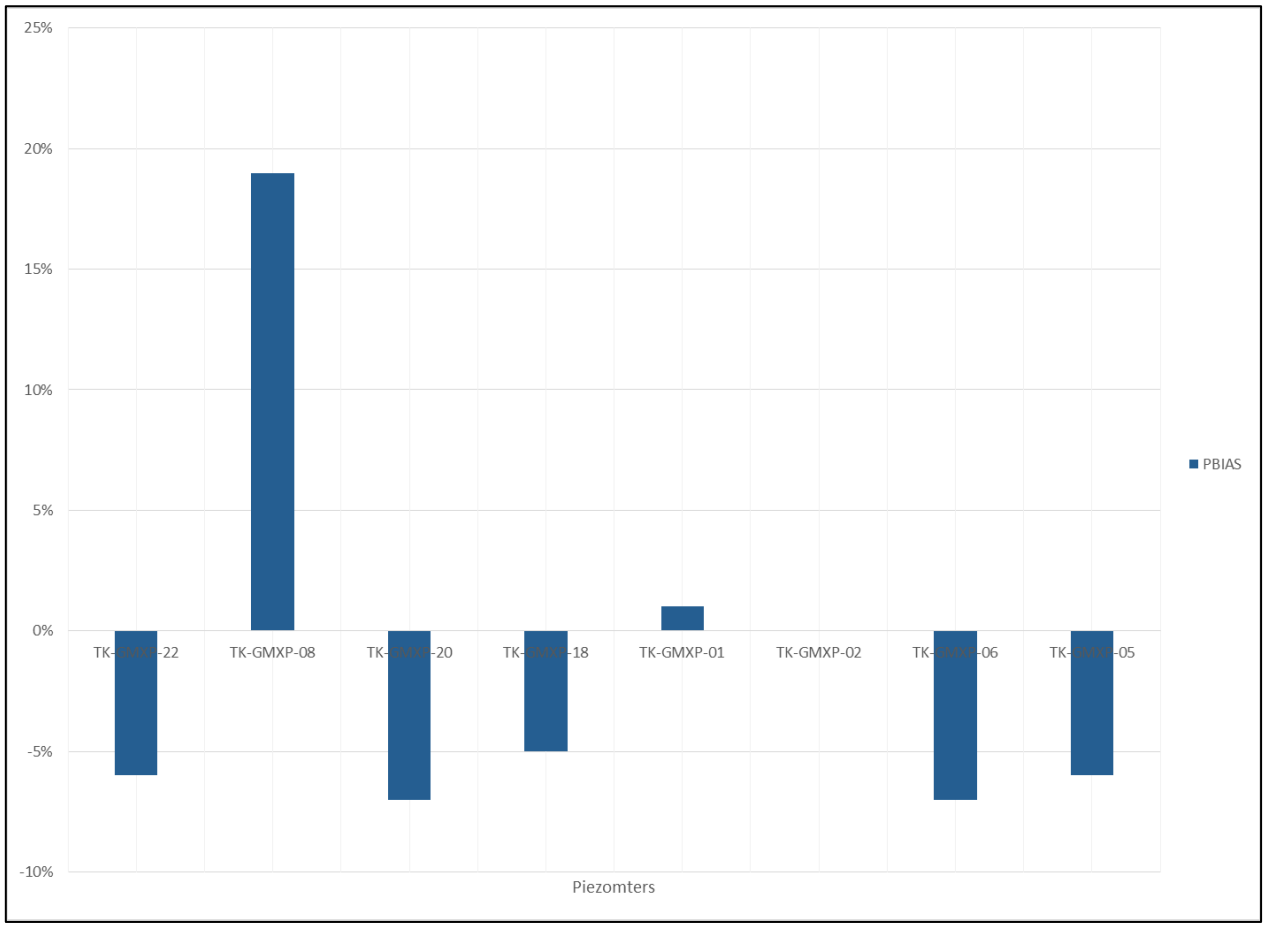

Figure 5-10: PBIAS of the ANN model for each piezometer

5.9.1 DISCUSSION

From the results of the different performance evaluation techniques used to assess the performance of the ANN, it can be concluded that the ANN was successful in predicting the hydraulic heads at the Kabwe and Shimbidi Mines under dewatering conditions. However, the accuracy of the predictions varied between the different piezometers. Particularly the predictions at piezometer TK-GMXP-08 were less accurate than the predictions at the other piezometers.

Piezometer TK-GMXW-08 is located between the two open pits (refer to Figure 5-6). The low hydraulic head observed at this piezometer was most probably due to the presence of two nearby dewatering wells (TK-GMXW-01 and TK-GMXW-04) which pumped continuously during the period from 05 October 2015 to 30 December 2015. Furthermore, dewatering well TK-GMXW-01 was drilled in the area between three mineralized zones and has a high yield. During the drilling of this well and piezometer TK-GMXP-08, a significant loss of water occurred in some layers. A fault is known to occur in the area where these two wells are located. This fault could

be responsible for the encountered water loss and may also be partly responsible for the low hydraulic head observed at piezometer TK-GMXW-08.

From the above observations it again appears that the ANN was more successful in predicting the hydraulic heads at positions of less drawdown in the groundwater. Near the dewatering wells, where larger drawdown occurred, the predictions of the ANN became worse, even though the difference between the observed and predicted hydraulic heads was rarely greater than 1.5 m.

5.10 APPROXIMATE MATHEMATICAL RELATIONS TO PREDICT HYDRAULIC HEADS

In mining environments, water management responsibilities often fall on the shoulders of geohydrologists and geohydrological engineers. When these professionals are off-site when mining operations have to continue, mining and construction engineers often have to take care of water management. Simplified methods of predicting the hydraulic heads in and around the mines are therefore required since mining and construction engineers are generally not familiar with groundwater modelling (or the use of ANNs to predict hydraulic heads).

As an example of how this may be done, equations approximating the drawdown in the hydraulic heads as a function of time were found for the Kabwe and Shimbidi Mines. The *CurveExpert* code was used to equations that approximate the hydraulic heads predicted by the ANN for the period 05 October to 30 December 2015. *CurveExpert Professional* is a code computed for data analysis and curve fitting. The particularity of this code is its ability to model data using linear regression, nonlinear regression or various splines (Solanki *et al.*, 2015). The equations for the drawdowns at the different piezometers are listed in Table 5-2, while graphs showing the modelled (FEM), predicted (ANN) and calculated (approximated) hydraulic heads at three piezometers are shown in Figure 5-11. The equations listed in Table 5-2 are all in a form known as the Richard's Equation and may be used to estimate the hydraulic heads at times later than 30 December 2015.

It should be kept in mind that the equations approximating the drawdown at the different piezometers were based on the hydraulic heads predicted by the ANN. This ANN was trained using input data recorded at the Kabwe and Shimbidi Mines during selected months (January to October 2015) when particular conditions

prevailed (i.e. pumping rates at dewatering wells, pumping duration, rainfall, etc.) The predicted hydraulic heads are therefore inherently based on the assumption that the future conditions will be similar to the conditions during the training period. If these conditions were to change significantly, both the predicted hydraulic heads and the equations approximating drawdown will no longer be valid. In such a case it would be necessary to retrain the ANN using input data representative of the new conditions before the predictions can be updated.

Table 5-2: Simplified relations between dewatering time and the predicted drawdown at the different piezometers

ID	NAME	FORMULAS
1	TK_GMXP_22	$\Delta(m) = \frac{9.52402}{(1+e^{112.427363-0.393106t})^{\frac{1}{102.296957}}}$
2	TK_GMXP_08	$\Delta(m) = \frac{12.471685}{(1+e^{106.770624-0.382018t})^{\frac{1}{41.314792}}}$
3	TK_GMXP_20	$\Delta(m) = \frac{9.384654}{(1+e^{20.039835-0.081411t})^{\frac{1}{5.996287}}}$
4	TK_GMXP_18	$\Delta(m) = \frac{9.662798}{(1+e^{100.947759-0.354335t})^{\frac{1}{94.413589}}}$
5	TK_GMXP_01	$\Delta(m) = \frac{9.722644}{(1+e^{122.910661-0.440679t})^{\frac{1}{48.28506}}}$
6	TK_GMXP_02	$\Delta(m) = \frac{3.648235}{(1+e^{87.934942-0.407278t})^{\frac{1}{45.949838}}}$
7	TK_GMXP_06	$\Delta(m) = \frac{10.534876}{(1+e^{29.980389-0.104830t})^{\frac{1}{28.99252}}}$
8	TK_GMXP_05	$\Delta(m) = \frac{8.096207}{(1+e^{107.385063-0.385063t})^{\frac{1}{56.565}}}$

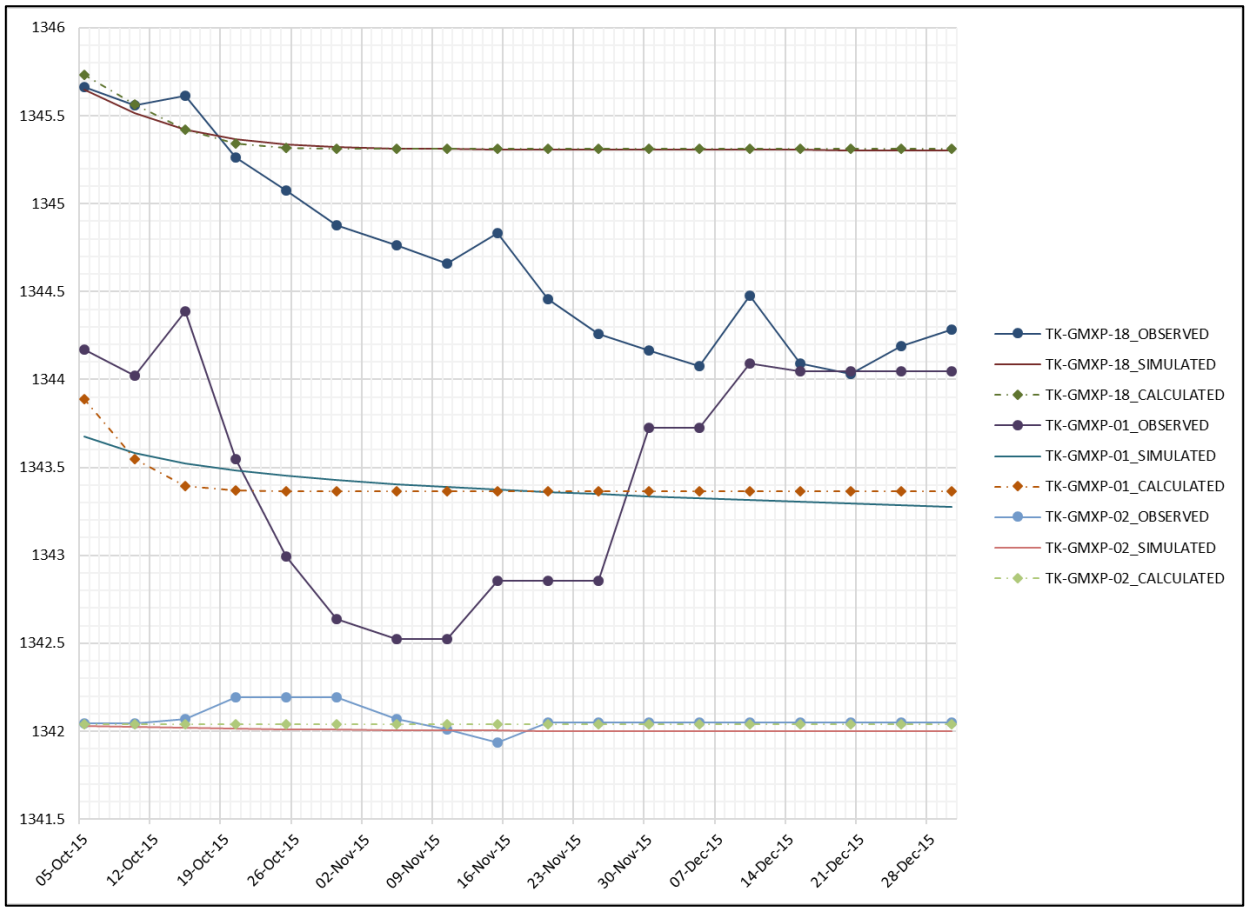

Figure 5-11: The observed, predicted (simulated) and calculated hydraulics heads at three piezometers

CHAPTER 6: CONCLUSIONS AND RECOMMENDATIONS

This study investigated the possibility of predicting the impact of dewatering operations at open pit mines where limited geohydrological data are available, by using ANNs. The advantage that ANNs offer is that these networks are able to recognise patterns in the observed data, without considering the underlying physical principles that govern the phenomena being studied. The values of specific parameters that influence the phenomena are also not required as inputs to the ANNs. ANNs can therefore operate in data-scarce environments.

Numerical groundwater modelling is commonly used to simulate the aquifer response during dewatering operations at mines. These methods are, however, expensive and require a lot of geohydrological data. At mines where limited data on the geohydrological conditions are available, ANNs offer the possibility of predicting the aquifer response to dewatering strategies by using historical datasets of the hydraulic heads recorded at different observation points over time. The ANNs can be trained using these historical datasets to make generalised predictions about the future behaviour of the aquifer under similar dewatering conditions.

In the current study, ANNs with different internal architectures were used to predict the aquifer response to dewatering strategies. First, the ANNs were applied to synthetic datasets, generated through a numerical groundwater model developed for a fictional mine. Different dewatering strategies, corresponding to different numbers of dewatering wells, were used to generate datasets of the hydraulic heads versus time at different observation points at the fictional mine. The ANNs were trained using parts of the generated datasets, and their performances were evaluated by using the remaining data in the datasets. Performance analyses were carried out by using different statistical and graphical evaluation techniques to assess the degree of agreement between the modelled and predicted datasets. The ANN that performed best in predicting the modelled hydraulic heads was selected for application to two real open pit mines.

The selected ANN was used to predict the hydraulic heads at the Kabwe and Shimbidi open pit mines where dewatering of the pits takes place. As with the

modelled fictional mine, hydraulic head data measured over a selected time period were used to train the ANN, while the hydraulic head data recorded over a subsequent time period were used to evaluate the performance of the ANN. Again, several statistical evaluation techniques were employed during the performance analyses.

The results of the performance analyses showed that the ANN was successful in predicting the general behaviour of the hydraulic heads at the two mines undergoing dewatering. However, the ANN was unsuccessful in predicting the short-term fluctuations in the hydraulic heads that result from changes in the abstraction rates at the dewatering wells. This is to be expected, since the ANN makes predictions based on patterns recognised in the training data. The ANN is therefore more adept at making predictions about the general temporal and spatial behaviour of the system, while short-period and localised fluctuations are inherently unpredictable. It should furthermore be noted that the ANN was more successful in predicting the hydraulic heads at positions of less drawdown than at positions of larger drawdown. This may prove to be a weakness of ANNs in predicting aquifer behaviour near dewatering wells.

An advantage of using ANNs to predict mine dewatering is the fact that the size of the dataset available for training constantly increases as new hydraulic head data are recorded. The potential of the ANNs to make accurate predictions increases accordingly as the historical record of the hydraulic heads expands.

To provide mining personal with a simple way of predicting the aquifer behaviour during mine dewatering operations, simplified mathematical equations describing the predicted drawdown over time were found. These equations give approximations of the predicted drawdowns in the different piezometers at the mines. It should, however, be kept in mind that the predictions made by the ANN are inherently based on the assumption that the future conditions at the mines will be similar to the conditions during the training period. If these conditions were to change significantly, both the predicted hydraulic heads and the equations approximating drawdown will no longer be valid.

Considering the performance of the ANN at the Kabwe and Shimbidi Mines, the following actions are recommended for future investigations into the application of ANNs for mine dewatering predictions:

- Four different ANN architectures were used in the current investigations. These architectures were found to give the best approximations to the hydraulic heads found from a numerical model developed for a fictional mine. The architectures were selected through a trial-and-error process. It is possible that the optimal architecture that would have yielded the best hydraulic head predictions was excluded during the trial-and-error selection of ANN architectures. It is therefore recommended that an investigation be launched to systematically study the impact of network architecture on network performance, specifically for ANNs used to predict hydraulic heads near mine dewatering operations.
- Only hyperbolic tangent and sigmoidal transfer functions were used in this study. These transfer functions were chosen because they are well suited to predict the non-linear behaviour of groundwater impacted by dewatering processes. For future studies, it is recommended that other non-linear transfer functions should be employed to evaluate whether such transfer functions could improve the performance of the ANNs in predicting hydraulic heads near dewatered open pit mines.
- In this study, an ANN was applied to only two adjacent open pit mines in the DRC. It is recommended that ANNs be used at more real mines to evaluate the performance of these networks under real world conditions. The application on the ANNs should also be extended to underground mines where dewatering is required for mining operations to continue.
- When ANNs are used at mines to predict the hydraulic heads, these networks should be retrained every six months using all the data recorded up to the date of retraining. In this way the training dataset will continually expand allowing for better pattern recognition and more accurate predictions to be made.

For mine wishing to implement ANNs to predict the groundwater response to dewatering based on the historic records of hydraulic heads recorded at piezometers, the following steps are recommended:

- An ANN should be developed using codes such as NeuroXL Predictor. The results of this thesis showed that a network with only one hidden layer with six neurons should suffice.
- The developed ANN should use non-linear transfer functions at its neurons to allow for better prediction of the non-linear response of the complex groundwater system. It is recommended that the Hyperbolic Tangent Function be used.
- It is recommended that the following values be used for the learning rate, momentum rate and initial weights of the ANN: 0.3, 0.2 and 0.2. These values were found to yield the best performance during the current investigations.
- For training purposes, it is recommended that the first 75% of the historical record of hydraulic heads during dewatering be used, while the last 25% be used to test the performance of the ANN in predicting the hydraulic head.
- If the performance of the ANN is poorer than desired, small adjustments (less than 10%) to the learning rate, momentum rate and initial weights of the ANN should be made in a trial-and-error manner until the performance of the ANN is satisfactory.
- The ANN should then be used to predict the future hydraulic heads in the vicinity of the dewatered mine. Validation of the predictions will be an ongoing process as new hydraulic head data recorded at the mine can be compared with the predicted hydraulic heads. If poor agreement is found, the ANN should be retrained using an adjusted training dataset which includes more recent hydraulic head data. Further adjustments to the learning rate, momentum rate and initial weights of the ANN may also be required.

REFERENCES

Abdulla, F.A., Al-Khatib, M.A., Al-Ghazzawi, Z.D. 2000. *Development of groundwater modeling for the AZROQ basin*. Environ Geol., 40(1/2):11–18.

Abrahart, R. J. and See L. M., 2007. *Neural network modelling of non-linear hydrological relationships*. Hydrol. Earth Syst. Sci., 11: 1563–1579.

Abramowitz, M. and Stegun, I. 1972. *Handbook of mathematical functions with formulas, graphs, and mathematical tables*, New York.

Acworth, R.I., Greenbaum, D. and Wyns, R. 2001. *The development of crystalline basement aquifers in a tropical environment*, Quarterly Journal of Engineering Geology. 20: 265-272.

Allende, H., Moraga, C. and Salas, R. 2002. *Artificial neural networks in time series forecasting: a comparative analysis*, Kibernetika, 38 (6): 685-707.

Amari, S., Murata, N., Muller, K., Finke, M. and Yang, H. 1997. *Asymptotic statistical theory of overtraining and cross-validation*, IEEE Transactions on Neural Networks, 8(5): 985-996.

Anderson, D., McNeill, G.1992. *Artificial Neural Networks Technology*. Kaman Sciences Corp., New York, 13502-4627.

Anderson, M. P., and Woessner, W. W. 1991. *Applied groundwater modeling, simulation of flow and convective transport*, Academic San Diego, Calif.

Anderson, M.P. and Woessner, W.W. 1992. *Applied groundwater modeling simulation of flow and advective transport*, Academic press, California, 373 p.

Anscombe, F., 1961. *Examination of residuals*. Proc. Fourth Berkeley Symp. Math. Statist. Prob. I, 1-36.

Anthony K. 2009. *An integrated surface–groundwater model of the Roper River Catchment, Northern Territory*, Dept of Natural Res., env, art and sport, Australian gov. 69 p.

Ardejani, D. and Tonkaboni, S. 2009. *Modeling the environmental field*. The University of Shahrood.

Ardejani, F.D., Sadeghiamirshahidi, M., Singh, R.N., Kish, T.E., Reed, S.M. 2013. *Prediction of the groundwater rebound process in a backfilled open cut mine using an artificial neural network*, Mine Water Env., 32: 251 – 257.

Aryafar, A., Ardejani, F., Singh, R. and Shokri, B. 2007. *Prediction of groundwater inflow and height of the seepage face in a deep open pit mine using numerical finite element model and analytical solutions*, IMWA Symposium: Water in Mining Environments, Cagliari, Italy.

ASCE, 2000a. *Task Committee on Application of Artificial Neural Networks in Hydrology. Artificial neural networks in hydrology. I: Preliminary concepts*. Journal of Hydrologic Engineering, 5 (2): 115–123.

ASCE, 2000b. *Task Committee on Application of Artificial Neural Networks in Hydrology. Artificial neural networks in hydrology. II: Hydrologic applications*. Journal of Hydrologic Engineering, 5 (2): 124–137.

Atkinson, A. 1985. *Plots, Transformations and Regression*. Oxford University Press, Oxford.

Azaïs, J, Bardet, J. 2005. *Le modèle linéaire par l'exemple*, Dunod.

Aziz, A. and Wong, K. 1992. *A neural network approach to the determination of aquifer parameters,* Ground Water, 30 (2): 164 – 166.

Bahrami, S., Ardejani, F.D., Baafi, E. 2016. *Application of artificial neural network couped with genetic algorithm and simulated annealing to solve groundwater inflow problem to an advancing open pit mine*, J. Hydrol., 536: 471 – 484.

Bakker, M. 1999. *Simulating groundwater flow in multi aquifer systems with analytical and numerical Dupuit models*, J. Hydrol., 222, 55-64.

Balint, S. and Balint A. 2007. *Mathematical models for mass and heat transport in porous media – Part I*, West University of Timisoara, Romania.

Banerjee, P., Singh, V.S., Chatttopadhyay, K., Chandra, P.C., Singh, B. 2011. *Artificial neural network model as a potential alternative for groundwater salinity forecsting*, J. Hydrol., 398: 212 – 220.

Barnett, B., Townley, L., Post, V., Evans, R., Hunt, R., Peeters, L., Richardson, S., Werner, A., Knapton, A. and Boronkay, A. 2012. *Australian groundwater*

modelling guidelines, Waterlines Report, National Water Commission, Canberra.

Batumike, M., Cailteux, J. and Kampunzu, A. 2007. *Lithostratigraphy, base metal deposits, and regional correlations of the Neoproterozoic Nguba and Kundelungu rock successions in central African Copperbelt*. Gondwana Research, 11 (3): 432 – 447.

Box, G. and Cox, D. 1982. *An analysis of transformations revisited*. J. Amer. Statist. Assoc., 77, 209-10.

Brawner, C. 1982. *Control of groundwater in surface mining. International journal of mine water*, 1: 1 – 16.

Brown, M. and Harris, C. 1994. *Neurofuzzy adaptive mmodeling and control*. Prentice hall, Englewood Cliffs, New Jersey.

Brown, K. and Trott Sh. 2014. *Groundwater flow model in open pit mining: can we do better?* , Mine Water Environ, 33: 187 – 190.

Cailteux, J., Kampunzu, A., Lerouge C., Kaputo, A. and Milesi J. 2005. *Genesis of sediments-hosted stratiform copper-cobalt deposits in central African Copperbelt*. Journal of African Earth Sciences, 42 (1-5): 134 – 158.

Cailteux, J., Kampunzu, A. and Lerouge C. 2007. *The Neoproterozoic Mwashya-Kansuki sedimentary rock succession in the central African Copperbelt, its mineralisation, and regional correlations*, Gondwana Research, 11 (3): 414 – 431.

Carslaw, H.S. and Jaeger, J.C. 1959. *Conduction of Heat in Solids*, Oxford University: Clarendon press.

Chai, T. and Draxler, R. 2014. *Interactive comment on « Root mean square error (RMSE) or mean absolute error (MAE)*. Geosci., Model Dev. Discuss., 7: 589 – 590.

Chambers, J., Cleveland, W., Kleiner, B. and Tukey, P. 1983. *Graphical Methods for Data Analysis*. Belmont, CA: Wadsworth.

Chang, D. and Lacy, H. 2008. *Artificial ground freezing in geotechnical engineering*. International Conference on Case Histories in Geotechnical engineering. Paper 55.

Chitsazam, M., Rahmani, G., Neyamadpour, A. 2013. *Groundwater level simulation using artificial neural network: study from Aghili plain, urban of Gotvand, south-west Iran*, J. Geope, 3: 35 – 46.

Cho, S. 2009. *Probabilistic stability analyses of slopes using the ANN-based response surface*, Computer and Geotechnics, 36: 787 – 797.

Cohen, J. and Cohen, P. 1983. *Applied multiple regression / correlation analysis for the behavioral sciences*. Hillsdale, NJ: Lawrence Erlbaum Associates, Inc.

Cook, R. and Weisberg, S. 1994. *An Introduction to Regression Graphics*. Wiley, New York.

Cortez, P., Rocha, M., Machado, J. and Neves, J. 1995. *A Neural Network Based Forecasting System,* In Proceedings of ICNN 95, International Conference on Neural Networks, Perth, Western Australia.

Coulibaly, P., Anctil,F.O., Aravena, R. and Bobe, B. 2001. *Artificial neural network modeling of water table depth fluctuation*. Water Resource Research, 37 (4): 885–896.

Craig, J. and Read, W. 2010. *The future of analytical solution methods for groundwater flow and transport simulation*. XVIII International Conference on Water Resources, CMWR, Carrera, Barcelona, P. 8.

Csoma, R. 2001. *The analytic element method for groundwater flow modelling*, Periodica Polytechnica Ser. Civ. Eng., 45 (1): 43 – 62.

Costabel, M and Stephan, E. 1985. *A direct boundary integral equation method for transmission problems*. Journal of Mathematical Analysis and Applications.106: 367 – 413.

Cybenko, G. 1989. *Approximation by superposition of a sigmoid function*. Mathematics for Control, Signals and Systems, 2 (4): 303 – 314.

Das, A. and Datta, B. 2001. *Application of optimisation techniques in groundwater quantity and quality management*, Sadhana, 26 (4): 293–316.

Daw, G. and Pollard, C. 2006. *Grouting for groundwater control in underground mining*. International Journal of Mine Water. 5 (4): 1 – 40.

Dhatt, G., Touzot, G., Lefrancois, E. 2012. *Finite Element Method*, John Wiley & Sons.

Diersch, H. 2004. *Feflow: interactive, graphic – based finite – element simulation system for modelling groundwater flow, contaminant mass and heat transport processes*. Getting Started. 5 (1).

Doherty, J.E., Hunt, R.J. and Tonkin, M.J. 2010. *Approaches to highly parameterized inversion: a guide to using PEST for model-parameter and predictive-uncertainty analysis*, US Geological Survey Scientific Investigations Report, 2010–5211.

Domenico, P., Schwartz, F. 1998. *Physical and chemical hydrogeology*, 2nd Edition, Wiley.

Dowling, J., Beale, G. and Bloom, J. 2013. *Designing a large pit scale pit slope depressurization system at Bingham Canyon*, Reliable mine water technology, 1: 119 – 125.

Ehrenberg, A. 1975. *Data Reduction: Analysing and Interpreting Statistical Data*, New York: Wiley.

Elango, L. 2005. *Numerical modelling- an emerging tool for sustainable management of aquifers*. Journal of applied hydrology, 18 (4): 40-46.

Ella, V.B. 2004. *Numerical groundwater models as powerful tools for sustainable groundwater resources management in the Philippines*. AGRIS 2013 - FAO of the United Nations.

Ellis, G., Yao, C., Zha, R. and Penumadu, D. 1995. *Stress – strain modeling of sand using artificial neural networks*. J. Geotech. Eng. 121 (5): 429 – 435.

Farrokhzad, F., Choobbasti, A., and Barari, A. 2010. *Artificial neural network model for prediction of liquefaction potential in soil deposits.* International Conferences on Recent Advances in Geotechnical Earthquake Engineering and Soil Dynamics, Paper 4.

Fay, I. and Barton, M 2011. *Alteration and ore distribution in the Proterozoic mines series, Tenke – Fungurume Cu- Co district in the Democratic republic of Congo*. Springer - Verlag. Miner Deposita.

FemLab User Guide, 2015. *An introduction to FEMLAB's Multiphysics modeling capabilities*. Burlington, 40p.

Feng, S., Kang, S. and Huo, Z. 2008. *Neural Networks to Simulate Regional Ground Water Levels Affected by Human Activities*, Ground Water, 46 (1): 80 – 90.

Ferraresi, M. 1989. *An integrated finite difference model for groundwater flow and quality simulation*, Groundwater Management: Quantity and Quality, IAHS, 188: 321 – 330.

Fowler, A. 1998. *Mathematical Models in the Applied Sciences*, Cambridge University Press.

France, P. 1974. *Finite element analysis of three dimensional groundwater flow problems,* J. Hydrol., 21: 381-398.

François, A. 1987. *Synthèse géologique sur l'arc cuprifère du Shaba (Rep. Du Zaïre).* Centenaire de la Société Belge de Géologie. 15 – 65.

François, A. 1995. *La structure tectonique du Katanguien dans la région de Kolwezi (Shaba, Rep. Du Zaïre).* Annales de la Société Géologique de Belgique. 116 (1): 87 –104.

François, A. 2006. *La partie centrale de l'Arc cuprifere du Katanga: étude géologique*, Tervuren African Geosciences Collection, 109 : 61.

Gilberto, E. and Urroz, E. 2004. *Numerical solution to ordinary differential equations.*http://ocw.usu.edu/Civil_and_Environmental_Engineering/Numerical_Methods_in_Civil_Engineering/ODEsMatlab.pdf.

Goh, A., Kulhawy, F. and Chua, C. 2005. *Bayesian neural network analysis of undrained side resistance of drilled shafts*, Journal of Geotechnical and Geoenvironmental Engineering, 131 (1): 84 – 93.

Golder Associates. 2007. *Environmental and social impact assessment. Report to Tenke Fungurume Mining, Democratic Republic of the Congo.* March 2007.

Gupta, H., Sorooshian, S. and Yapo, P. 1999. *Status of automatic calibration for hydrologic models*, Journal of Hydrologic Engineering, 4 (2): 135 – 143.

Gomez, H., Lorenzis, L. 2016. *The variational collocation method*, Computer Methods in Applied Mechanics and Engineering, 309: 152-181.

Haitjema, H. and Mitchell-Bruker, S. 2005. *Are a water table a subdued replica of the topography?* Ground Water, 43: 781 – 786.

Hajek, M. 2005. *Neural Networks*, University of Kwazulu Natal, 114p.

Hantush, M. 1964. *Hydraulics of wells*, in Advances Hydro-Sciences. Academic press. PP. 281 – 442.

Härdle, W. 1990. *Applied nonparametric regression*, Cambridge University Press, 1990.

Hashash, Y.M.A., Jung, S. and Ghaboussi, J. 2004. *Numerical implementation of a neural network based material model in finite element analysis*, International Journal for Numerical Methods in Engineering, 59: 989–1005.

Heinl M., Brinkmann P.J. 1989. *A groundwater model of the Nubian aquifer system*, Hydrol. Sci. J., 34: 425–447.

Heinz, W.F. 1997. *Cover grouting: a rational approach*. Proceedings of the 6th International Mine Water Congress, Bled, Slovenia.

Holland, K., Overton, I., Jolly, I., Walker, G. 2004. *An analytical model to predict regional groundwater discharge patterns on the floodplains of s semi – arid Lowland River*. CSIRO Land and Water Technical Report No. 6/04. 35p.

Hsieh, C. 1993. *Some potential applications of artificial neural systems in financial management*, Journal of Systems Management, 44(4), 12-15.

Huet, S., Bouvier, A., Gruet, M. and Jolivet, E. 1996. *Statistical Tools for Nonlinear Regression*, Springer.

Hsu, K., Gupta, H., and Sorooshian, S. 1995. *Artificial neural network modeling of the rainfall-runoff process*, Water Resources, 31 (10), 2517 -2530.

Igboekwe, M.U. 2014. *Finite Element Method of Modeling Solute Transport in Groundwater Flow*. Pacific Journal of Science and Technology, 15(1):85-92.

Joorabchi, A., Zhang, H. and Blumenstein, M. 2009. *Application of artificial neural networks to groundwater dynamics in coastal aquifers*. Journal of Coastal research, 56: 966 – 970.

Jorgensen, G. 1974. *Analog-model studies of groundwater hydrology in the Houston district, Texas*, U.S. Geol. Survey open file report, 87p.

Juan, C., Genxu, W., Tianxu, M. 2015. *Simulation and prediction of suprapermafrost groundwater level variation in response to climate change using neural network model*, J. Hydrol., 529: 1211 -122.

Karahan, H. and Ayvaz, M.T. 2005. *Time-Dependent Groundwater Modeling Using Spreadsheet*, Computer applications in engineering education, 13: 192 -199.

Karahan, H. and M. T. Ayvaz, M.T. 2005. *Transient groundwater modeling using spreadsheets*, Adv. Eng. Software, 36: 374-384.

Karplus, W.J. 1976. *The future of mathematical models of water resources systems*. In System Simulation in Water Resources, 11 – 18.

Kelson, V.A., Hunt, R.J., Haitjema, H.M. 2002. *Improving a regional model using reduced complexity and parameter estimation*, Groundwater, 40 (2): 132 – 143.

Khashei, M. and Bijari, M. 2009. *An artificial neural network (p, d, q) model for time series forecasting*, Expert Systems with Applications, 37 (2010) 479–489.

Khashei, M., Hejazi, S. R., & Bijari, M. 2008. *A new hybrid artificial neural networks and fuzzy regression model for time series forecasting*, Fuzzy Sets and Systems, 159: 769–786.

Kipata, L. 2013. *Brittle tectonics in the Lufilian foldand- thrust belt and its foreland: an insight into the stress field record in relation to moving plates (Katanga, DRC)*, Phd thesis KU Leuven, Faculty of Science, 160p.

Kipata, L., Delvaux, D., Sebagenzi, M., Cailteux, J. and Sintubin, M. 2013. *Brittle tectonic and stress field evolution in the Pan-African Lufilian arc and its foreland (Katanga, DRC): from orogenic compression to extensional collapse, transpressional inversion and transition to rifting*, Geologica belgica, 16 (1-2): 1 – 17.

Kipko, E.Y., Polozov, Y.A. and Lushinkova O.Y. 1993. *Integrated grouting and hydrogeology of fractured rock in the former USSR*, U.S. Society for Mining, Metallurgy and Exploration, Denver, Colorado.

Koch, D. 1985. *Analytical modeling of ground water impact by mining*. Colorado, 7p.

Konikow, L. 1996. *Numerical models of groundwater flow and transport. In: Manual on Mathematical Model in Isotope Hydrogeology,* International Atomic Energy Agency Rept. 910: 59 – 112.

Könnö, J. 2011. *Finite element methods for flow in porous media.* Department of Mathematics and Systems Analysis., School of science, Aalto University.

Kourakos G and Mantoglou, A. 2009. *Pumping optimization of coastal aquifers based on evolutionary algorithms and surrogate modular neural network models*. Advanced in Water Resources, 32 (4): 507 – 521.

Knapton, A. 2009. *An integrated surface – groundwater model of the Roper River Catchment*. Alice Springs, Dept. Natural Resources, Environment, the Arts and Sports.

Kumar, C. 1992. *Groundwater Modelling in Hydrological Developments in India since Independence: a Contribution to Hydrological Sciences*, National Institute of Hydrology, Roorkee, pp. 235-261.

Kumar, S., Ghosh, N., Singh, S. 2013. *A comparative study of artificial neural network and hybrid model for prediction of groundwater level*. Journal of Indian Water Resources Society, 33 (4): 7.

Laznicka, P. 2010. *Giant metallic deposits: future source of industrial metals*, Springer, 950p.

Leech, S. and McGann, M. 2007. *Open pit depressurization using horizontal drains – a case study*, 13p.

Levasseur, S. 2007. *Analyse inverse en géotechnique: Development d'une méthode à base d'algorithme génétique*, Thèse de doctorat, Université Joseph Fourier, 209p.

Li, E. 1994. *Artificial neural networks and their business applications*. Institute of Information Management, National Chung Cheng University. Information and Management 27:303 - 313.

Libicki, J. 1985. *Proposal of Criteria for the Selection of Dewatering Methods in Surface Mining*. Mine Water Granaga, 105 -112.

Libicki, J. 1993. *Proposal of Criteria for the Selection of Dewatering Methods in Surface Mining*. International Mine Water Symposium, 53-332.

Lin, Y. and Cunningham, G.A. 1995. *A new approach to fuzzy – neural system modeling*. IEEE Transactions on fuzzy system, 3 (2).

Little, R. and Rubin, D. 1987. *Statistical analysis with missing data*. Wiley, New York.

Lohani, A. and Krishan, G. 2015. *Application of artificial neural network for groundwater level simulation in Amritsar and Gurdaspur District of Punjab*. J. Earth Sci. Clim. Change. 6; 274.

Mabmann, J. 2012. *Development of a Groundwater Information & Management Program for the Lusaka Groundwater Systems*. Hannover, P. 58.

McCuen, R. H. 1997. *Hydrologic analysis and design*, 2nd Ed., Prentice Hall, Upper Saddle River, N.J.

McWhorter, D. 1981. *Predicting groundwater response to disturbance by mining – selected problems*. Surface Mining Hydrology, Sedimentology and Reclamation, Lexington, Kentucky.

Merbruk, M., Watanabe, K., Takeuchi, S. 2009. *Combined used of finite element method and neural networks for the prediction of pore pressure change*. Annual Journal of Hydraulic Engineering, 53 (6).

Mercer J.W. and Faust C.R. 1980. *Ground water modeling: an overview*, Groundwater, 18 (2): 8.

Millar, D. and Calderbank, P. 1995. *On the investigation of a multi-layer feedforward neural network model of rock deformability behaviour*. International Congress on Rock Mechanics, 933 – 938.

Mohanty, S., Madan, K., Kumar, A., Panda, D.K. 2013. *Comparative evaluation of numerical model and artificial neural network for simulating groundwater flow in Kathajodi–Surua Inter-basin of Odisha, India*, Journal of Hydrology, 495: 38-51.

Mohammadi, K. 2008. *Groundwater table estimation using MODFLOW and artificial neural netwaroks*, Water Science and Technology Library, 68 (2): 127 – 138.

Moriasi, D., Arnold, J., Van Liew, M., Bingner, R., Harmel, R. and Veith, T. 2007. *Model for evaluation guidelines for systematic quantification of accuracy in watershed simulations*, American Society of Agricultural and Biological Engineers, 50(3): 885−900.

Morris, D.A. and Johnson, A.I. 1967. *Summary of hydrologic and physical properties of rock and soil materials as analyzed by the Hydrologic Laboratory*

of the U.S. Geological Survey, U.S. Geological Survey Water-Supply, Paper 1839-D, 42p.

Morton, K.L and van Niekerk F.A. 1993. *A Phase Approach to Mine Dewatering*. Mine Water and the Environment, 12: 27-34.

Morton, K.L. 2009. *Comparison of Designs for the Dewatering of Coal, Gold and Diamonds,* KLM Consulting Services, Lanseria, Gauteng, South Africa.

MWR. 2009. *Ground water resource estimation methodology*. Report of the Ground Water Resources Estimation Committee, Minister of Water Resources, Government of India, New Delhi.

Nash, J. and Sutcliffe, J. 1970. R*iver flow forecasting through conceptual model, Part I – A discussion of principles*, Journal of hydrology, 10: 282 – 290.

Nel, P. 1997. *A critical overview of a completed shaft project and the disposal of excessive water inflows into the up-cast ventilation compartment.* International Mine Water Congress, Bled, Slovenia.

Norris, S. 1983. *Aquifer tests and well field performance, Scioto River Valley*, Ground Water, 21 (3): 287 – 292.

Obe, O., Shangodoyin, D. 2010. *Artificial neural network based model for forecasting sugar cane production*, J. Comput. Sci., 6: 439–445.

Osborne, J. and Waters, E. 2002. *Four assumptions of multiple regression that researches should always test*, Pratical assessment, Research and Evaluation., 8 (2). Retrieved from: http://PAREonline.net/getvn.asp?v=8&n=2.

Park, H., Keon, G., and Lee, S. 2009. *Prediction resilient modulus of granular subgrade soils and subbase materials based on artificial neural network*, Road Materials and Pavement Design, 10 (3): 647 – 665.

Parkin, G., Younger P., Birkinshaw, S., Murray, M., Rao, Z. and Kirk, S. 2001. *A new approach to modelling river-aquifer interactions using a 3-D numerical model and neural networks*, Impact of Human Activity on Groundwater Dynamics, IAHS, 269: 1 – 8.

Parkin, G., Birkinshaw, S.J., Younger, P.L. and Kirk, S. 2007. *A numerical modelling and neural network approach to estimate the impact of groundwater abstractions on river flows*, Journal of Hydrology, 339 (1-2): pp 15 – 28.

Pedhazur, E. 1997. *Multiple regression in behavioural research*, 3rd ed.

Plummer E.A. 2000. *Time series forecasting with feed-forward neural networks: Guidelines and limitations*, Master Thesis, University of Wyoming.

Pushpa, P. and Manimala, K. 2014. *Implementation of hyperbolic tangent activation function in VLSI*, International Journal of Advanced Research in Computer Science & Technology, Vol. 2.

Quinion, D.W. and Quinion, G.R. 1987. *Control of Groundwater*, ICE Works Construction Guides, Thomas Telford Pub.Co, London.

Rojas, R. 1993. *Backpropagation in General Networks*, Joint Meeting of the AMS and MAA, San Antonio.

Rojas, R. 1996. Neural Networks: *A Systematic Introduction*, Springer-Verlag, Berlin, pp. 5-9.

Rumelhart, D. E., Hinton, G. E., and Williams, R. J. 1986. *Learning internal representations by error propagation*. Parallel distributed processing, 1: 318–362.

Santing, G. 1957. *A horizontal scale model based on the viscous flow analogy of studying groundwater flow in an aquifer having storage*, IASH, 44: 105 – 114

Saporta, G. 2006. *Probabilités, Analyse des données et Statistique*, Dunod.

Sarkar, R. 2012. *Groundwater modeling: a comparison between multiple regression and artificial neural network approaches*, LAP Lambert Academic Publishing, 137p.

Saunders, G.P. 1983. *Aquifer dewatering and drawdown at an open mine pit in North-eastern Colorado*, Ground Water Monitoring Review, 3 (1): 122 – 126.

Schmidt, G. 2002. *Groundwater quantification – Validation of groundwater models*, Federal Institute for Geosciences and Natural Resources, 3: 29-47.

Seyam, M. 2010. *Groundwater Salinity Modeling Using Artificial Neural Networks, Gaza Strip case study*, Msc thesis, Islamic University of Gaza, 156p.

Shamim, M. A., Ghumman, A. R., Ghani, U. 2004. *Forecasting groundwater contamination using artificial neural networks*, International Conf. on Water Resources and Arid Environment, p.8.

Shaopei C. and Boru. D. 1998. *Modeling of fuzzy machine learning and fuzzy neural network in structural design, chapter Uncertainty modeling and analysis in civil engineering*, CRC Press, pp. 337–355.

Shewchuk, J. R. 2002. *Delaunay refinement algorithms for triangular mesh generation, Computational geometry: theory and application*, Amsterdam, 22: 21-74.

Shi, J. 2000. *Reducing prediction error by transforming input data for neural networks*, Journal of computing in civil engineering, 14 (2): 109 – 116.

Singh, J., Knapp, H. and Demissie, M. 2005. *Hydrologic modeling of the Iroquois River watershed using HSPF and SWAT*, Journal of American Water Resources Association, 41 (2): 361 – 375.

Smith, J. and Eli, R. 1995. *Neural networks models of rainfall – runoff process.* Journal of Water Resources, ASCE, 121 (6): 499 – 508.

Smith, M. 1993. *Neural networks for statistical modeling*. Van Nostrand Reinhold, New York.

Solanki, L.S., Singh, S., Singh, D. 2016. *Development and modelling of the dielectric properties of tissue-mimicking phantom materials for ultra-wideband microwave breast cancer detection*, Optik (Elsevier) 127: 2217 - 2225.

Stone, D.B. and Fontaine, R.C. 1998. *Simulation of groundwater fluxes during open-pit filling and under steady state pit lake conditions*. Conference on Hazardous Waste Research, P. 11.

Straskraba V. and Effner S. 1998. *Water control in underground mines – grouting or drainage?,* Mine Water Environmental Impacts in IMWA, 1: 213 – 220.

Straskraba V. and Effner S. 2012. *Water control in underground mines – grouting or drainage?* International Mine Water Association, Lakewood, Colorado, P. 18.

Sudheer, K.P., Gosain, A.K., Ramasastri, K.S. 2002. *A data driven algorithm for constructing artificial neural network rainfall-runoff models*, Hydrol. Process, 16: 1325-1330.

Szidarovszky, F., Coppola, E.A., Long, J., Hall, A.D., Poulton, M.M. 2007. *A hybrid artificial neural network-numerical model for ground water problems*, Ground Water, 45(5): 590-600.

Tapoglu, E., Karatzas, G.P., Trichakis, I.C., Varouchakis, A. 2014. *A spatio-temporal hybrid neural netwok-krigging model for groundwater level simulation,* J. Hydrol., 519: 3193 – 3203.

Thomas, R.G. 1973. *Groundwater models: Irrigation and drainage, Paper 21,* Food and Agriculture Organization of the United Nations. 192p.

Thangarajan, M. 1999. *Modeling multi-layer aquifer system to evolve pre-development management schemes*, Environmental Geology, 38 (4): 285 – 295.

Todd, D. 1954. *Unsteady flow in porous media by means of Hele-Shaw viscous fluid model*. Trans. Amer. Geophys. Union, 35 (6): 905-916.

USGS, 2008. *The Water Cycle: Water Storage in Oceans.*

Varrin, D. and Fang H. 1967. *Design and construction of a horizontal viscous flow model*. Groundwater. 5 (3): 55 – 41.

Veysseyre, R. 2006. *Aide-mémoire - Statistique et probabilités pour l'ingénieur*, Dunod.

Wang, P. and Anderson, M. 1982. *Introduction to Groundwater Modeling*. W. H. Freeman and Company, San Francisco. 237p.

Wang, P. and Chunmaio, Z. 1998. *An efficient approach for successively perturbated groundwater models*, Adv. Water Res., 21: 499-508.

Wilamowski, B. 2003. *Neural network architectures and learning (tutorial)*, International Conference on Industrial Technology (ICIT 03), Maribor, Slovenia, December 10 –12.

Wilamowski, B. 2007. *Neural networks and fuzzy systems for nonlinear applications*. Intelligent Engineering Systems, 11: 13–19.

Wilcox, R. 2012. *Introduction to robust estimation and hypothesis testing*, Elsevier.

Willmott, C. and Matsuura, K. 2005. *Advantages of the absolute mean error (MAE) over the root mean square error (RMSE) in assessing average model performance,* Clim. Res., 30: 70 – 82.

Wilson, R., McCaffrey, K., Jones, R., Clegg, P. and Holdsworth, R. 2005. *Digital mapping of Lofoten's faults*, Geoscientist, 15 (2): 4 – 9.

Winter, T. 2001. *The concept of hydrologic landscapes*, J. Am. Water Resources Assoc., 37:335–349.

Woessner, W. and Anderson, M. 2002. *The hydro-malaprop and the ground water table,* Ground Water, 40 (5): 465.

Yan, W., Alcoe, D., Morgan L., Li, C., Howles, S. 2010. *Protocol for development of numerical groundwater model, version 1*, report prepared for the Government of South Australia, Department for Water.

Yeh, W. 1992. *Systems analysis in groundwater planning and management*, J. Water Resour. Planning Manag. Div., Am. Soc. Civ. Eng., 118: 224–237.

Yoon, H., Hyun, Y., Lee, K.K. 2007. *Forecasting solute breakthrough curves through the unsaturated zone using artificial neural networks*, J. Hydrol., 335, 68–77.

Yoon, H., Jun, S.C., Hyun, Y., Bae, G.O., Lee, K.K. 2011. *Comparative study of artificial neural networks and support vector machines for predicting groundwater levels in a coastal aquifer*, J. Hydrol., 396: 128 – 138.

ABSTRACT

Open pit mines often experience problems related to groundwater inflows. To perform mineral extraction in safe conditions with high productivity, it is essential to have dry working conditions. For this reason, the groundwater table is often lowered below the elevation of the floors of the pits by using various dewatering schemes.

Numerical groundwater models are powerful tools that can be used to simulate the behaviour of aquifers during dewatering operations. However, these models typically require a lot of geohydrological data which are often expensive and time-consuming to collect. When geohydrological input data are limited, artificial neural networks (ANNs) provide an alternative way of predicting the behaviour of the groundwater system under dewatering conditions. ANNs can simulate complex systems, and have been used to provide simple and accurate solutions to problems encountered in many disciplines of the earth sciences.

This study investigated the possibility of predicting the impacts of pit dewatering on the aquifer system in the vicinity of open pit mines where geohydrological inputs are limited, using ANNs. First, the performance of the ANNs in predicting hydraulic head responses was evaluated by using synthetic datasets generated by a numerical groundwater model developed for a fictional mine. The synthetic datasets were then used to both train and evaluate the performance of the ANNs. The ANN found to give the best predictions of the hydraulic heads had an architecture of 2-6-1 (input-hidden-output layers) and was based on the hyperbolic tangent transfer function. This network was selected for application to real open pit mines.

The selected ANN was next used to predict hydraulic heads at a number of piezometers installed at two open pit mines in the Democratic Republic of the Congo. The only input to the ANN was the recorded hydraulics heads and the time of recording. A portion of the real dataset was used to train the ANN, while the remaining portion was used to evaluate the performance of the ANN in predicting the hydraulic heads. The results of the performance analyses indicated that the

ANN successfully predicted the general behaviour of the aquifer system under dewatering conditions, using only limited input data.

The results of this investigation illustrate the great potential of using ANNs to predict aquifer responses during dewatering operations in the absence of comprehensive geohydrological datasets. Since these networks recognise patterns in the training datasets without considering the underlying physical principles that govern the processes, the responses of complex systems that are dependent on numerous parameters may be predicted.

APPENDICES

A. MODELLED AND PREDICTED HYDRAULIC HEADS

A.1 THREE DEWATERING WELLS

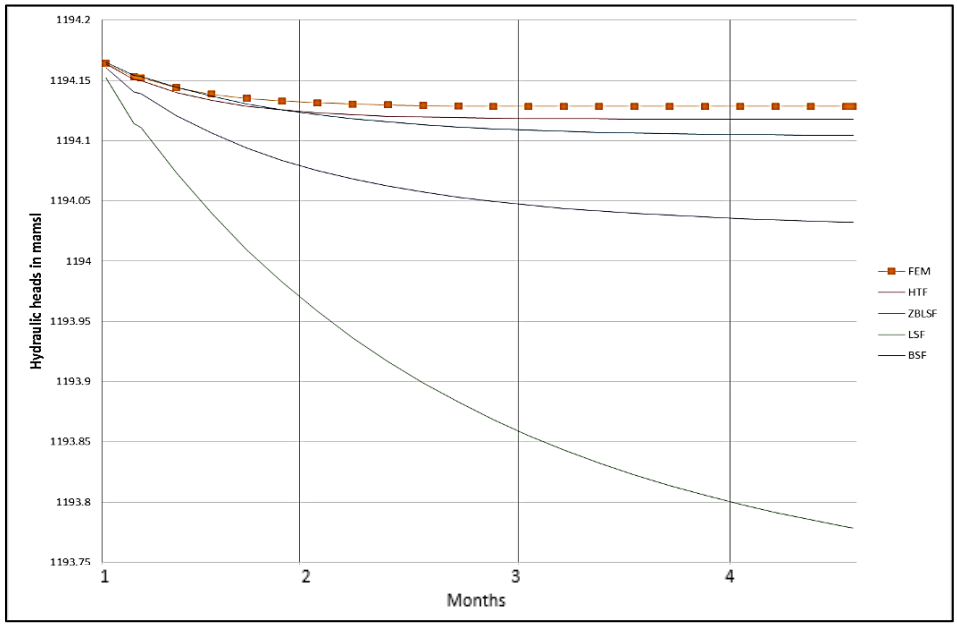

Figure A-1: Modelled and predicted hydraulic heads at observation well OBS_1

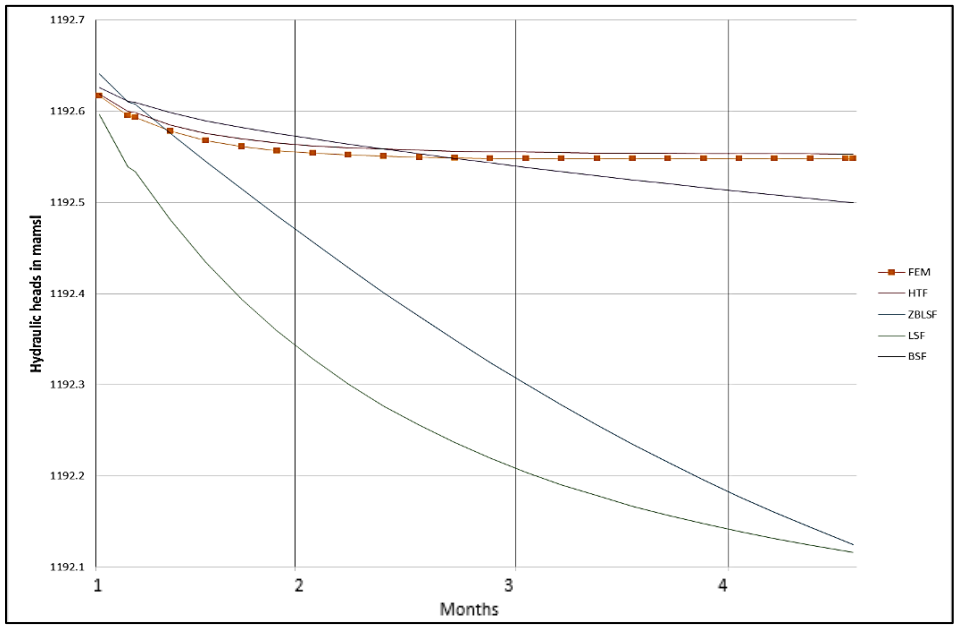

Figure A-2: Modelled and predicted hydraulic heads at observation well OBS_2

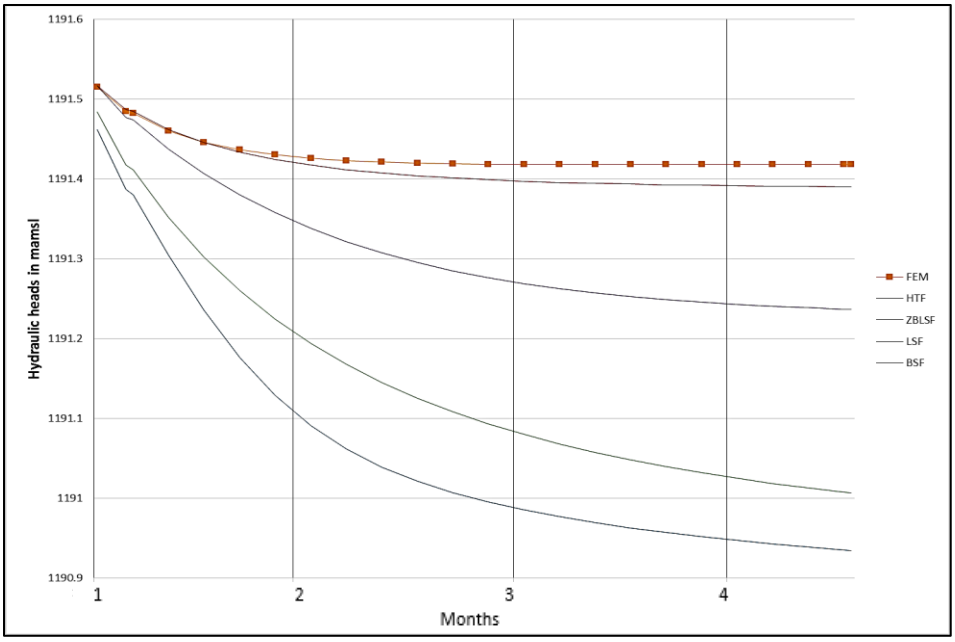

Figure A-3: Modelled and predicted hydraulic heads at observation well OBS_3

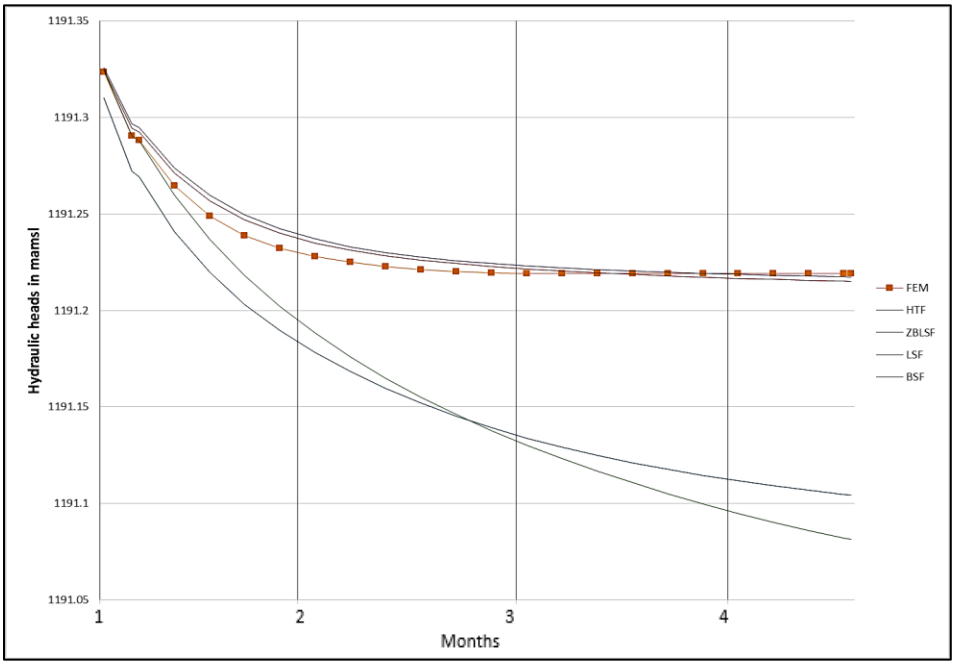

Figure A-4: Modelled and predicted hydraulic heads at observation well OBS_4

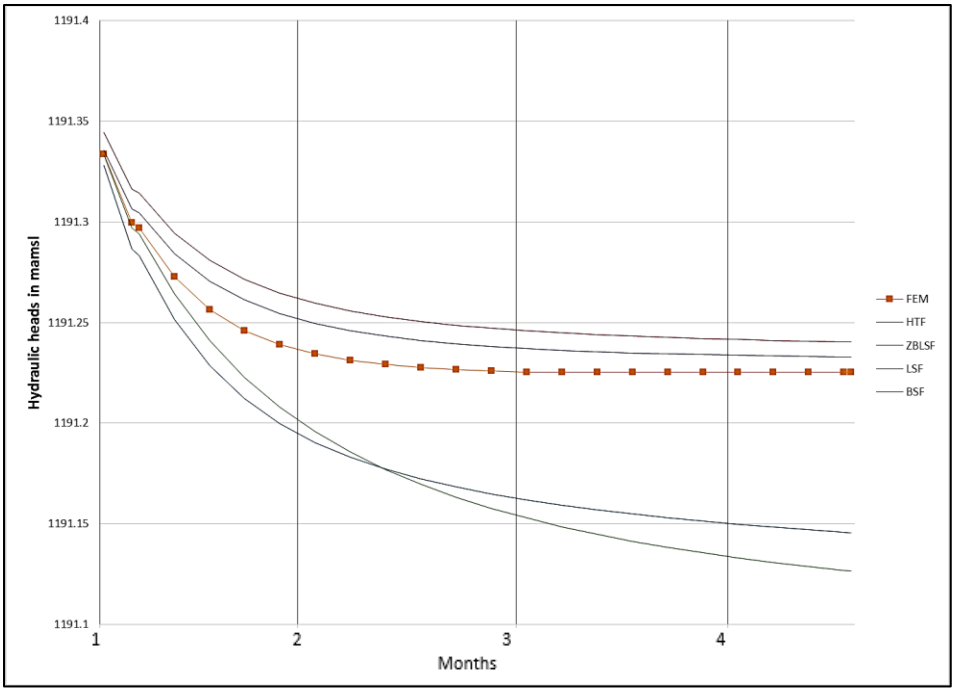

Figure A-5: Modelled and predicted hydraulic heads at observation well OBS_5

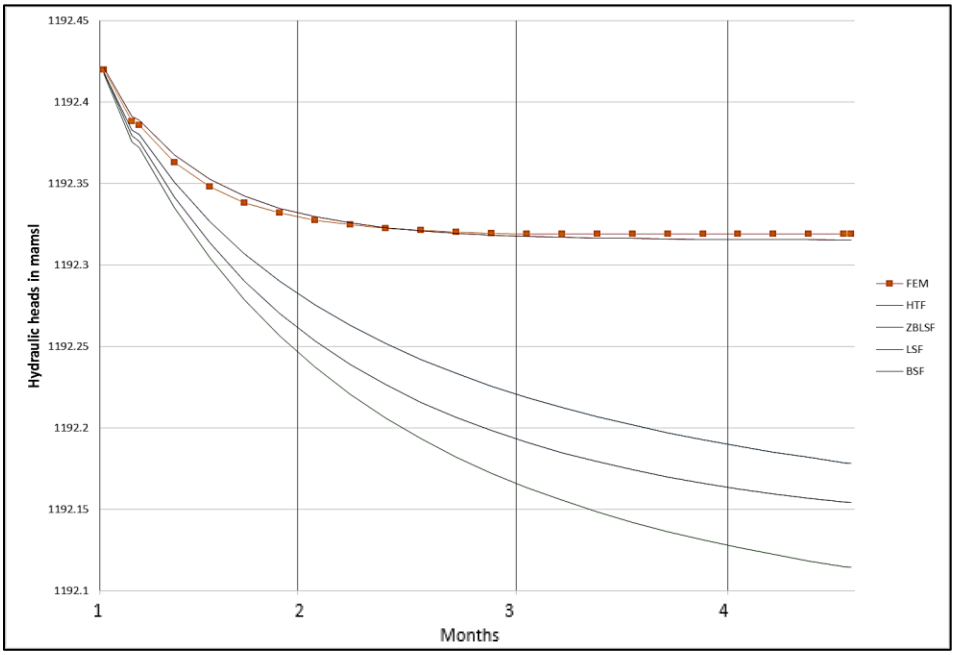

Figure A-6: Modelled and predicted hydraulic heads at observation well OBS_6

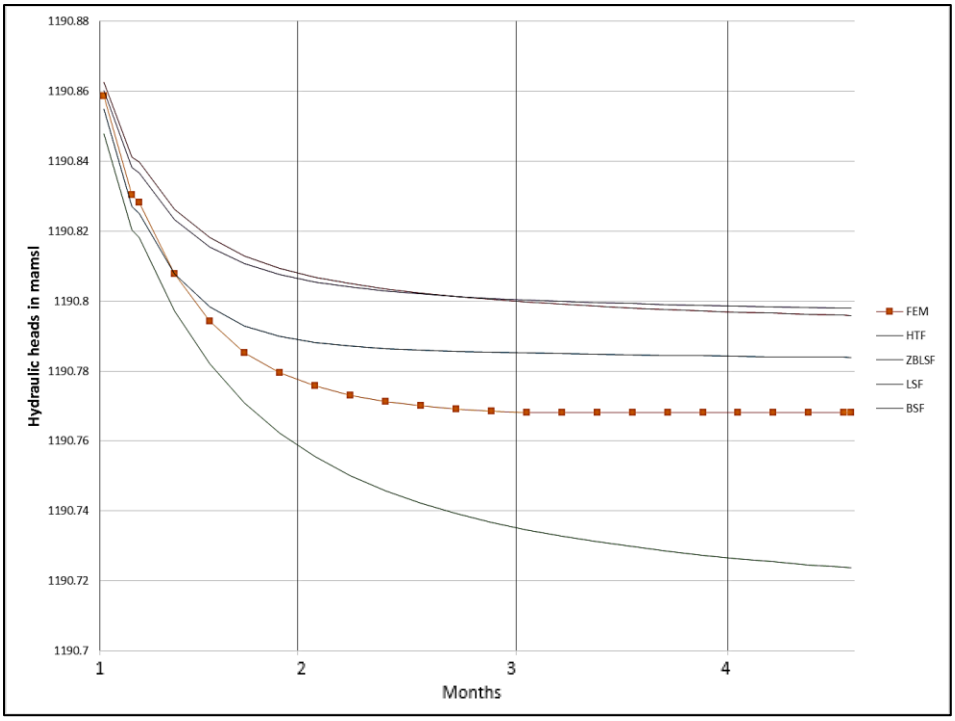

Figure A-7: Modelled and predicted hydraulic heads at observation well OBS_7

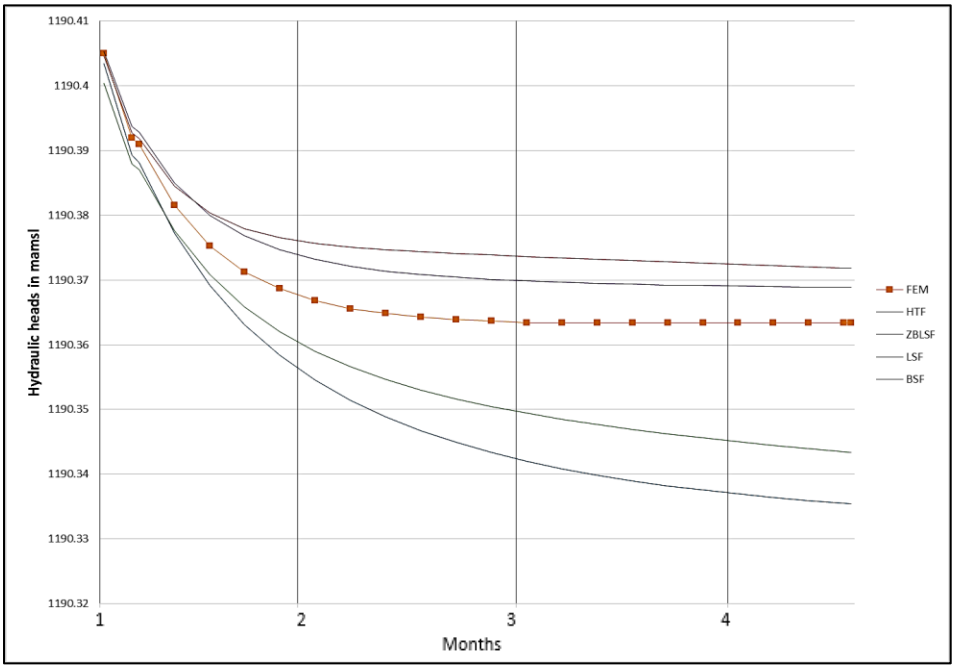

Figure A-8: Modelled and predicted hydraulic heads at observation well OBS_8

A.2 SIX DEWATERING WELLS

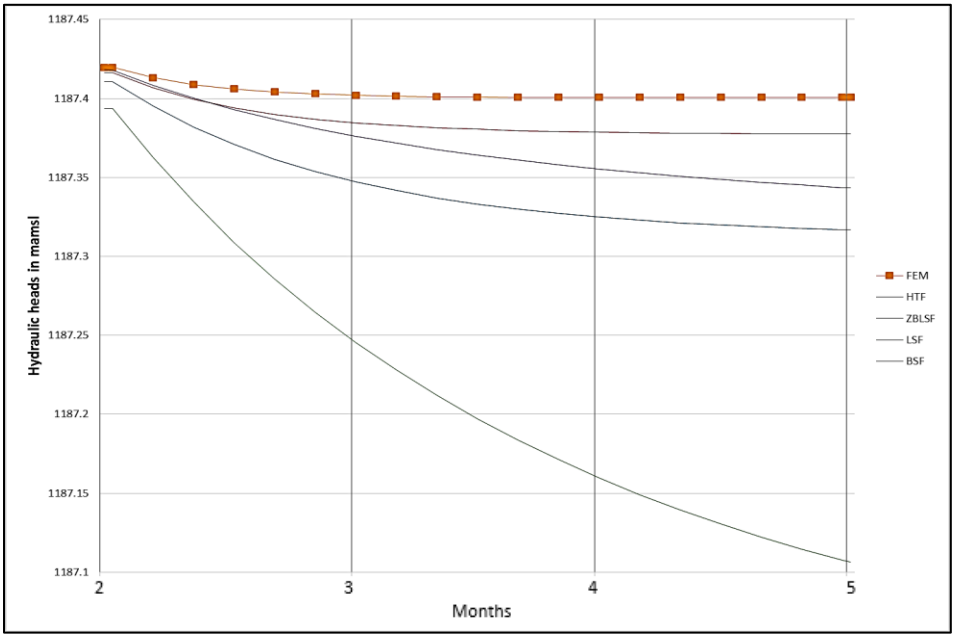

Figure A-9: Modelled and predicted hydraulic heads at observation well OBS_1

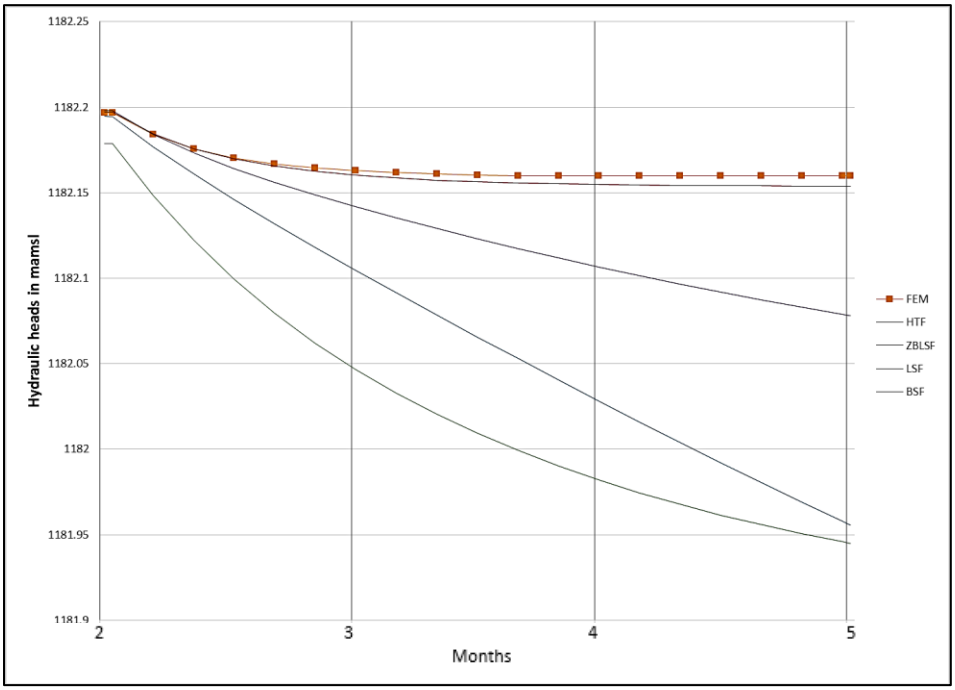

Figure A-10: Modelled and predicted hydraulic heads at observation well OBS_2

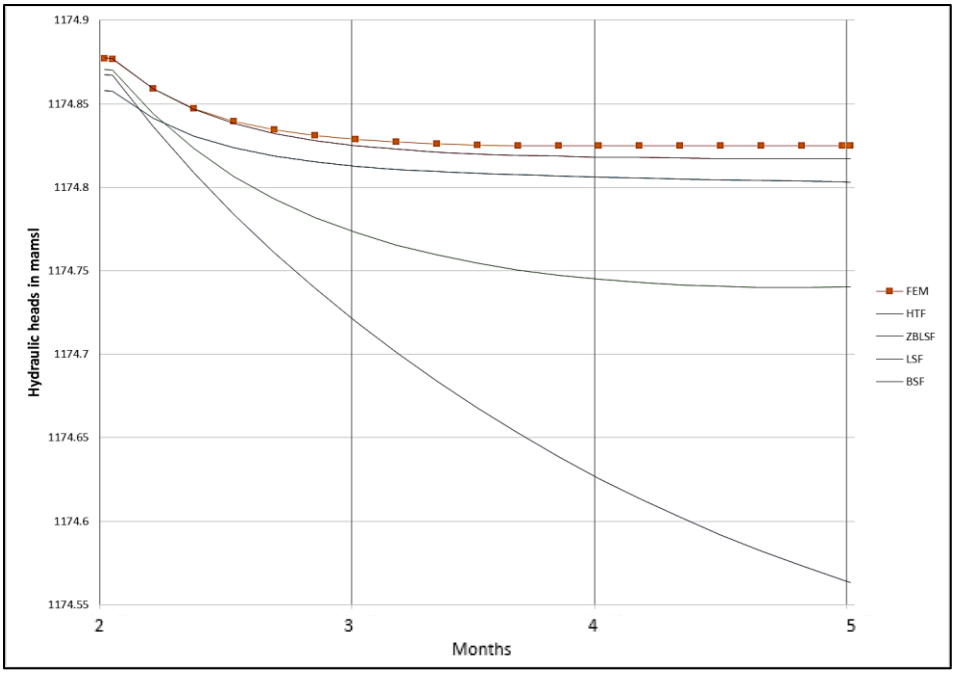

Figure A-11: Modelled and predicted hydraulic heads at observation well OBS_3

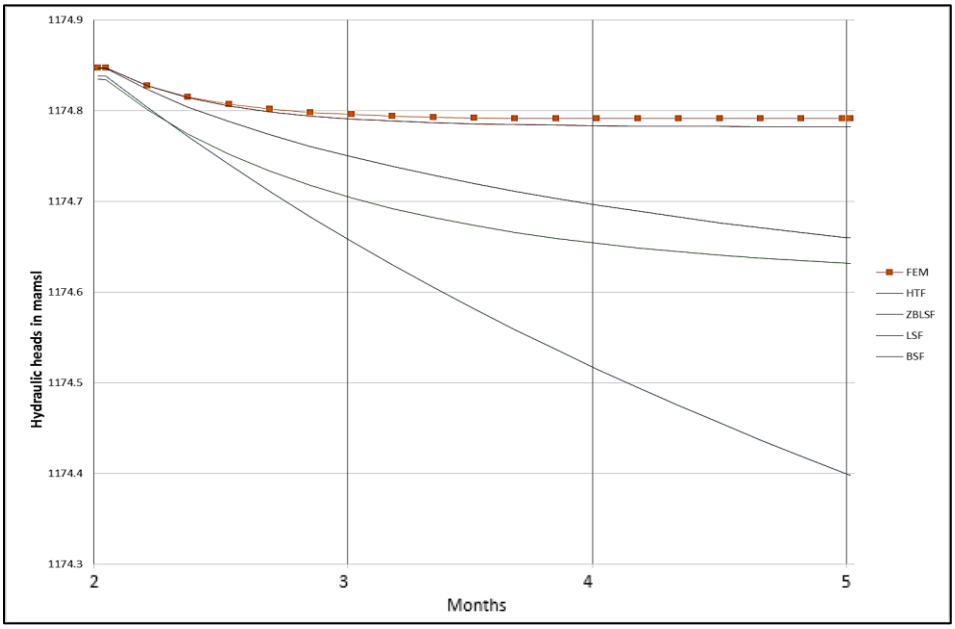

Figure A-12: Modelled and predicted hydraulic heads at observation well OBS_4

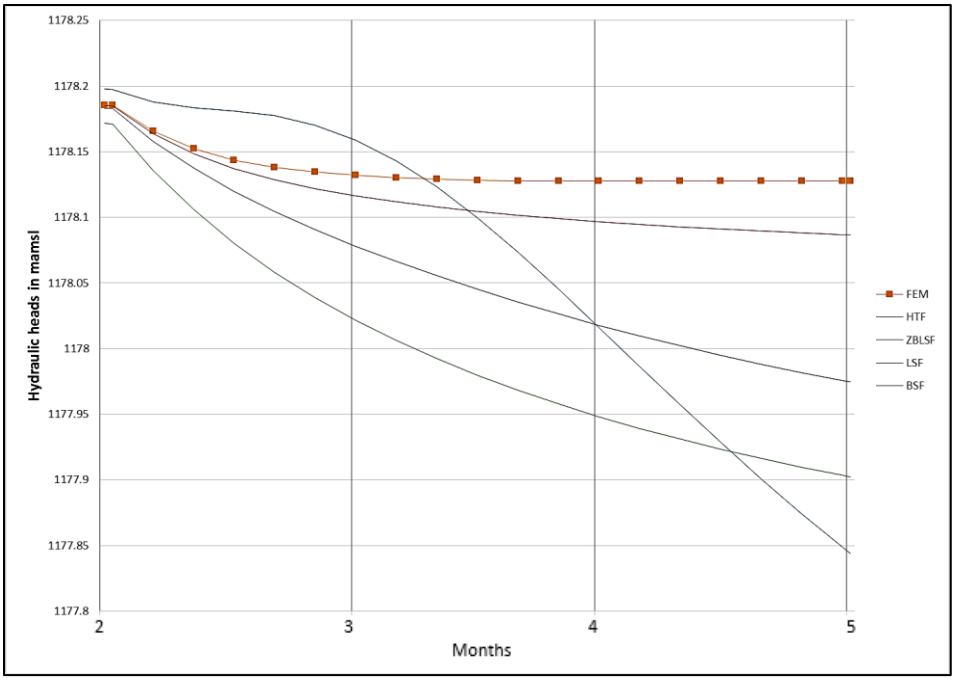

Figure A-13: Modelled and predicted hydraulic heads at observation well OBS_5

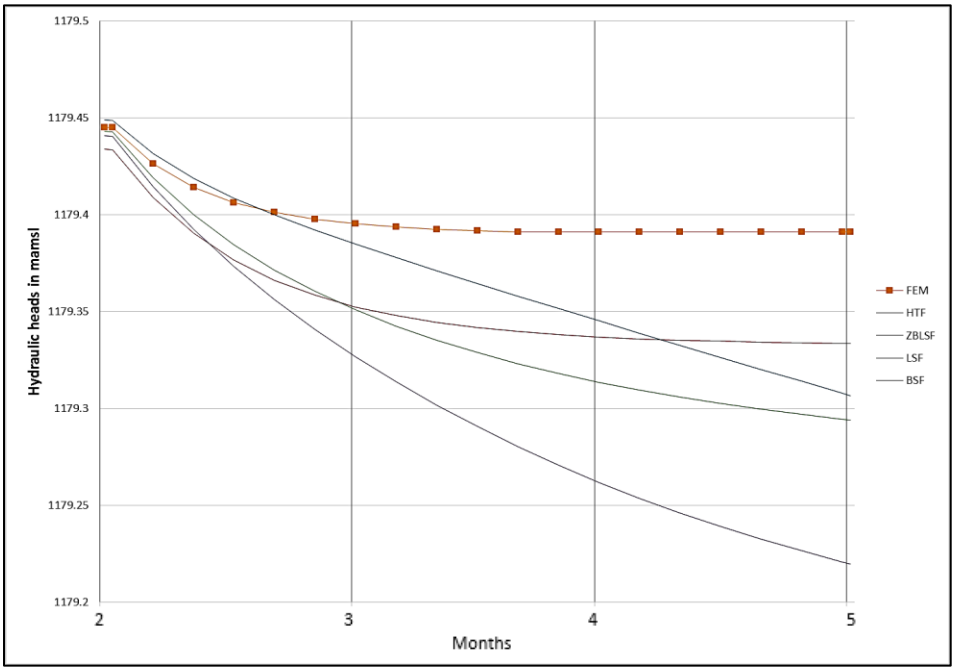

Figure A-14: Modelled and predicted hydraulic heads at observation well OBS_6

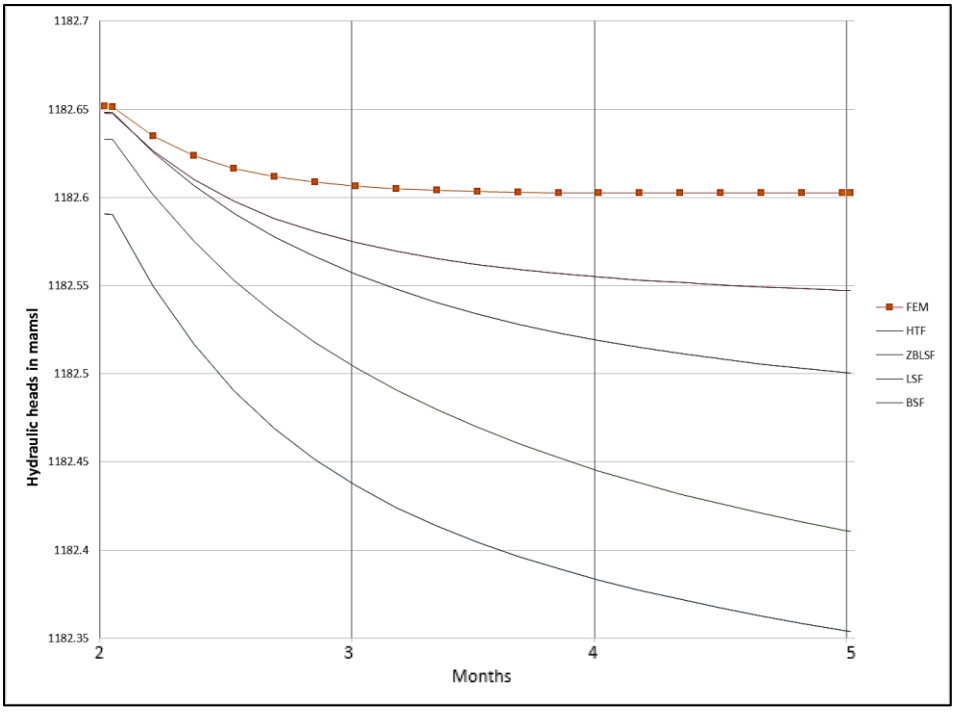

Figure A-15: Modelled and predicted hydraulic heads at observation well OBS_7

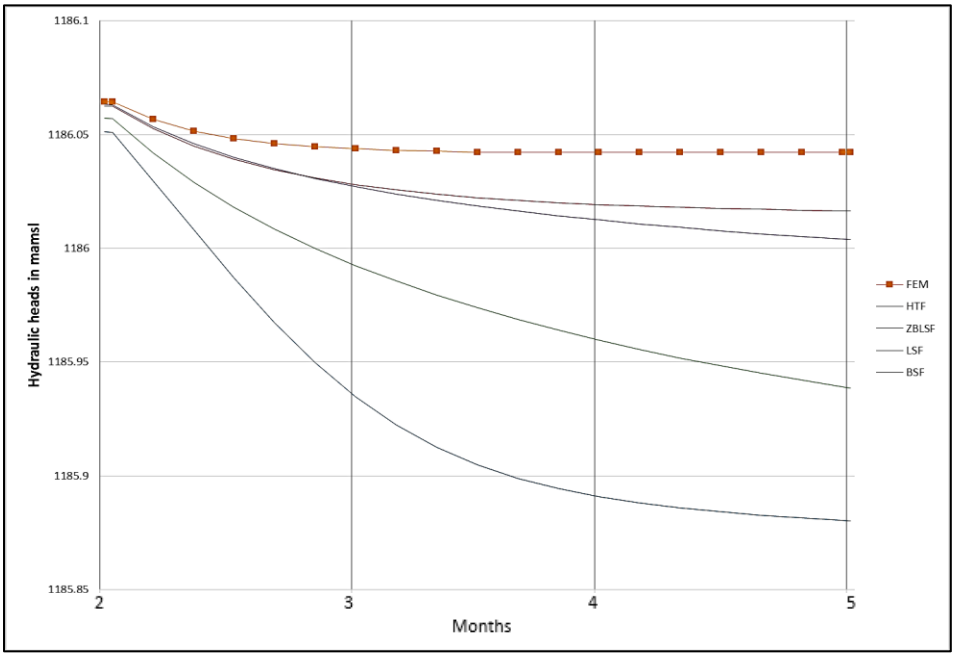

Figure A-16: Modelled and predicted hydraulic heads at observation well OBS_8

A.3 NINE DEWATERING WELLS

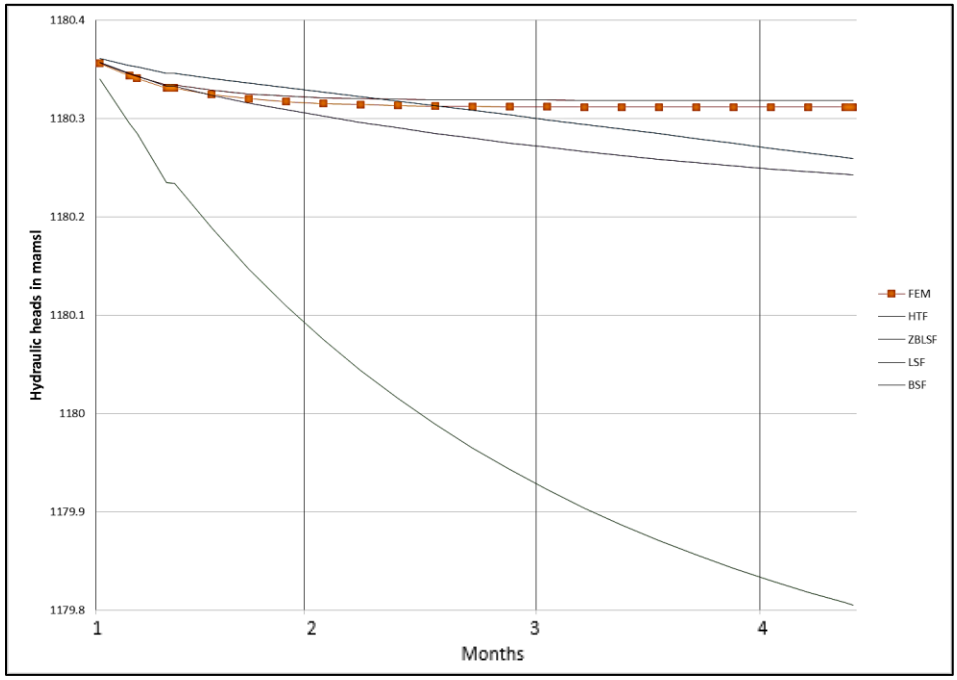

Figure A-17: Modelled and predicted hydraulic heads at observation well OBS_1

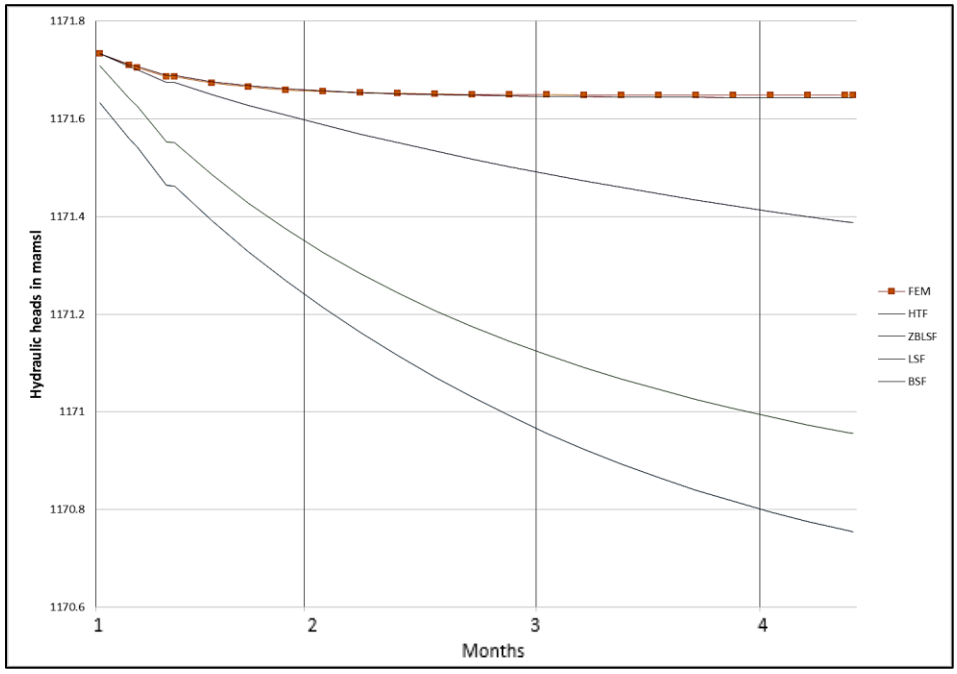

Figure A-18: Modelled and predicted hydraulic heads at observation well OBS_2

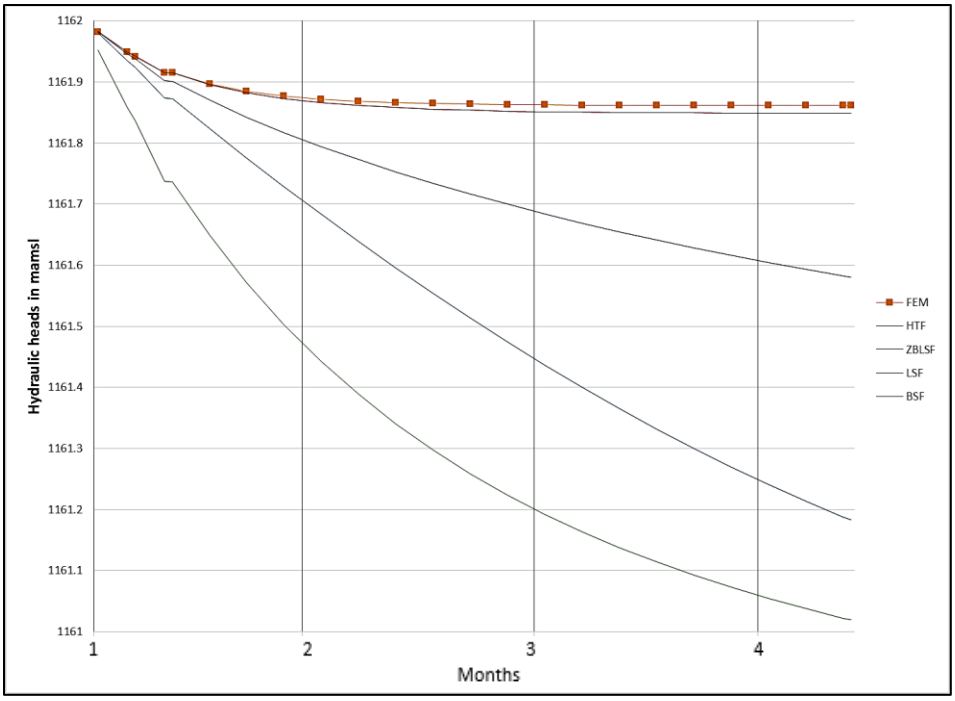

Figure A-19: Modelled and predicted hydraulic heads at observation well OBS_3

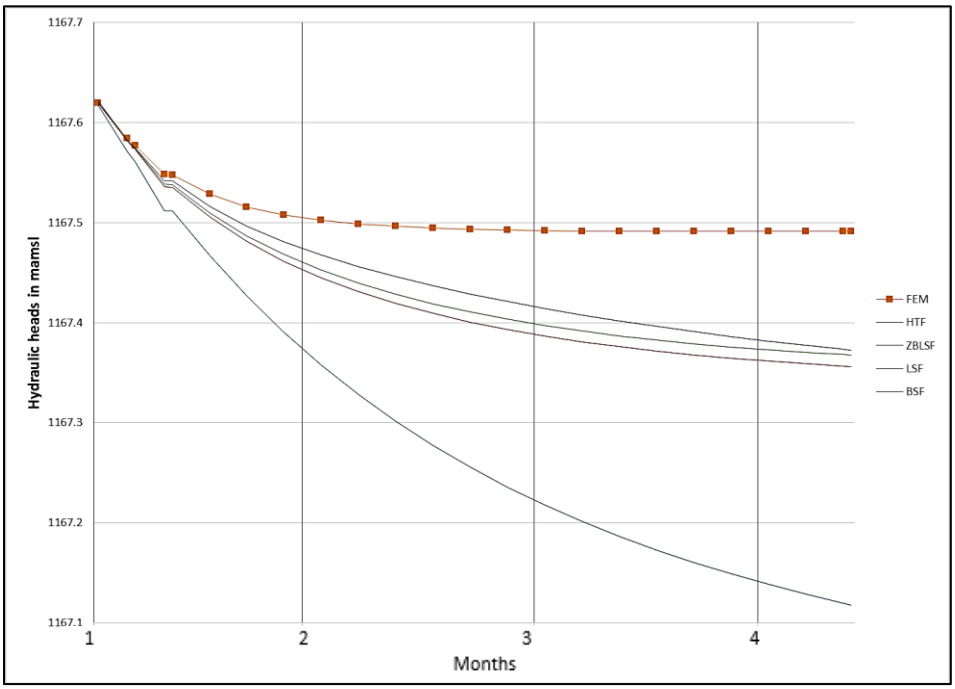

Figure A-20: Modelled and predicted hydraulic heads at observation well OBS_4

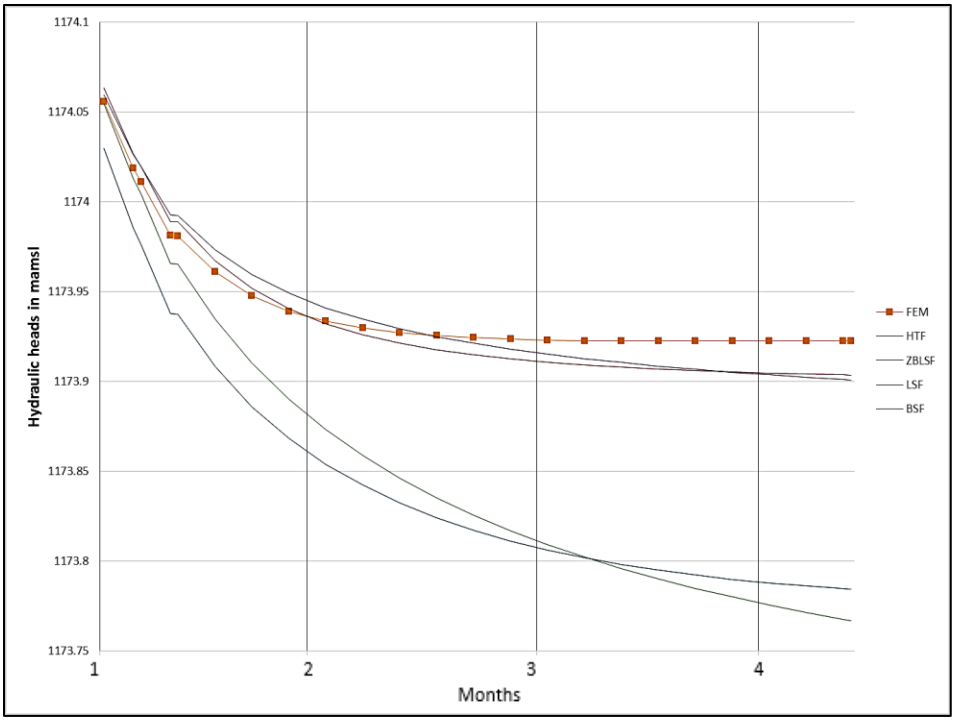

Figure A-21: Modelled and predicted hydraulic heads at observation well OBS_5

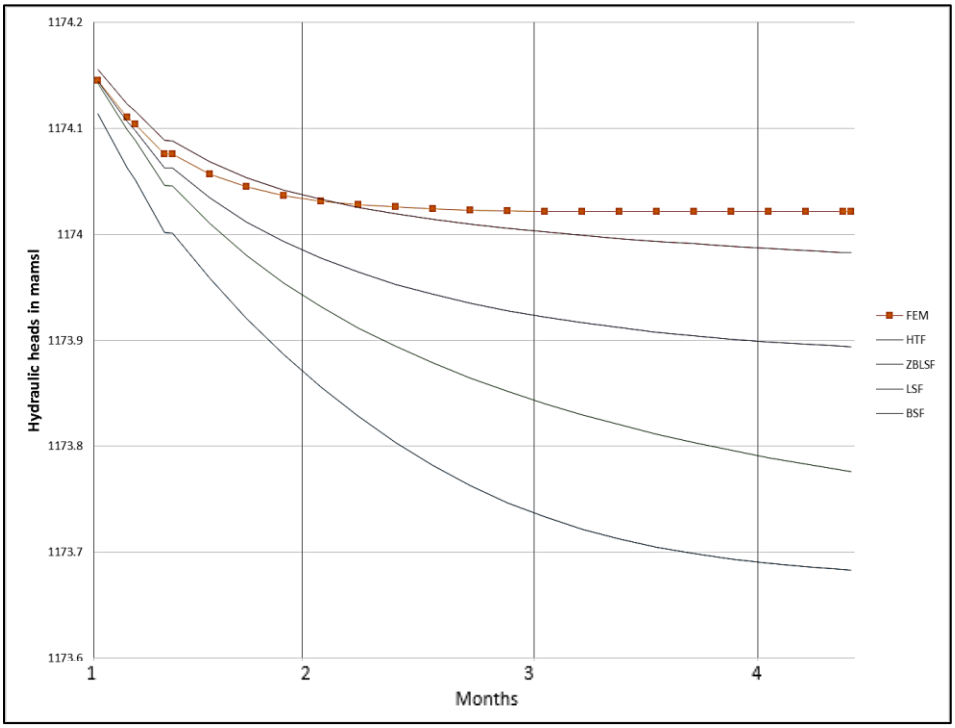

Figure A-22: Modelled and predicted hydraulic heads at observation well OBS_6

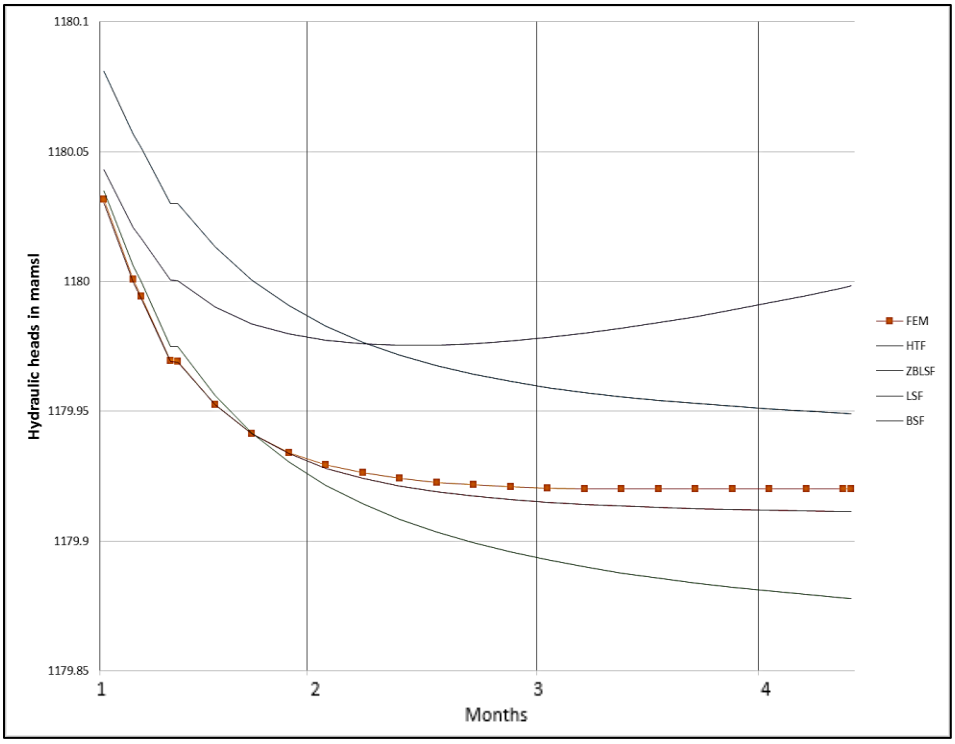

Figure A-23: Modelled and predicted hydraulic heads at observation well OBS_7

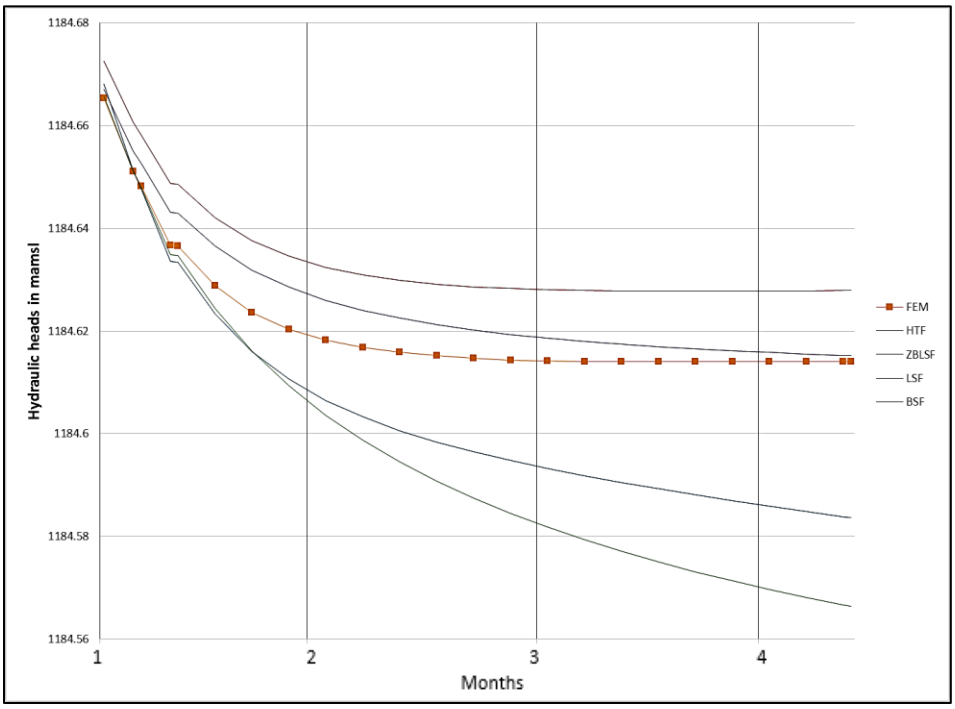

Figure A-24: Modelled and predicted hydraulic heads at observation well OBS_8

A.4 TWELVE DEWATERING WELLS

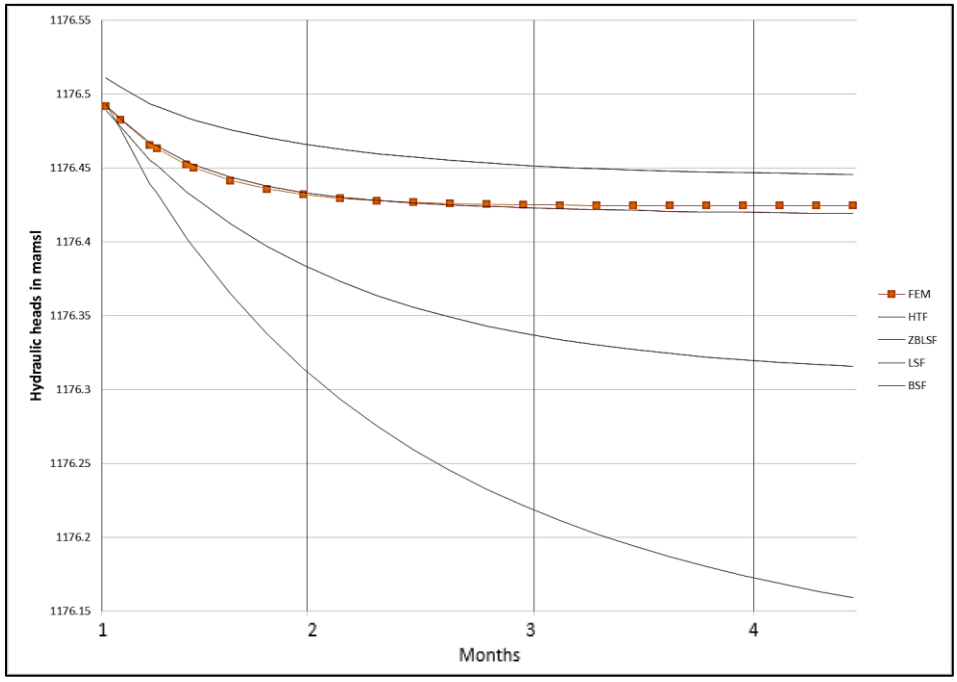

Figure A-25: Modelled and predicted hydraulic heads at observation well OBS_1

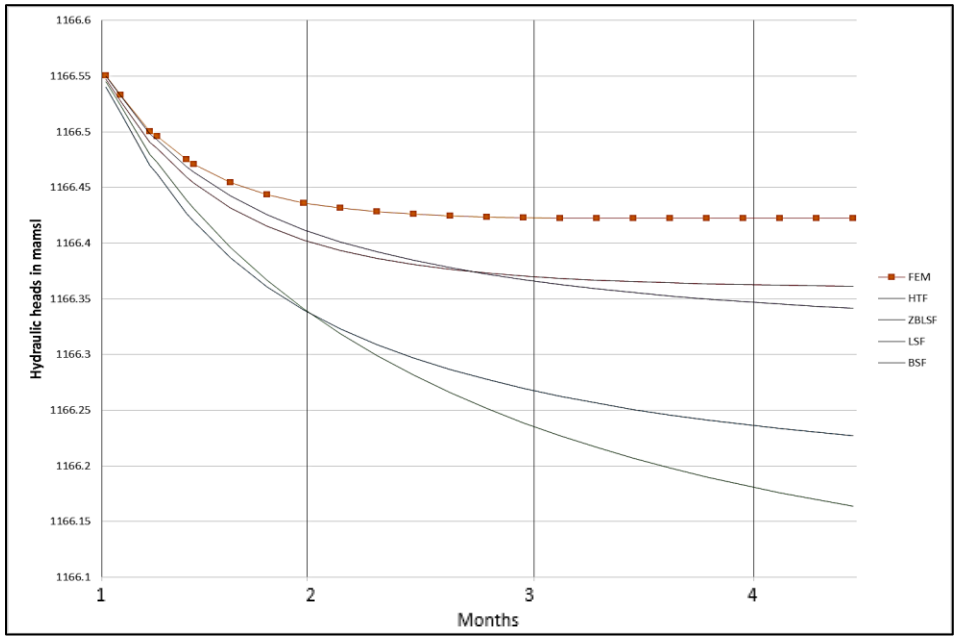

Figure A-26: Modelled and predicted hydraulic heads at observation well OBS_2

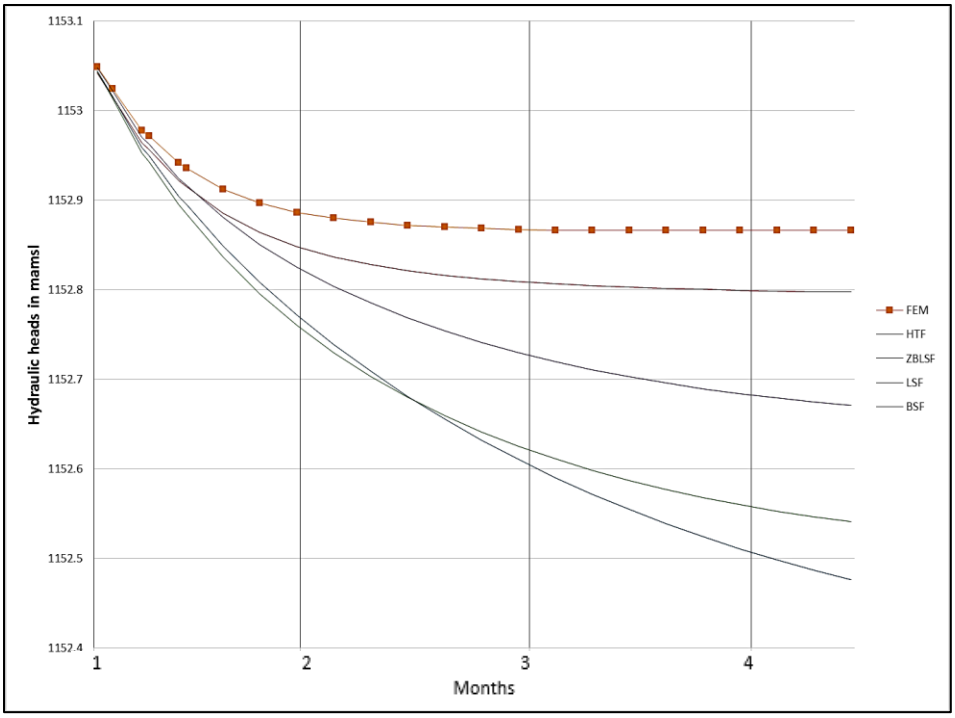

Figure A-27: Modelled and predicted hydraulic heads at observation well OBS_3

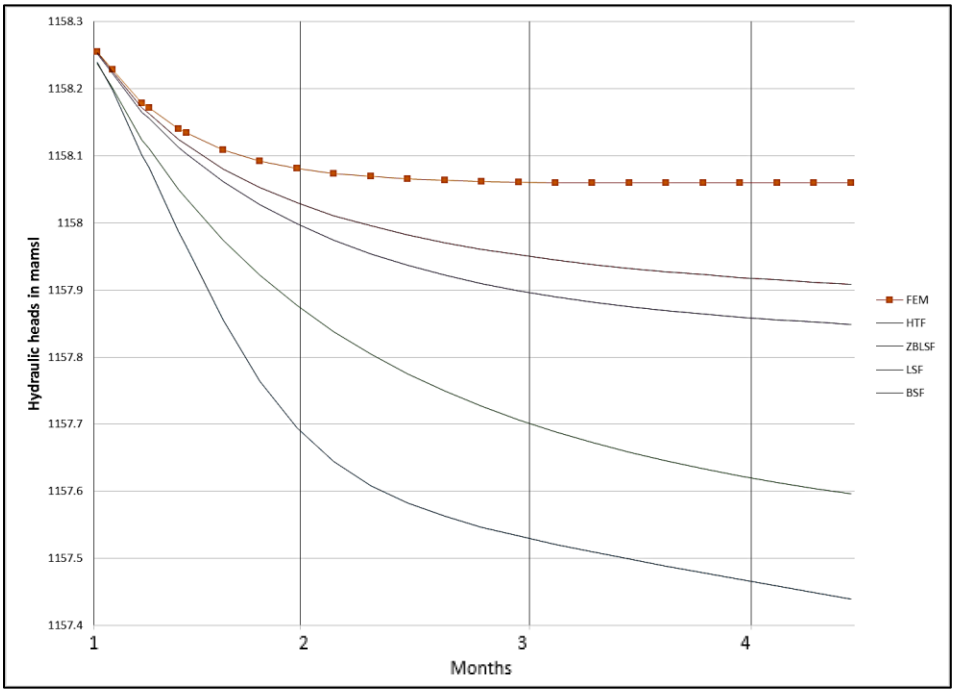

Figure A-28: Modelled and predicted hydraulic heads at observation well OBS_4

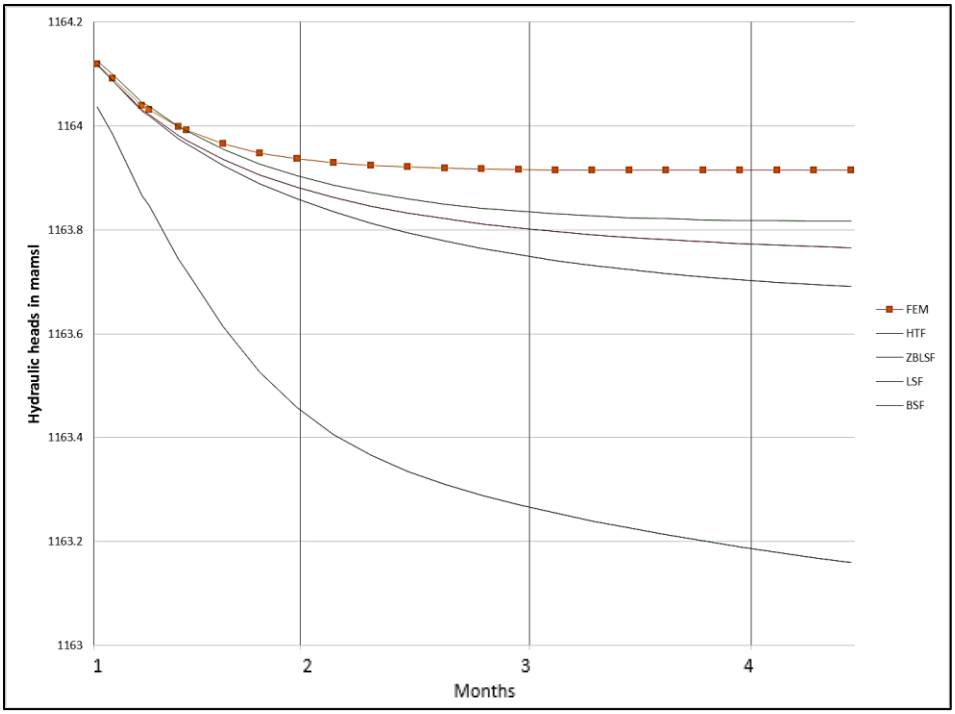

Figure A-29: Modelled and predicted hydraulic heads at observation well OBS_5

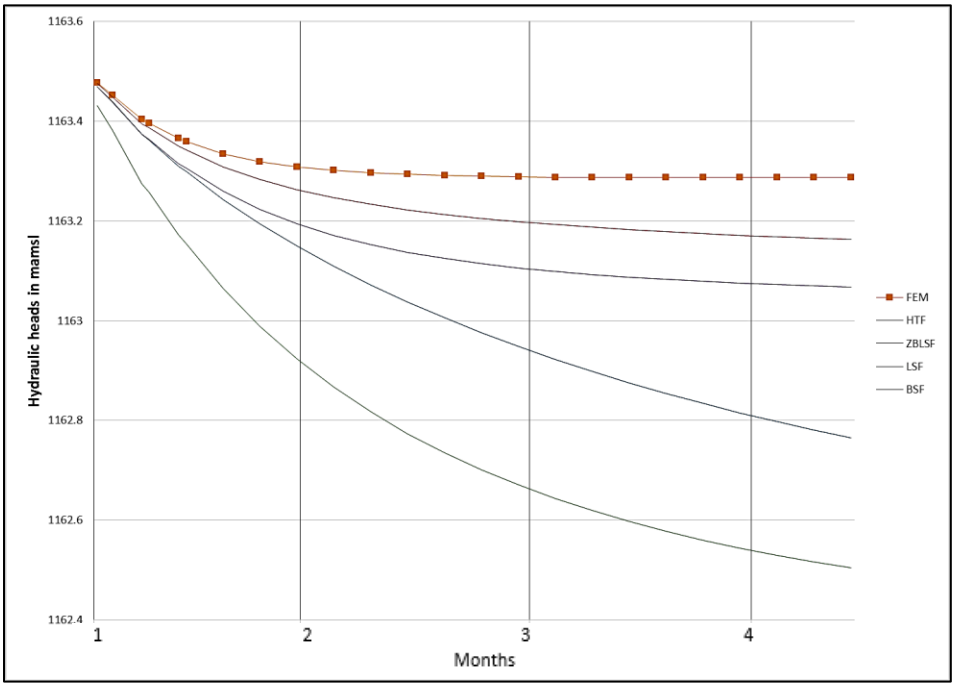

Figure A-30: Modelled and predicted hydraulic heads at observation well OBS_6

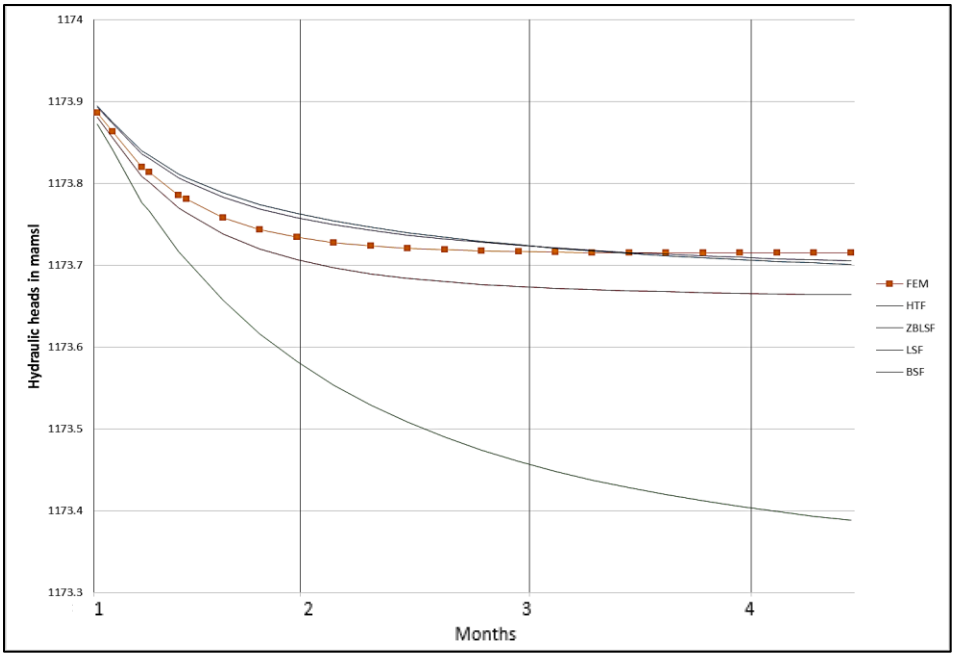

Figure A-31: Modelled and predicted hydraulic heads at observation well OBS_7

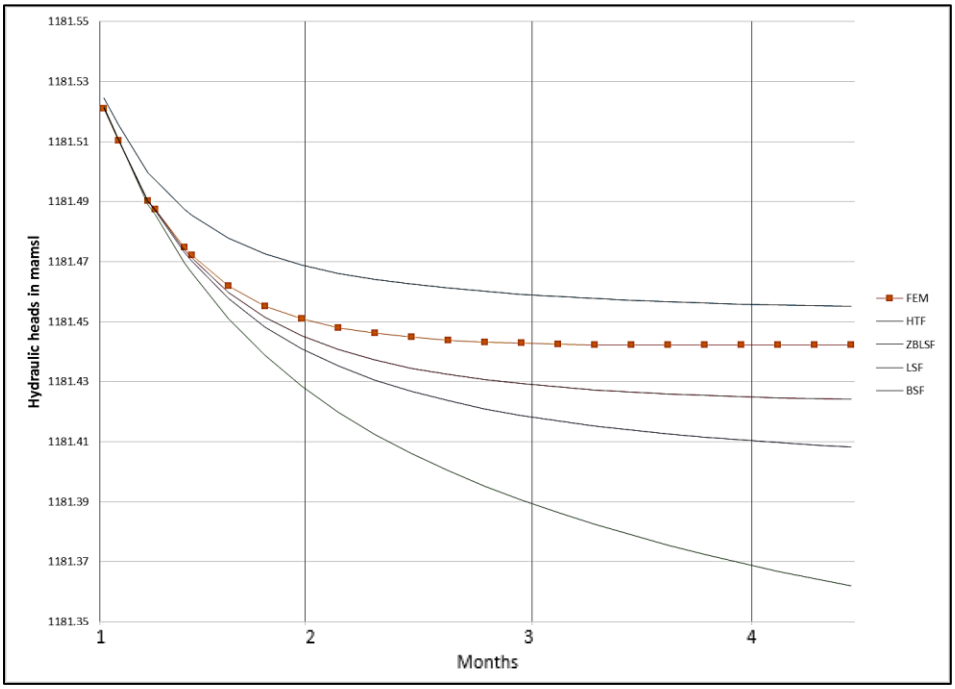

Figure A-32: Modelled and predicted hydraulic heads at observation well OBS_8

B. PREDICTED VERSUS MODELLED HEADS

B.1 THREE DEWATERING WELLS

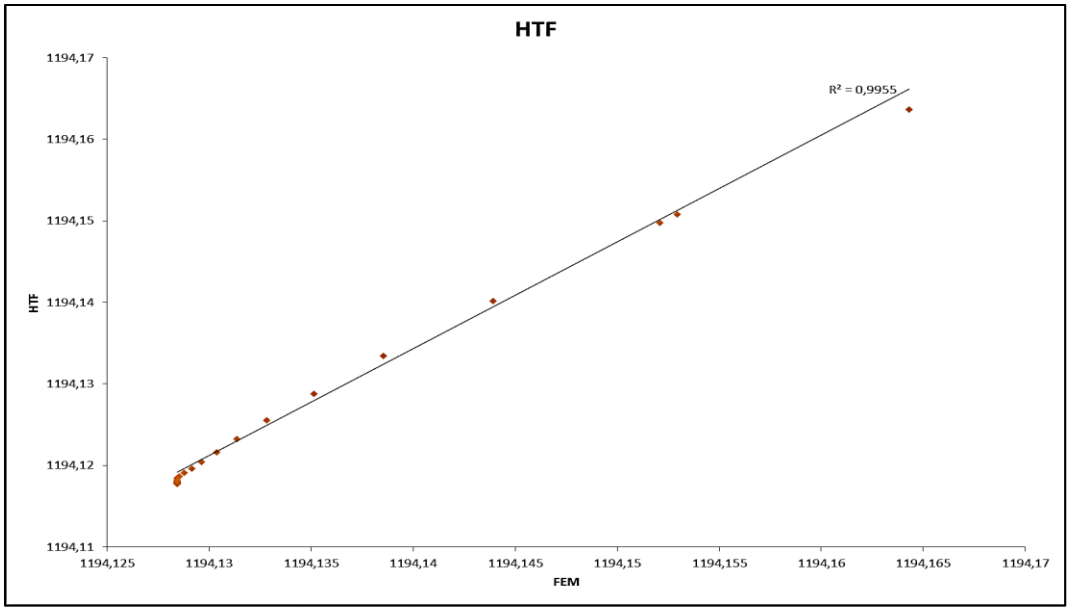

Figure B-1: Modelled versus predicted hydraulic heads for observation well OBS_1

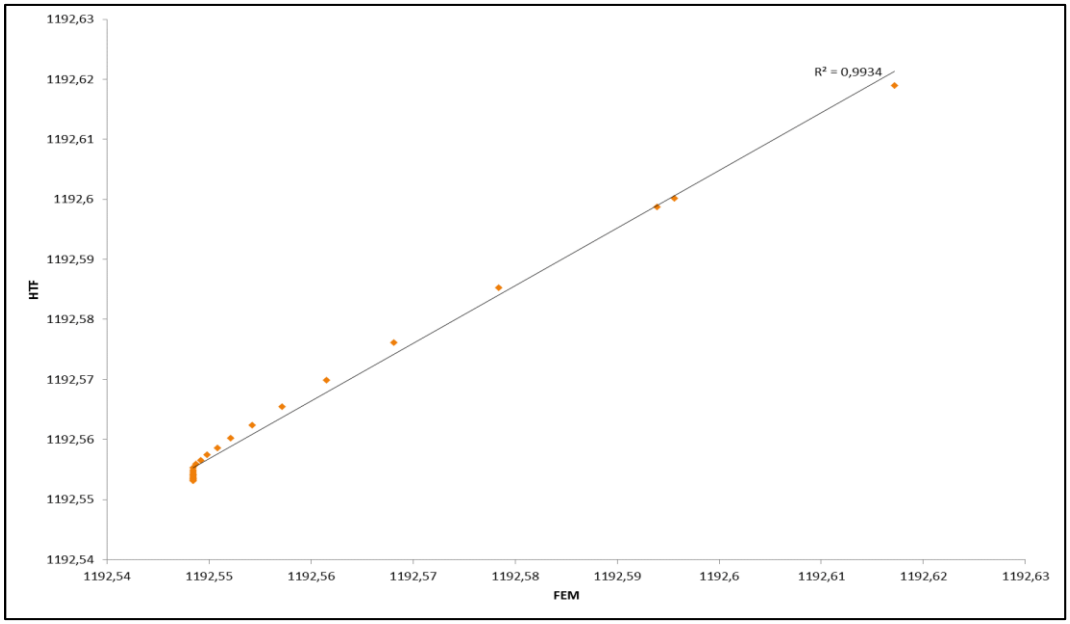

Figure B-2: Modelled versus predicted hydraulic heads for observation well OBS_2

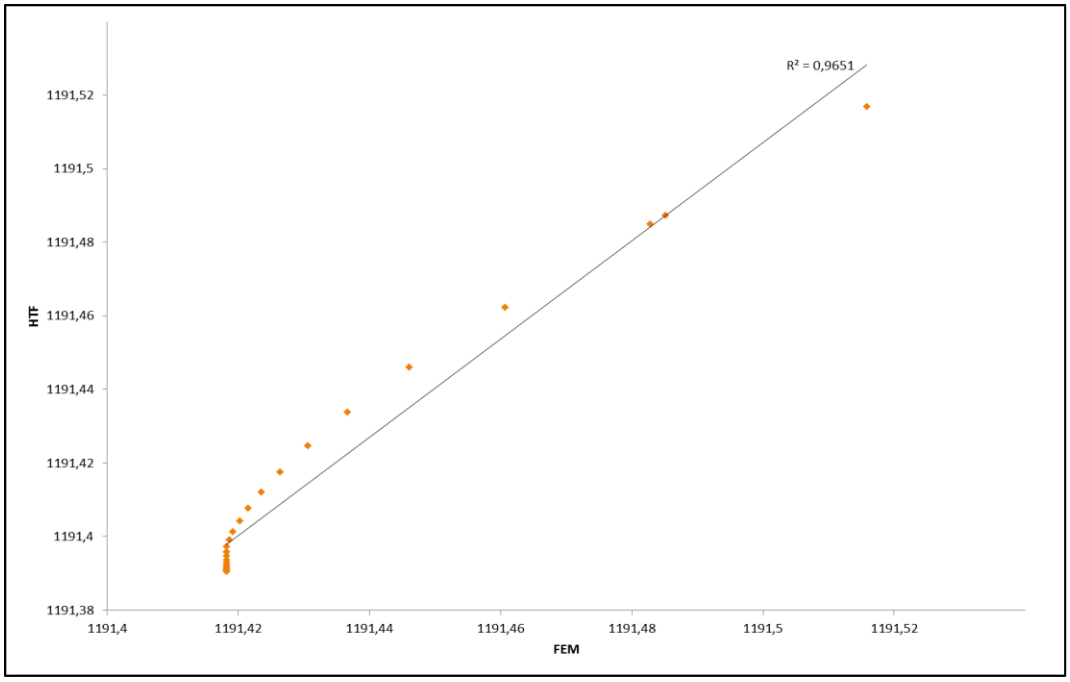

Figure B-3: Modelled versus predicted hydraulic heads for observation well OBS_3

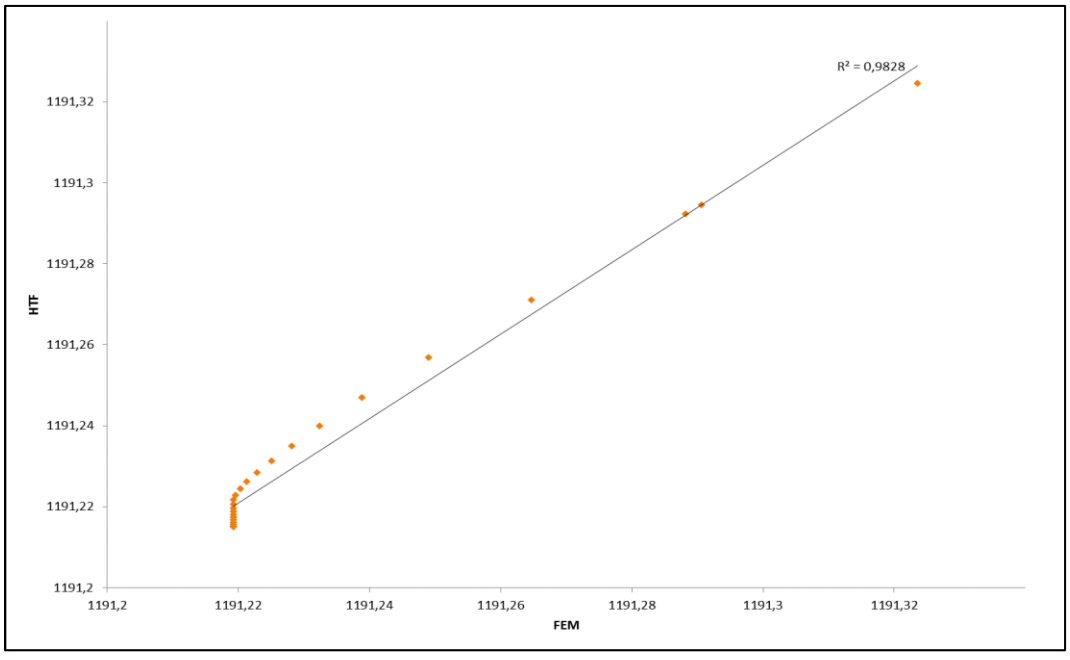

Figure B-4: Modelled versus predicted hydraulic heads for observation well OBS_4

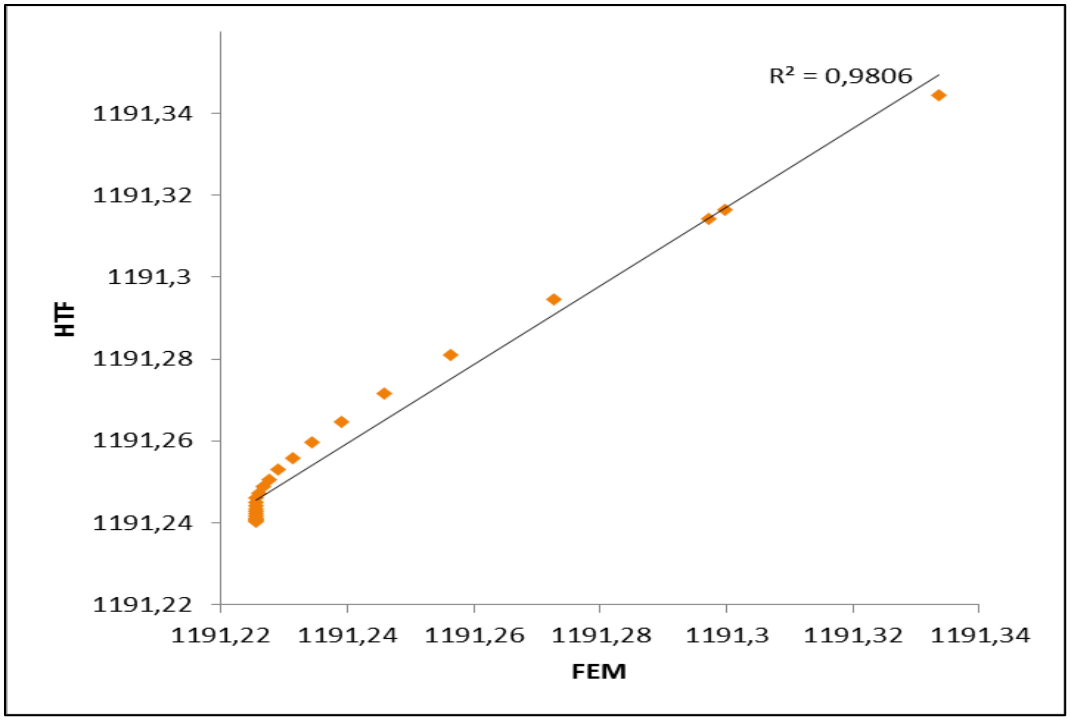

Figure B-5: Modelled versus predicted hydraulic heads for observation well OBS_5

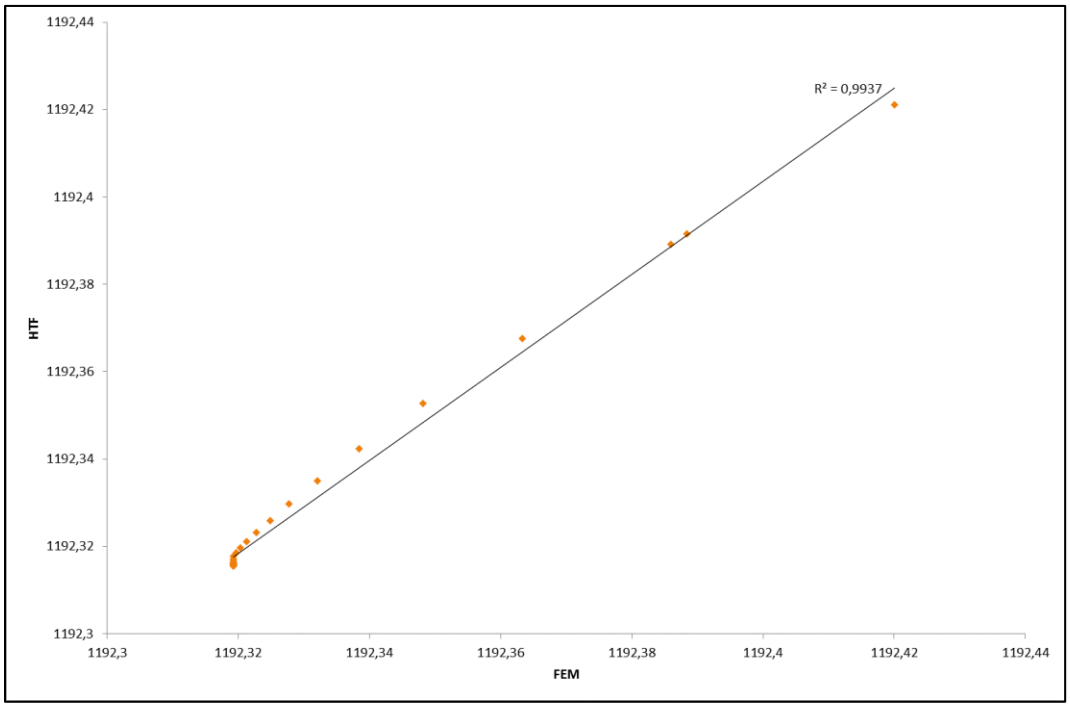

Figure B-6: Modelled versus predicted hydraulic heads for observation well OBS_6

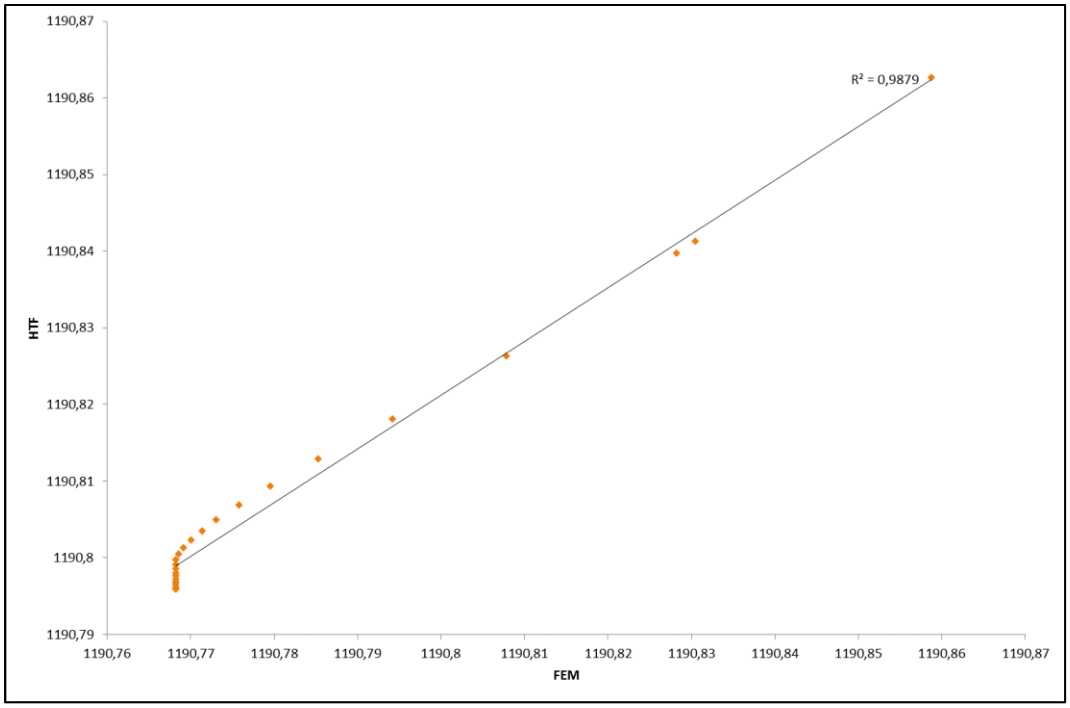

Figure B-7: Modelled versus predicted hydraulic heads for observation well OBS_7

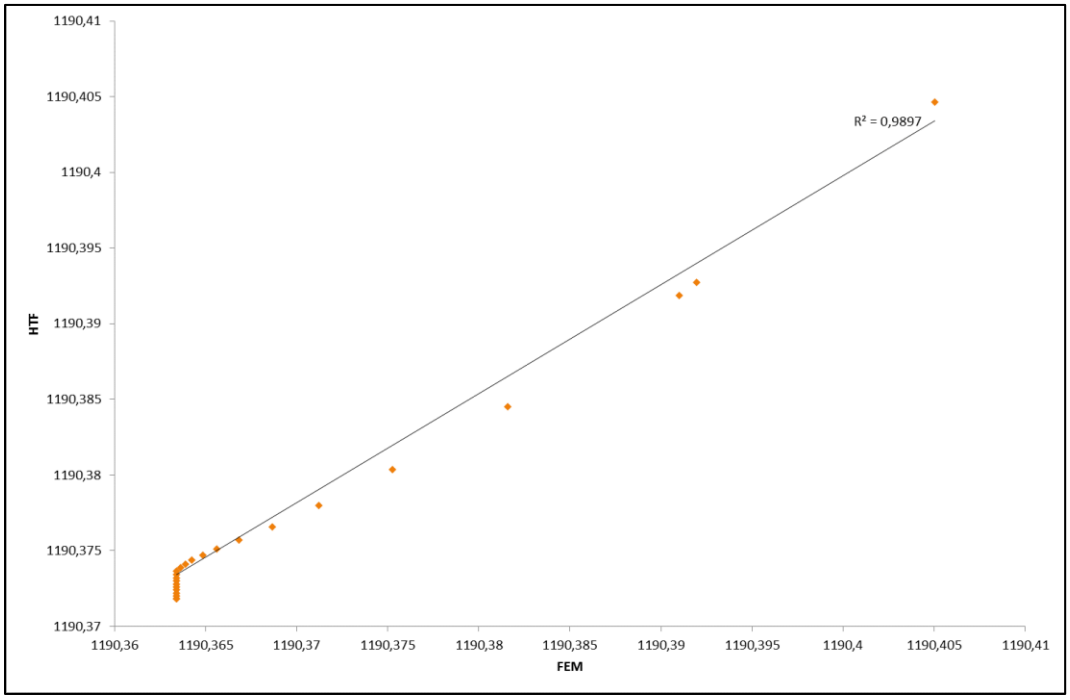

Figure B-8: Modelled versus predicted hydraulic heads for observation well OBS_8

B.2 SIX DEWATERING WELLS

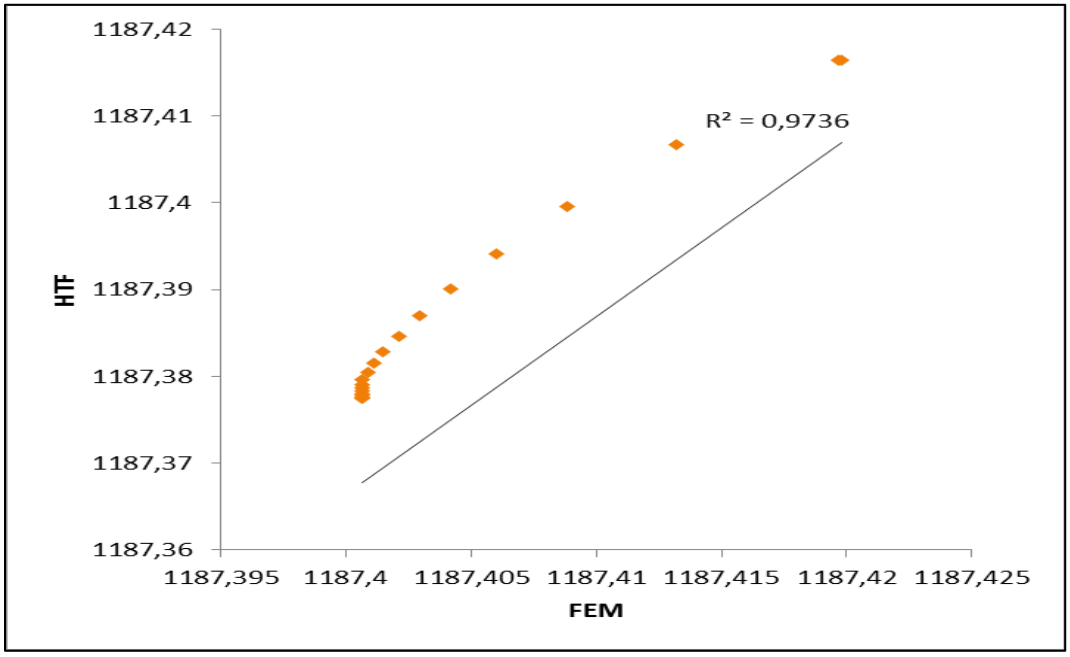

Figure B-9: Modelled versus predicted hydraulic heads for observation well OBS_1

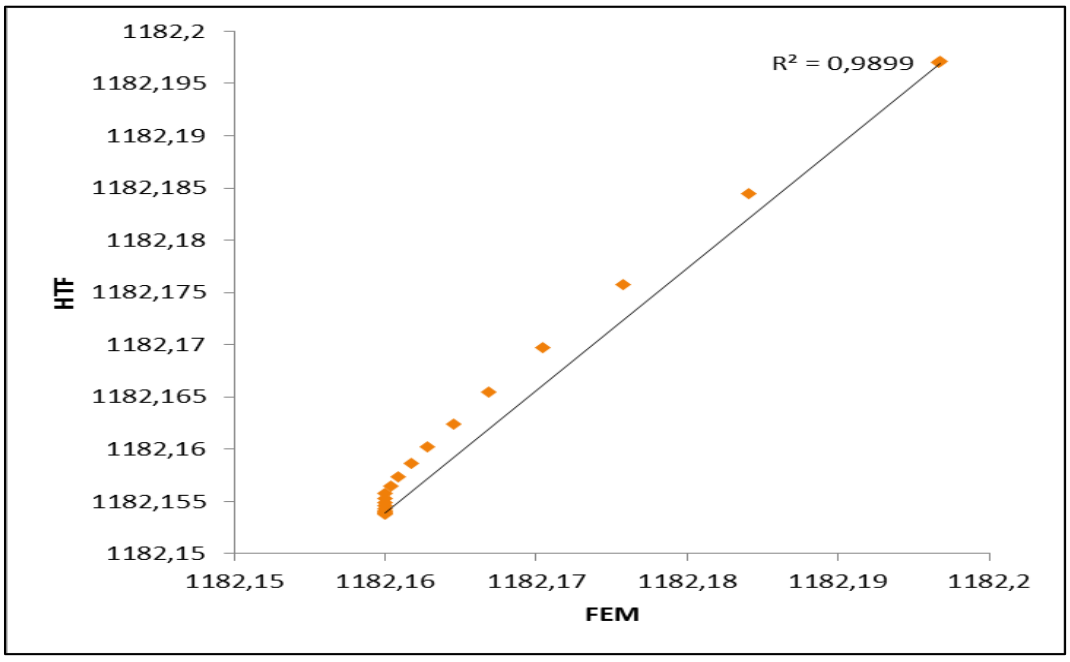

Figure B-10: Modelled versus predicted hydraulic heads for observation well OBS_2

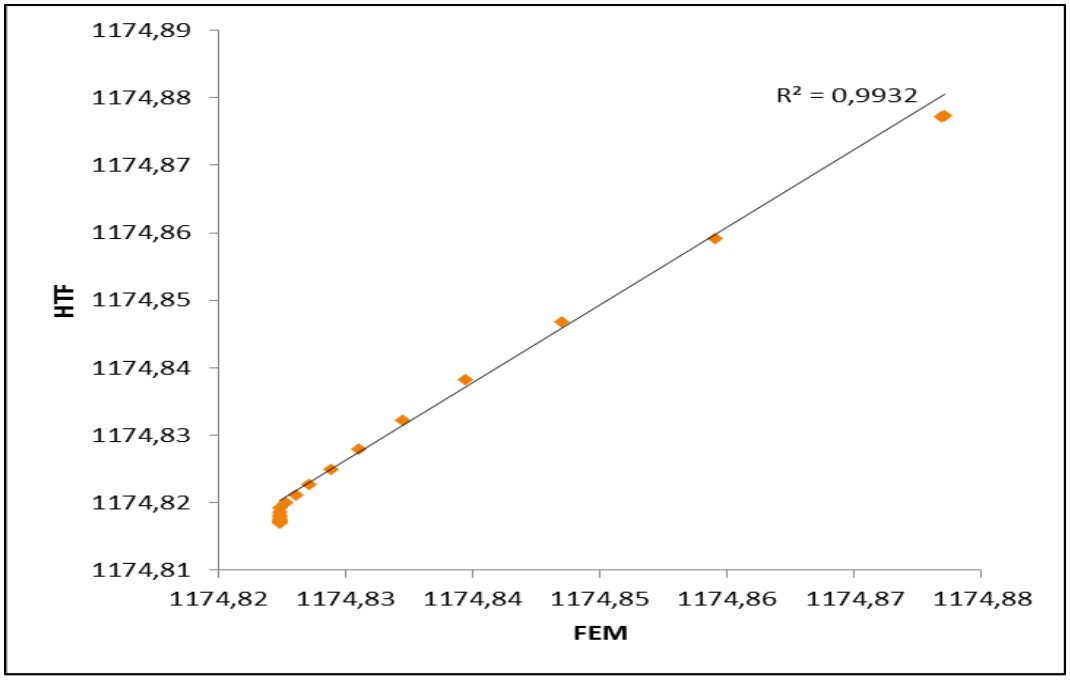

Figure B-11: Modelled versus predicted hydraulic heads for observation well OBS_3

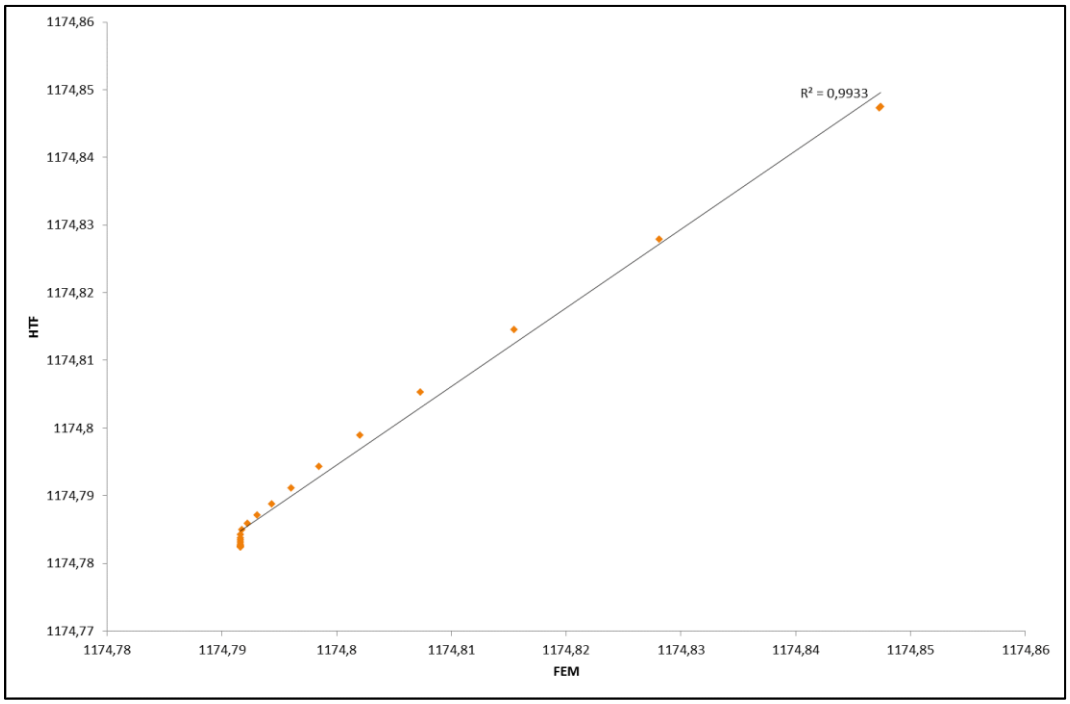

Figure B-12: Modelled versus predicted hydraulic heads for observation well OBS_4

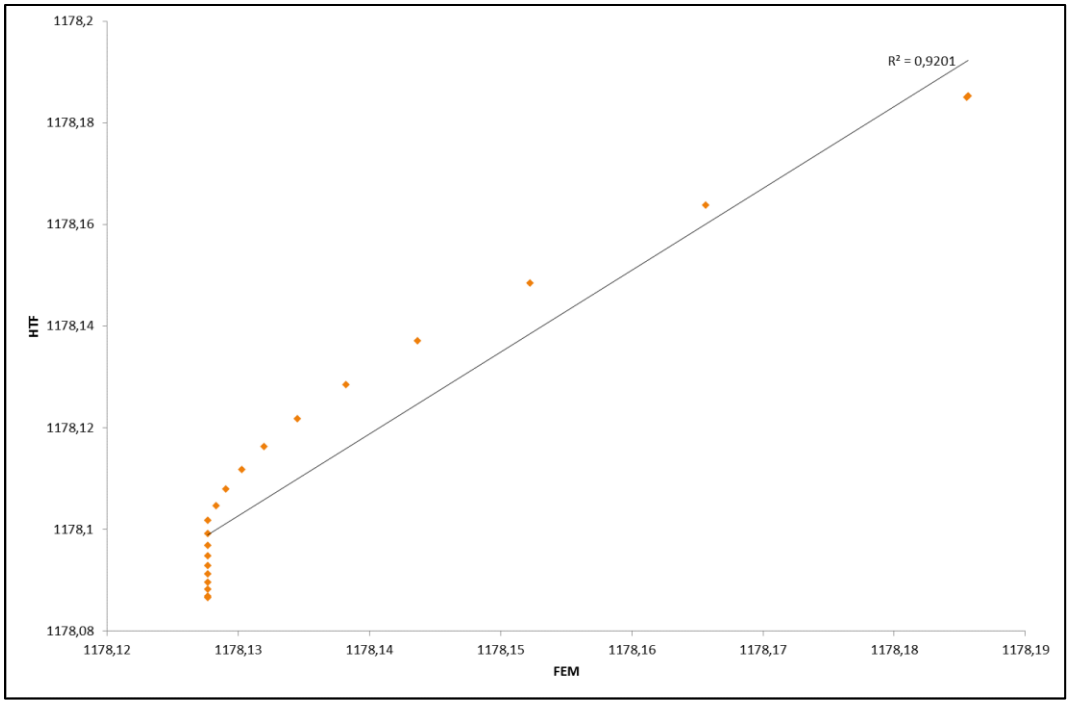

Figure B-13: Modelled versus predicted hydraulic heads for observation well OBS_5

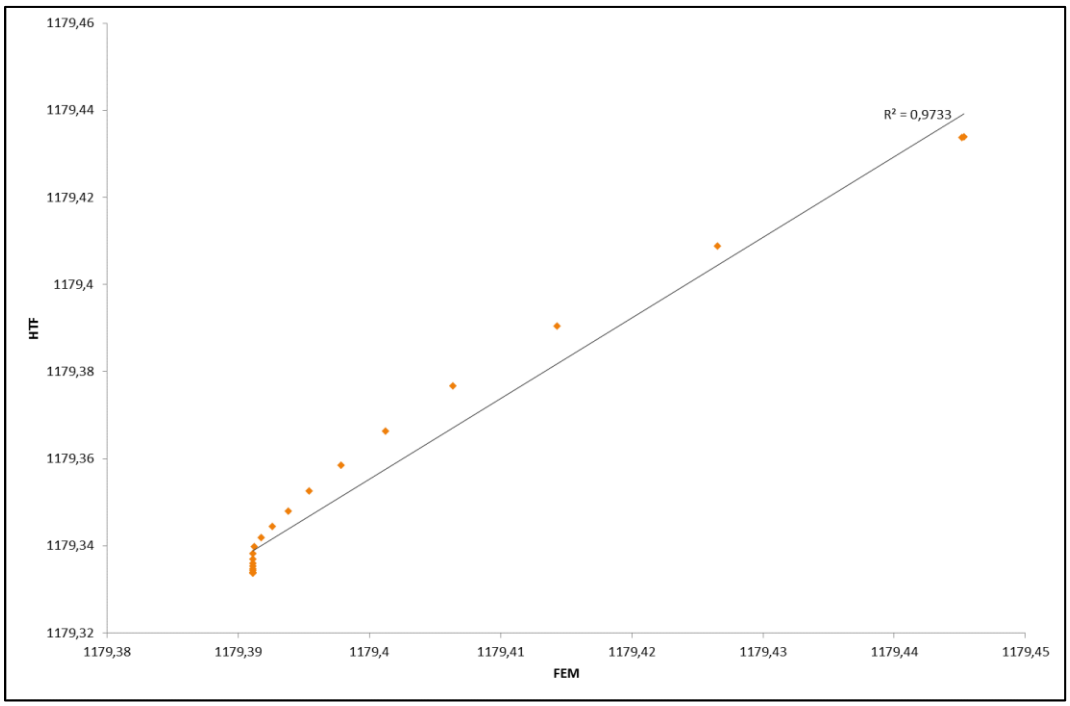

Figure B-14: Modelled versus predicted hydraulic heads for observation well OBS_6

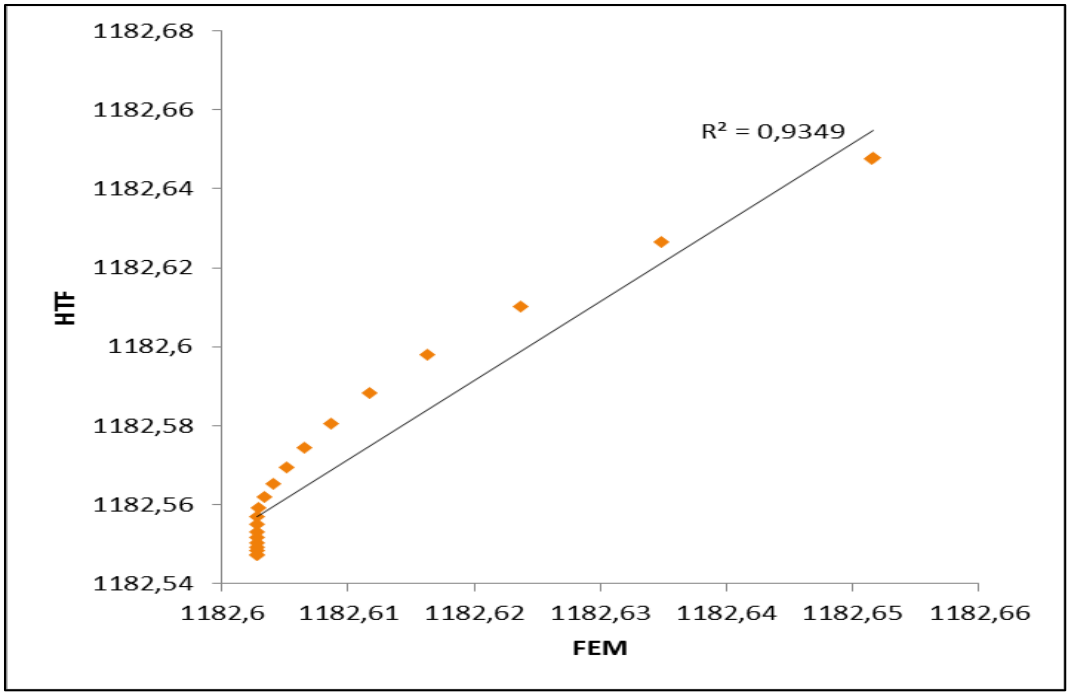

Figure B-15: Modelled versus predicted hydraulic heads for observation well OBS_7

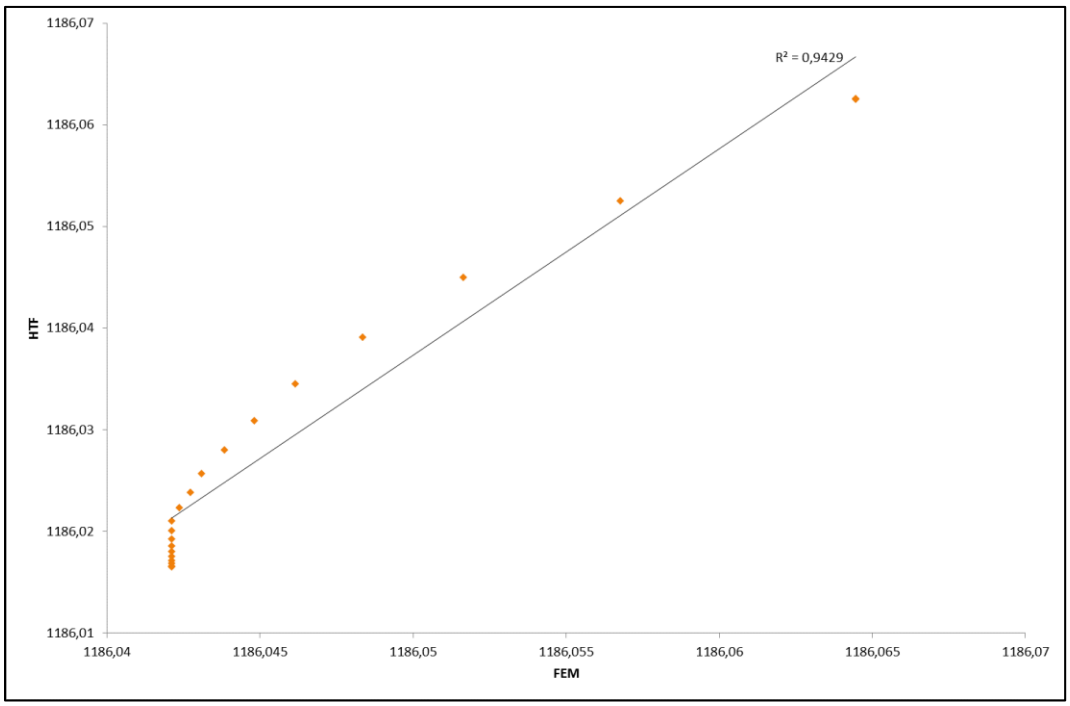

Figure B-16: Modelled versus predicted hydraulic heads for observation well OBS_8

B.3 NINE DEWATERING WELLS

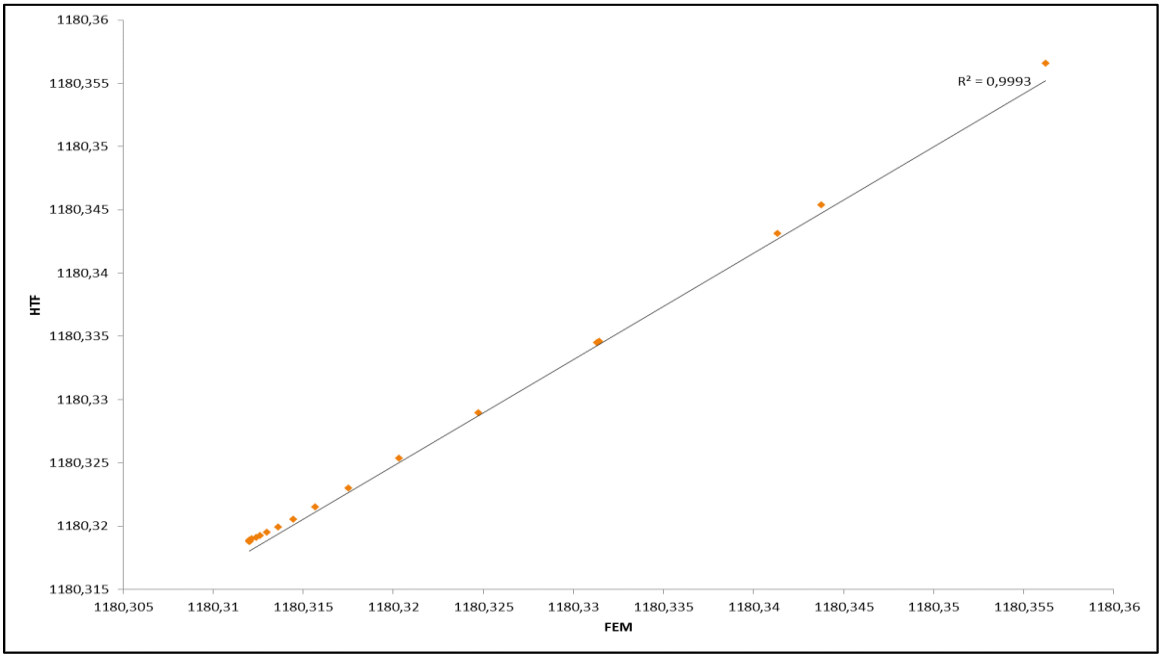

Figure B-17: Modelled versus predicted hydraulic heads for observation well OBS_1

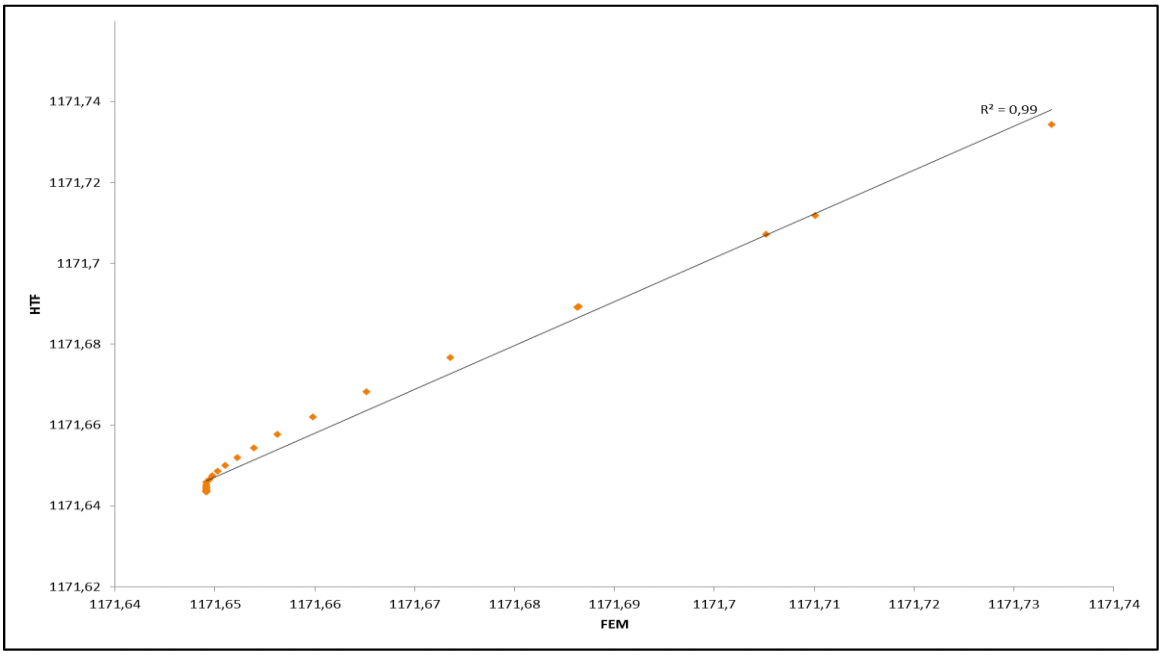

Figure B-18: Modelled versus predicted hydraulic heads for observation well OBS_2

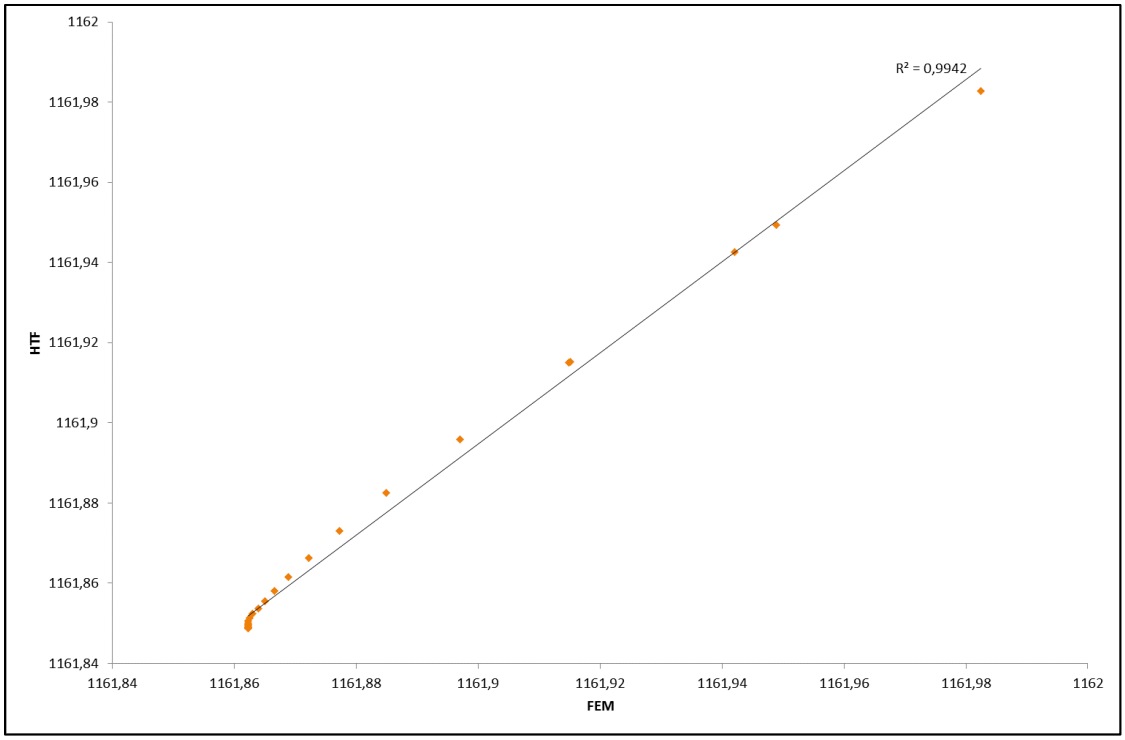

Figure B-19: Modelled versus predicted hydraulic heads for observation well OBS_3

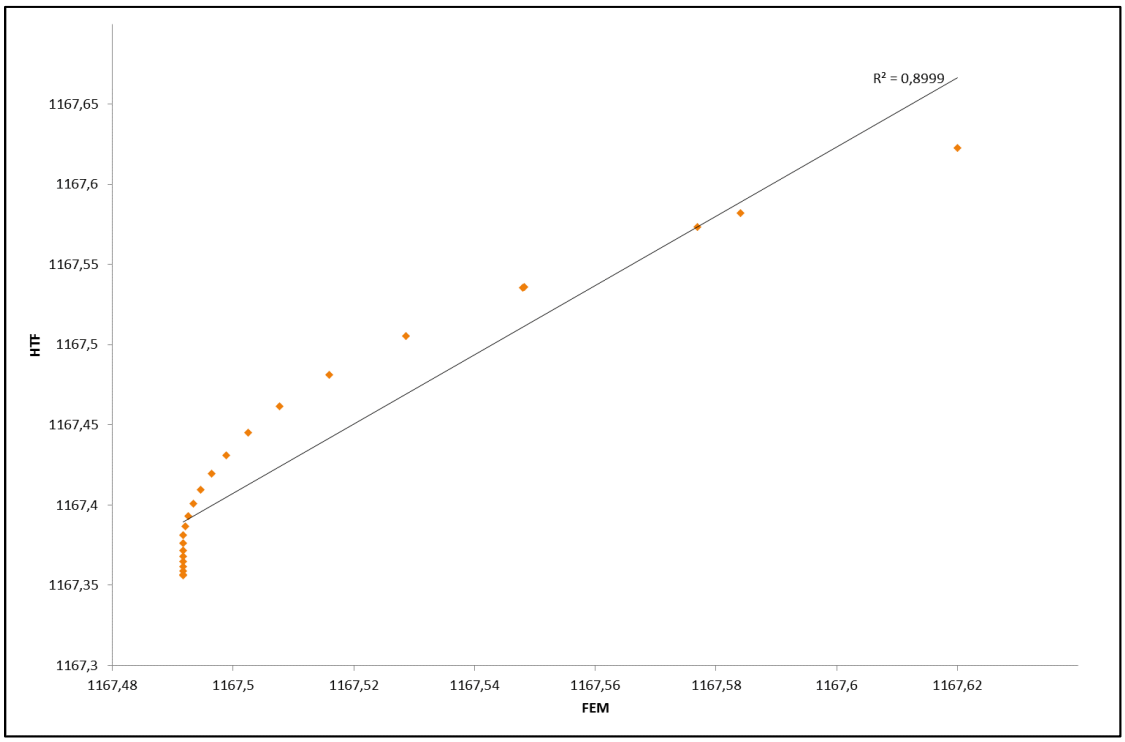

Figure B-20: Modelled versus predicted hydraulic heads for observation well OBS_4

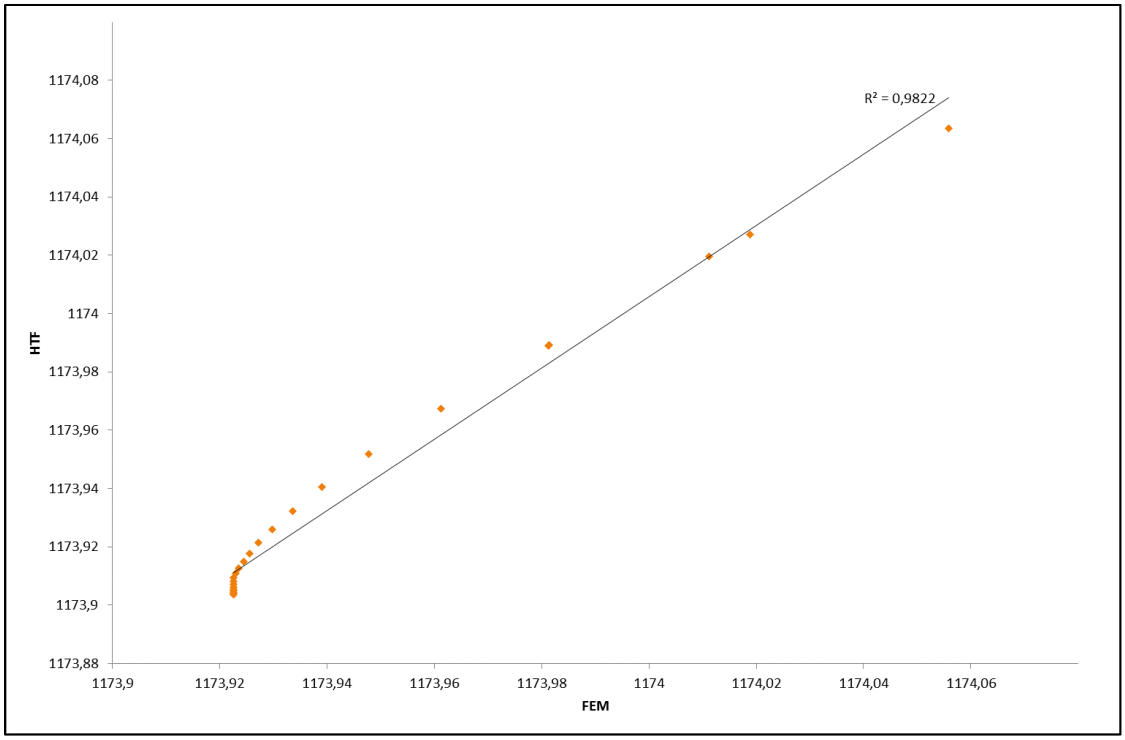

Figure B-21: Modelled versus predicted hydraulic heads for observation well OBS_5

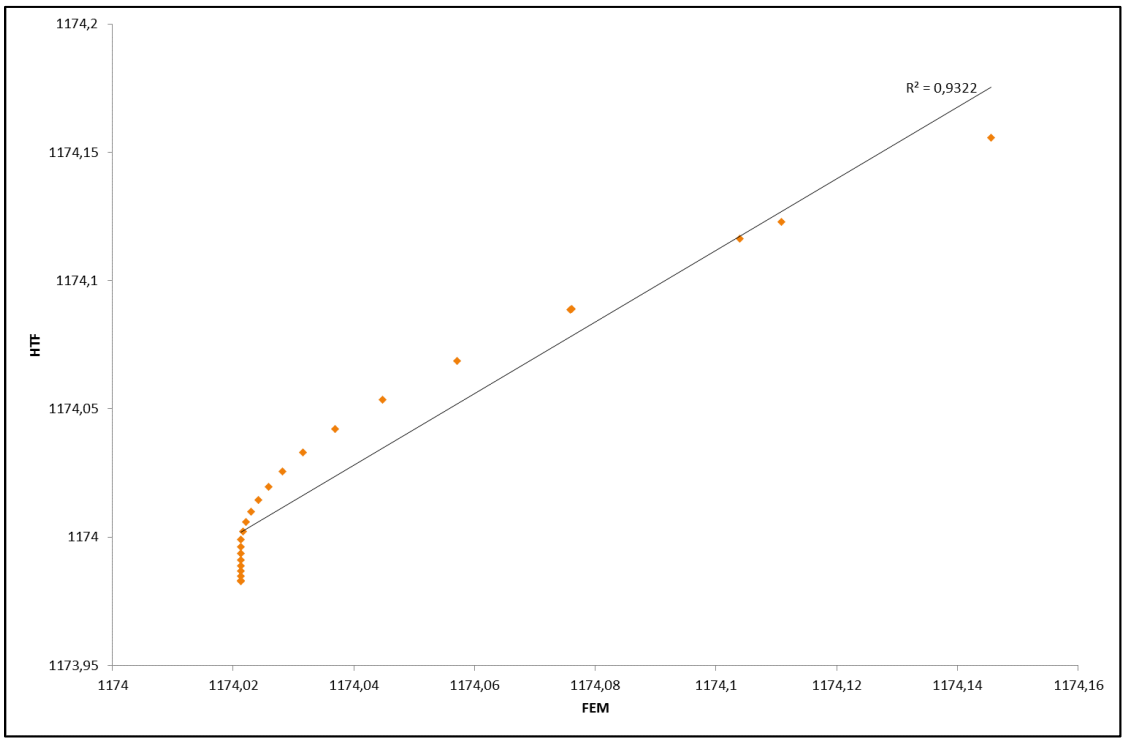

Figure B-22: Modelled versus predicted hydraulic heads for observation well OBS_6

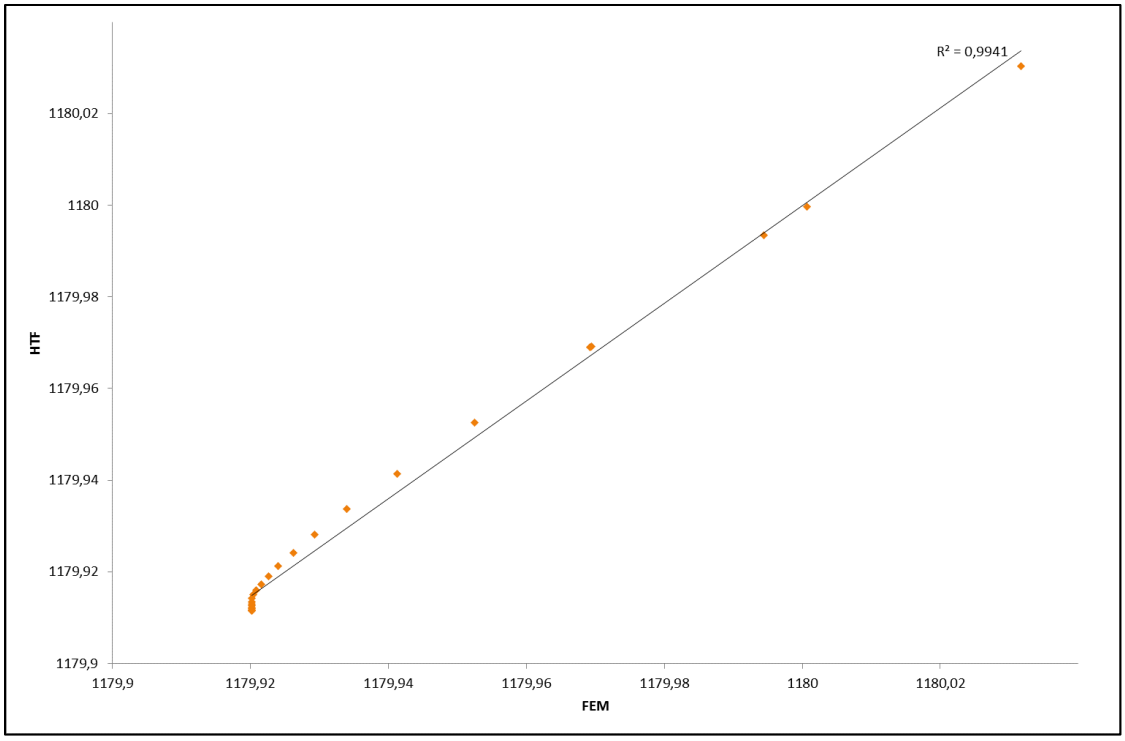

Figure B-23: Modelled versus predicted hydraulic heads for observation well OBS_7

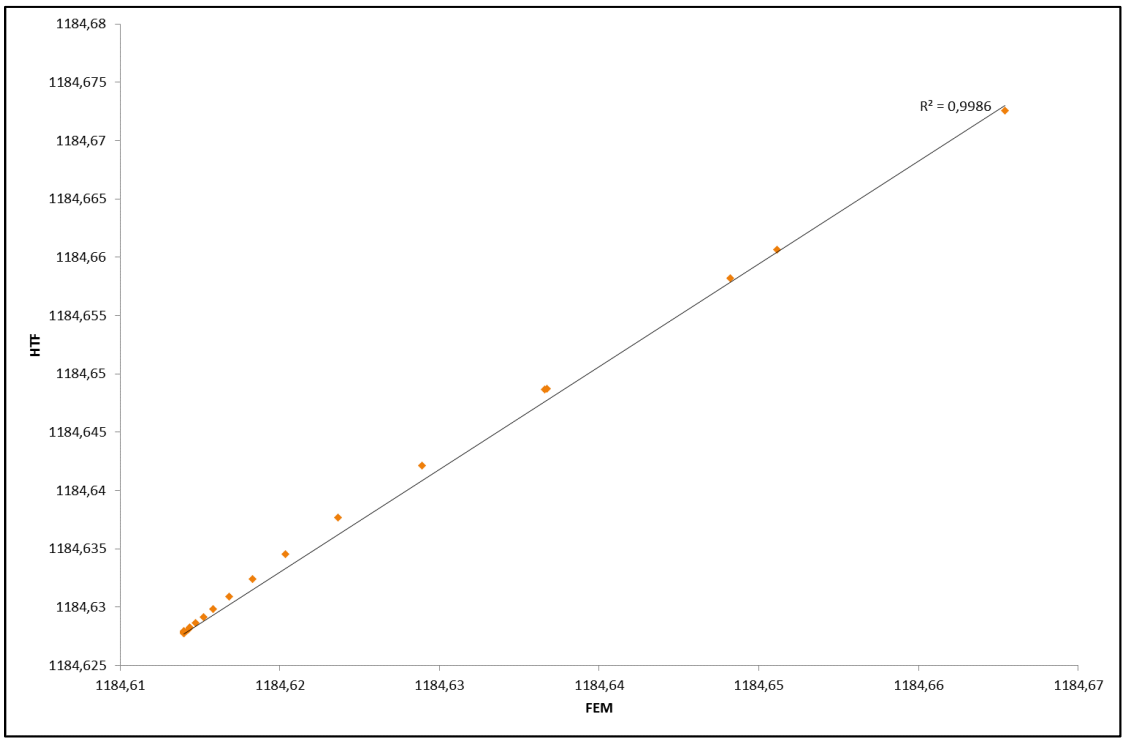

Figure B-24: Modelled versus predicted hydraulic heads for observation well OBS_8

B.4 TWELVE DEWATERING WELLS

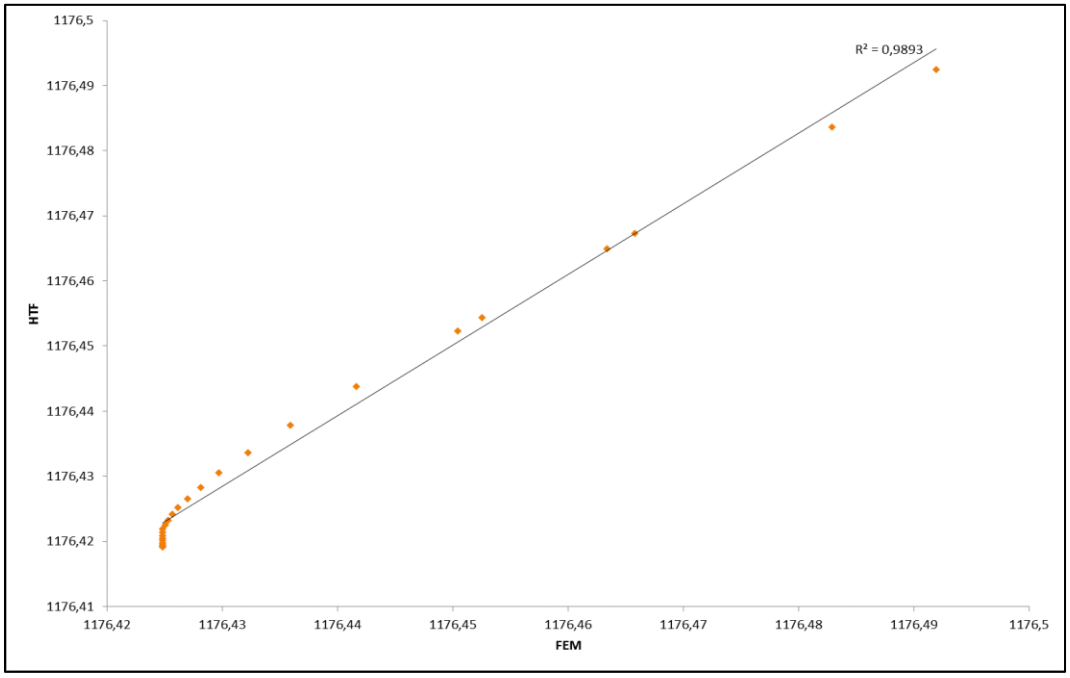

Figure B-25: Modelled versus predicted hydraulic heads for observation well OBS_1

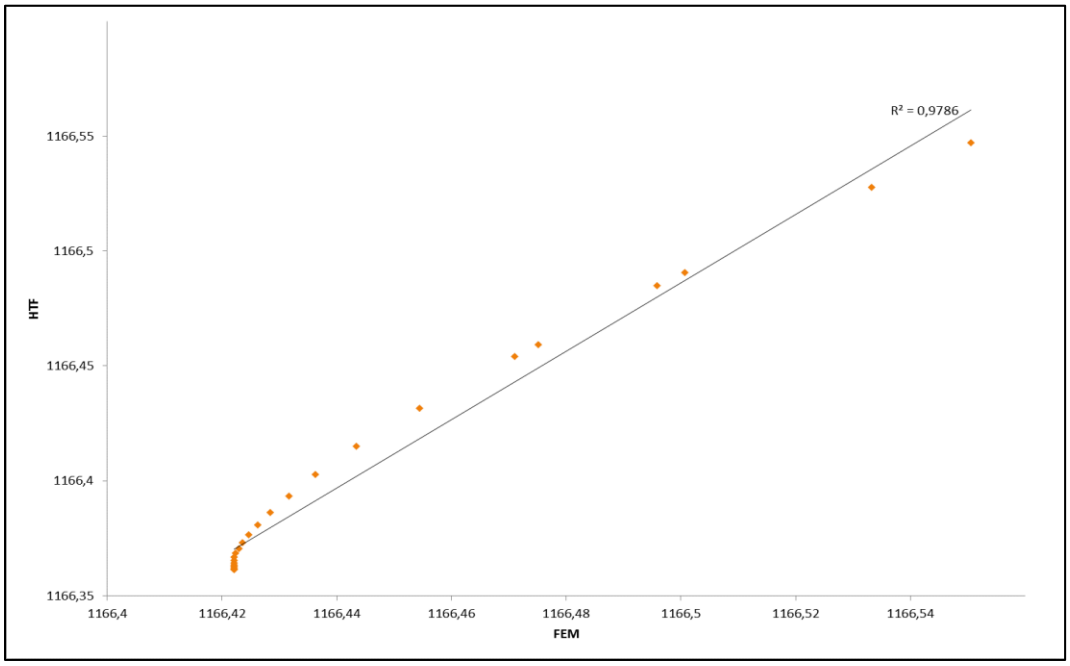

Figure B-26: Modelled versus predicted hydraulic heads for observation well OBS_2

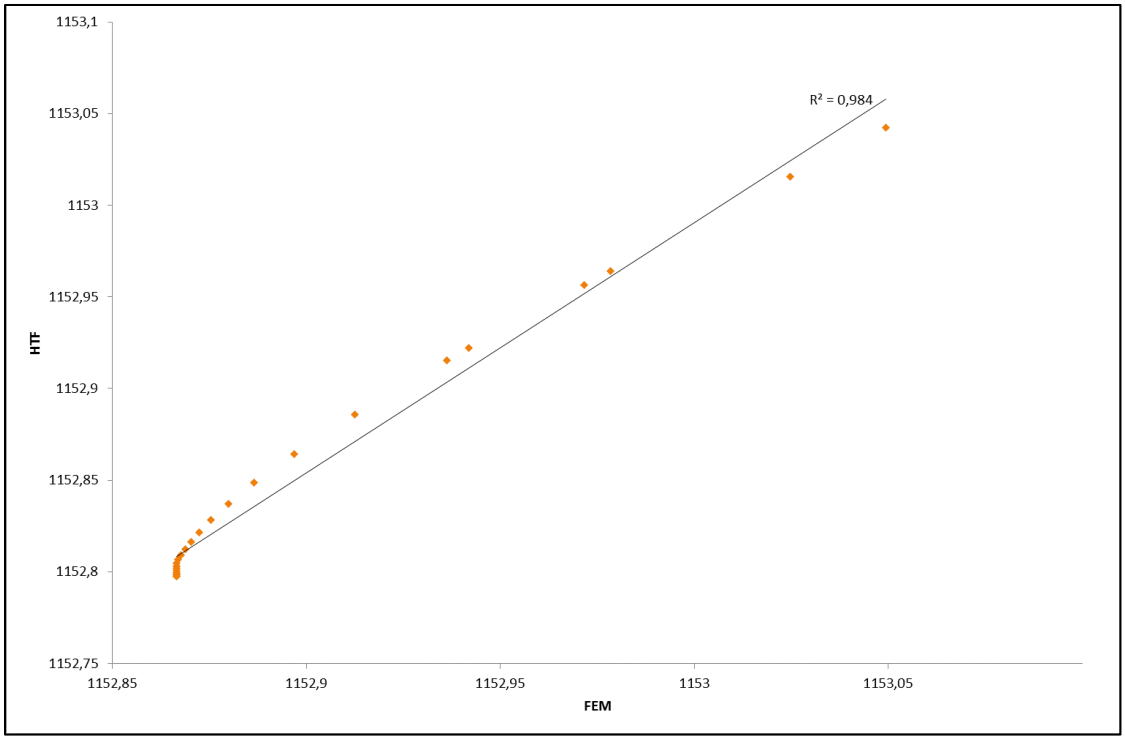

Figure B-27: Modelled versus predicted hydraulic heads for observation well OBS_3

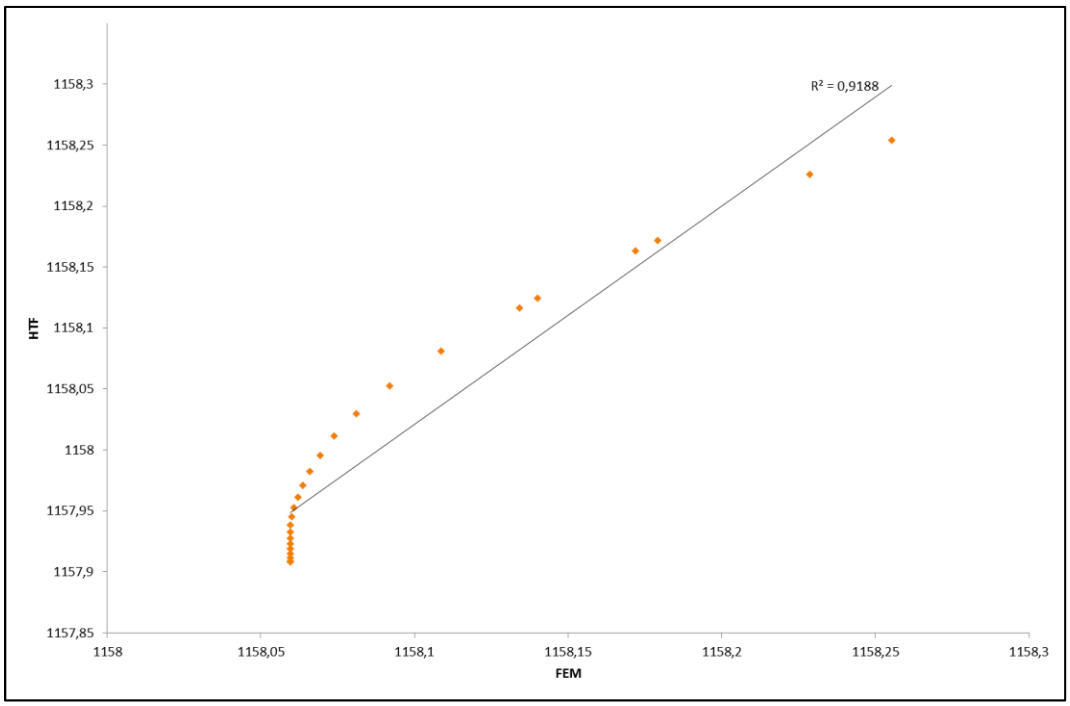

Figure B-28: Modelled versus predicted hydraulic heads for observation well OBS_4

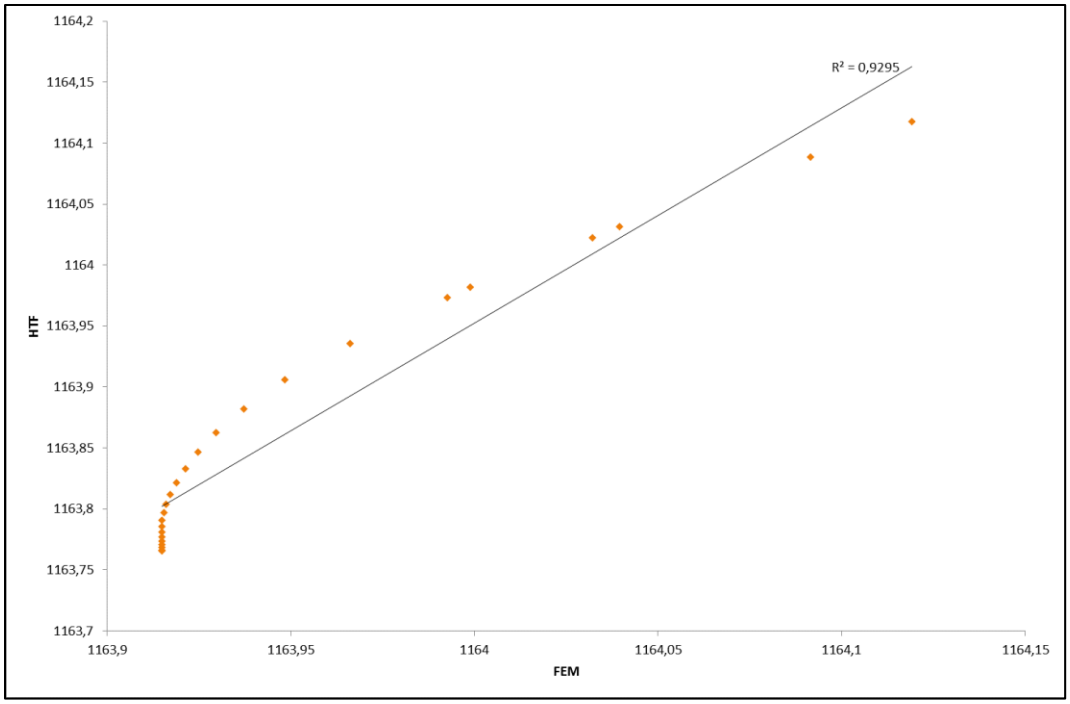

Figure B-29: Modelled versus predicted hydraulic heads for observation well OBS_5

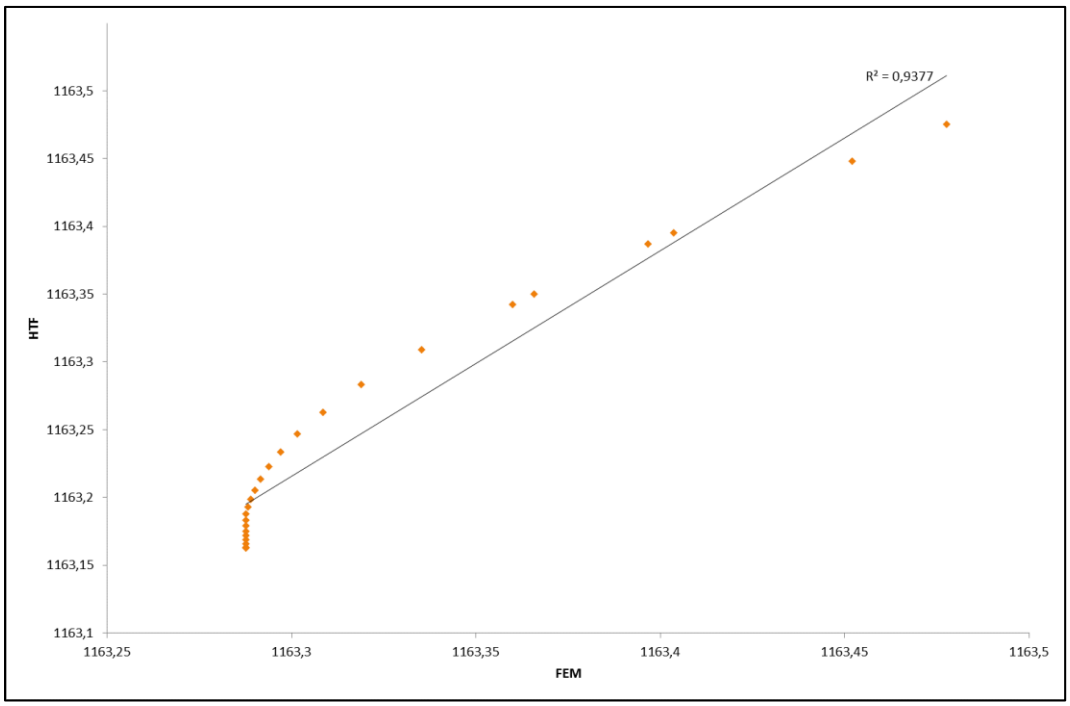

Figure B-30: Modelled versus predicted hydraulic heads for observation well OBS_6

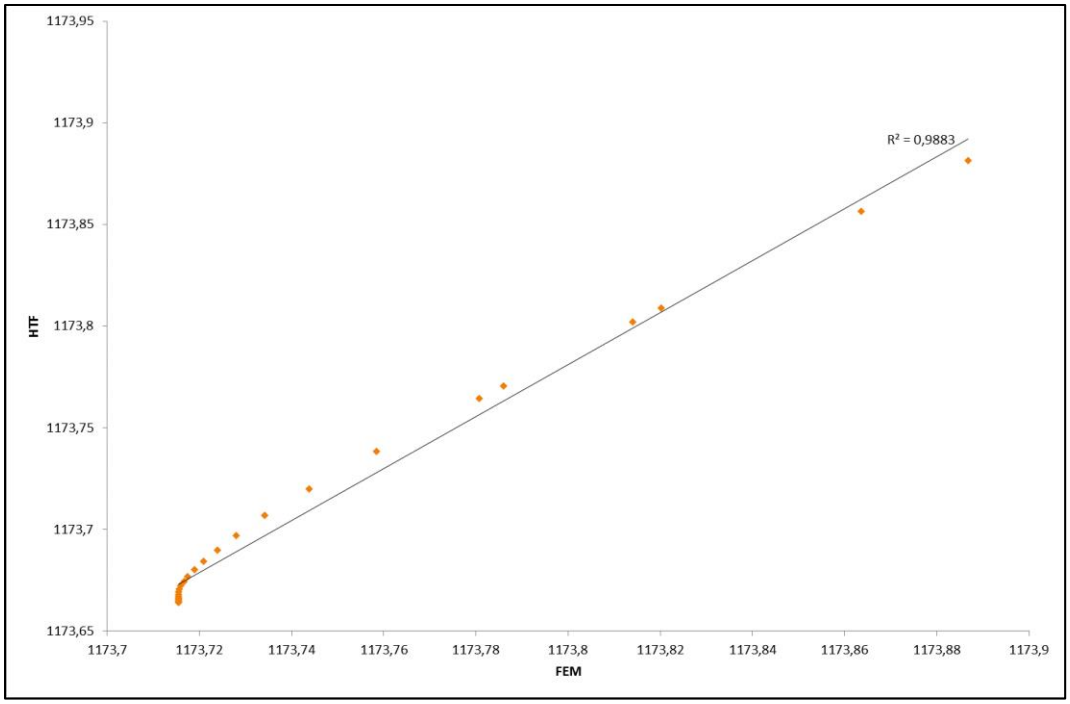

Figure B-31: Modelled versus predicted hydraulic heads for observation well OBS_7

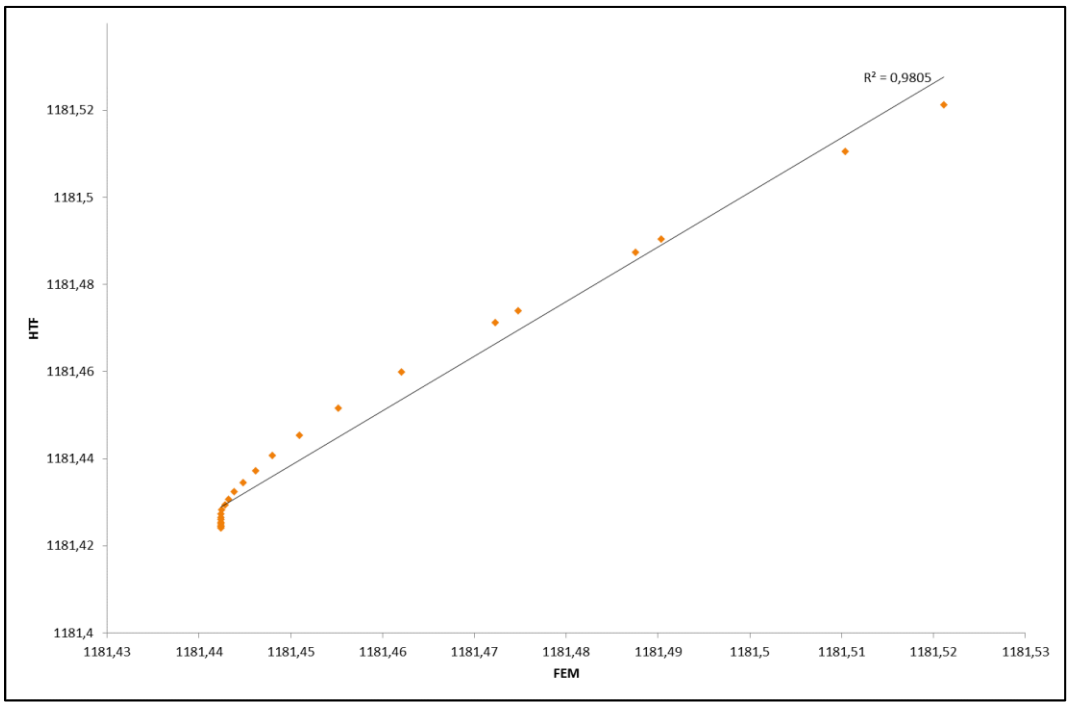

Figure B-32: Modelled versus predicted hydraulic heads for observation well OBS_8

C. NORMAL PROBABILITY PLOTS

C.1 THREE DEWATERING WELLS

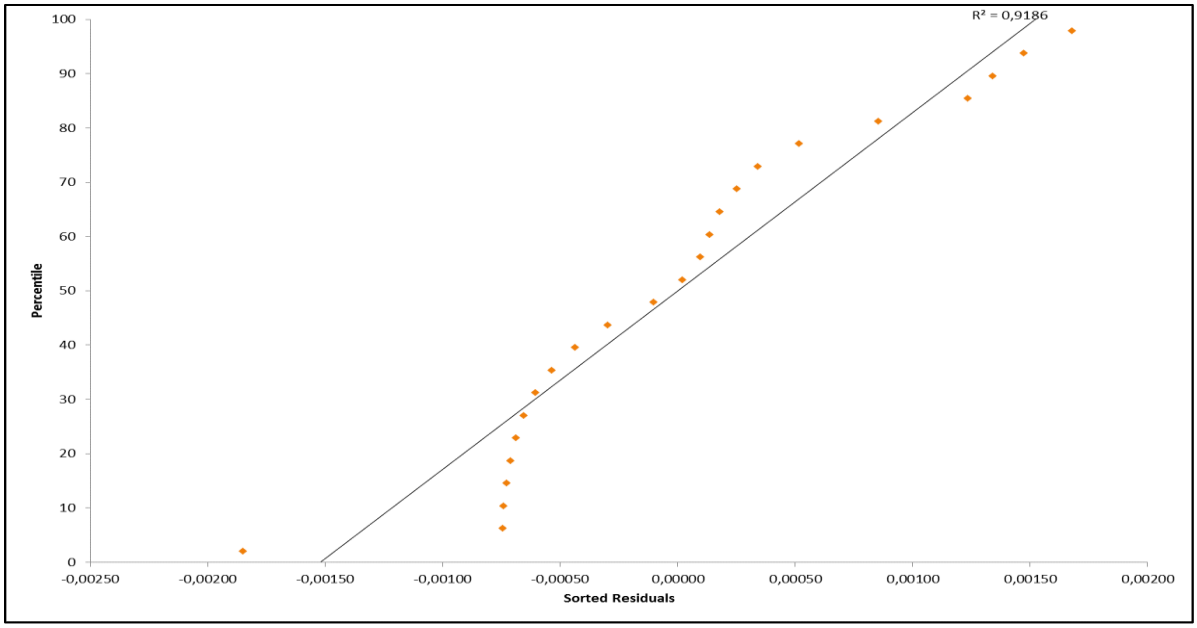

Figure C-1: Normal probability plot for observation point OBS_1

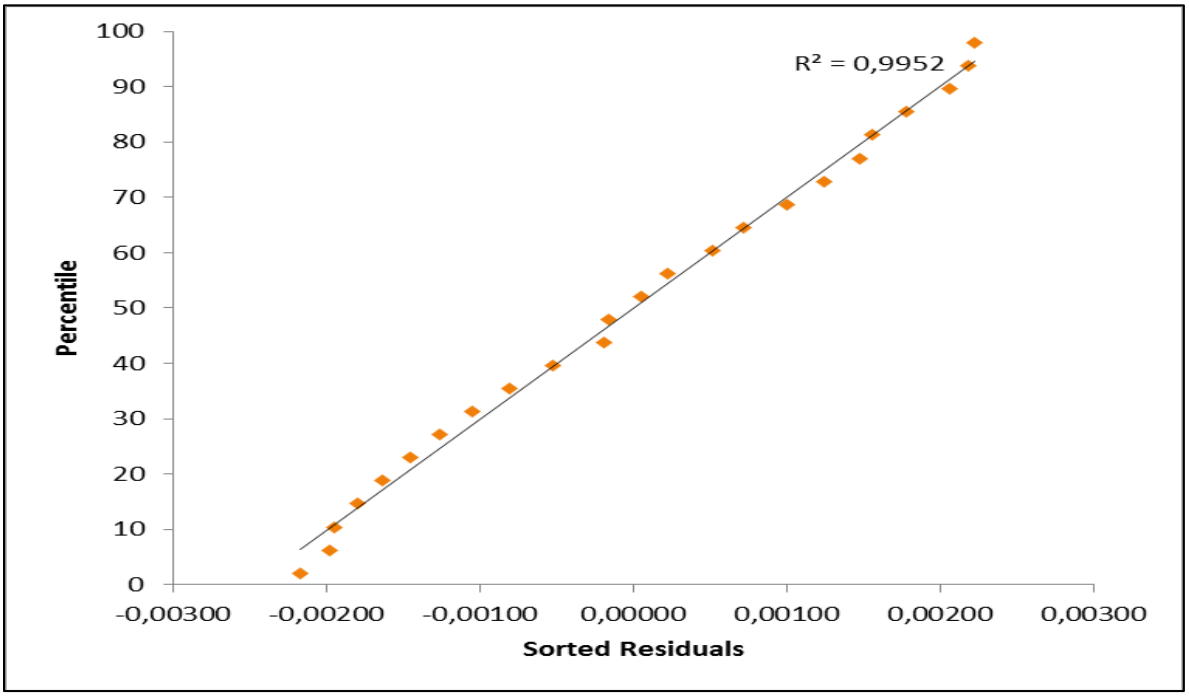

Figure C-2: Normal probability plot for observation point OBS_2

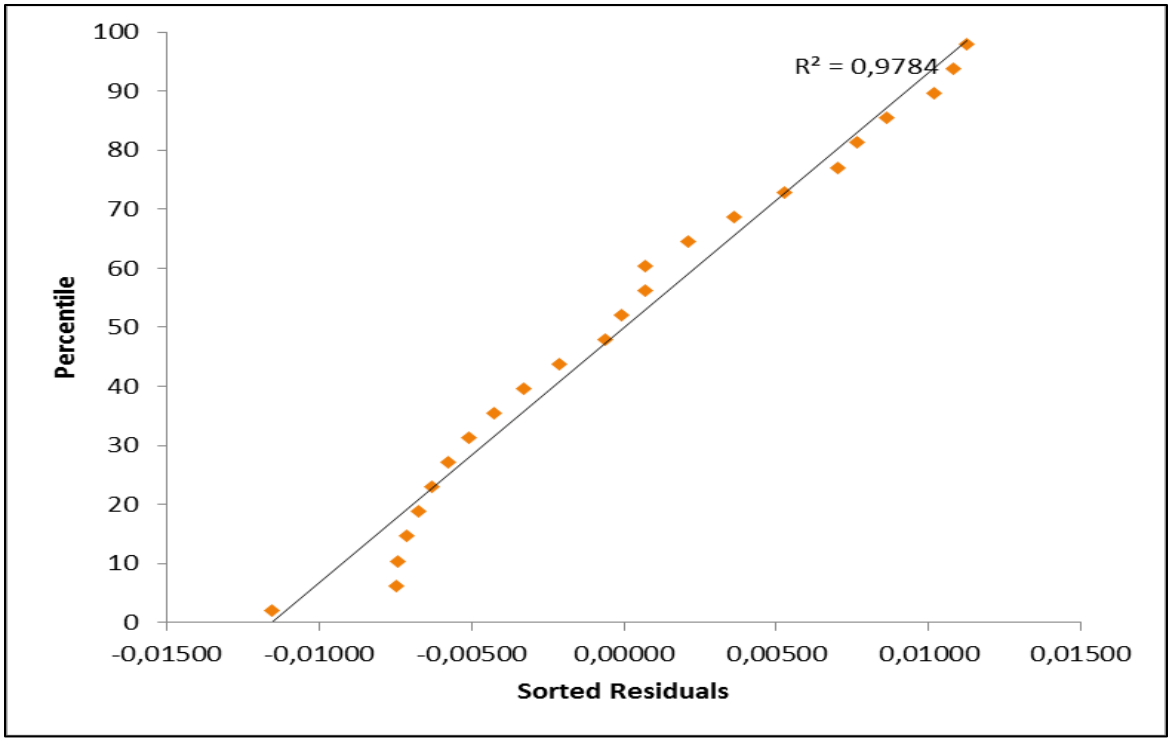

Figure C-3: Normal probability plot for observation point OBS_3

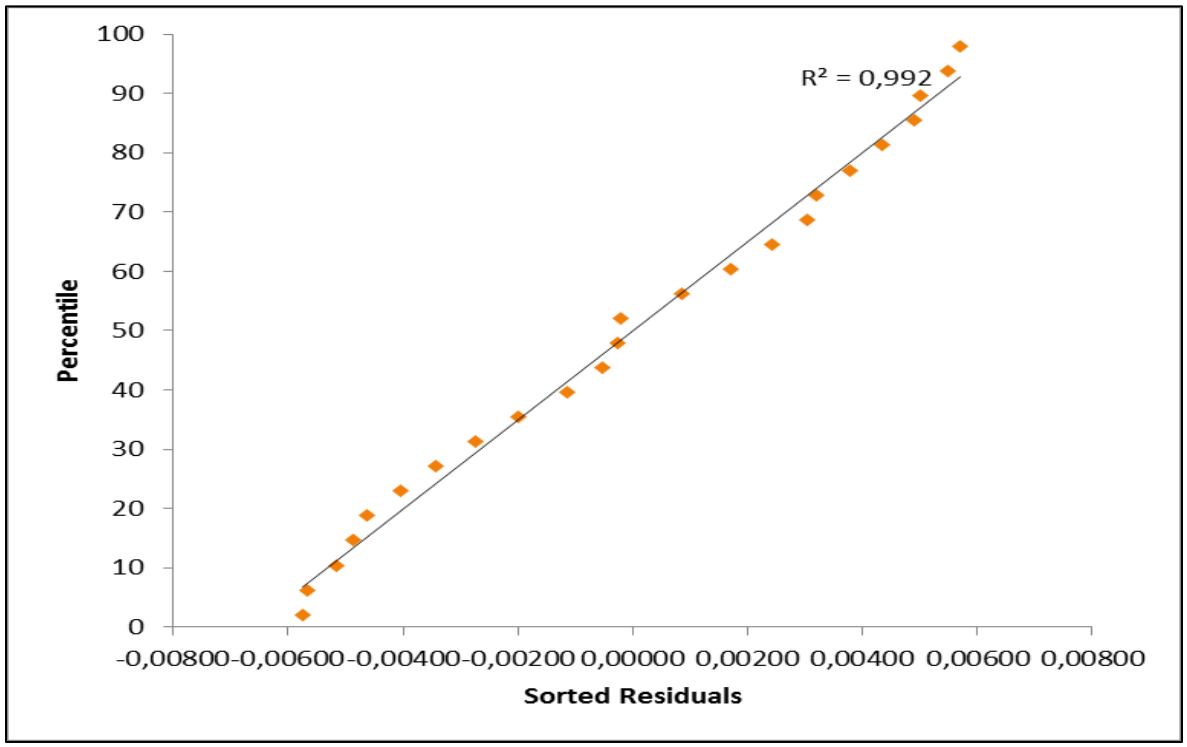

Figure C-4: Normal probability plot for observation point OBS_4

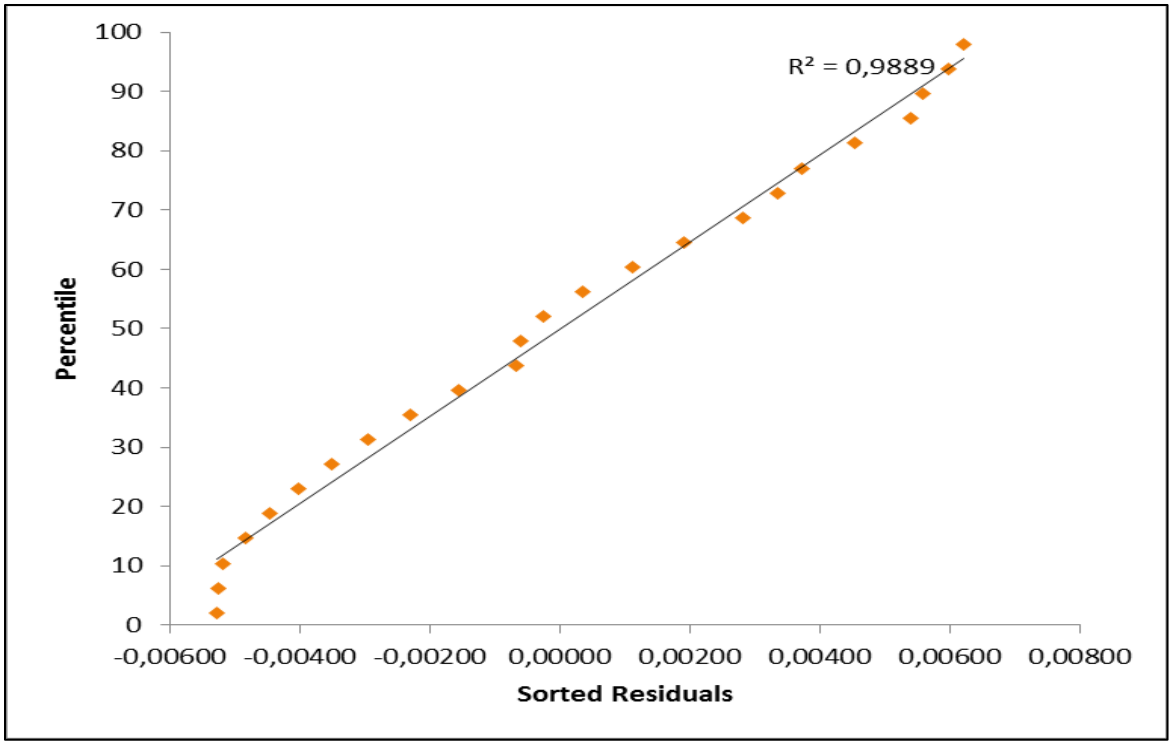

Figure C-5: Normal probability plot for observation point OBS_5

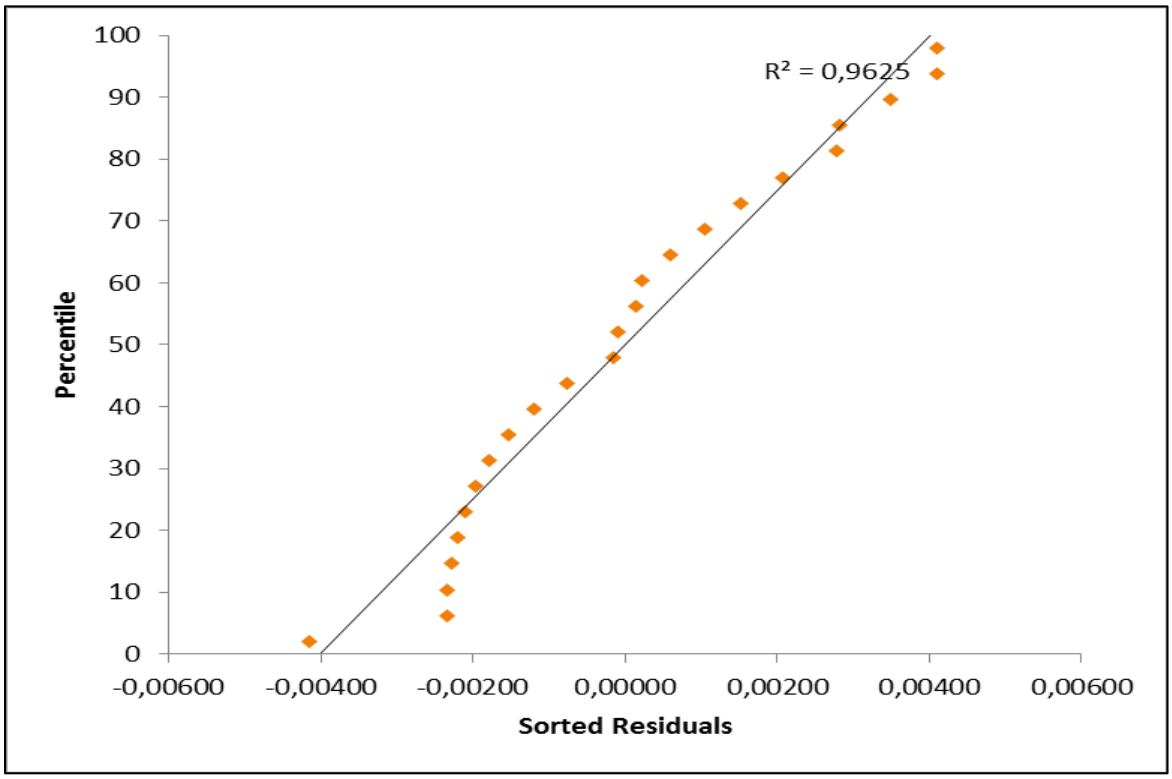

Figure C-6: Normal probability plot for observation point OBS_6

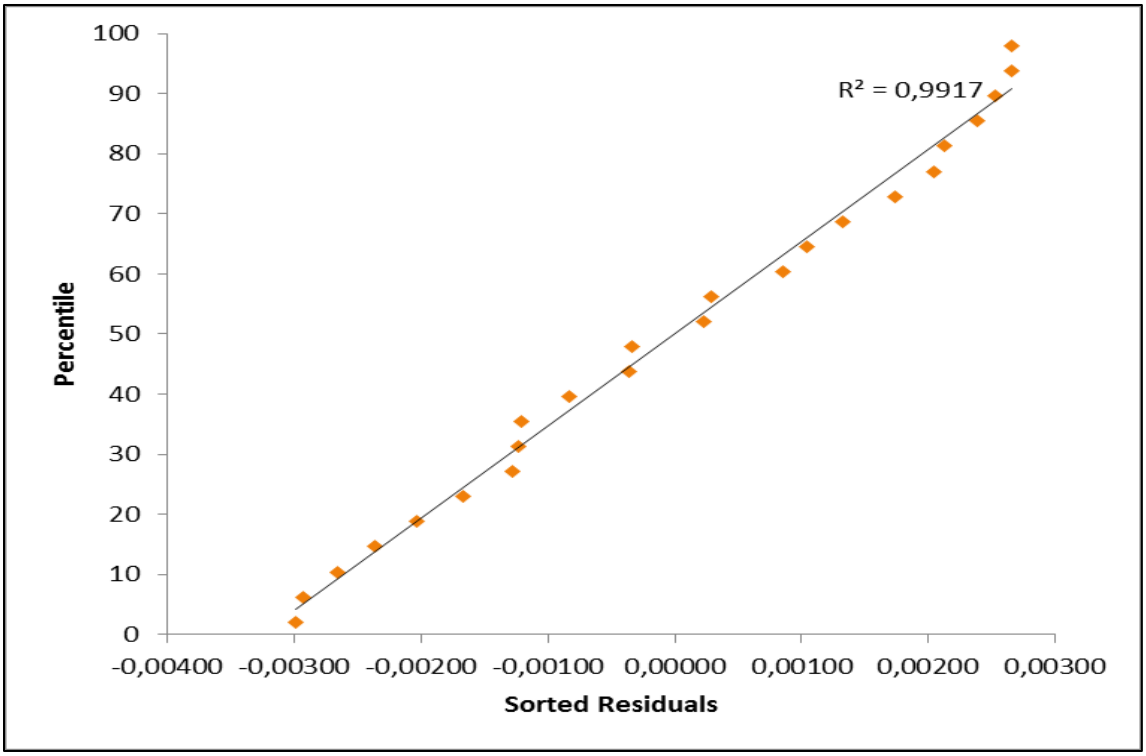

Figure C-7: Normal probability plot for observation point OBS_7

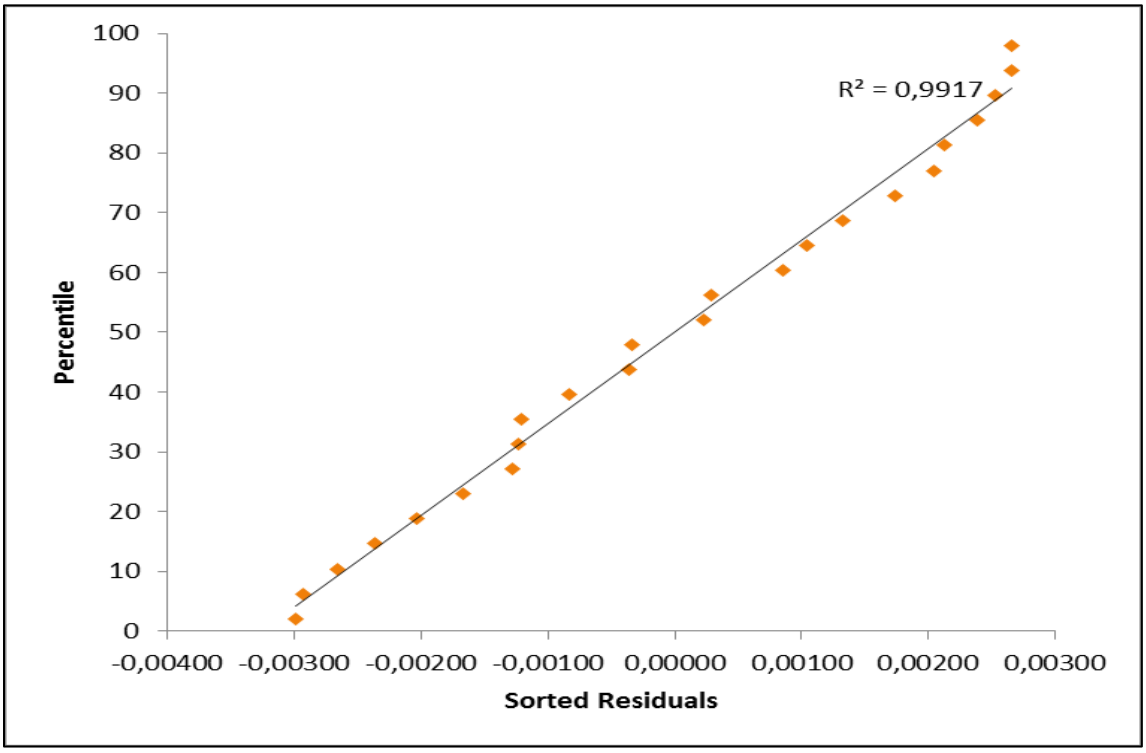

Figure C-8: Normal probability plot for observation point OBS_8

C.2 SIX DEWATERING WELLS

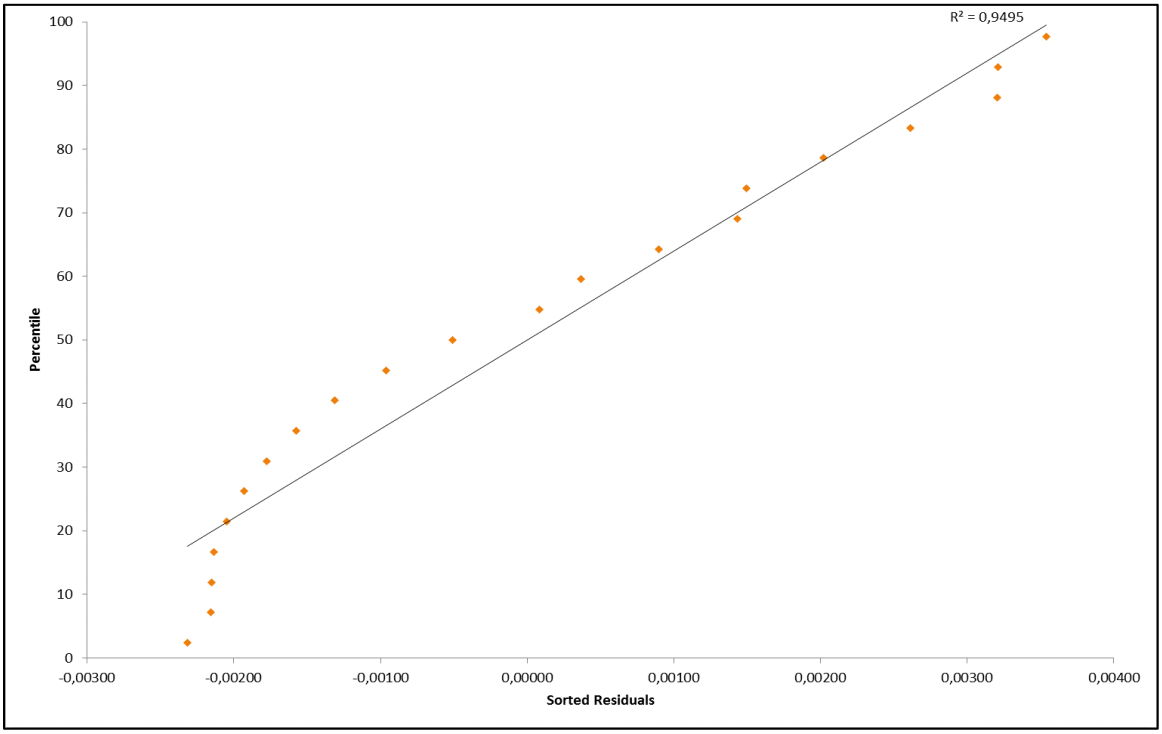

Figure C-9: Normal probability plot for observation point OBS_1

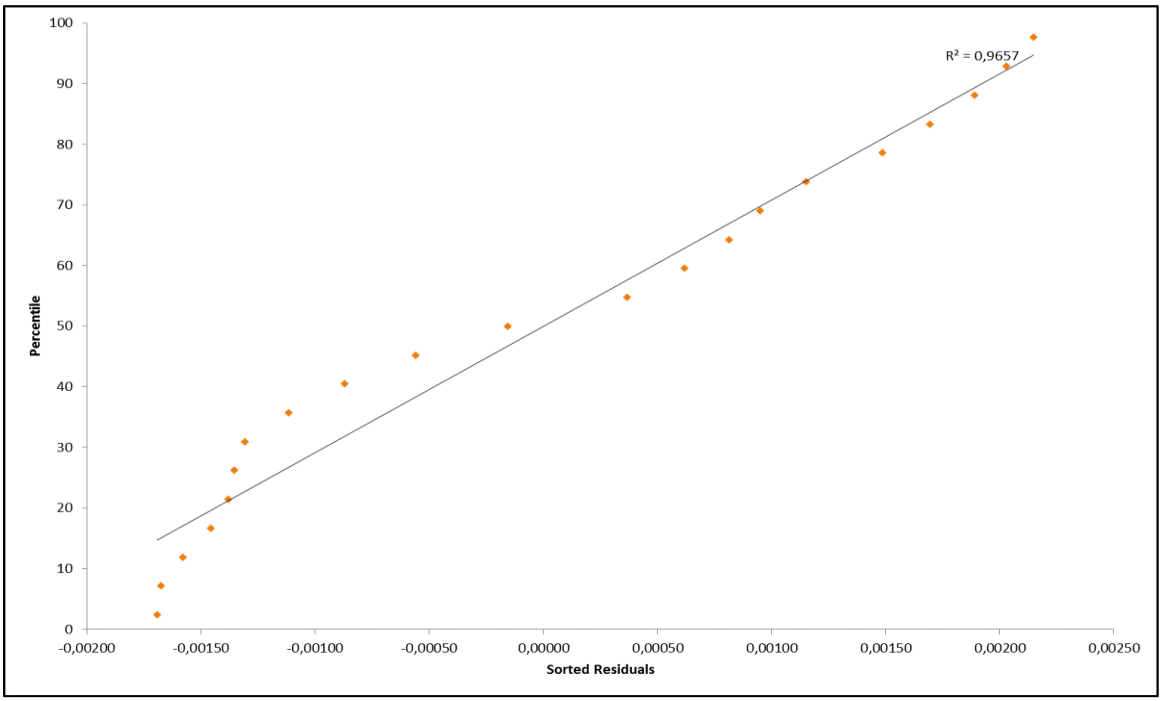

Figure C-10: Normal probability plot for observation point OBS_2

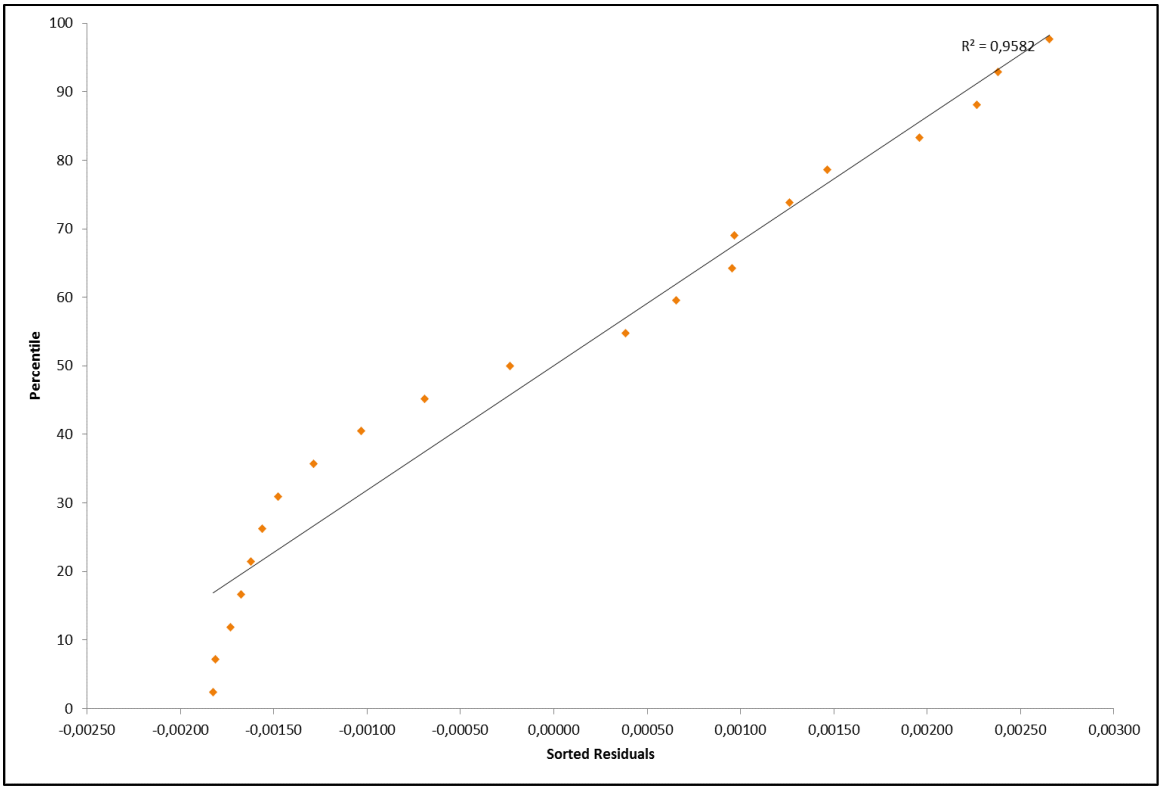

Figure C-11: Normal probability plot for observation point OBS_3

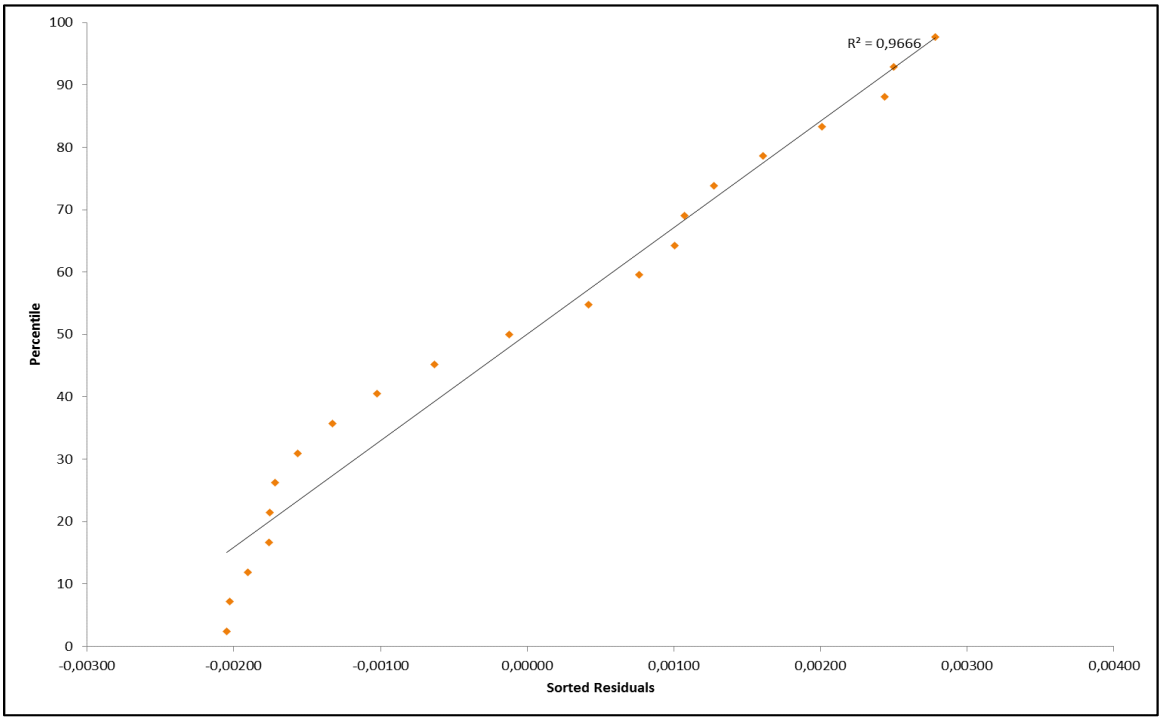

Figure C-12: Normal probability plot for observation point OBS_4

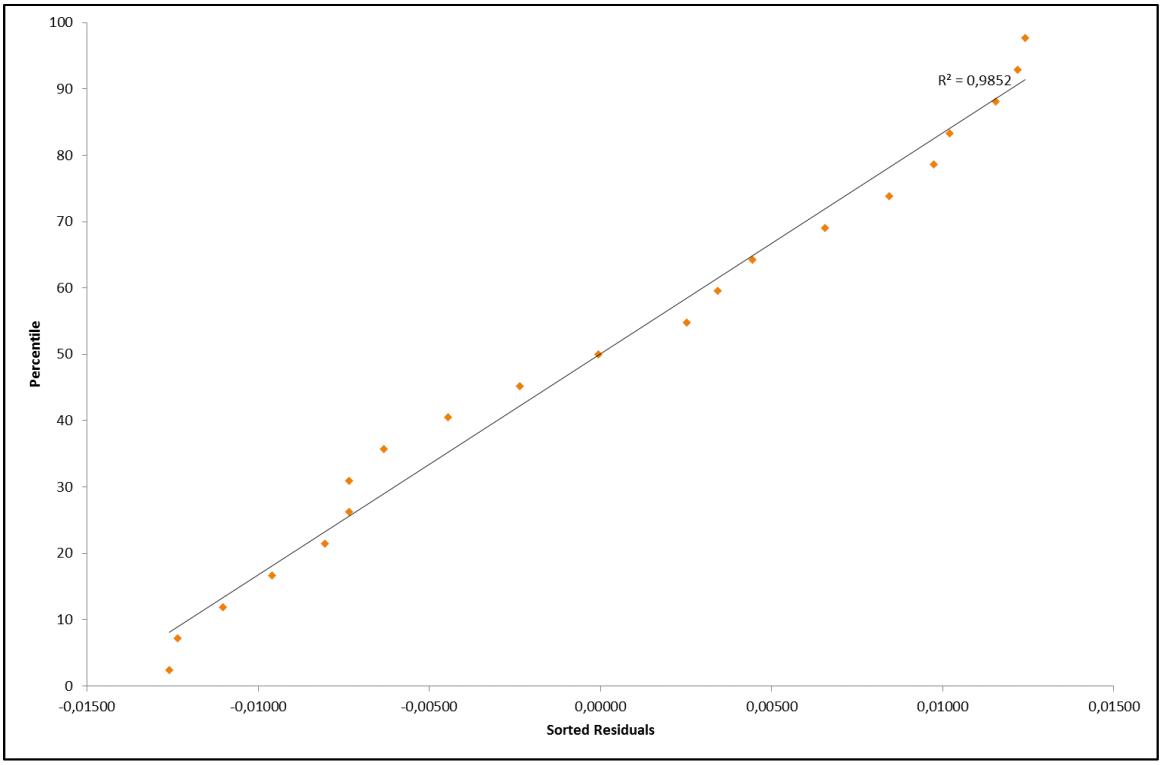

Figure C-13: Normal probability plot for observation point OBS_5

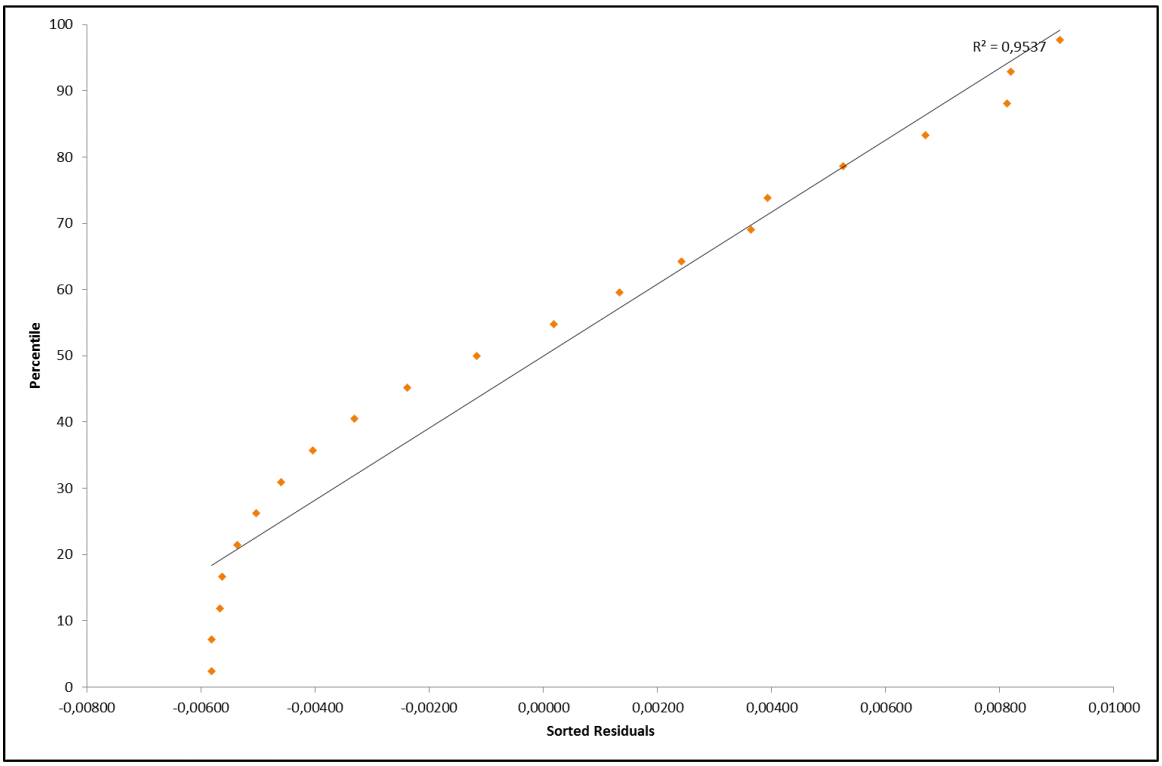

Figure C-14: Normal probability plot for observation point OBS_6

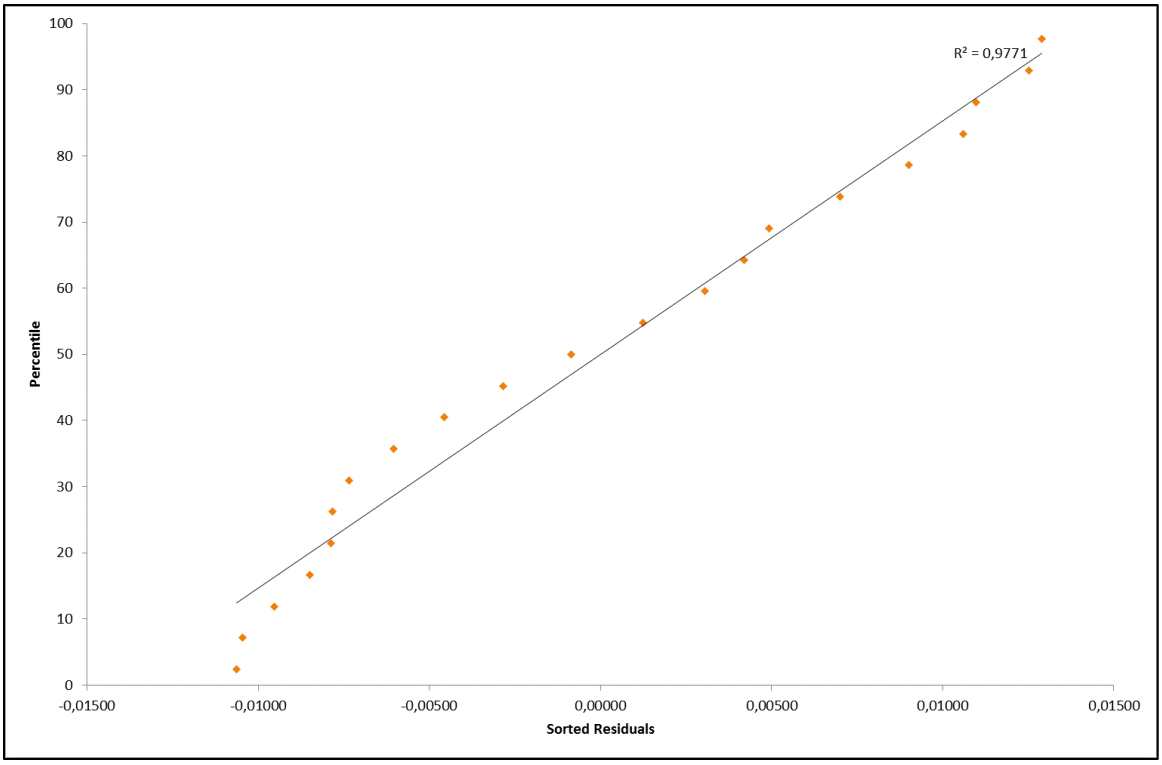

Figure C-15: Normal probability plot for observation point OBS_7

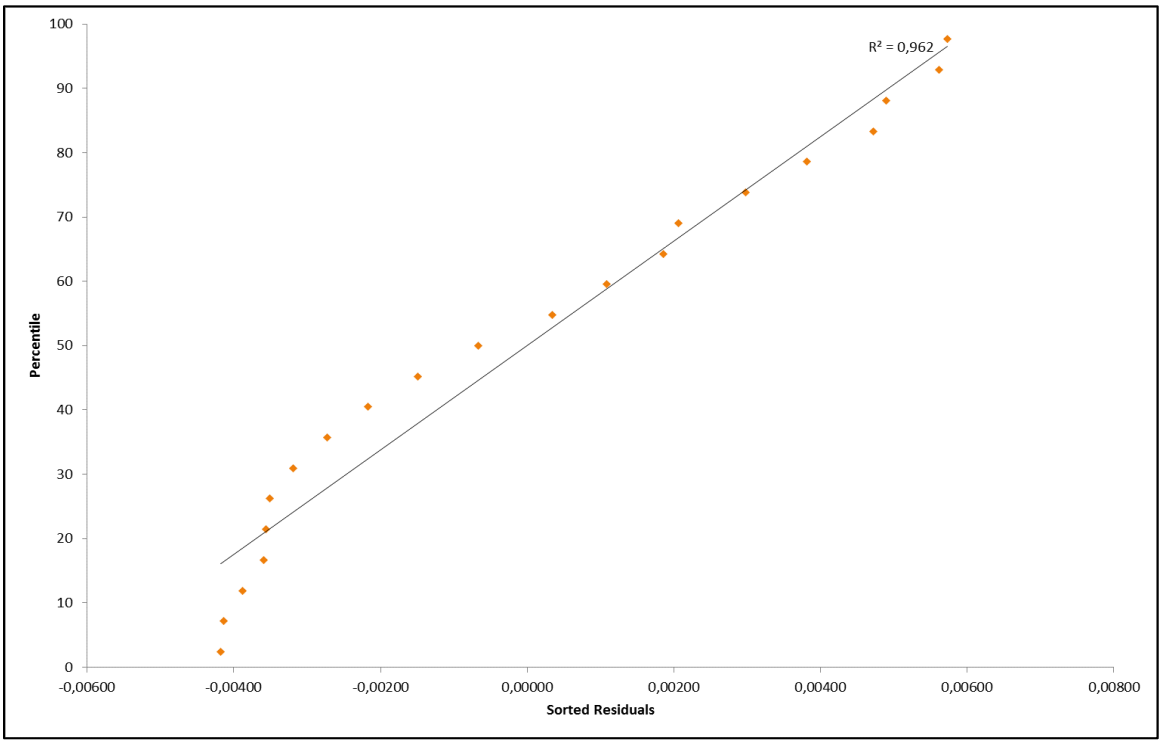

Figure C-16: Normal probability plot for observation point OBS_8

C.3 NINE DEWATERING WELLS

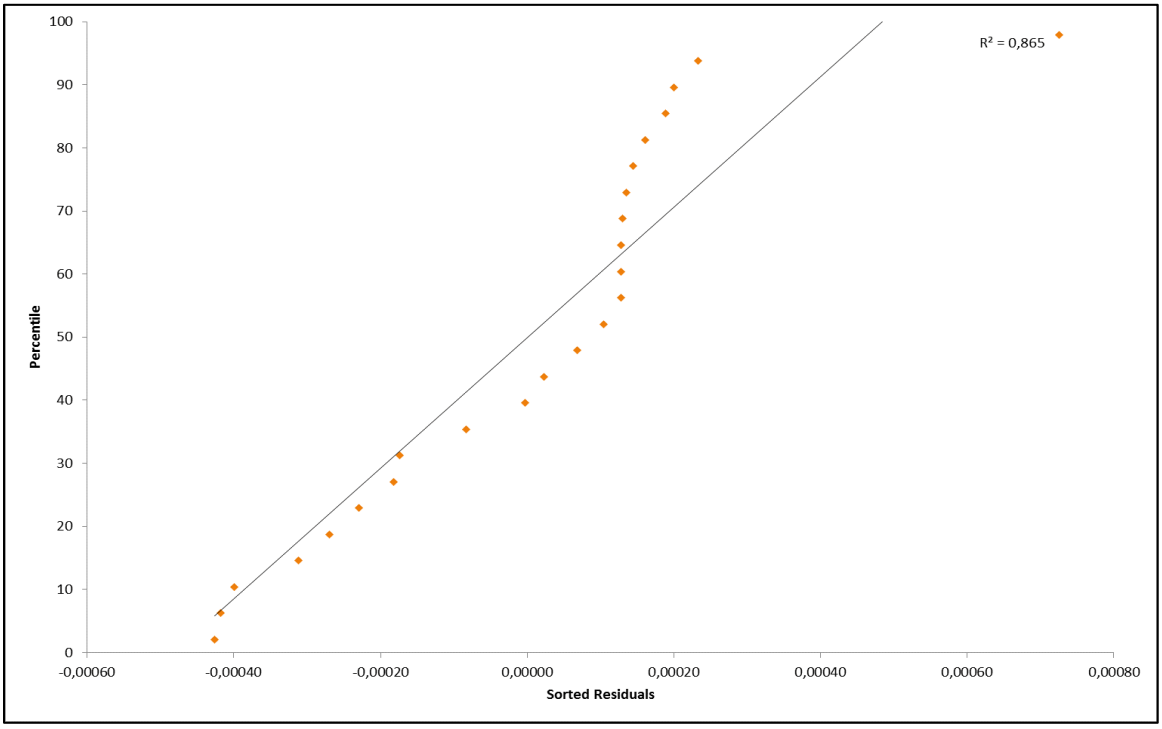

Figure C-17: Normal probability plot for observation point OBS_1

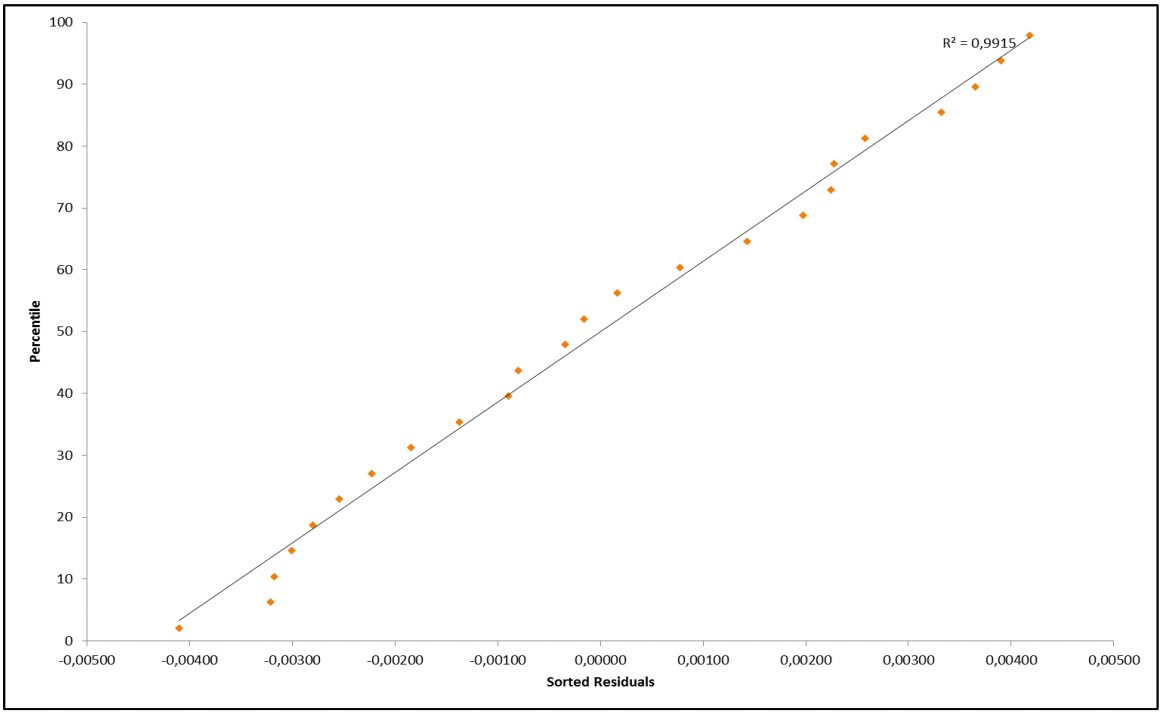

Figure C-18: Normal probability plot for observation point OBS_2

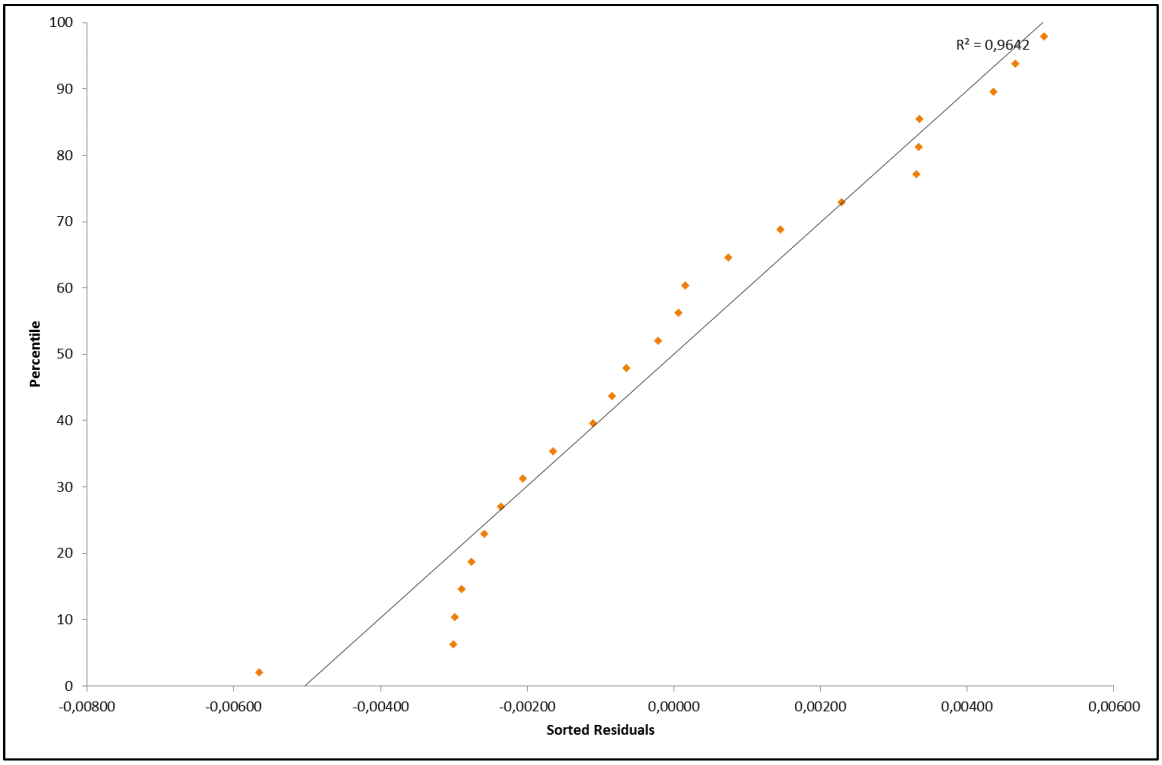

Figure C-19: Normal probability plot for observation point OBS_3

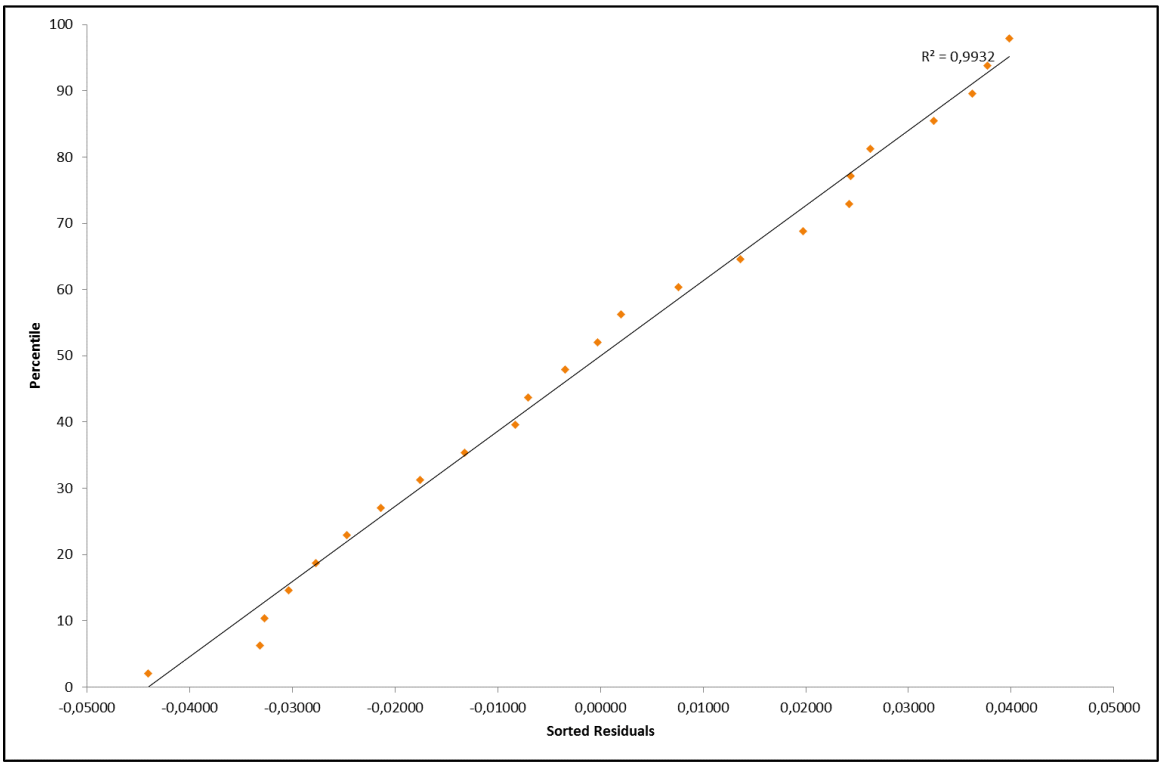

Figure C-20: Normal probability plot for observation point OBS_4

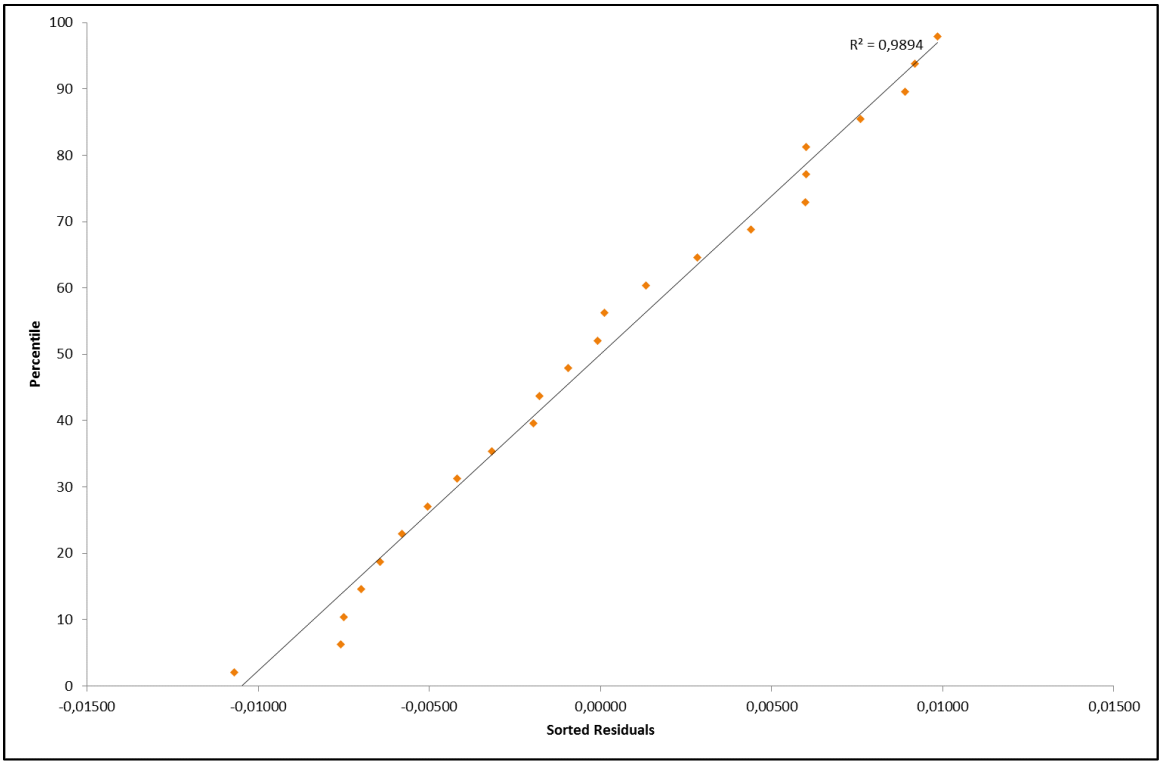

Figure C-21: Normal probability plot for observation point OBS_5

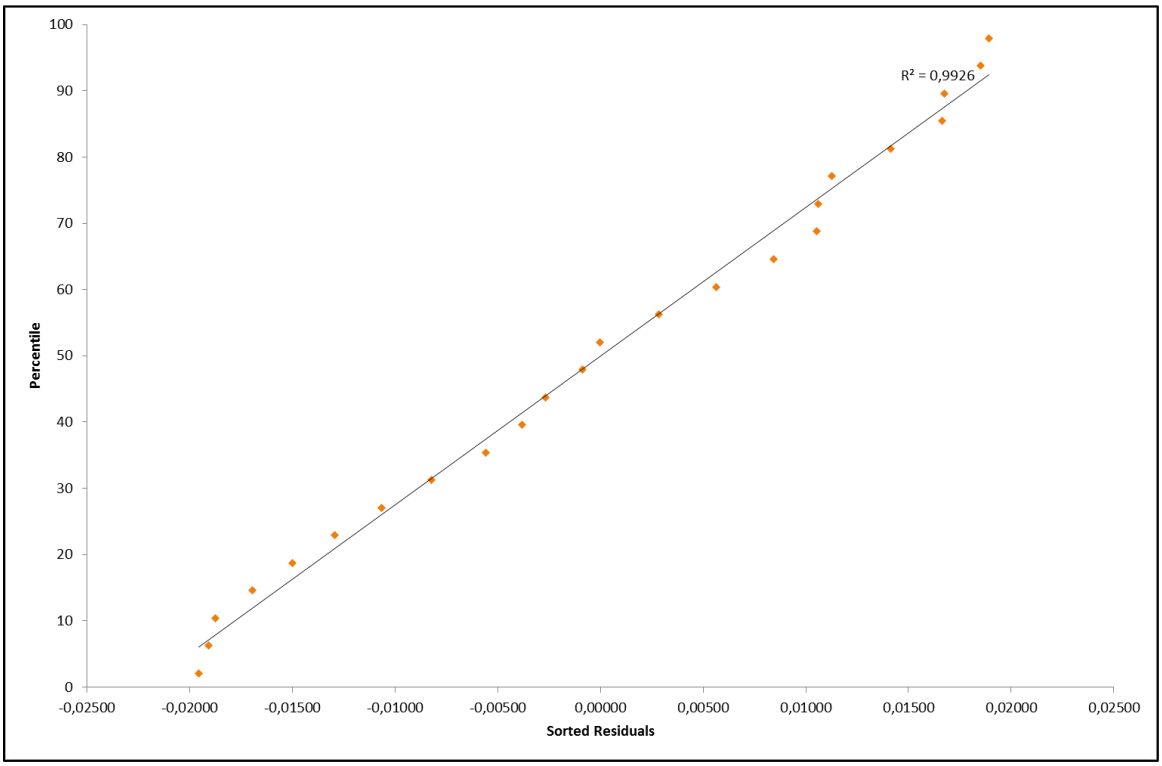

Figure C-22: Normal probability plot for observation point OBS_6

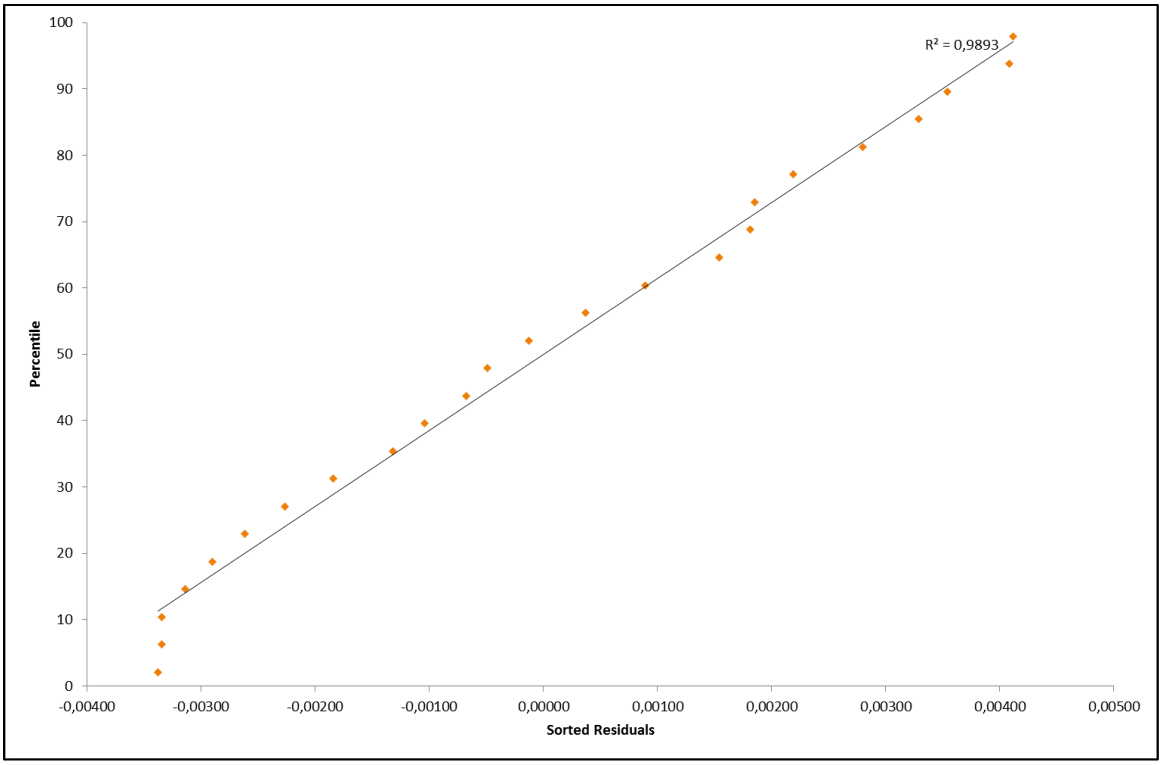

Figure C-23: Normal probability plot for observation point OBS_7

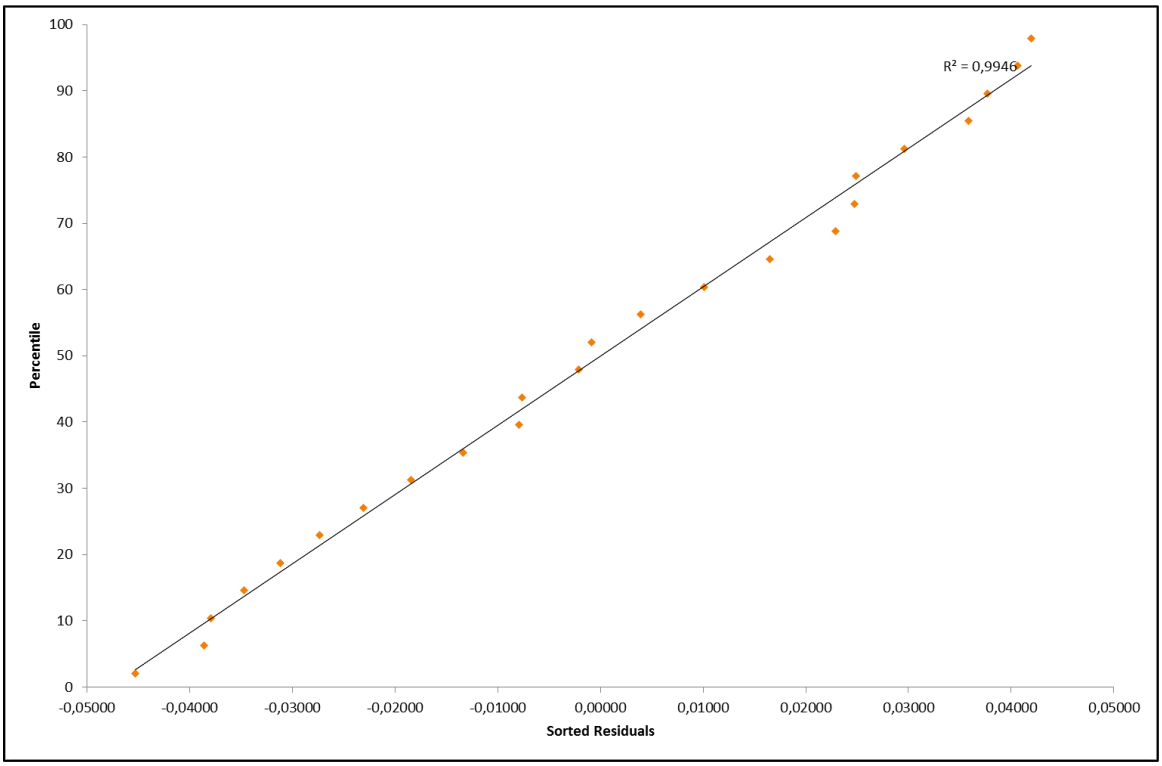

Figure C-24: Normal probability plot for observation point OBS_8

C.4 TWELVE DEWATERING WELLS

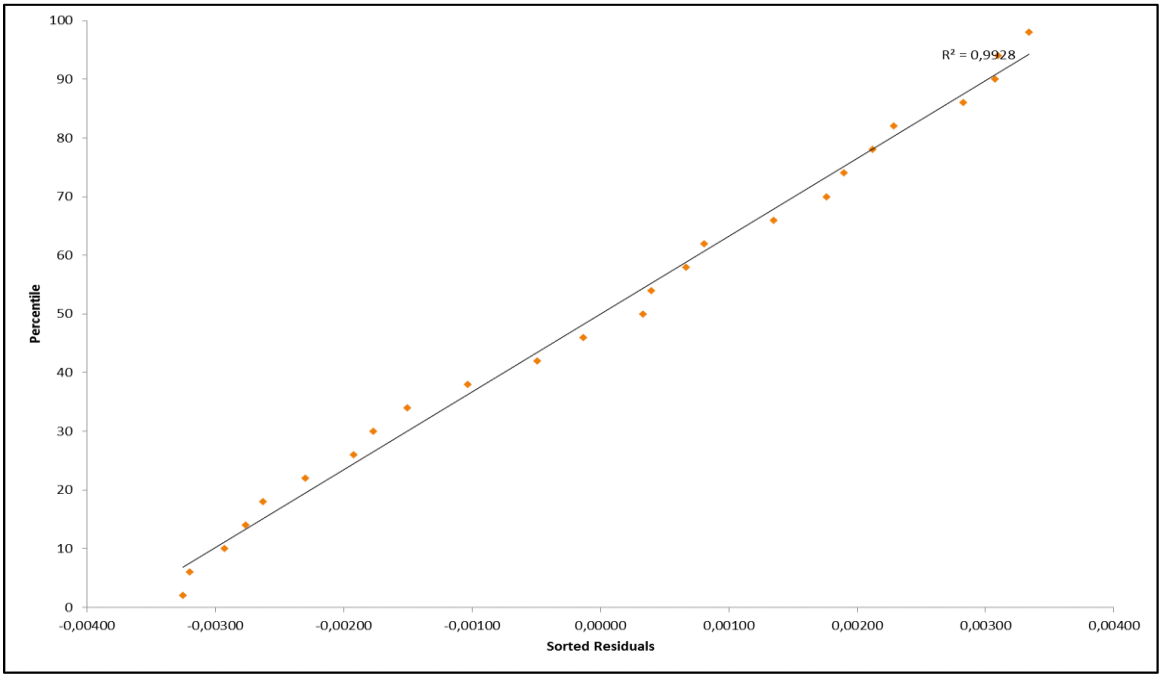

Figure C-25: Normal probability plot for observation point OBS_1

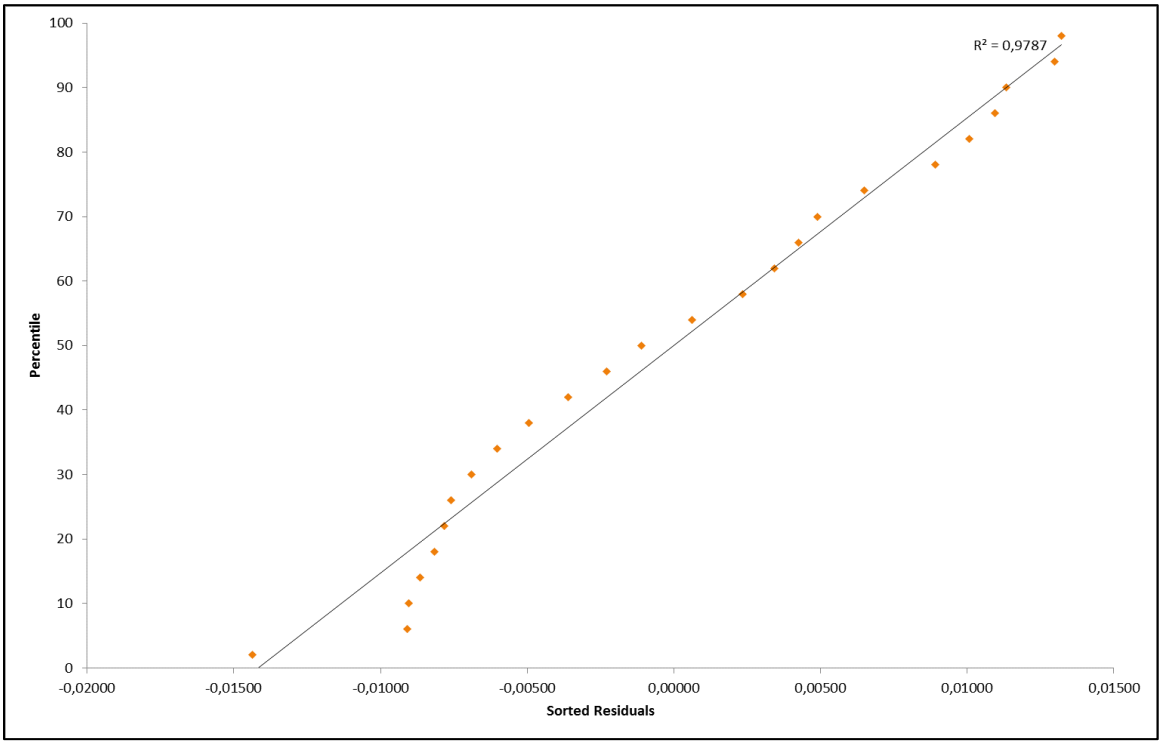

Figure C-26: Normal probability plot for observation point OBS_2

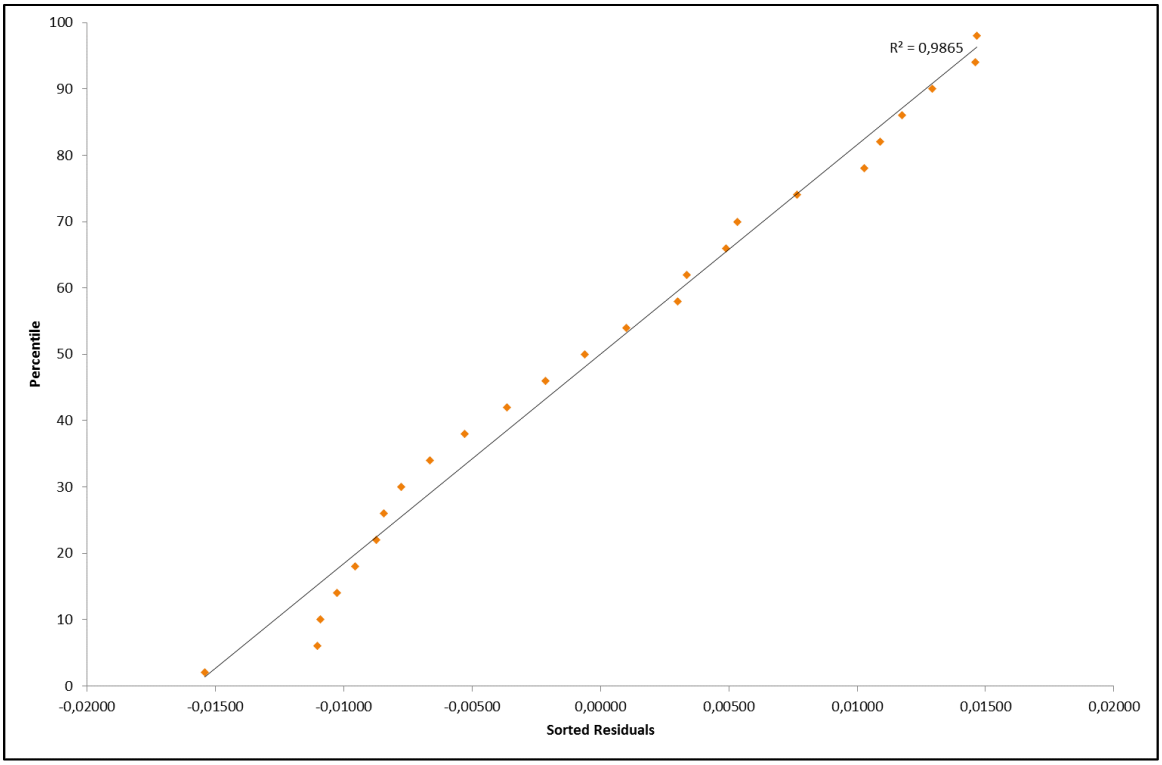

Figure C-27: Normal probability plot for observation point OBS_3

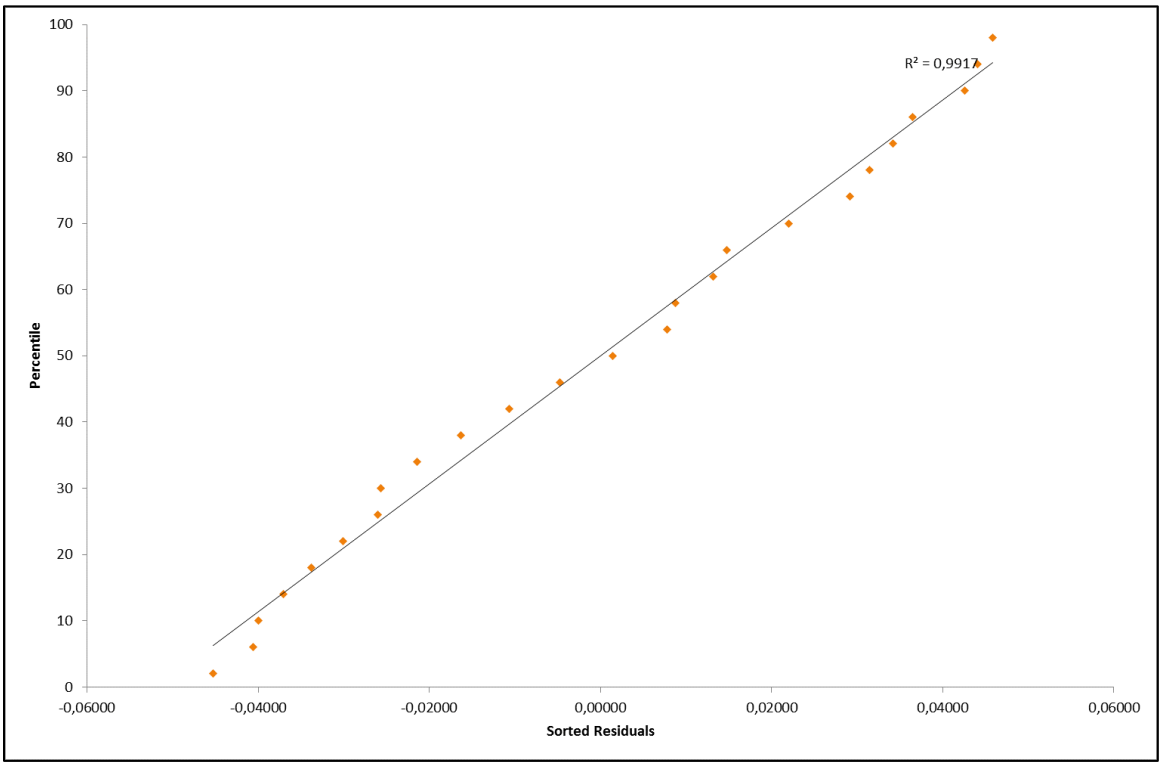

Figure C-28: Normal probability plot for observation point OBS_4

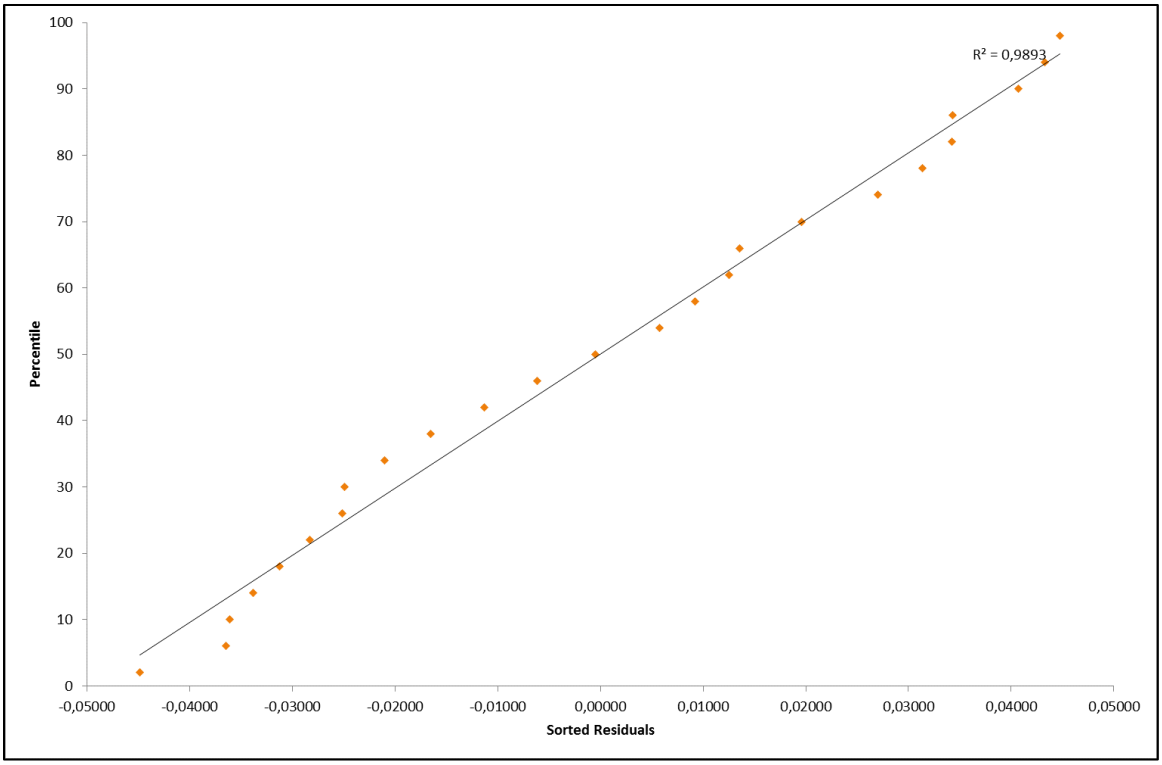

Figure C-29: Normal probability plot for observation point OBS_5

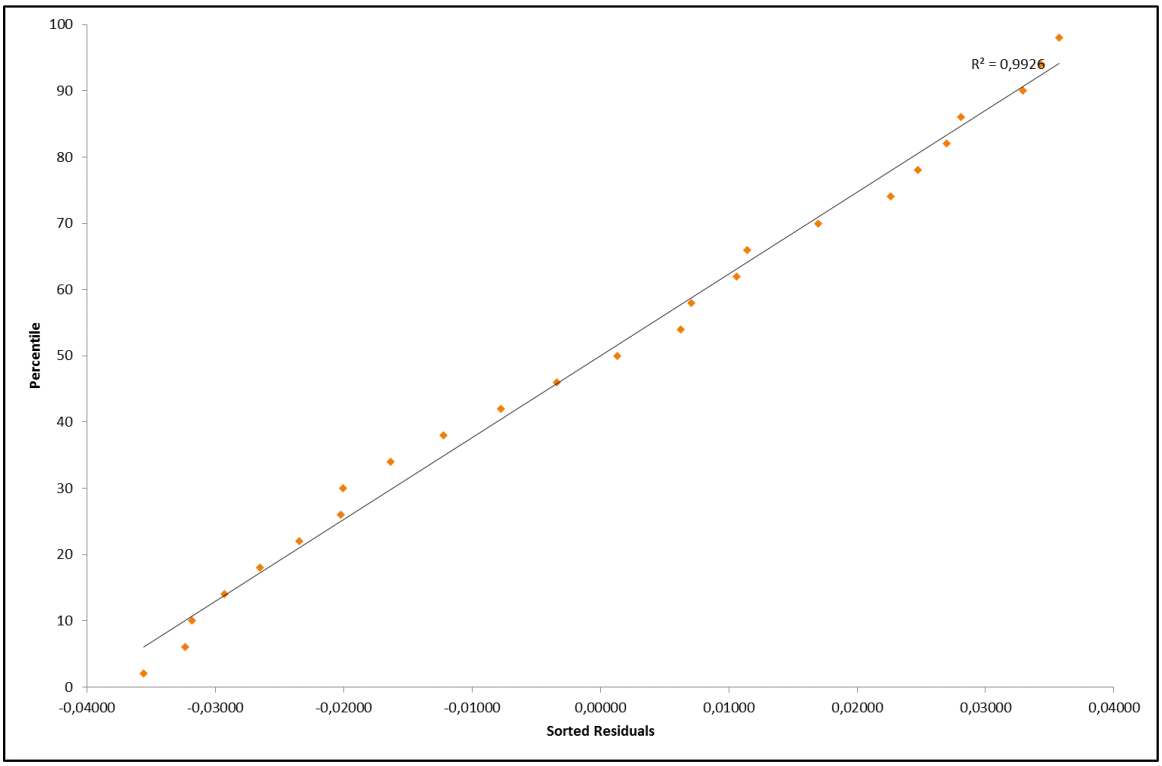

Figure C-30: Normal probability plot for observation point OBS_6

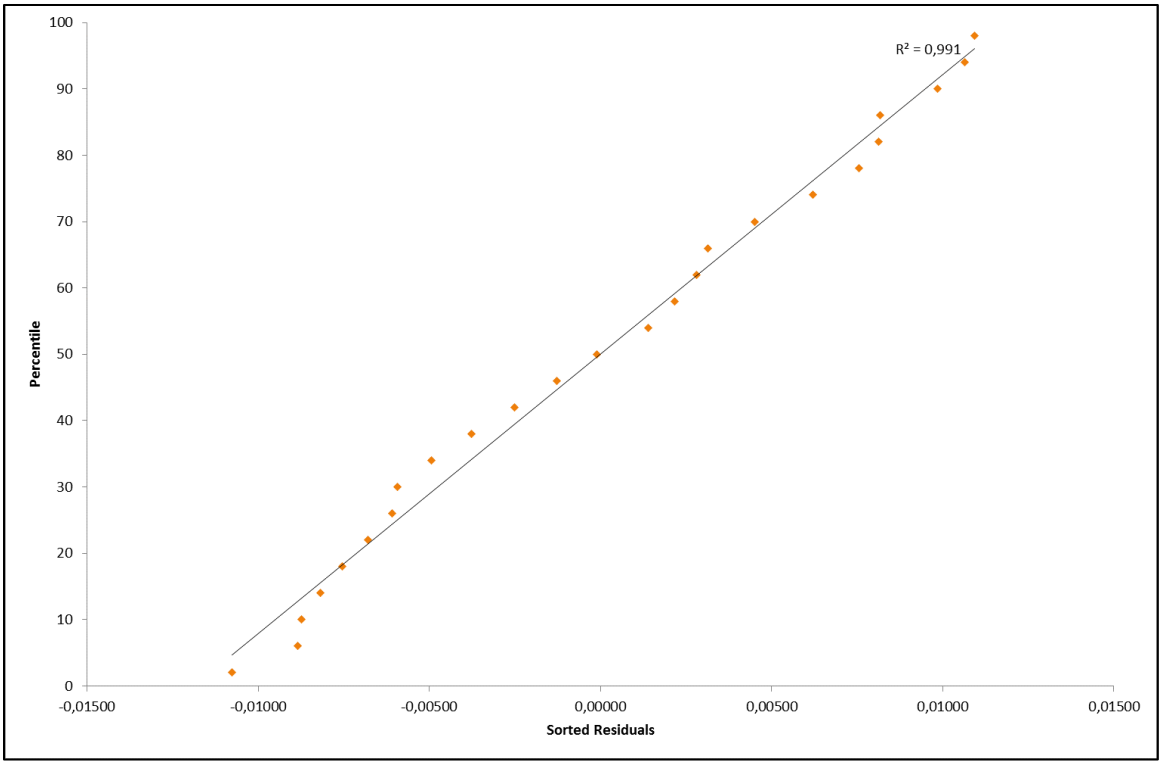

Figure C-31: Normal probability plot for observation point OBS_7

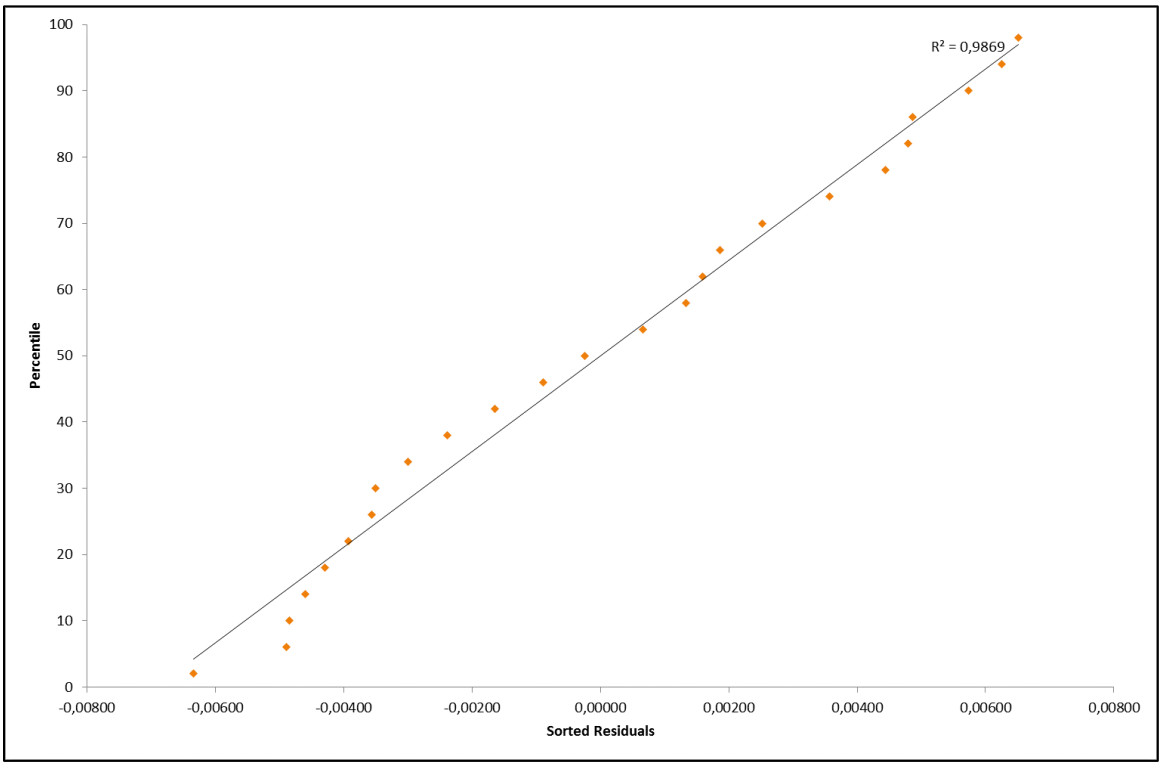

Figure C-32: Normal probability plot for observation point OBS_8

D. RESIDUAL PLOTS

D.1 THREE DEWATERING WELLS

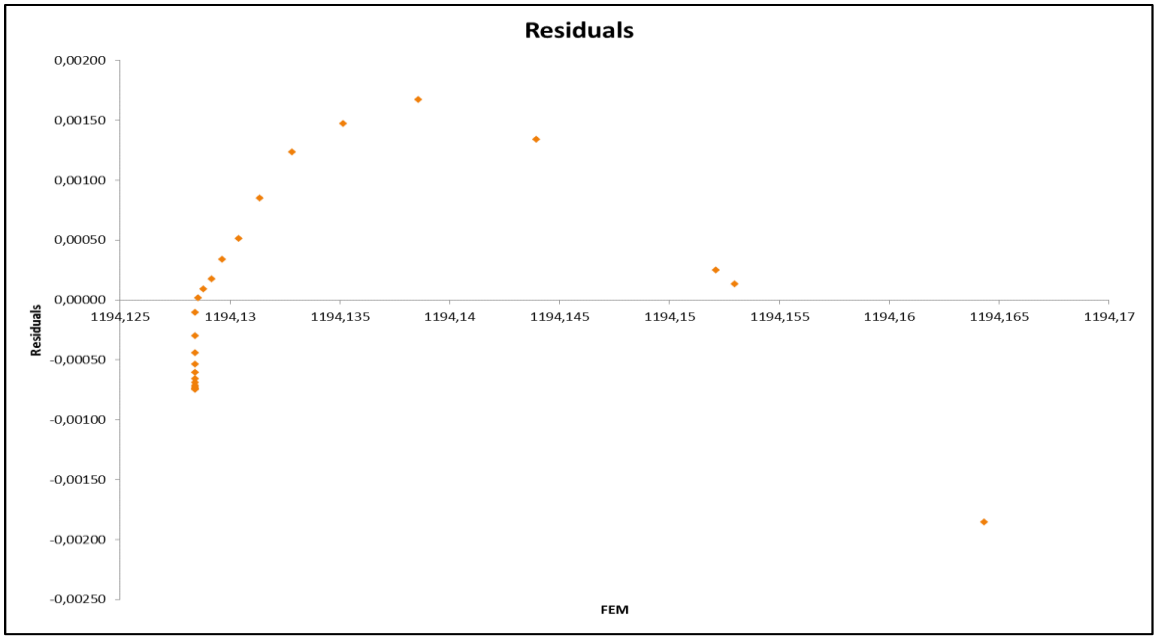

Figure D-1: Residuals plots for observation point OBS_1

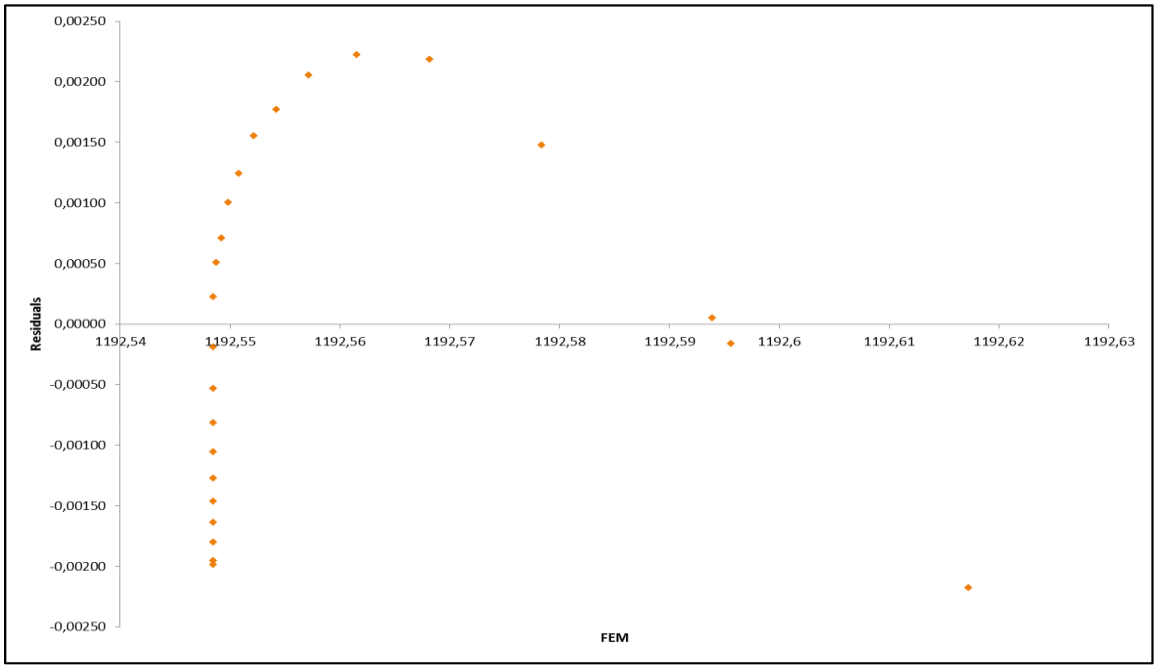

Figure D-2: Residuals plots for observation point OBS_2

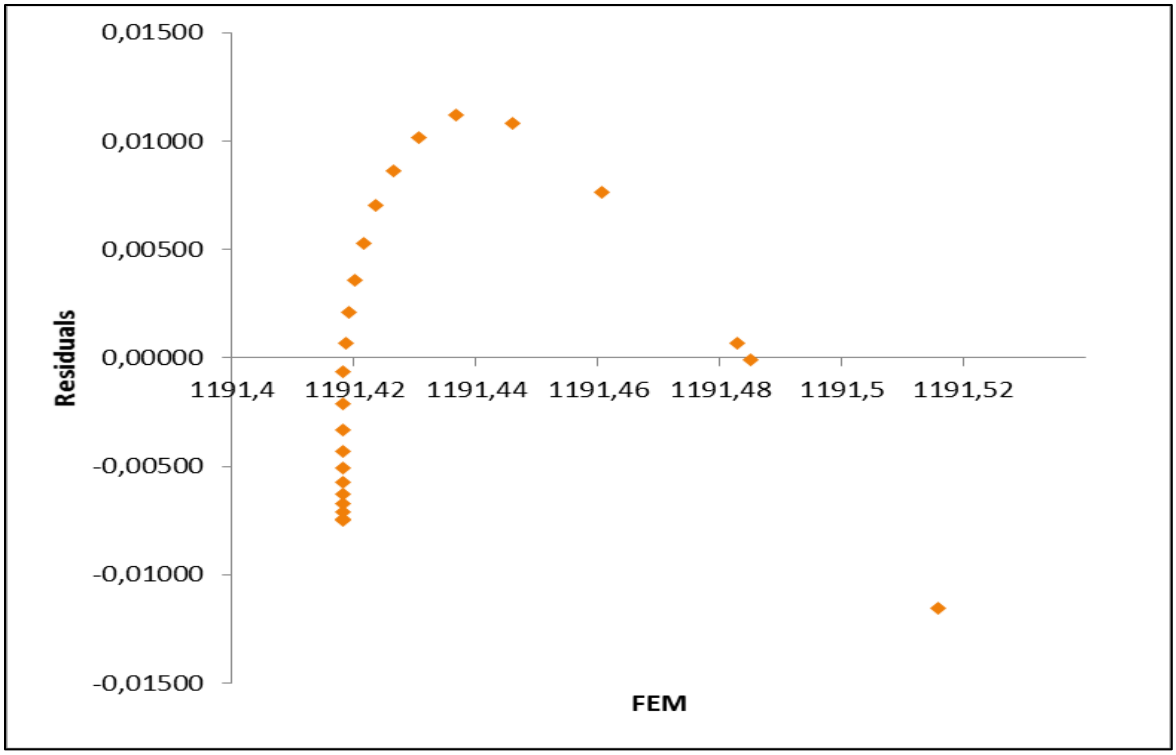

Figure D-3: Residuals plots for observation point OBS_3

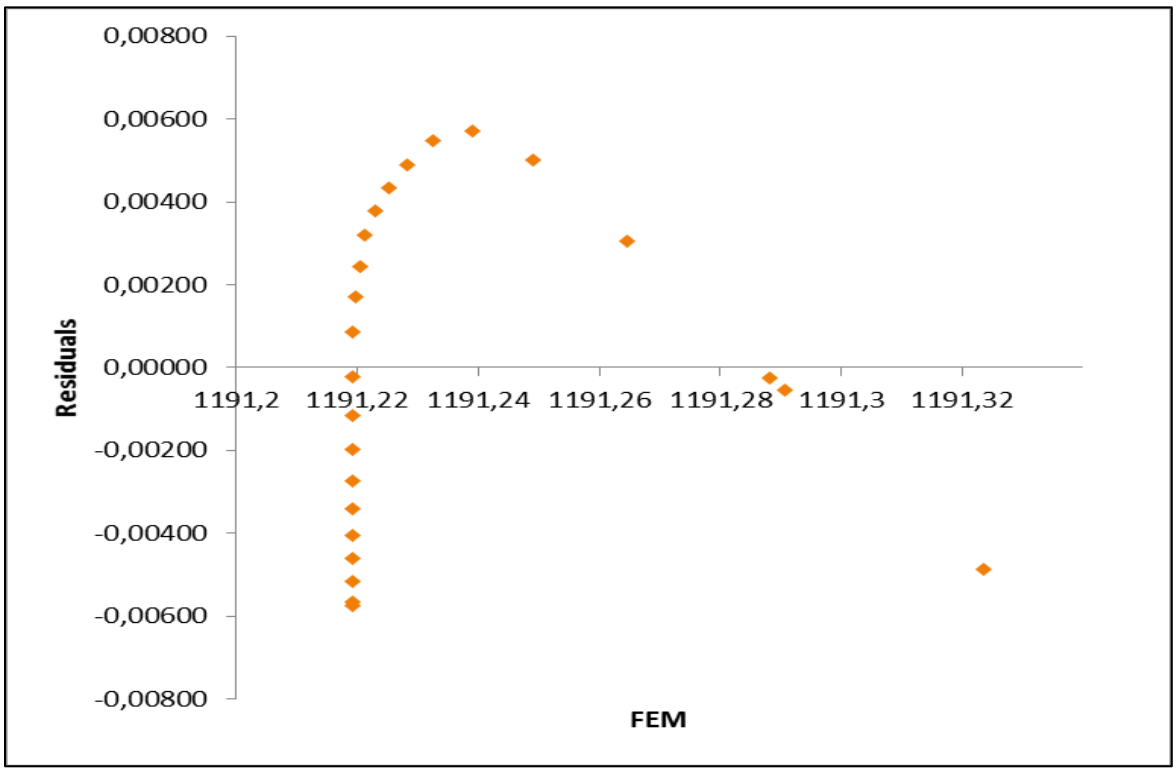

Figure D-4: Residuals plots for observation point OBS_4

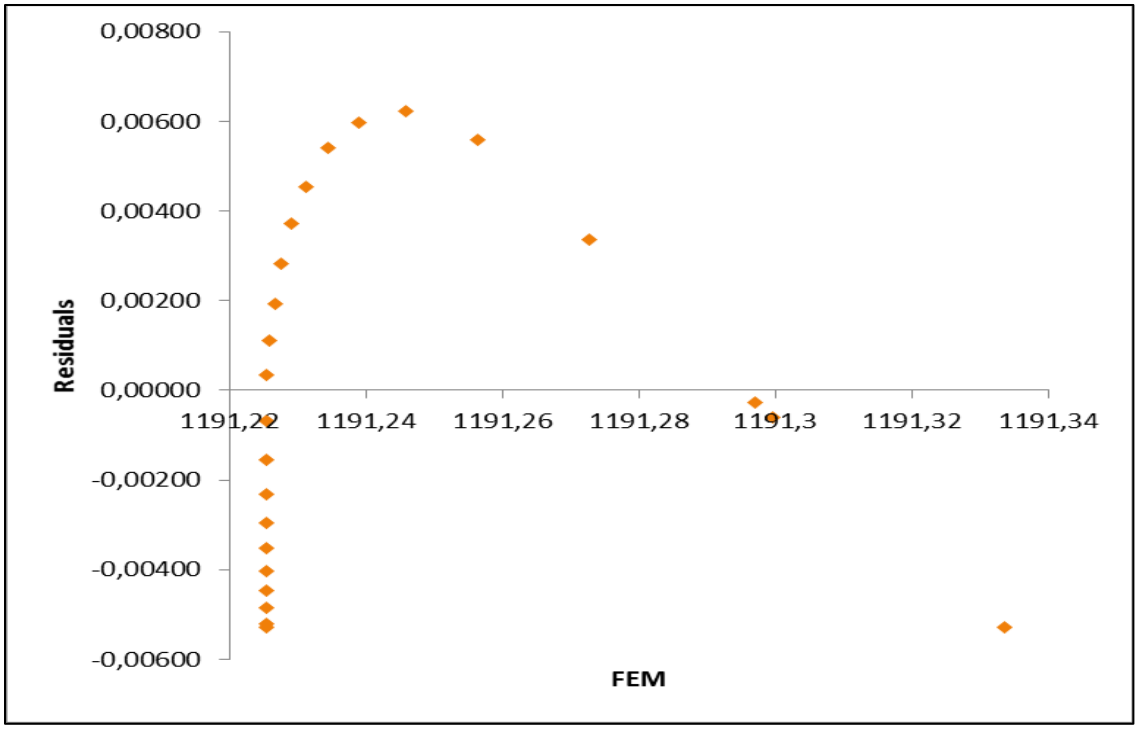

Figure D-5: Residuals plots for observation point OBS_5

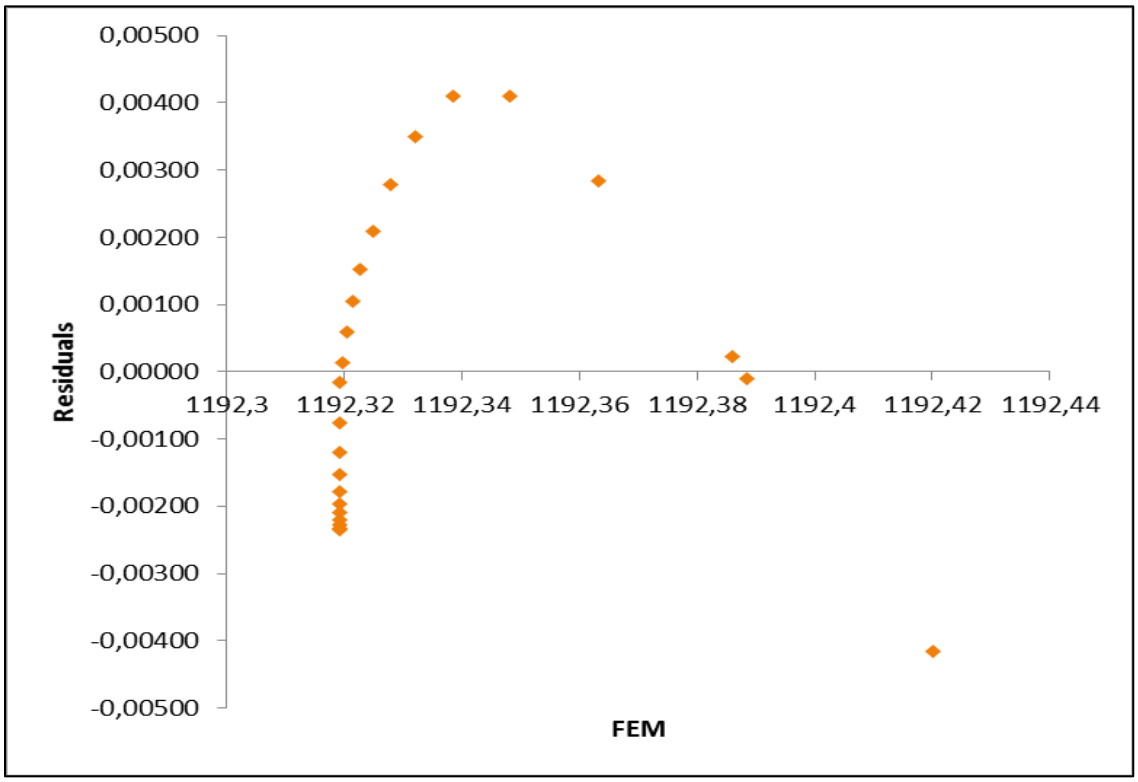

Figure D-6: Residuals plots for observation point OBS_6

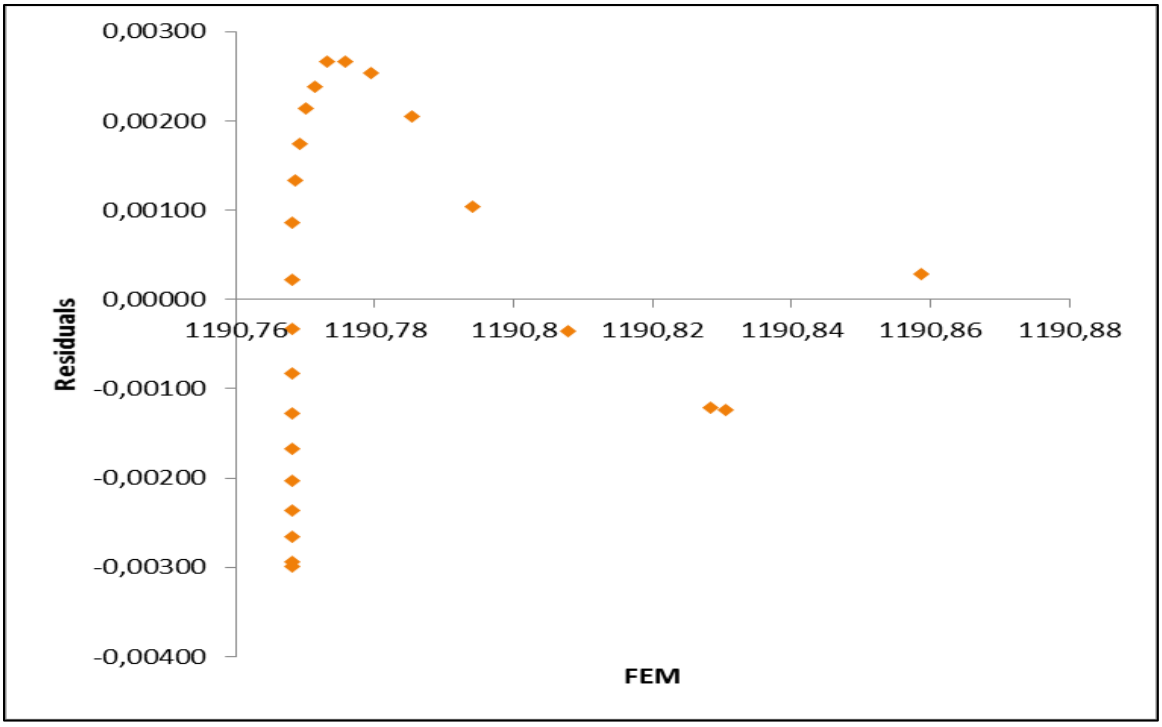

Figure D-7: Residuals plots for observation point OBS_7

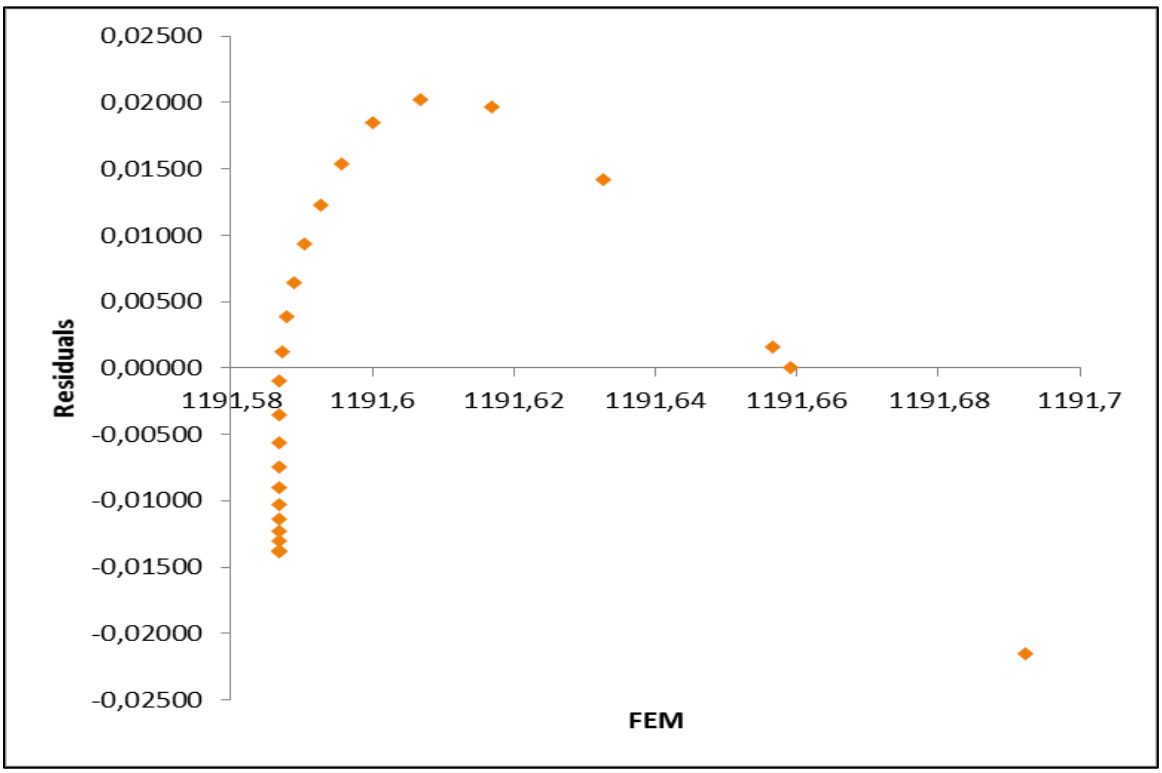

Figure D-8: Residuals plots for observation point OBS_8

D.2 SIX DEWATERING WELLS

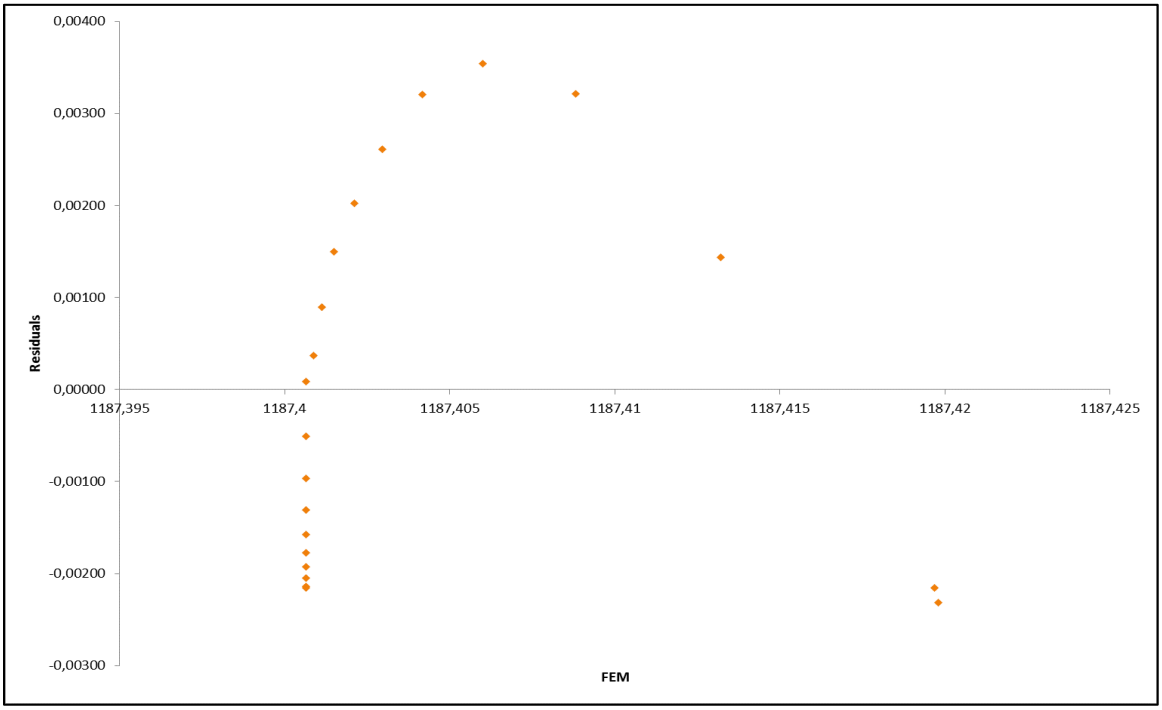

Figure D-9: Residuals plots for observation point OBS_1

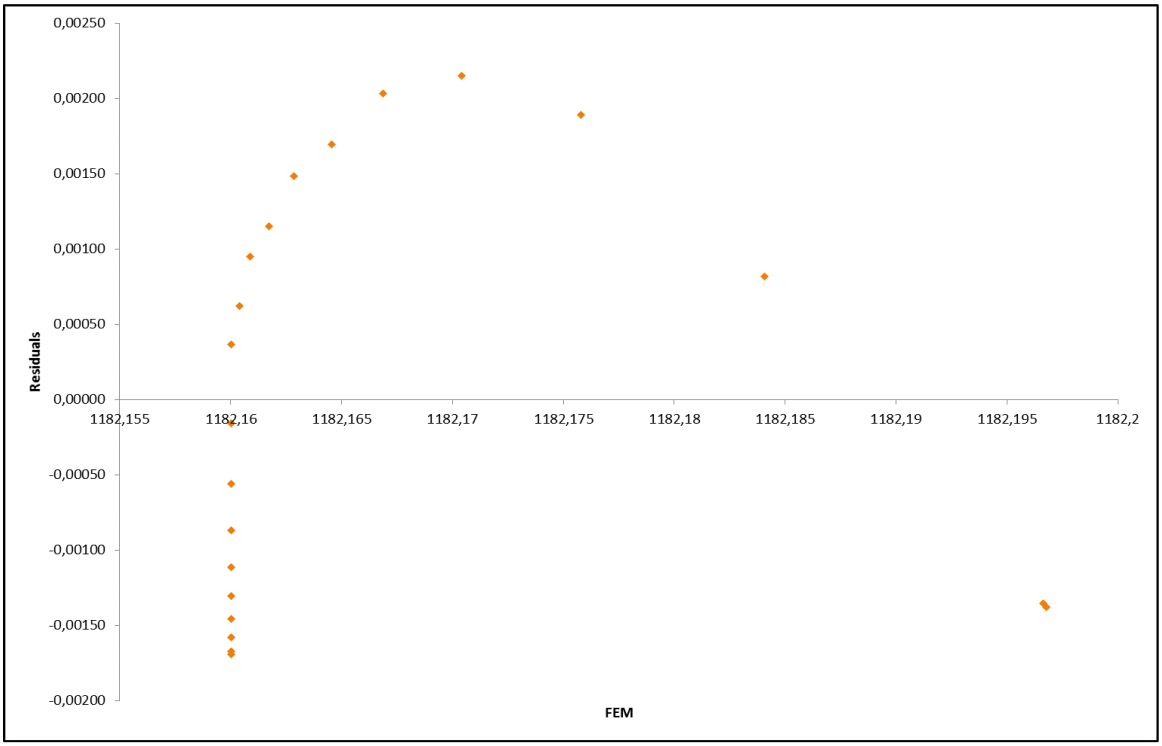

Figure D-10: Residuals plots for observation point OBS_2

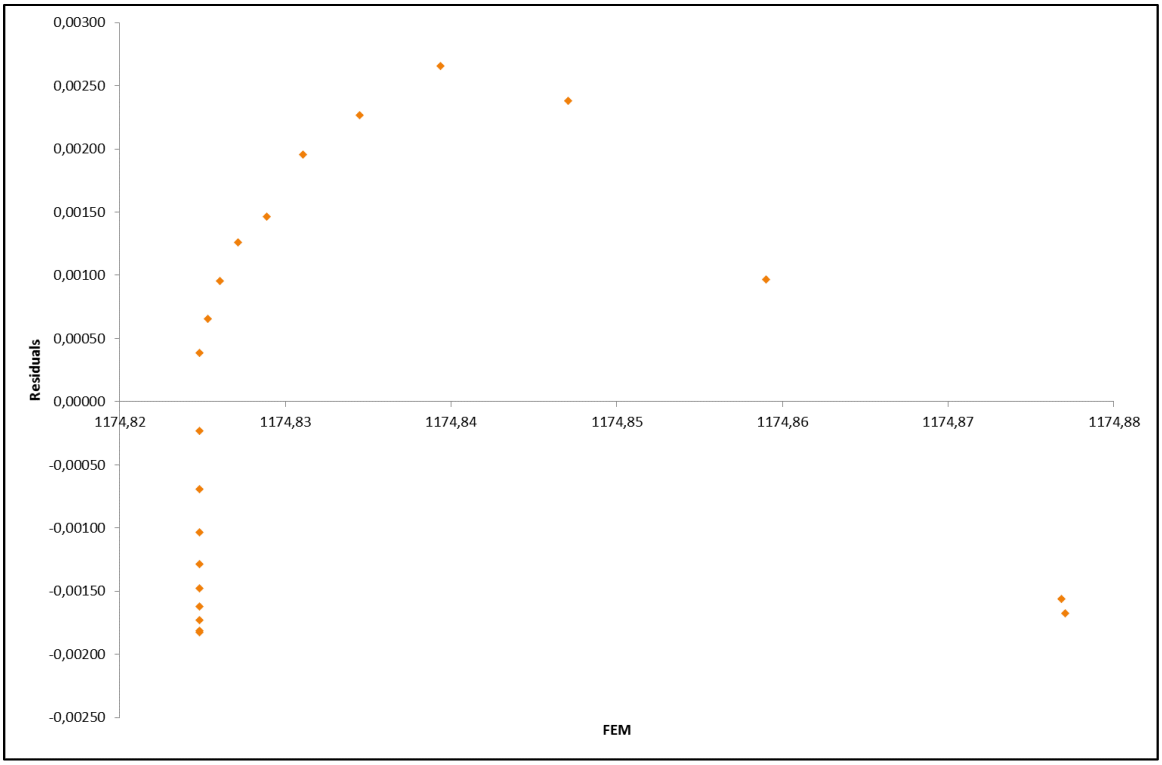

Figure D-11: Residuals plots for observation point OBS_3

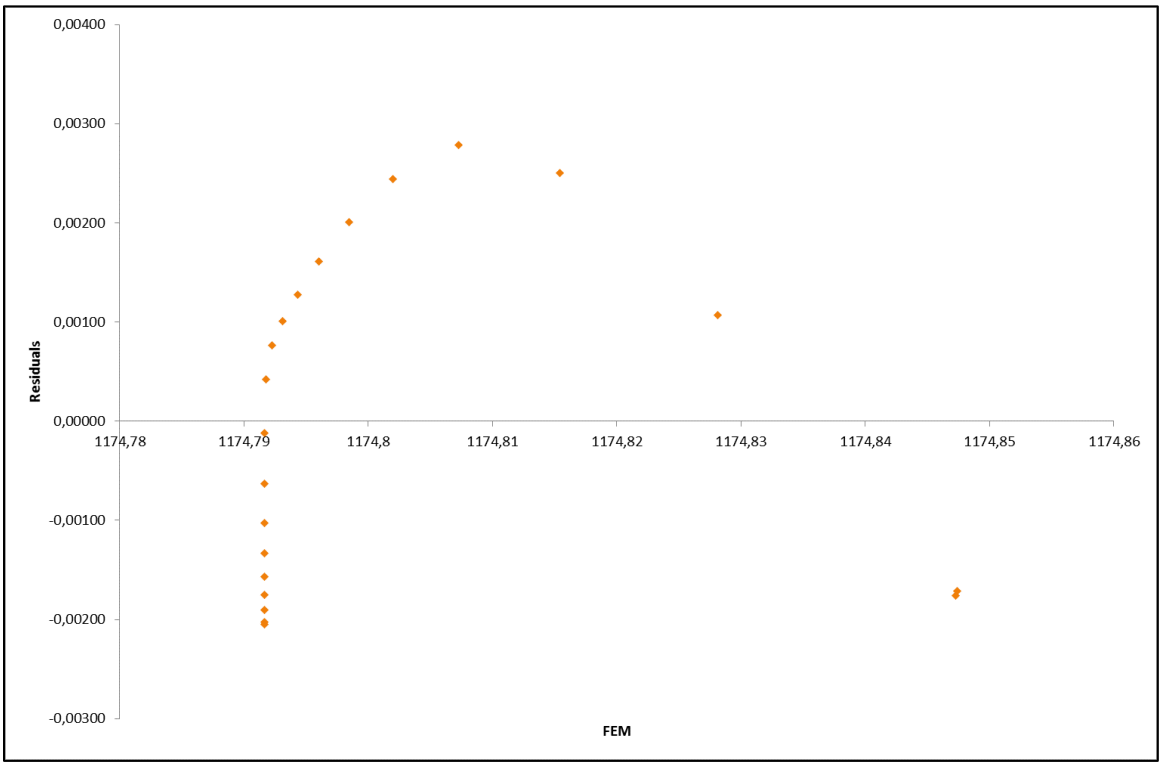

Figure D-12: Residuals plots for observation point OBS_4

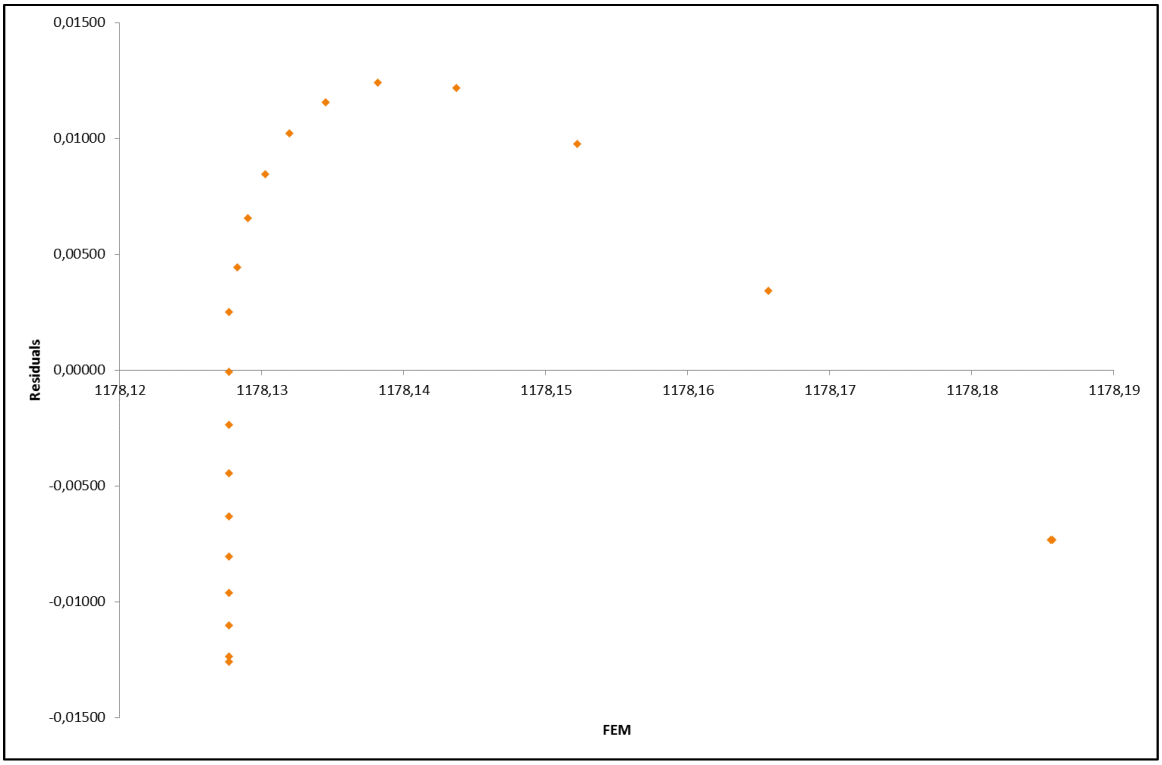

Figure D-13: Residuals plots for observation point OBS_5

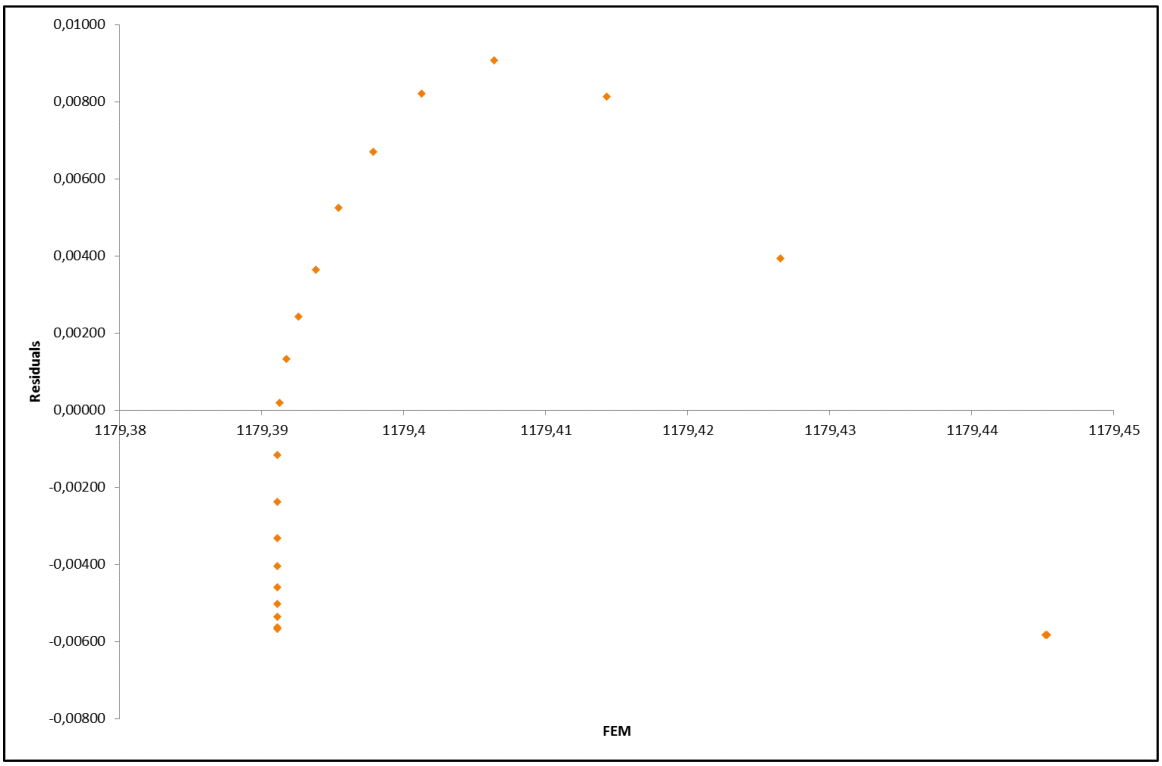

Figure D-14: Residuals plots for observation point OBS_6

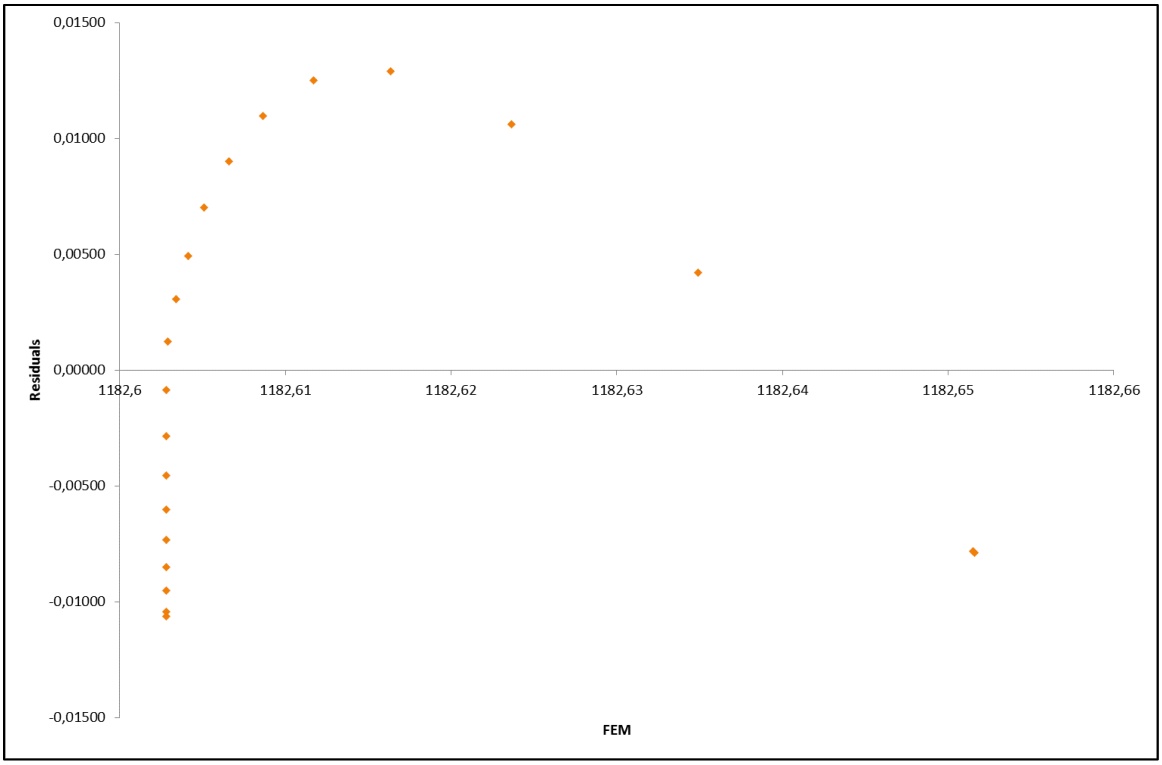

Figure D-15: Residuals plots for observation point OBS_7

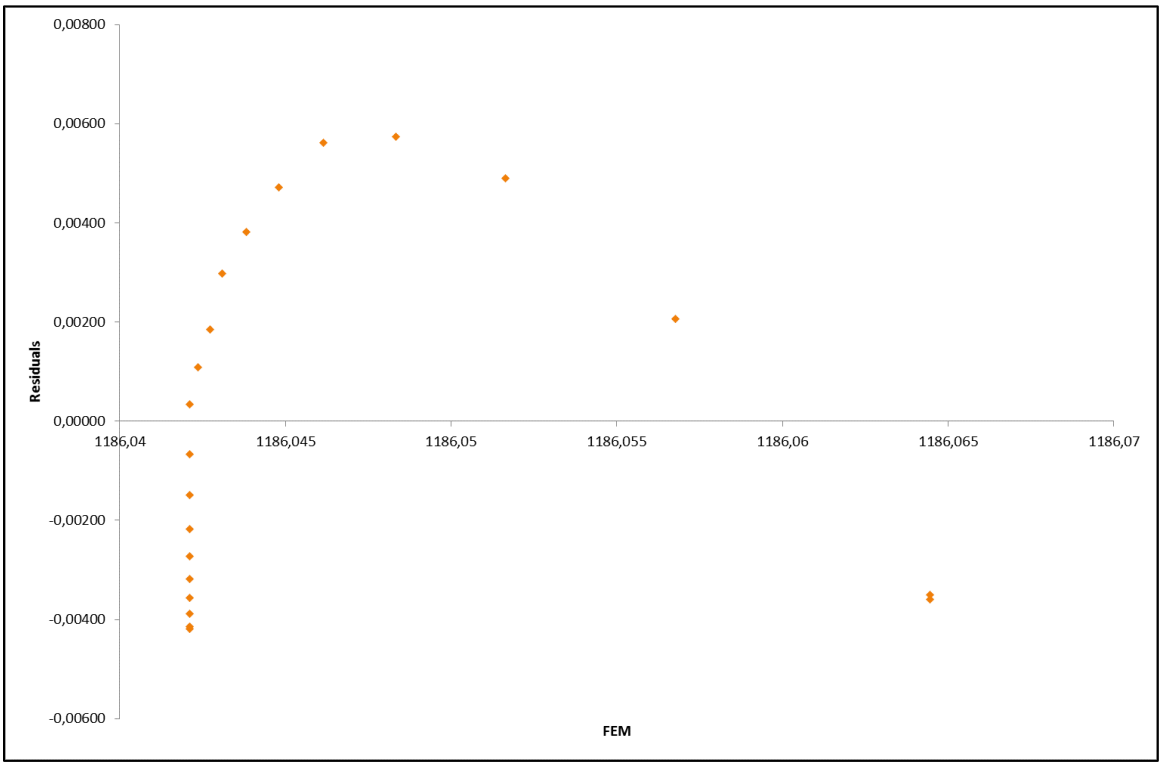

Figure D-16: Residuals plots for observation point OBS_8

D.3 NINE DEWATERING WELLS

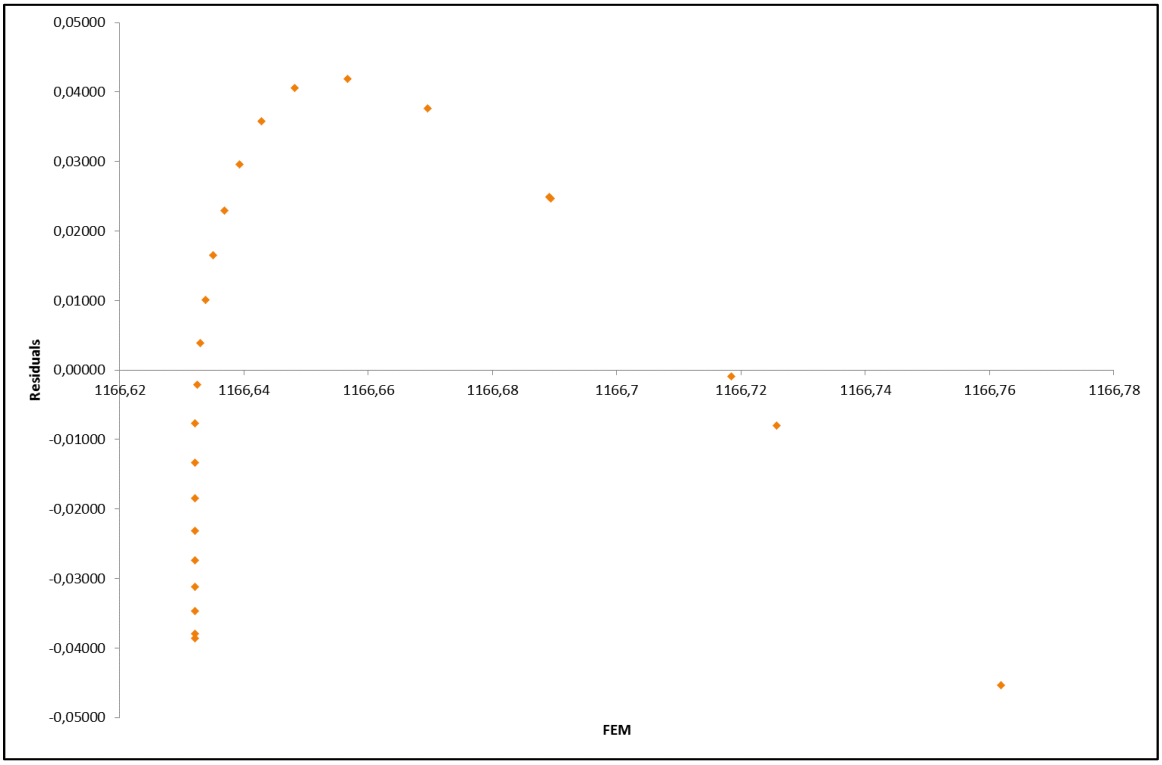

Figure D-17: Residuals plots for observation point OBS_1

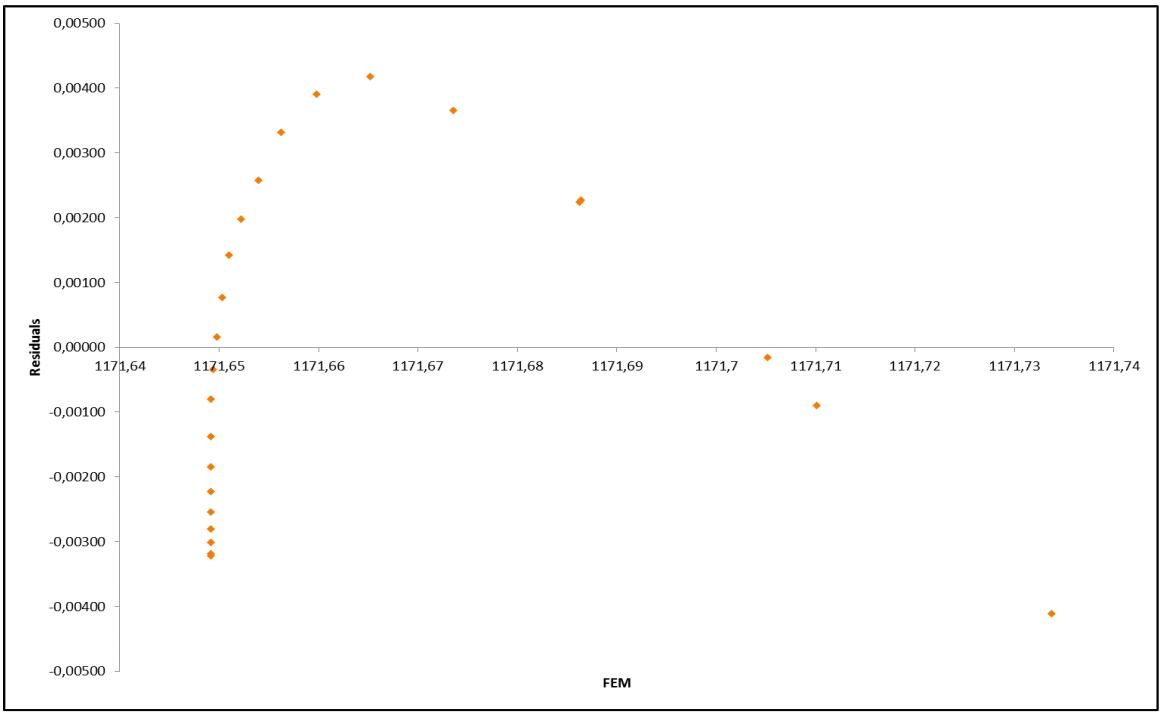

Figure D-18: Residuals plots for observation point OBS_2

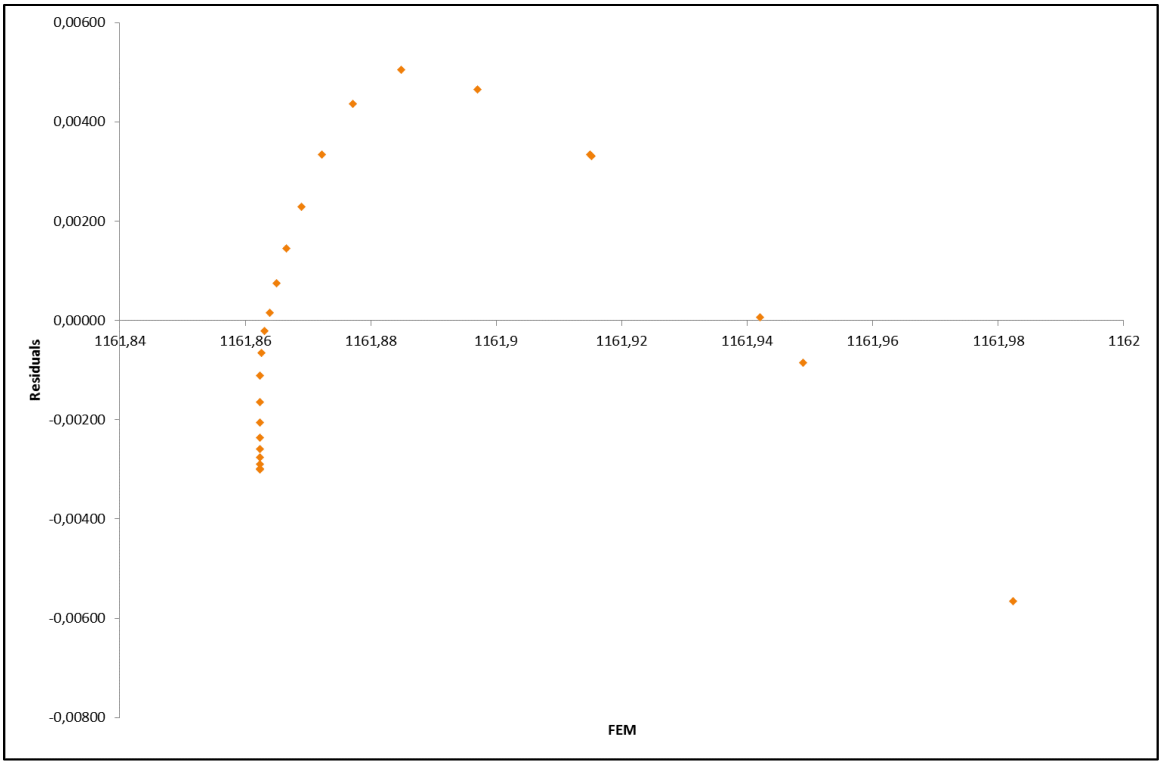

Figure D-19: Residuals plots for observation point OBS_3

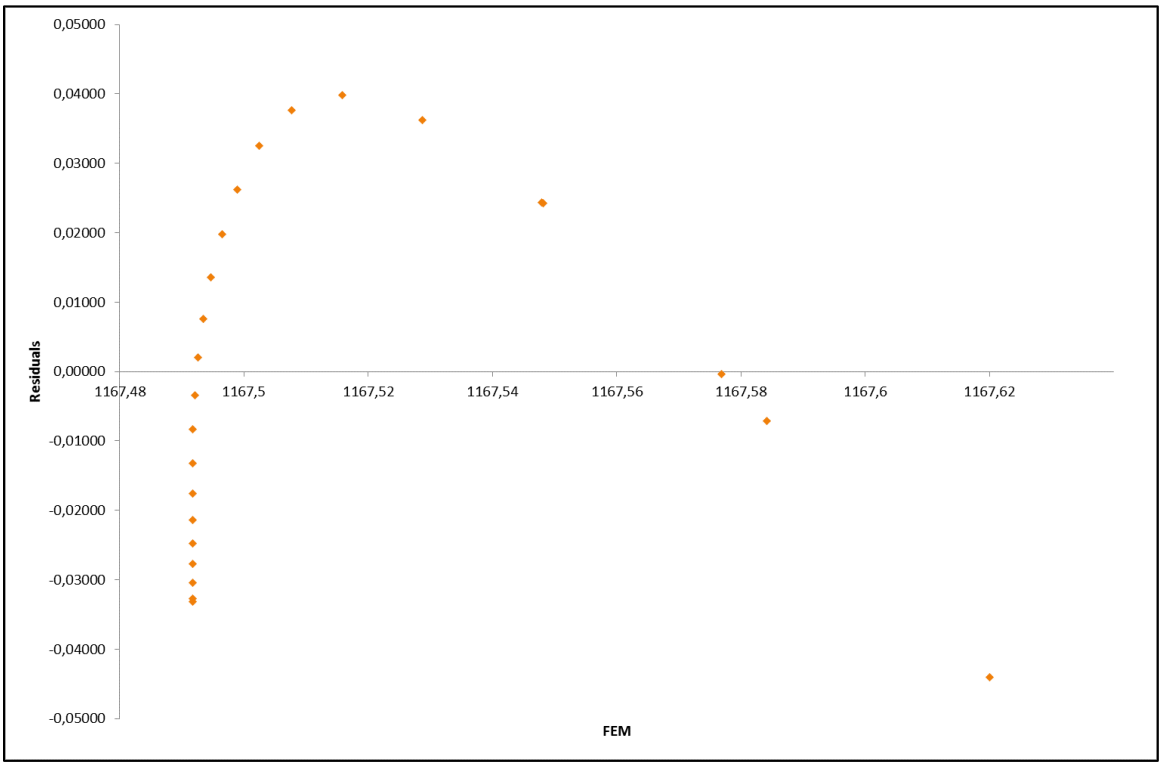

Figure D-20: Residuals plots for observation point OBS_4

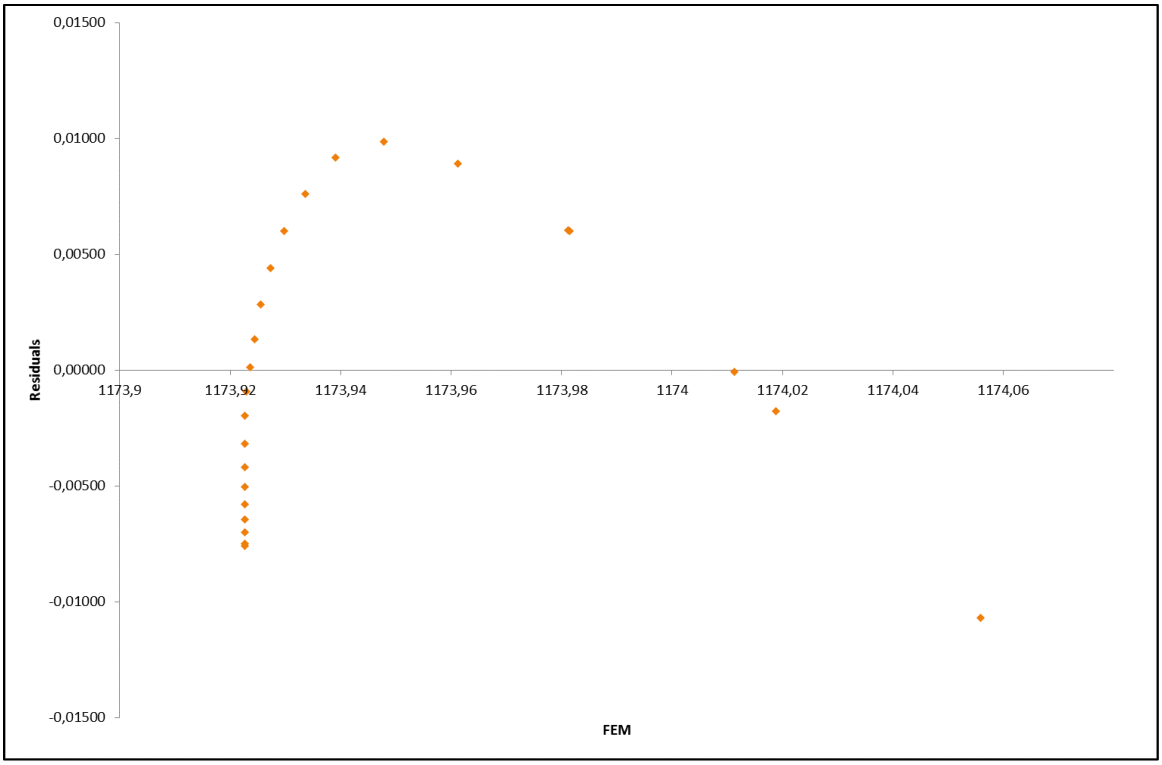

Figure D-21: Residuals plots for observation point OBS_5

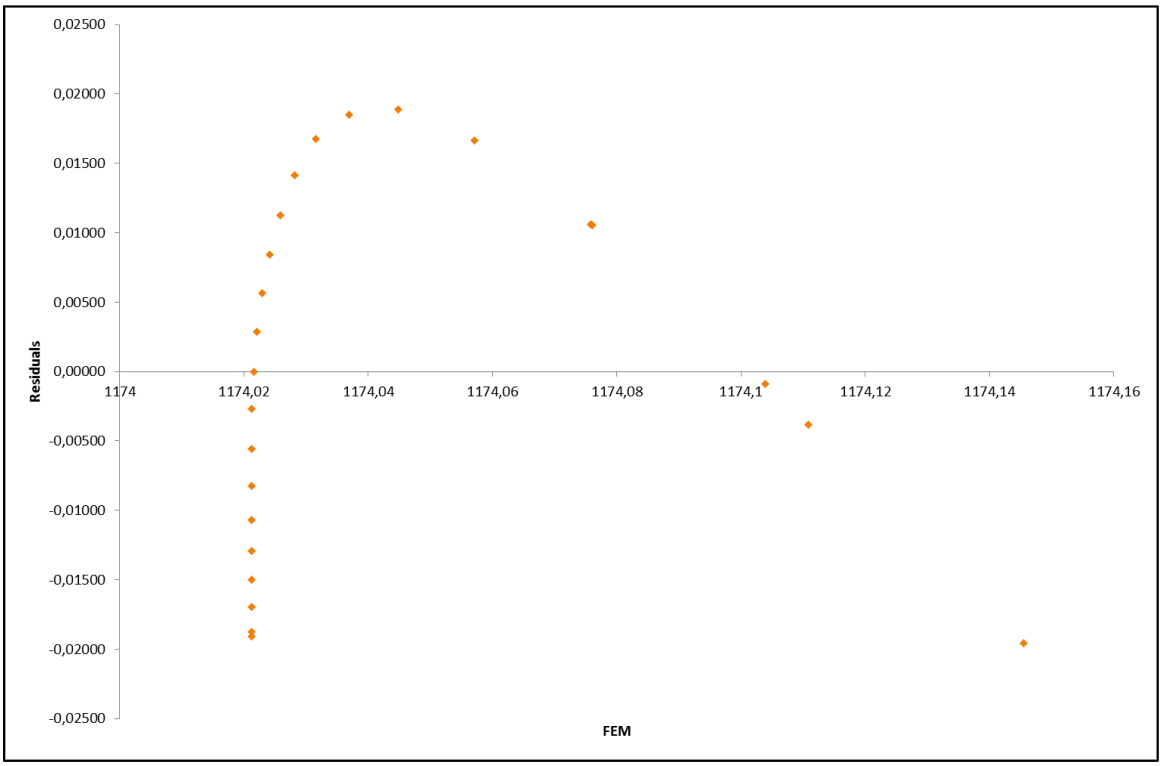

Figure D-22: Residuals plots for observation point OBS_6

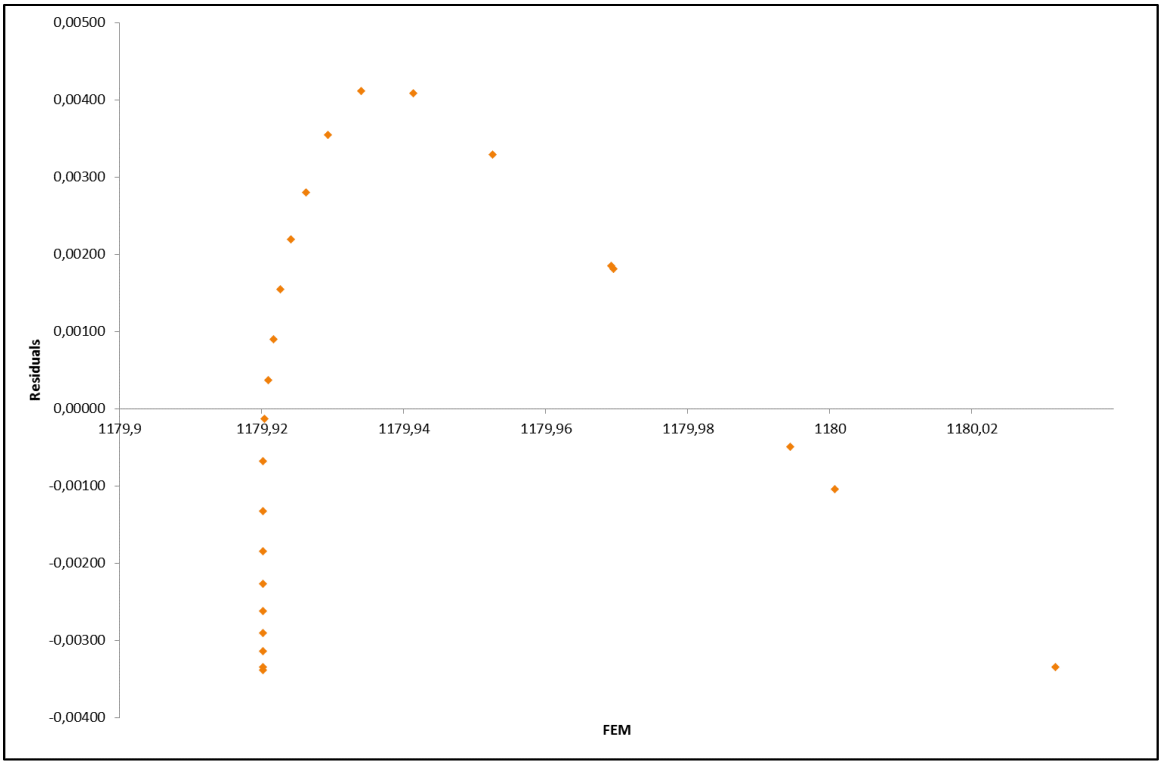

Figure D-23: Residuals plots for observation point OBS_7

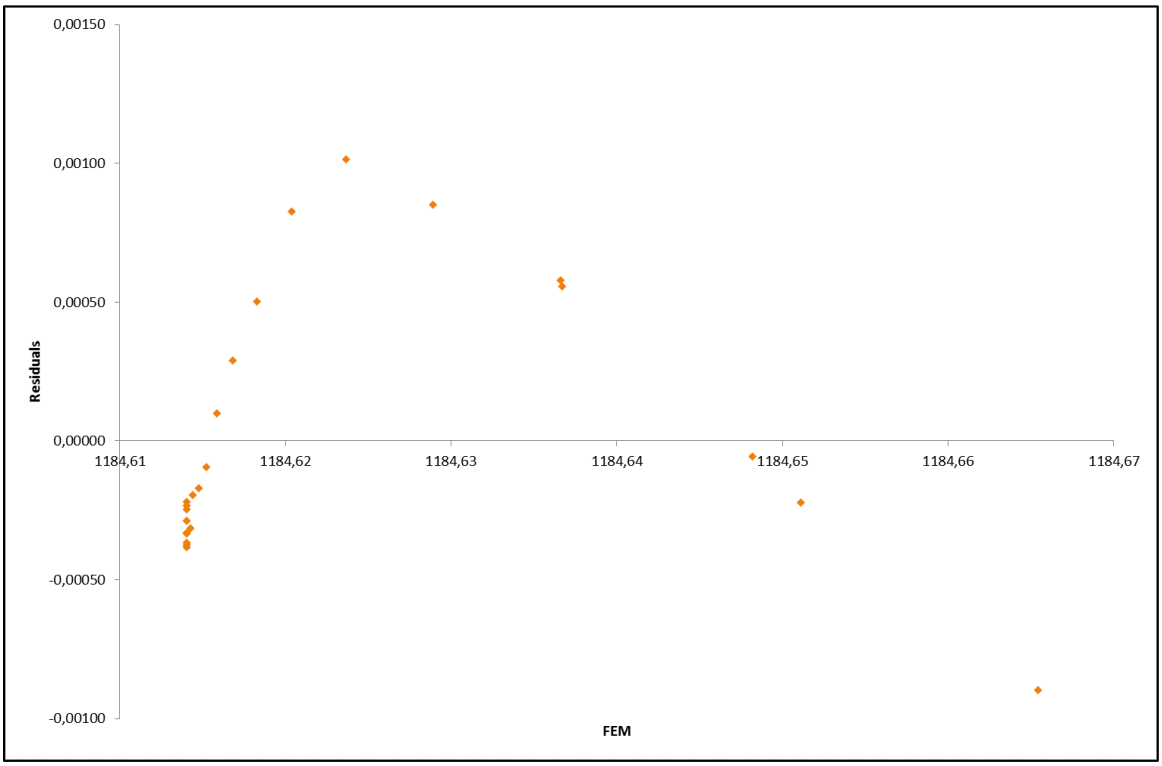

Figure D-24: Residuals plots for observation point OBS_8

D.4 TWELVE DEWATERING WELLS

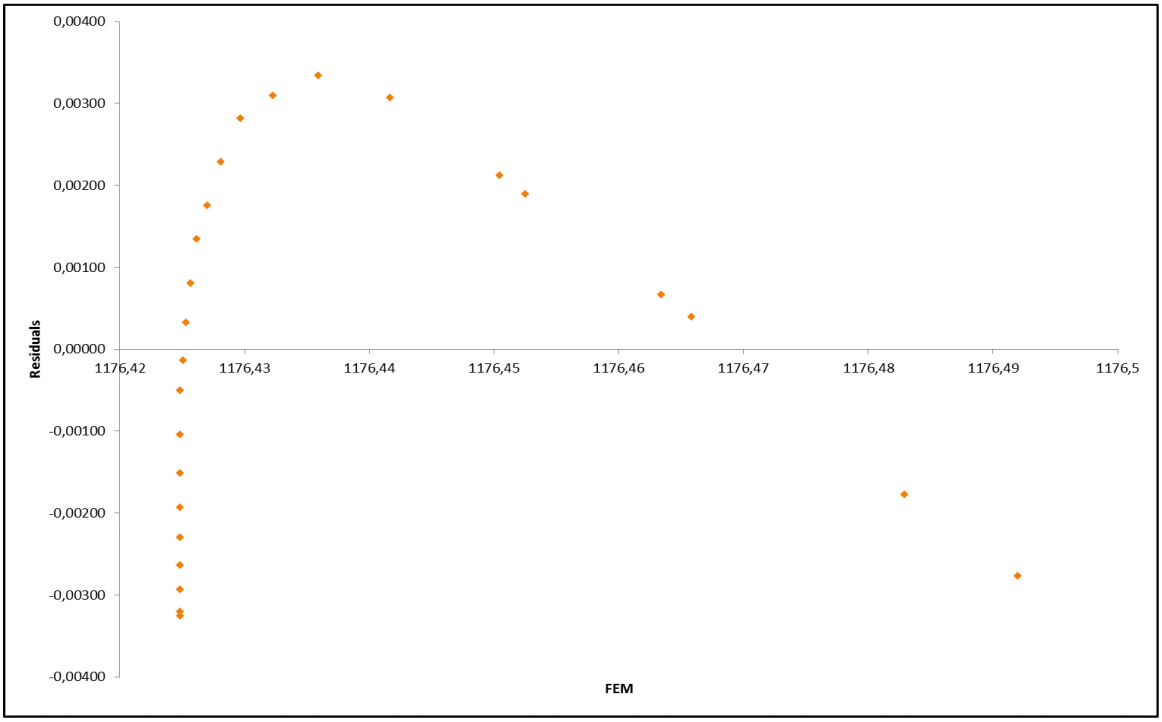

Figure D-25: Residuals plots for observation point OBS_1

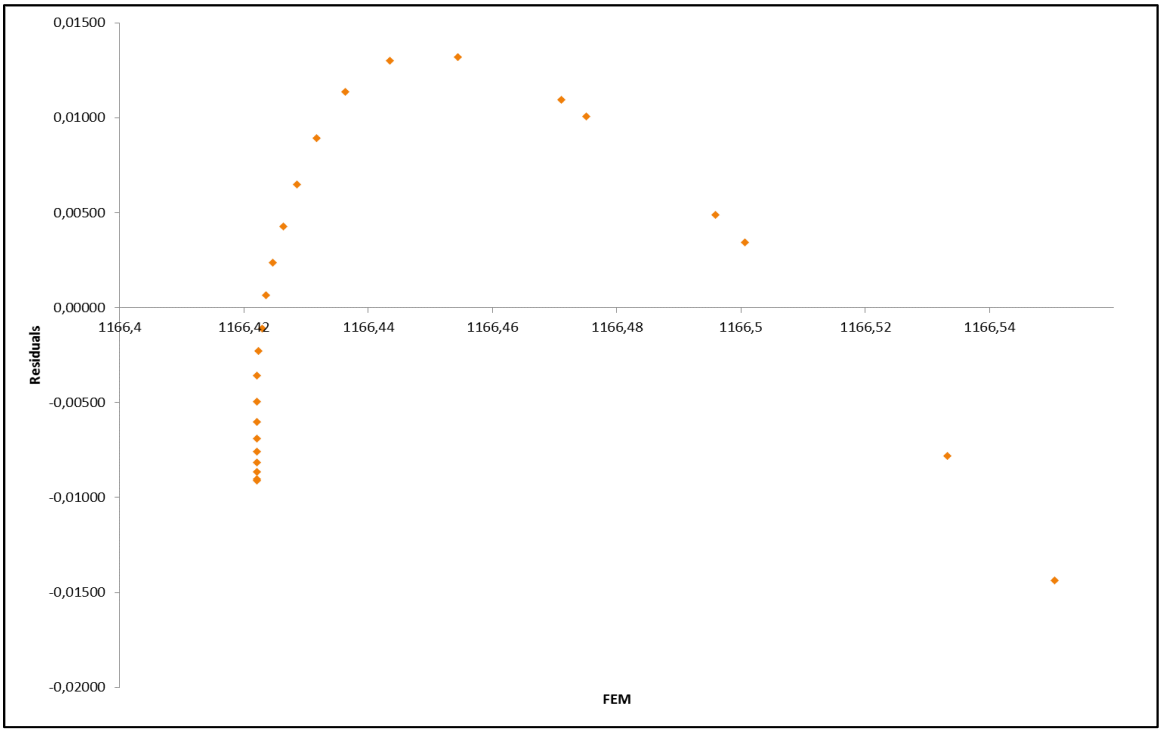

Figure D-26: Residuals plots for observation point OBS_2

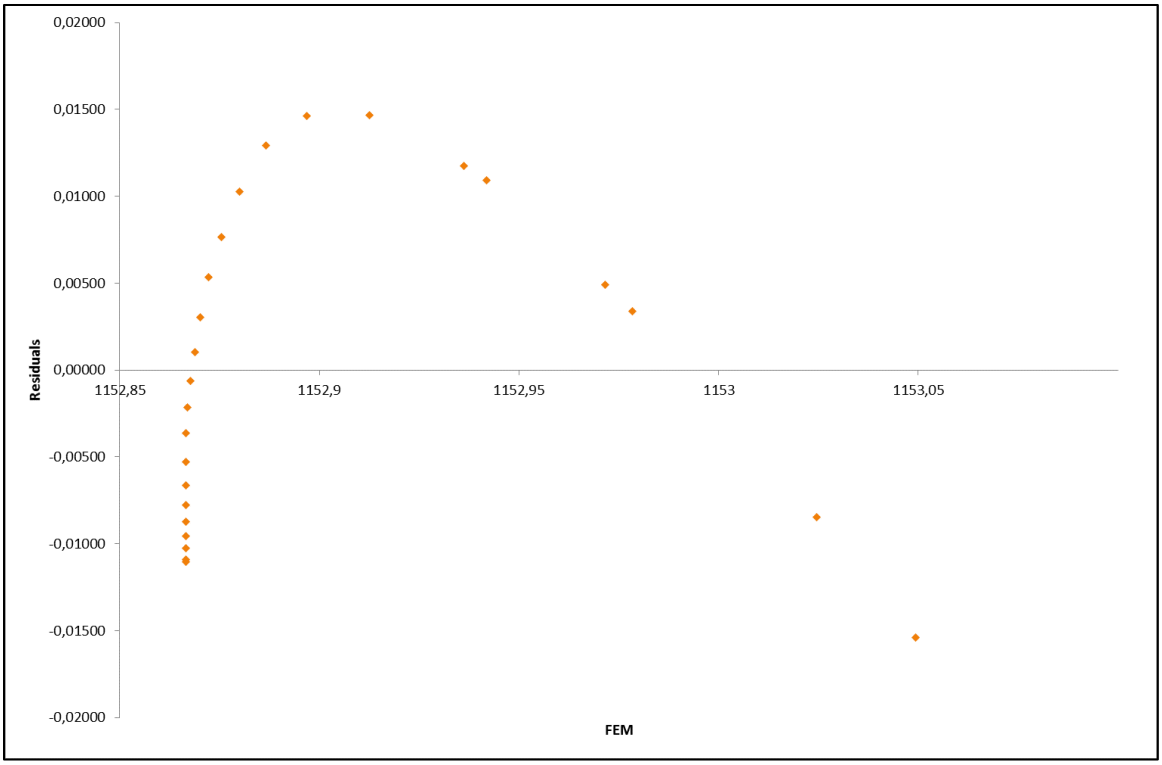

Figure D-27: Residuals plots for observation point OBS_3

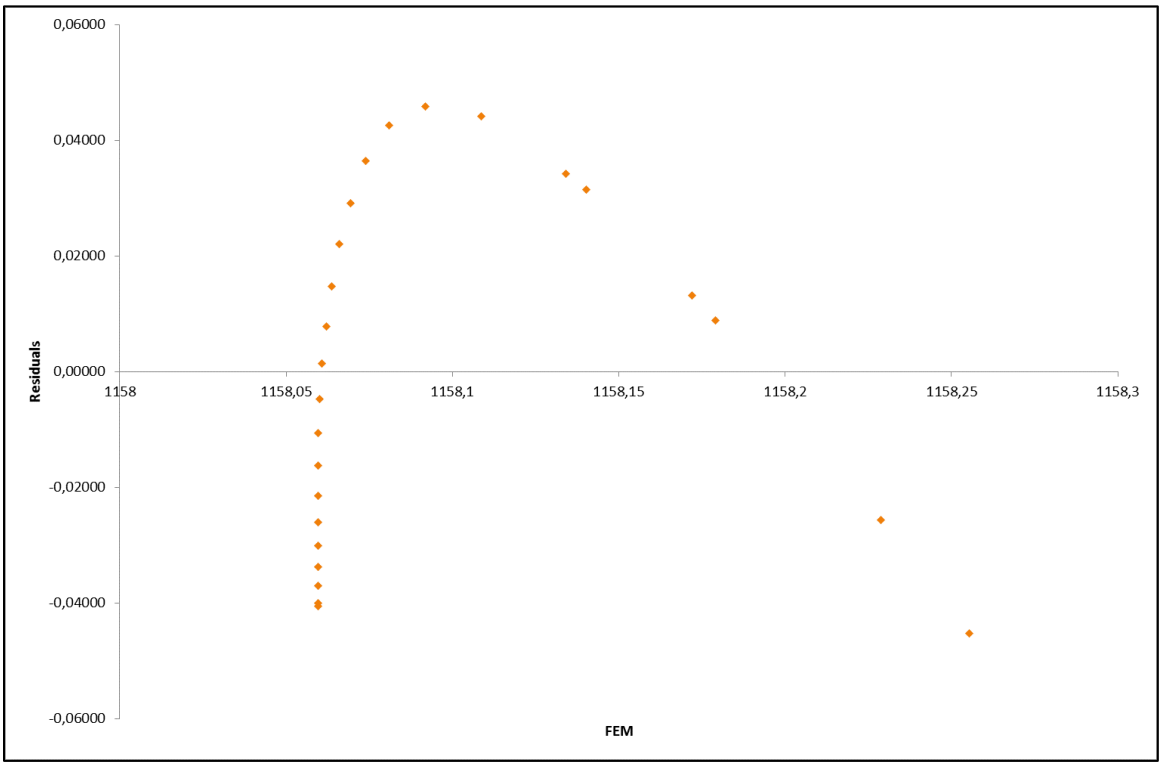

Figure D-28: Residuals plots for observation point OBS_4

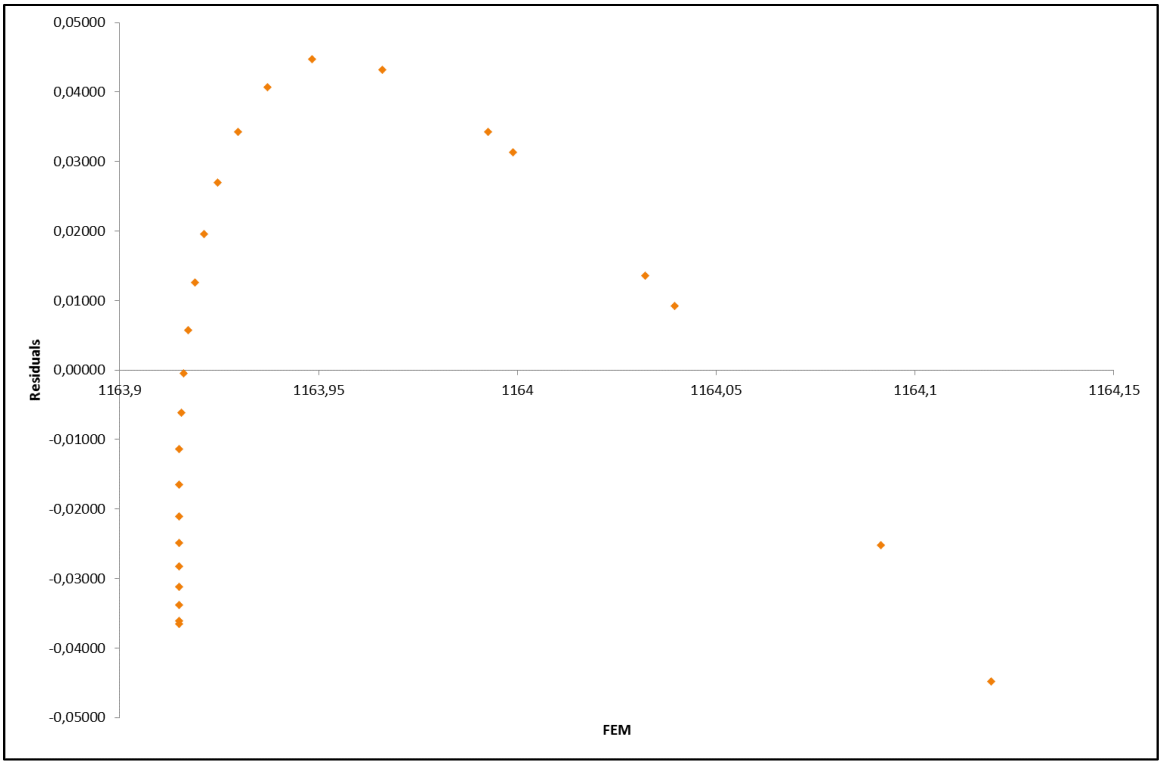

Figure D-29: Residuals plots for observation point OBS_5

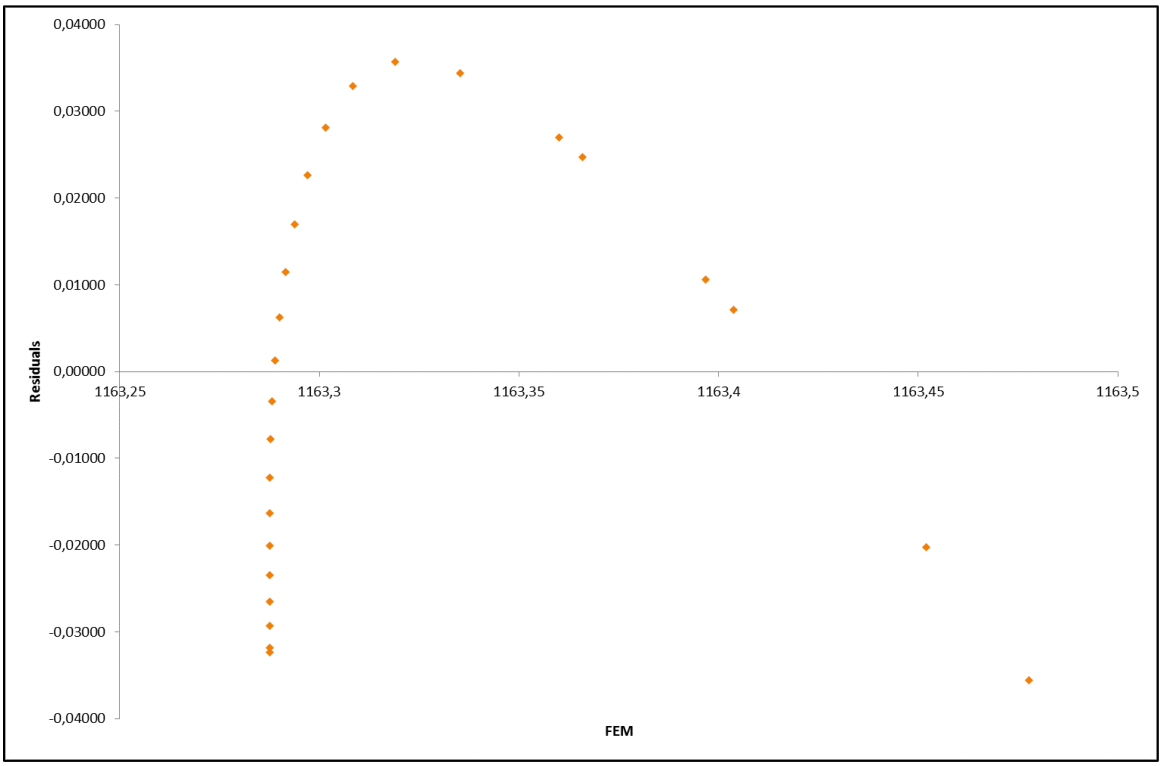

Figure D-30: Residuals plots for observation point OBS_6

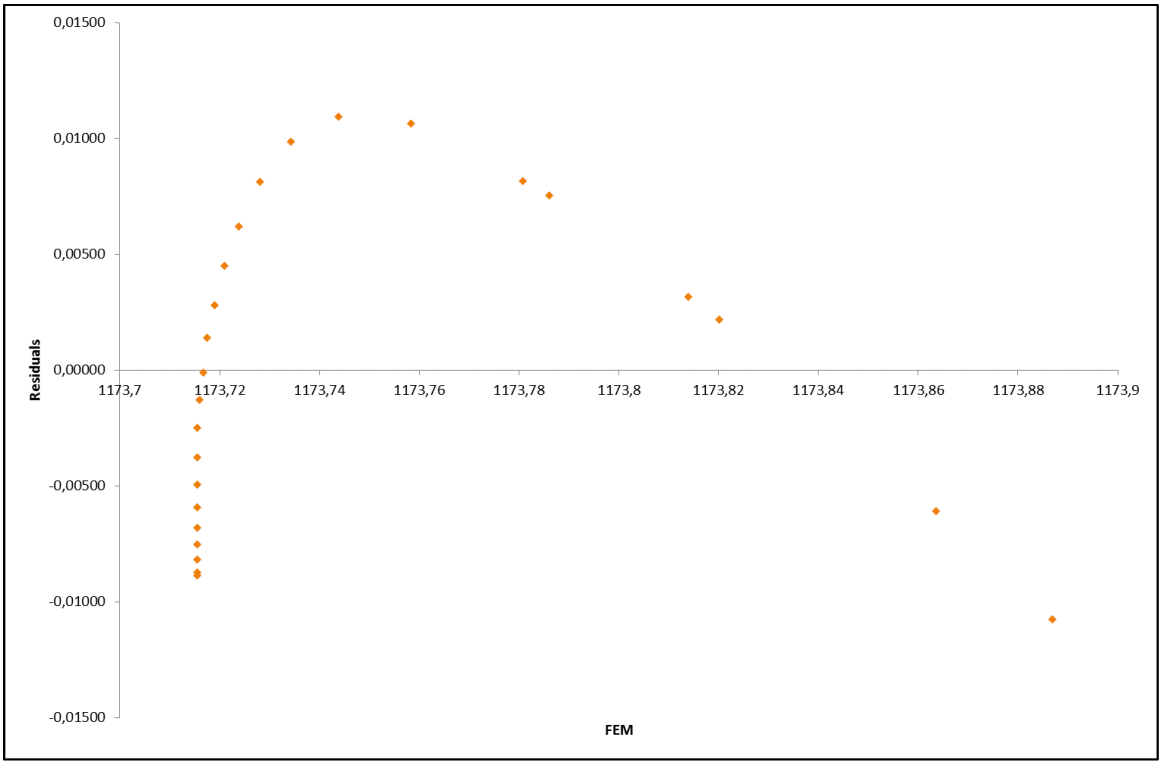

Figure D-31: Residuals plots for observation point OBS_7

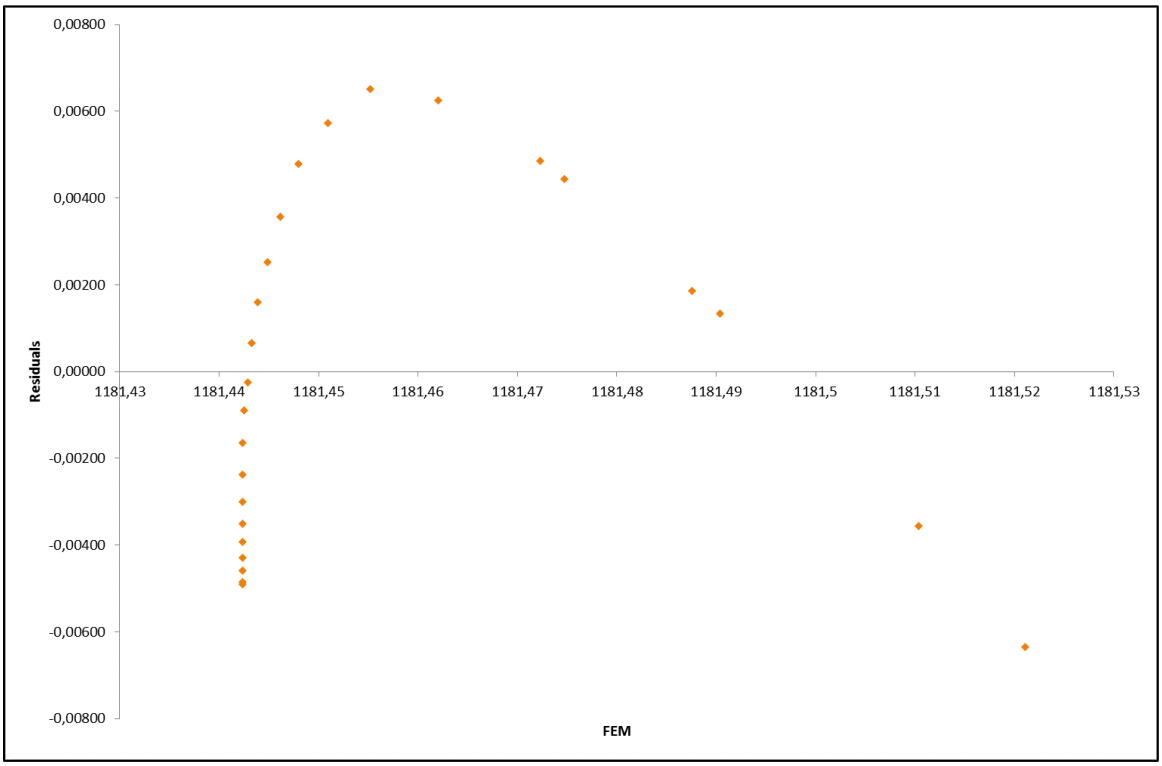

Figure D-32: Residuals plots for observation point OBS_8